Analysis of a nuclear role for *pebble*, a gene required for cytokinesis in *Drosophila*.

This thesis is submitted in fulfilment of the requirements for a Doctor of Philosophy (PhD) in the Faculty of Science at the University of Adelaide.

By Alyssa Harley

May 2002.

Centre for the Molecular Genetics of Development,
Department of Molecular Biosciences,
The University of Adelaide.

Declaration

I hereby declare that the thesis presented does not contain any material written by another person except where due reference is given in the text, nor has it been previously presented as a component of any other academic course,

I agree to my thesis being made available for photocopying and for loan

Signed

Alyssa Harley

07/05/02

Dedicated to the memory of Bruce Stuart Harley

July 1962 – March 2002

A loving brother and a constant source of inspiration.

Remembered always.

In loving memory of Patch Harley

1987 – 2001

A childhood friend and faithful companion for 14 years.

Remembered fondly.

Acknowledgments

This has been such a major part of my life so far and there are so many people I need to thank for their encouragement and support.

First and foremost I would like to thank my supervisor Rob Saint. No matter how busy or how far away, you were never too busy to discuss ideas, suggest experiments and read chapters. For this I will always be grateful.

Thanks to the many members of the Saint lab for their support and invaluable advice over the years. In particular I would like to thank Tatiana and Steve for always knowing everything, Masha for her friendship and support, Louise for her Pebble knowledge, and Jane, Gabby, Hazel, Donna and Julianne for making the lab complete.

Special thanks must also go to Michelle (MII), Tara, Volkan and Paul Moir for their many hours of technical assistance, to Velta for the laughs over the past 8 years, to my friends in other labs, and to Paul Tosch for going through the whole experience with me and for always knowing everything there is to know about computers. Cambridge here we come!

To my friends, "the group", Jenny, Lisa, Tonia, Melissa, Nga and Toby, for their friendship over the past 13 years, half our lives. You guys have provided me with just enough distraction to maintain my sanity over the years, looking forward to the next 50 years. "Oldsville" here we come! Special thanks must go to Jenny, for always being there. Your friendship and support have been boundless.

And finally, thanks in particular to my family for their support and understanding over the years. Especially to my father for providing a taxi service at all hours, and my mother and sisters Andrea and Mandy and brother-in-law Tony, for all of their support and faith. To Bruce for our discussions, for being the only family member who would have read this thesis and tried to understand it, and to my niece and four nephews for always making life interesting. Thanks also to Daisy for being a loving spaniel and constant thesis writing companion.
I owe a great debt of gratitude to you all.

Abstract

Cellular division is a vital process that must be tightly regulated to ensure the faithful replication and segregation of the genetic material of a cell. Previous experiments have shown that the *Drosophila* gene *pebble* plays an essential role in this process, and is thought to be required for the activation of the Rho G protein and the stimulation of cytokinesis. However, in addition to the DH/PH domains deemed responsible for this activation of Rho, Pebble (PBL) also contains two highly conserved nuclear BRCT domains, and a third conserved region, named the RadECl region. BRCT domains have previously been implicated in the response to and repair of DNA damage. The presence of such domains within a Rho GEF protein is both unique and intriguing in that it could enable PBL to play a dual role in both cytokinesis and DNA repair. This would not only be a novel mechanism, but it could also provide a link between the sensing of DNA damage and cell cycle control. A potential nuclear role for PBL was therefore examined in this thesis.

Through the use of a variety of biochemical and genetic techniques, the importance of the nuclear localisation of PBL was examined, as well as the function of its RadECl and BRCT domains. While nuclear localisation was found to be non-essential for the role of PBL in cytokinesis, sequestering the protein to the nucleus at the appropriate time was found to be highly important for the maintenance of normal cellular processes. In a completely novel and exciting finding, the RadECl/BRCT domains were found to be required in the cytoplasm for cytokinesis, extending the range of function attributed to these domains. PBL was also shown to shuttle between the nucleus and the cytoplasm, providing an explanation for the observed ability of nuclear PBL to influence cytoplasmic structure.

In addition to its role in cytokinesis, the phenotypes observed when PBL and its mutant forms were expressed in non-cytokinetic tissues suggested a novel cytoplasmic and/or nuclear role for PBL in interphase. In line with the documented function for BRCT domains, preliminary evidence also suggested a role for PBL in the response to DNA damage.

The results of this study have therefore provided numerous novel findings concerning the function of PBL, indicating that it is a multifunctional protein that utilises multiple domains for its diverse cellular roles.

Table of Contents

Chapter 1: Introduction

1:1 Introduction

Cellular division is a vital process that must be tightly regulated to ensure the faithful replication and segregation of the genetic material of a cell. During the development of a multicellular organism this process must not only be tightly regulated, but it must also be strictly coordinated with the process of development itself. In addition to this, cells are constantly under the threat of genetic mutation through continuous errors in DNA replication and the damaging effect of an unstable environment. A large number of spontaneous errors occur every day in a typical human cell. Thus it is obvious that accurate and thorough mechanisms must have evolved to cope with this high level of damage and maintain genomic integrity. Despite these mechanisms, failures in this process are evident from the numerous types of cancers that plague our existence. The massive detrimental impact of these diseases on our society is one of the many reasons why cell proliferation and DNA repair are of such high social and experimental interest. However, despite this interest and the many decades of research devoted to the understanding of these processes, there is still much to learn. The classical model organism *Drosophila melanogaster* provides an ideal system in which to study this vital regulation of proliferation, as it is a genetically manipulable metazoan whose cellular basis of development has been extremely well characterised. The high conservation of genes and their function across the broadest range of eukaryotic species makes *Drosophila* an invaluable research tool in the understanding of these complex cellular processes.

1:2 The eukaryotic cell cycle

The eukaryotic cell cycle can be divided into four distinct phases;

1) S phase, during which the genome is replicated.

2) M phase, consisting of mitosis, the process during which the duplicated genome is divided into two daughter nuclei before the cell itself divides during cytokinesis.

3) G1 phase, the period of time between cell division and the start of DNA synthesis and

4) G2 phase, the period between the completion of DNA synthesis and the next M phase.

Coordination of genome replication during S phase with its segregation during M phase is of vital importance to the correct development of a eukaryotic organism. If this process is not correctly controlled, cell death or cancer can result. Studies of mammalian cultured cells suggest that the two main control points of the cell cycle, G1 and G2, play different roles in the regulation of the cell cycle. During G1, cells respond to growth factors and other environmental signals, and a decision is made by the cell to continue through another cell cycle or to cease proliferating. During G2, cells monitor the fidelity of replication of the genome before the decision is made to commit to division. Throughout development, the emphasis on these control points is thought to differ at different developmental stages and in different tissue types (reviewed by Saint and Wigley, 1992; Edgar, 1995).

Studies in a multitude of different organisms have indicated the importance of two key families of proteins in the regulation of the cell cycle. The cyclin dependent kinase (CDK) family of serine/threonine protein kinases exert their effect by phosphorylating selected proteins involved in cell cycle processes. Their activity depends on association with a second family of proteins, termed cyclins because of the cyclic oscillations in the level of these proteins observed throughout the cell cycle. The cyclic assembly, activation, and disassembly of cyclin/CDK complexes is thought to act as the engine that drives the cell cycle (reviewed by O'Farrell, 1992).

1:3 The process of cytokinesis

Cytokinesis itself, the division of the cell into two daughter cells, is a process about which surprisingly little is known. Despite the fact that many of the structural components involved have been identified on the basis of their mutant phenotypes or cellular localisation, the actual mechanics and regulation of this fundamental process remains relatively poorly understood. The process of cytokinesis varies widely in eukaryotes, from budding in yeast, to septation in plants, and to contractile ring-driven cytokinesis in animal cells. Although a great deal is known about the components of yeast budding and plant septation, this discussion will focus on the factors identified in animal cell cytokinesis.

Cytokinesis in animal cells can be divided into a series of steps (**Figure 1.1**). The first step is cleavage plane specification, i.e. specifying the plane along which the cell will divide (**Figure 1.1a**). This is thought to involve the transmission of a signal, derived from the mitotic spindle and targeted to the cellular cortex, which directs the accumulation and alignment of proteins involved in the next step in cytokinesis, the formation of the contractile ring (**Figure 1.1b**) (reviewed by Glotzer, 1997b).

The contractile ring is proposed to consist of filamentous actin, arranged in a circumferential ring around the equator of a dividing cell, and non-muscle myosin II, which is arranged into minifilaments that interdigitate the actin filaments. ATP hydrolysis by myosin leads to constriction of the actin bundles via a slide filament mechanism, similar to that which drives muscle contraction. Thus constriction of the ring applies tension to the attached plasma membrane, generating the cleavage furrow which divides the cell in two (**Figure 1.1c**).

The ingression of this cleavage furrow continues until the cell membrane has been pulled in towards the microtubule bundles forming the central spindle region. The intercellular bridge structure generated after the furrow ingresses completely, which links the two daughter cells, is known as the midbody (**Figure 1.1d**). It is a transient structure consisting of an aggregate of overlapping microtubules from the spindle.

This final remaining link between the cells is resolved when the cells separate (**Figure 1.1e**). Very little is known about this process, apart from the assumption that it must involve the insertion of new membrane between the two now separate daughter cells (reviewed by Glotzer, 1997a; Glotzer, 1997b).

Figure 1.1 Cytokinesis in animal cells.

A schematic diagram of the steps involved in cytokinesis in animal cells. Nuclear material and the outline of the cell are shown in black, microtubules are shown in blue, the contractile ring is shown in red, the central spindle region is shown in green, and the signal that specifies the position of the cleavage plane is represented by yellow triangles.

A. Cleavage plane specification. This is thought to involve the transmission of a signal from
the mitotic spindle to the cell cortex.

B. Contractile ring formation. The contractile ring consists of filamentous actin and myosin
arranged in a circumferential ring around the equator of the dividing cell.

C. Furrow ingression. The constriction of the acto-myosin contractile ring leads to the formation of the cleavage furrow that divides the cell in two.

D. Midbody formation. After furrow ingression, the two daughter cells are joined by a small bridge termed the midbody. It is a transient structure consisting of an aggregate of overlapping microtubules from the spindle.

E. Cell separation. Resolution of the midbody structure and insertion of new membrane results in the formation of two separate daughter cells.

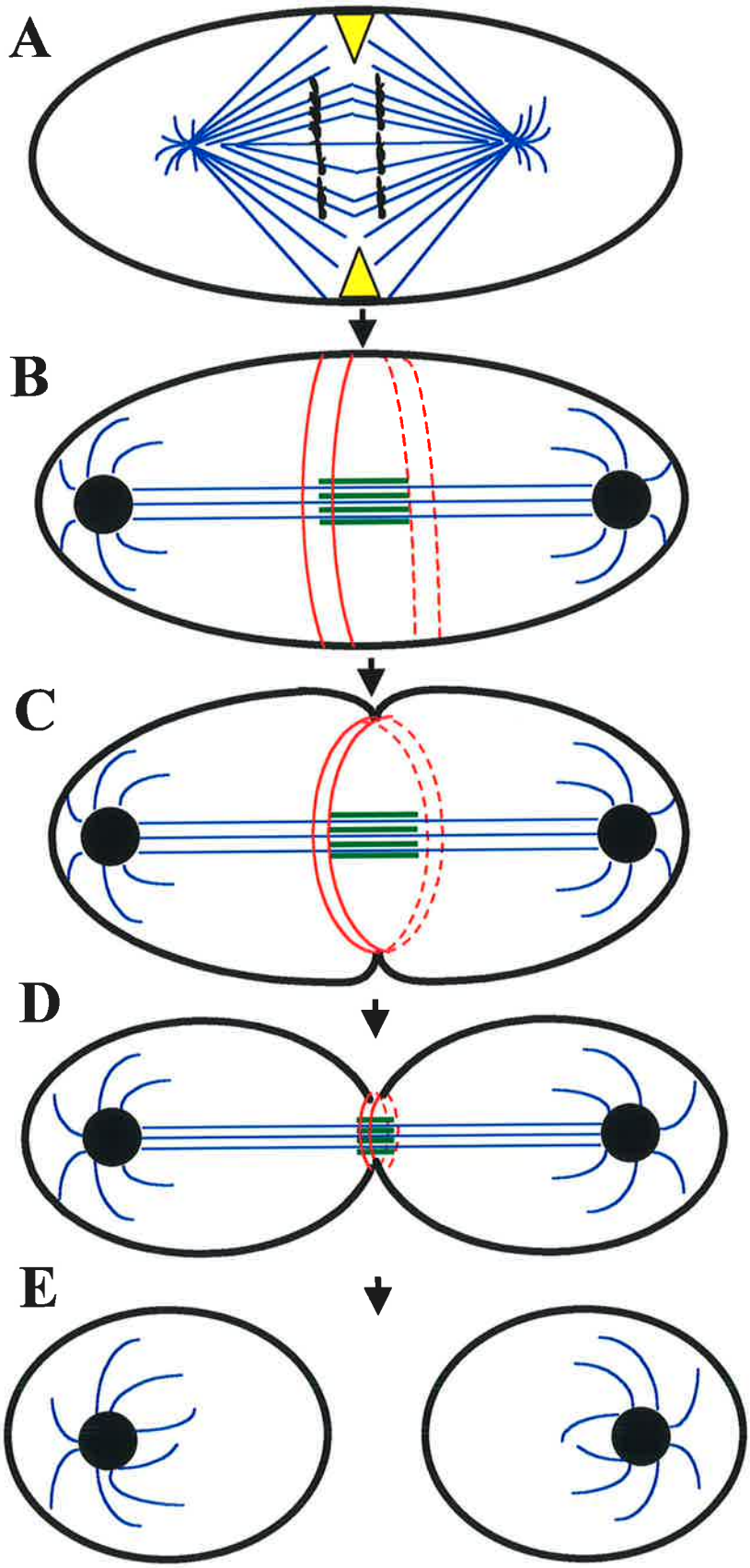
A
B
C
D
E

1:4 The initiation of cytokinesis: when?

Cytokinesis begins shortly after the onset of anaphase, the stage in mitosis in which the duplicated sister chromatids move apart to the opposite poles of the cell. The tight temporal correlation between the processes of mitosis and cytokinesis is of upmost importance to ensure that the cell does not divide until its genetic material has been completely segregated. The exit from mitosis itself is triggered by the degradation of the mitotic B type cyclins and by decreased levels of their associated CDK activity (reviewed by Zachariae, 1999). However, it has also been shown that these mitotic proteins can control the onset of cytokinesis. Inactivation of CDK1 has been shown to be required for cytokinesis to proceed in cultured rat cells (Wheatley *et al.*, 1997). Similarly, the expression of stable forms of cyclin B (CYC-B) in a variety of cell types has shown that the degradation of B-type cyclins is essential not only for late mitotic stages, but also for cytokinesis to proceed (Murray *et al.*, 1989; Sigrist *et al.*, 1995; Yamano *et al.*, 1996; Parry and O'Farrell, 2001). In support of this, *cycB* mutant *Drosophila* embryos form premature cytokinetic furrows (Knoblich and Lehner, 1993). Thus it appears that mitotic cyclin and CDK activity must be removed for both the exit from mitosis and the initiation of cytokinesis, allowing these processes to be precisely coordinated.

1:5 The initiation of cytokinesis: where?

How does a cell decide where it is going to initiate the process of cleavage furrow specification and divide itself in two? How does it ensure that this process is initiated so that each daughter receives its appropriate share of nuclear and cellular material? Mitosis is a process that is driven by reorganisation of microtubule filaments. These filaments are one of the three major protein components that make up the cytoskeleton. During the mitotic process, microtubules are reorganised and proteins are recruited to form the structure known as the mitotic spindle. This mechanical structure divides the duplicated genome in two by applying opposing forces to the sister chromatids aligned on the metaphase plate. Microtubule organising centres (MTOCs) or centrosomes play important roles in the

assembly of the spindle, the alignment of sister chromatids at the metaphase plate, and the movement of the sister chromatids to opposite poles during mitosis.

1:5.1 Cleavage plane specification: the importance of the mitotic spindle

The results of numerous studies have indicated the importance of the mitotic spindle structure to the initiation of cytokinesis. This is not at all surprising given that such connection would enable the processes of mitosis and cytokinesis to be precisely coordinated, ensuring both the correct timing and positioning of the cleavage furrow between the two daughter nuclei after successful mitotic separation. However, there remains some controversy as to which part of the mitotic spindle is responsible for this stimulus. The initial experiments performed on sea urchin embryos originally suggested that the microtubules emanating from the asters of the mitotic spindle specify the position of the cleavage furrow (Rappaport, 1961). In this system, the positioning of two polar asters from different spindles within the same cell was sufficient to induce furrowing. It was therefore proposed that a signal, originating at the asters, would travel along the astral microtubules to the cell cortex where it would stimulate constriction of the cleavage furrow (Devore *et al.*, 1989). However, more recent experiments using cultured cells have suggested that it is the central spindle that determines the position of the cleavage furrow (Cao and Wang, 1996; Wheatley and Wang, 1996; Eckley *et al.*, 1997; Wheatley *et al.*, 1998). The central spindle is made up of cross-linked bundles of antiparallel non-kinetochore spindle microtubules. In one study, tubulin was fluorescently labelled to monitor the organisation of these microtubules. An ectopic furrow was observed to form only when microtubule bundles formed between the asters, suggesting that the asters themselves were insufficient to induce furrow formation (Wheatley and Wang, 1996). The differences between the sea urchin and the mammalian tissue culture system possibly reflect inherent differences in the structures of these cells. However, it is also possible that in the original sea urchin experiments, a central spindle structure was able to form between the two asters, and it was this structure that acted as the source of the signal.

More recent studies using *Drosophila* have lent further support to the theory that it is the central spindle that provides the source of the signal. In *asterless* mutants, both spermatocytes and neuroblasts form a normal central spindle that has the ability to initiate cytokinesis (Bonaccorsi *et al.*, 1998; Giansanti *et al.*, 2001). In addition to this, *Drosophila* female meiosis is normally anastral (Theurkauf and Hawley, 1992). During male meiosis, a strong correlation between the presence of a central spindle and the formation of a contractile

ring has also been demonstrated in a variety of different mutant backgrounds (Giansanti *et al.*, 1998). Thus it seems that a wealth of data in both *Drosophila* and mammalian cells points to the central spindle as the source of the signal that initiates cytokinesis.

1:6 Formation and function of the contractile ring

Once sister chromatid segregation has been initiated, the structure known as the contractile ring forms between the segregating chromosomes. This consists of filamentous actin arranged in a circumferential ring around the equator of the dividing cell. Non muscle myosin II is arranged into minifilaments which interdigitate these actin filaments. ATP hydrolysis by myosin leads to constriction of the actin bundles via a mechanism, similar to that which drives muscle contraction. This constriction of the ring applies tension to the attached plasma membrane, generating the cleavage furrow that divides the cell in two. In addition to the actin filaments that run parallel to the cell cortex, several analyses have indicated that in the equatorial regions of the contractile ring, many actin filaments also run perpendicular to the length of the mitotic spindle (Opas and SoÇtyÑska, 1978; Fishkind and Wang, 1993). Thus the organisation of actin within the contractile ring is quite complex (Glotzer, 1997a). It is also known that actin is recruited to this region from a cytoplasmic pool (Cao and Wang, 1990). Thus the formation and function of the contractile ring requires significant changes in the actin cytoskeleton.

A host of other proteins also localise to the cleavage furrow and are involved in the formation and activity of the contractile ring. A few of these are described briefly below.

1:6.1 The role of actin binding proteins

Profilin (encoded by *chickadee* in *Drosophila*) and cofilin (*twinstar* in *Drosophila*) are actin binding proteins required for cytokinesis, which are thought play a role in the regulation of actin assembly. While Profilin binds actin monomers and is involved in filament formation (Verheyen and Cooley, 1994; Giansanti *et al.*, 1998), cofilin promotes the disassembly of actin filaments (Gunsalus *et al.*, 1995; Bamburg, 1999). Thus both the assembly and disassembly of actin filaments are required for the function of the contractile ring.

Another actin binding protein, anillin, colocalises with myosin II in the cleavage furrow and has been shown to bundle actin filaments *in vitro*. As such, it may play a role in stabilising the contractile ring by bundling cortical actin (Field and Alberts, 1995).

Thus it appears that the opposing effects of Profilin and cofilin, together with the actin bundling activity of anillin, are required for the cytoskeletal reorganisation events necessary for the formation and function of the contractile ring.

1:6.2 The role of septins

The septins are a conserved family of proteins that are required for cytokinesis in a wide range of organisms. They contain a characteristic GTP binding domain near the N-terminus, and a coiled-coil domain near the C-terminus (reviewed in Longtine *et al.*, 1996). They colocalise with actin and myosin to the cleavage furrow and in *Drosophila* are capable of forming filaments *in vitro* (Neufeld and Rubin, 1994; Field *et al.*, 1996). They are also capable of forming complexes and are thought to function as a scaffold on which other proteins assemble (Longtine *et al.*, 1998). In *Drosophila* 5 septins have been identified, PEANUT (PNUT), and SEP1, SEP2, SEP4 and SEP5 (Adam *et al.*, 2000). A 340 kD complex of PNUT, SEP1 and SEP2 has been shown to be responsible for the filament-forming activity (Field *et al.*, 1996). In vertebrate cells, septins have been shown to associate with actin-containing structures, including the contractile ring (Kinoshita *et al.*, 1997). In addition to their ability to bind actin, they are also capable of binding microtubules in *Xenopus*. This dual ability may be part of a link between the cell cortex and the central spindle that promotes furrow ingression (Glotzer, 1997b).

1:6.3 The role of Formin Homology proteins

Formin Homology (FH) proteins are known to be required for cytokinesis in a variety of species and to localise to contractile ring structures (Chang *et al.*, 1997; Harris *et al.*, 1997; Imamura *et al.*, 1997). In *Drosophila*, the FH protein Diaphanous localises to the contractile ring and is required for cytokinesis in the male germline and embryonic divisions (Castrillon and Wasserman, 1994; Afshar *et al.*, 2000). Mutations in the nematode FH gene *cyk-1* also lead to cytokinetic defects (Swan *et al.*, 1998).

Formin Homology proteins contain a number of characteristic FH domains that are responsible for their function in the reorganisation of the actin cytoskeleton. The FH1 domain is a polyproline rich region that has been demonstrated in both budding and fission yeast to

bind the actin polymerising protein Profilin (Chang *et al.*, 1997; Imamura *et al.*, 1997), suggesting that FH proteins are upstream regulators of actin reorganisation. In addition to this actin regulatory ability, FH proteins are also capable of binding Rho GTPases through an amino terminal domain (Evangelista *et al.*, 1997; Imamura *et al.*, 1997; Watanabe *et al.*, 1997). Among many cellular roles, Rho GTPases regulate the reorganisation of the actin cytoskeleton during cytokinesis. Thus FH proteins may form a crucial link between these GTPases and actin.

1:7 The importance of the central spindle and midbody

During cytokinesis, the ingression of the cleavage furrow continues until the cell membrane has been pulled in towards the microtubules forming the central spindle region (shown in green in **Fig1.1b** and **c**). Once the furrow ingresses completely, an intercellular bridge structure linking the two daughter cells remains. This structure is referred to as the midbody and consists of an aggregate of overlapping microtubules from the spindle (shown in **Fig 1.1d**). The function of the midbody is not yet entirely understood, but a variety of proteins that localise to both the central spindle region and the midbody have been shown to be required for cytokinesis. These are briefly discussed below.

1:7.1 The role of chromosomal passenger proteins

Chromosomal passenger proteins are proteins with a dynamic pattern of localisation. They are observed to initially concentrate at the centromeric regions of chromosomes before relocating to the microtubules of the central spindle and the region of the cell cortex where the cytokinetic furrow will form. Their localisation to the future furrow site occurs before any other evidence of furrowing, suggesting that these proteins may be involved in the earliest stages of furrow formation (Earnshaw and Cooke, 1991; Eckley *et al.*, 1997). However, the observation that cytokinesis can occur in the absence of chromosomes in grasshopper spermatocytes, suggests that, at least in these cells, passenger proteins are either not essential for cytokinesis or can be delivered to the central spindle via a separate mechanism (Zhang and Nicklas, 1996).

1:7.2 The role of kinesin-like motor proteins

Numerous kinesin motor proteins have also been implicated in the processes of mitosis and cytokinesis (Moore and Endow, 1996). In *Drosophila* the Kinesin-like protein KLP3A exhibits defects in cytokinesis during the meiotic divisions of spermatogenesis. It is observed to concentrate at the midbody during anaphase and telophase and is thought to be involved in the bundling of microtubules at the midzone to form the central spindle (Williams *et al.*, 1995). These observations provide further evidence that it is the central spindle that is the source of the signal that initiates the cleavage furrow.

Pavarotti is a mitotic kinesin-like protein in *Drosophila* that has also been shown to be required for cytokinesis during embryonic divisions. It is observed to localise to the centrosomes early in mitosis and to the microtubules of the midbody during late anaphase and telophase. Pavarotti associates with Polo kinase, and together they show an overlapping pattern of subcellular mitotic localisation. This distribution is disrupted in *pavarotti* mutants, and Pavarotti has also been shown to be required for the correct localisation of the septin Peanut, actin, and the actin-associated protein Anillin. Cells of *pavarotti* mutant embryos develop an abnormal telophase spindle and fail to initiate cytokinesis (Adams *et al.*, 1998). Thus this kinesin-like protein is required for both spindle and contractile ring formation and to mobilise other regulatory proteins.

1:7.3 The role of Serine/Threonine protein kinases

In addition to their earlier roles in mitosis, the serine/threonine kinases Polo and Aurora localise to the midbody and play a role in the regulation of cytokinesis. Polo hypomorphic mutant spermatocytes in *Drosophila* fail to form correct midzone and midbody structures at telophase. Interestingly, *polo* mutant cells also fail to correctly localise the kinesin-like protein Pavarotti, and actin and the septin Peanut are not incorporated into the contractile ring. Thus it appears that Polo and Pavarotti are mutually dependent for their correct localisation, and are both essential for cytokinesis (Carmena *et al.*, 1998).

The first Aurora kinase identified in *Drosophila* was initially found to be required for the centrosomes to separate and form a bipolar spindle (Glover *et al.*, 1995). A second Aurora-like kinase, Aurora B, was subsequently found to be involved in cytokinesis in addition to its mitotic role in chromosome condensation and segregation. (Giet and Glover, 2001). In support of this finding, an Aurora B kinase in *C. elegans*, *AIR-2*, was also found to play a role in cytokinesis and chromosome condensation (Schumacher *et al.*, 1998; Kaitna *et*

al., 2000; Severson *et al.*, 2000). Interestingly AIR-2 was found to act as a passenger protein, associating with chromosomes early in mitosis before being transferred to the midbody microtubules, where it is required for correct organisation of the spindle and localisation of the Pavarotti kinesin-like protein orthologue ZEN-4 (Schumacher *et al.*, 1998; Kaitna *et al.*, 2000; Severson *et al.*, 2000). Thus it seems that a complex interplay between a multitude of proteins, including Polo and Aurora kinases, is required for the precise regulation of mitosis and cytokinesis.

1:8 Cell separation

After the furrow has ingressed to completion and the midbody is the only remaining structure linking the two cells, the final process of cell separation must begin. This involves the resolution of the midbody, and the insertion of new membrane to form two now separate daughter cells.

1:8.1 The insertion of new membrane

In animal cell divisions, new membrane is thought to be inserted just behind the leading edge of the ingressing furrow (Bluemink and deLaat, 1973; Drechsel *et al.*, 1997). Although very little is known about the mechanics and regulation of this process, it is thought to occur by targeted vesicle insertion, similar to the process of cell separation in plants. In plant cells, vesicles are transported via microtubules to the region between the separated sister chromatids. These vesicles then fuse into a tubulo-vesicular network that ultimately matures into a continuous membranous structure, dividing the cell in two. The syntaxin protein KNOLLE and the dynamin-like protein phragmoplastin have been identified as playing essential roles in this process (reviewed in Gu and Verma, 1996; Lukowitz *et al.*, 1996; Glotzer, 1997b). Syntaxins are known to be involved in membrane fusion events, while dynamin has been implicated in endocytosis in a wide range of organisms (Bennett *et al.*, 1993; Hinshaw and Schmid, 1995). Interestingly, syntaxins have more recently been identified as playing cytokinetic roles in animal cells, suggesting that plants and animals may use similar mechanisms to incorporate new membrane during cytokinesis (reviewed in Bowerman and Severson, 1999). Studies in *C. elegans* have identified the syntaxin protein

Syn-4 as playing a role in cytokinesis, possibly in membrane addition at the cleavage furrow (Jantsch-Plunger and Glotzer, 1999). In further support of the role of membrane addition, the inactivation by RNA interference of *rab-11* in *C. elegans* results in a similar cytokinetic defect to that caused by inactivation of *syn-4*. *rab-11* encodes a member of the Rab family of small GTPases that have previously been implicated in specific membrane fusion events (reviewed by Bowerman and Severson, 1999).

In *Drosophila*, inhibition of syntaxin activity inhibited the process of cellularisation (Burgess *et al.*, 1997). Cellularisation is a process related to cytokinesis, which occurs very early in the development of *Drosophila* before any cytokinetic division, and involves the growth of membranes from the periphery of the embryo to encapsulate the syncitial nuclei within it (Campos-Ortega and Hartenstein, 1985). Therefore the possible role of this protein in cytokinesis itself has not yet been determined. Similarly, mutants in *lavalamp* also show an inhibition of cellularisation. *lavalamp* encodes a golgi-associated protein that facilitates membrane insertion required for the formation of furrows during cellularisation (Sisson *et al.*, 2000). Further studies are required to determine whether these proteins also function in the analogous process of cytokinesis in *Drosophila*.

1:8.2 The role of centrosomes in final separation

The use of centrin-GFP to follow the localisation of the centrosomes in live cells during cytokinesis, provided surprising evidence that the centrosomes could also be involved in the final stages of cytokinesis (Piel *et al.*, 2001). Each centrosome consists of a mother and a newly synthesised daughter centriole, which is produced with each cell division. Real time imaging revealed that final separation of the two daughter cells coincided with the movement of one or other of the mother centrioles toward the vicinity of the midbody region. Analysis of fixed cells had also suggested a similar movement of the centrosome (Mack and Rattner, 1993). However, there remains some controversy as to the importance of the centrosome in the final separation of the daughter cells. Cells in which the centrosome has been laser ablated are observed to complete cytokinesis, albeit with an increased frequency of cytokinetic defects (Khodjakov and Rieder, 2001). Also, flies with a mutation in the centrosomin gene that lack functional centrosomes, survive to adulthood, suggesting that centrosomes are not essential for cytokinesis (Megraw *et al.*, 2001) (reviewed by Glotzer, 2001).

In conclusion, a range of proteins, possibly related to those involved in plant membrane addition, are involved in the insertion of new membrane behind the leading edge of the ingressing furrow. The movement of the centrosomes toward the midbody region may signal the final separation of the cells, leading to the creation of two separate daughter cells.

1:9 Rho family GTPases

Members of the Ras superfamily of small G proteins (GTPases) have been shown to be essential for a wide range of intracellular signalling pathways involved in multiple cellular functions. One subclass of this superfamily, the Ras Homology (Rho) family of small GTPases, has been shown to regulate many essential cellular processes including acto-myosin dynamics, cell adhesion, gene transcription and cell cycle progression. This discussion however, will focus on their roles in cytokinesis.

1:9.1 Rho GTPases: molecular switches with important regulatory roles

Multiple members of the Rho GTPase family have been identified, but the most extensively characterised of these are Rho, Rac and Cdc42. In common with all members of the Ras superfamily, each of these GTPases acts as a molecular switch, cycling between an active GTP bound form and an inactive GDP bound form (**Figure 1.2**). In their active state they localise to plasma membranes and are capable of interacting with downstream effector molecules to bring about changes in acto-myosin structures (reviewed by Bishop and Hall, 2000). Most of the initial work on these Rho family members was carried out in mammalian tissue culture cells where active Rho was found to induce the bundling of actin to form stress fibres, Rac was found to induce the accumulation of actin filaments to form membrane ruffles and lamellopodia, while Cdc42 induced the formation of filopodia (Ridley and Hall, 1992; Ridley *et al.*, 1992; Nobes and Hall, 1995). Once they have initiated a downstream response, their intrinsic GTPase activity returns these G proteins to the GDP-bound inactive state to terminate further signal transduction.

1:9.2 The regulation of Rho GTPases: GEFs and GAPs

The ratio of the GTP bound active form, and the GDP bound inactive form of Rho proteins in a cell is largely controlled by the opposing effects of GEFs, GAPs and GDIs (**Figure 1.2**). GTP Exchange Factors (GEFs) catalyse the exchange of GDP for GTP and thus promote the active GTP bound form. All Rho GEFs contain a characteristic tandem arrangement of Dbl-homology (DH) and pleckstrin homology (PH) domains. The DH domain is responsible for the catalytic activity of the GEF, promoting the uptake of GTP in exchange for GDP (Hart *et al.*, 1994; Cherfils and Chardin, 1999). The PH domain is thought to enable the localisation of the protein to the plasma membrane through lipid binding (Zheng *et al.*, 1996; Rameh *et al.*, 1997). However, the PH domain is also thought to directly affect the activity of the DH domain. For example, in the GEF Trio which contains two DH/PH modules, the DH/PH domains together have a 100-fold higher GEF activity than the DH domain alone (Liu *et al.*, 1998).

GTPase Activating Proteins (GAPs) increase the intrinsic GTPase activity of G proteins, thus promoting the inactive GDP bound form (Lamarche and Hall, 1994). A third class of Rho family interactors, Guanine nucleotide Dissociation Inhibitors (GDIs), bind to RhoGDP in the cytosol, sequestering it in this inactive form (Olofsson, 1999). Thus the combined effects of GEFs, GAPs and GDIs act to regulate the activity of Rho family members.

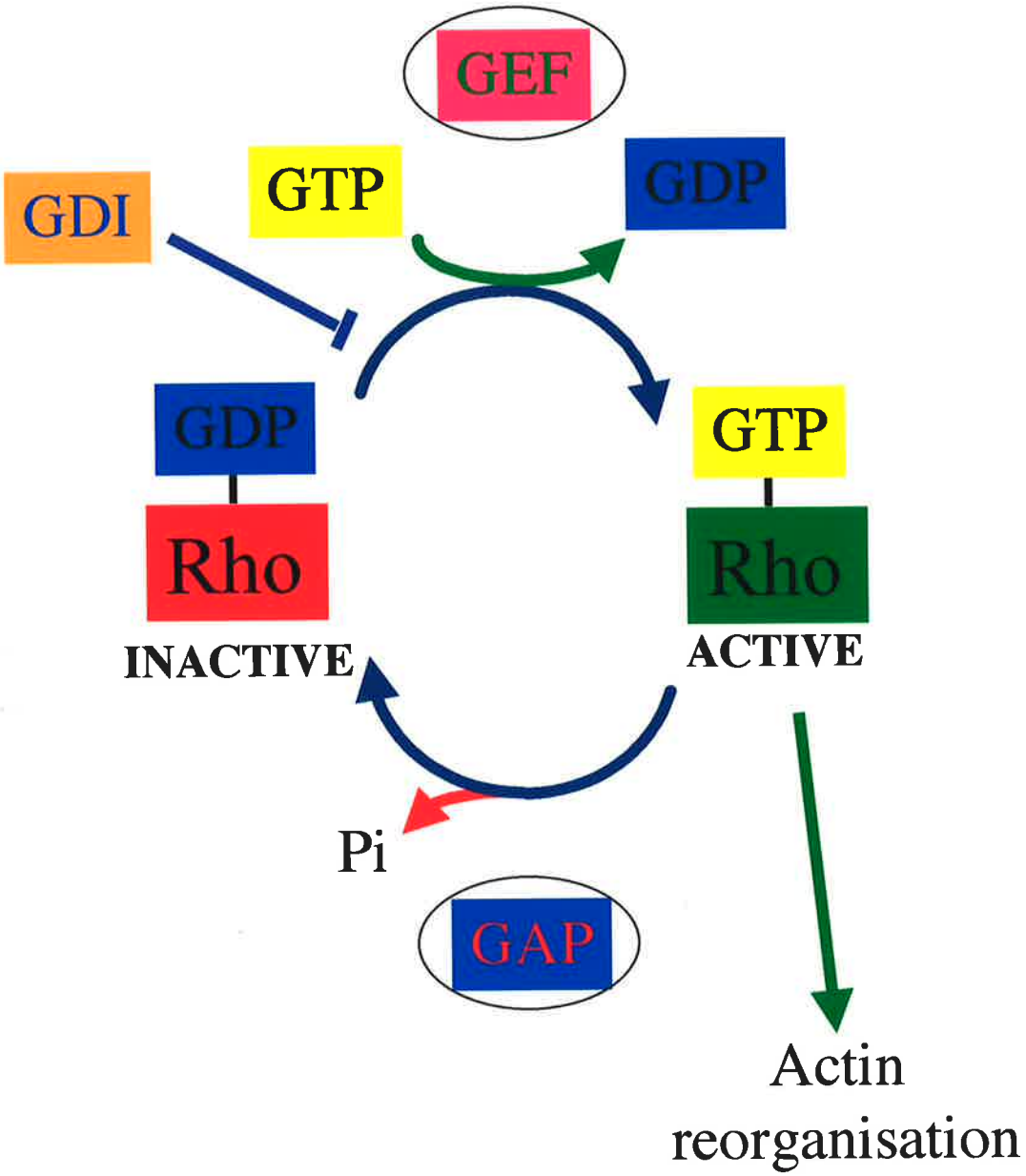

Figure 1.2 The regulation of Rho G protein activity by GEFs, GAPs, and GDIs.

Rho G proteins cycle between an active GTP bound form, and an inactive GDP bound form. The ratio of these two forms in the cell is controlled by the opposing effects of GEFs, GAPs, and GDIs. GTP Exchange Factors (GEFs) promote the uptake of GTP in exchange for GDP and therefore promote the active form. GTPase Activating Proteins (GAPs) catalyse the intrinsic GTPase activity of G proteins, thus promoting the GDP bound inactive form. Guanine nucleotide Dissociation Inhibitors (GDIs) bind to RhoGDP, maintining it in an inactive form. GTP bound active Rho localises to the plasma membrane and interacts with downstream effector molecules to bring about changes in acto-myosin structures.

1:10 Rho GTPases and their role in cytokinesis

The major role that has been identified for Rho GTPases is to regulate the organisation and assembly of the actin cytoskeleton. Therefore it is not at all surprising that they have been found to play important roles in cytokinesis. A role for Rho in cytokinesis was first demonstrated using the botulinum C3 toxin, which specifically inactivates Rho, and by microinjecting constitutively active and dominant negative versions of Rho family members in cultured cells.

Rho itself was found to be required for cytokinesis in *Xenopus* (Kishi *et al.*, 1993; Drechsel *et al.*, 1997) and sea urchin embryos (Mabuchi *et al.*, 1993), as well as in human cultured cells (O'Connell *et al.*, 1999). Injection of the C3 toxin and of modified forms of Rho in this range of organisms was found to inhibit furrow ingression through a failure of proper actin reorganisation to form a functional contractile ring. Interestingly, newly inserted cleavage membranes were observed to form aberrantly on the outer surface of the modified *Xenopus* embryos, suggesting that furrow ingression and membrane insertion are not necessarily linked (Drechsel *et al.*, 1997).

Rho has also been shown to be required for cytokinesis in *D. melanogaster* and *C. elegans*. In *Drosophila*, mutations in *RhoA* or expression of a dominant negative form of *RhoA* disrupt cytokinesis (Prokopenko *et al.*, 1999), while in *C. elegans*, RNA interference revealed a requirement for RhoA in cytokinesis (Jantsch-Plunger *et al.*, 2000).

Other Rho family members have also been demonstrated to play essential roles during cytokinesis in a variety of organisms. Expression of modified forms of Cdc42 has been shown to inhibit cytokinesis in both human cultured cells and *Xenopus* (Dutartre *et al.*, 1996; Drechsel *et al.*, 1997). Similarly, expression of constitutively active or dominant negative forms of Rac1A, Rac1B and Rac1C inhibited cytokinesis demonstrating their involvement in this process in the amoeba *Dictyostelium discoidium* (Dumontier *et al.*, 2000; Palmieri *et al.*, 2000). RacE was isolated in a molecular genetic screen in *Dictyostelium* to identify genes required for cytokinesis (Larochelle *et al.*, 1996). This gene was subsequently shown to be involved in the regulation of cortical tension and actin organisation at the cell cortex (Larochelle *et al.*, 2000).

Therefore Rho, Rac and Cdc42 all play important roles in cytokinesis in different systems. However, their involvement seems to differ depending on the organism. For example, although RhoA was shown to be required for cytokinesis in *C. elegans*, Rac1 and

Cdc42 were shown not to be required in this system (Jantsch-Plunger *et al.*, 2000). Multiple Rac proteins have been shown to be required for cytokinesis in *Dictyostelium discoidium*, however Rho and Cdc42 have not been found in this system (Larochelle *et al.*, 1996; Dumontier *et al.*, 2000; Palmieri *et al.*, 2000). In *Drosophila*, mutants were not, until very recently, available for Rac or Cdc42. Although ectopic expression of modified forms of these proteins demonstrated an affect on actin cytoskeletal structures, no specific role in cytokinesis was identified for these proteins (Luo *et al.*, 1994; Harden *et al.*, 1995; Murphy and Montell, 1996). Subsequently, lethal mutations in *cdc42* were isolated by a reverse genetic screen (Fehon *et al.*, 1997). Further analysis demonstrated a role for Cdc42 in actin filament assembly, epithelial cell morphogenesis and cell signalling during *Drosophila* development. However, no role in cytokinesis was identified. (Genova *et al.*, 2000). Thus it appears that there are either organism or cell type specific requirements for particular Rho family members during cytokinesis.

1:11 Downstream effectors of Rho GTPases mediate cytokinetic functions

Rho family members are obviously highly important in cytokinesis, but what is the exact nature of their roles? A clue came with the identification of a range of proteins that act downstream of the Rho family. Yeast 2 hybrid experiments and a variety of biochemical approaches have led to the identification of more than 30 potential effectors for Rho, Rac and Cdc42, which interact specifically with the GTP bound active form of these GTPases (reviewed in Bishop and Hall, 2000). These downstream effector proteins fall into 3 distinct classes: Ser/Thr kinases, lipid kinases and scaffold proteins, and mediate a wide variety of cellular processes. This discussion, however, will focus on 3 recently identified downstream effectors of RhoA that have been implicated in cytokinesis; Rho-associated kinase, citron kinase and Formin Homology proteins.

1:11.1 The role of Rho-associated kinase

Rho-associated kinase (also known as Rho-kinase, ROK or ROCK) is a Ser/Thr kinase that is activated by binding specifically to Rho-GTP. Once activated by Rho, Rho-kinase strongly concentrates at the cleavage furrow during cytokinesis (Kosako *et al.*, 1999). Several of the identified Rho-kinase substrates have been identified as playing roles in cytokinesis, suggesting that Rho-kinase may play an important regulatory role. A clue to its potential functional role in cytokinesis came with the observation that Rho-kinase can phosphorylate and activate myosin regulatory light chain (RLC) *in vitro* (Amano *et al.*, 1996). In support of this, pharmacological inhibition of Rho-kinase *in vivo* has been shown to reduce the amount of phosphorylated myosin RLC (Kosako *et al.*, 2000). Phosphorylation of myosin RLC stimulates the ATPase activity of myosin II and promotes the assembly of acto-myosin filaments that, as discussed previously, are essential for the formation and function of the contractile ring (**Figure 1.3**). In further support of this, phosphorylation of myosin RLC was also shown to be important for cytokinesis by the injection of non-phosphorylatable RLC into mammalian cells (Komatsu *et al.*, 2000). Also, mutational analysis has shown that the phosphorylation sites of the *Drosophila* myosin RLC, encoded by the *spaghetti squash* (*sqh*) gene, are essential for cytokinesis (Jordan and Karess, 1997).

In addition to its ability to phosphorylate myosin RLC, Rho-kinase can also indirectly regulate myosin activity by phosphorylation and inhibition of the myosin binding subunit of myosin phosphatase. Myosin phosphatase negatively regulates myosin RLC by dephosphorylating it. Thus inhibition of myosin phosphatase by Rho-kinase also results in an increase in the amount of active phosphorylated myosin RLC (Kimura *et al.*, 1996) (**Figure 1.3**).

A third Rho-kinase substrate, LIM kinase, may also contribute to assembly of the contractile ring through the stabilisation of filamentous actin. Cofilin destabilises filamentous actin, and the downregulation of cofilin is required for cytokinesis (Abe *et al.*, 1996). Rho-kinase has been shown to phosphorylate and activate LIM kinase (Maekawa *et al.*, 1999), which in turn phosphorylates and inactivates cofilin (Moriyama *et al.*, 1996; Sumi *et al.*, 1999), providing another mechanism by which Rho-kinase can regulate the formation and function of the contractile ring (**Figure 1.3**).

Other substrates of Rho-kinase that could play a role in the regulation of intermediate filament organisation during cytokinesis have also been characterised. Intermediate filaments, along with actin filaments and microtubules form the three most abundant components of the vertebrate cytoskeleton (reviewed by Goto *et al.*, 2000). During

cytokinesis, the intermediate filaments vimentin and glial fibrillary acidic protein (GFAP) are specifically phosphorylated by Rho-kinase at the cleavage furrow causing filament disassembly and allowing the daughter cells to separate for the completion of cytokinesis (Kosako *et al.*, 1997; Goto *et al.*, 1998; Yasui *et al.*, 1998) (**Figure 1.3**).

Thus there exists substantial evidence for the involvement of Rho-kinase in both the regulation of the acto-myosin contractile ring and intermediate filaments. Despite this, genetic analysis in some systems has failed to identify a clear role for Rho-kinase during cytokinesis. Although a dominant negative form of Rho-kinase inhibited cleavage furrow formation in *Xenopus* embryos and cytokinesis in mammalian cells (Yasui *et al.*, 1998), surprisingly, Rho-kinase in *Drosophila* (*Drok*), is not essential for cytokinesis. Homozygous mutant clones in the eye were found to be capable of proliferation (Winter *et al.*, 2001). Cytokinesis is also not affected in mutant embryos homozygous for the *C. elegans* Rho-kinase *let-502* (Wissmann *et al.*, 1997). It is possible however, that other Rho-associated kinases also play important roles in cytokinesis.

1:11.2 The role of citron kinase

Another kinase that has been shown to be activated by RhoA and is implicated in cytokinesis is Citron kinase. Once activated, Rho binds to Citron kinase and translocates to the cell cortex, where the complex becomes concentrated at the cleavage furrow (Eda *et al.*, 2001). Citron kinase has been shown to be required for cytokinesis in mammalian tissue culture cells through the overexpression of Citron kinase deletion mutants (Madaule *et al.*, 1998). Citron kinase knockout mice display a high incidence of multinucleate cells in the cerebellum, suggesting a defect in cytokinesis. Surprisingly, this phenotype is not observed in most other tissues, suggesting a degree of tissue specificity (Di Cunto *et al.*, 2000) (**Figure 1.3**). The exact nature of the biochemical role of Citron kinase in cytokinesis remains unknown, although it has been suggested that it could be involved in the contraction of the acto-myosin ring. Citron kinase is structurally similar to Rho-kinase, suggesting a similarity in function. In cells in which mutant forms of Citron kinase were expressed, contractile ring defects were observed (Madaule *et al.*, 1998). Thus citron kinase, like Rho kinase, could be involved in the regulation of the contraction of the acto-myosin ring.

1:11.3 The role of Formin Homology proteins

A class of RhoA effector molecules that may promote actin polymerisation for cytokinesis is the Formin Homology family. As discussed previously, Formin Homology proteins (FH) are known to localise to the contractile ring and are required for cytokinesis in a variety of species (Chang *et al.*, 1997; Harris *et al.*, 1997; Imamura *et al.*, 1997). FH proteins bind Rho through an amino terminal domain (Evangelista *et al.*, 1997; Imamura *et al.*, 1997; Watanabe *et al.*, 1997), and also bind the actin polymerising protein profilin via their FH1 domain (Chang *et al.*, 1997; Imamura *et al.*, 1997). As discussed previously, profilin is an actin binding protein that promotes F-actin polymerisation and is required for cytokinesis (Verheyen and Cooley, 1994; Giansanti *et al.*, 1998). Thus, through its interaction with Formin Homology proteins, which bind to and regulate profilin, Rho can ultimately stimulate the polymerisation of F-actin required for the formation and function of the contractile ring (**Figure 1.3**).

Therefore, through a variety of different biochemical pathways, Rho can regulate both the formation and function of the acto-myosin contractile ring, as well as the disassembly of intermediate filaments to ensure efficient cell separation. A summary of these RhoA dependent pathways involved in cytokinesis is shown in **Figure 1.3**.

Figure 1.3 Summary of the RhoA dependent pathways in cytokinesis.

Rho GTPases cycle between an active GTP-bound form and an inactive GDP-bound form. The ratio of these two forms in a cell is controlled by the opposing effects of GEFs and GAPs. Rho GEFs promote the GTP-bound active form, while Rho GAPs promote the GDP-bound inactive form. Once activated, Rho-GTP can initiate a downstream signalling cascade that can regulate cytokinesis.

The activation of citron kinase by Rho-GTP is thought to stimulate contraction of the contractile ring, although this pathway is yet to be defined. The activation of Rho-kinase by Rho-GTP initiates several different pathways that could lead to the activation of cytokinesis. The intermediate filaments vimentin and glial fibrillary acidic protein (GFAP) are specifically phosphorylated by Rho-kinase at the cleavage furrow causing filament disassembly and allowing the daughter cells to separate for the completion of cytokinesis. Rho-kinase can also phosphorylate and activate myosin regulatory light chain (RLC). Phosphorylation of myosin RLC stimulates the ATPase activity of myosin II and promotes the assembly of acto-myosin filaments, which is essential for the formation and function of the contractile ring. Rho-kinase can also indirectly regulate myosin activity by phosphorylation and inhibition of the myosin binding subunit of myosin phosphatase. Myosin phosphatase negatively regulates myosin RLC by dephosphorylating it. Thus, inhibition of myosin phosphatase by Rho-kinase also results in an increase in the amount of active phosphorylated myosin RLC. Rho-kinase has also been shown to phosphorylate and activate LIM kinase, which in turn phosphorylates and inactivates cofilin. Cofilin destabilises filamentous actin, and the downregulation of cofilin is required for cytokinesis. Formin Homology proteins bind Rho-GTP through an amino terminal domain and also bind the actin polymerising protein profilin via their FH1 domain. Profilin is an actin binding protein that promotes F-actin polymerisation and is required for the formation and function of the contractile ring. Thus through a variety of different biochemical pathways, Rho-GTP can regulate cytokinesis.

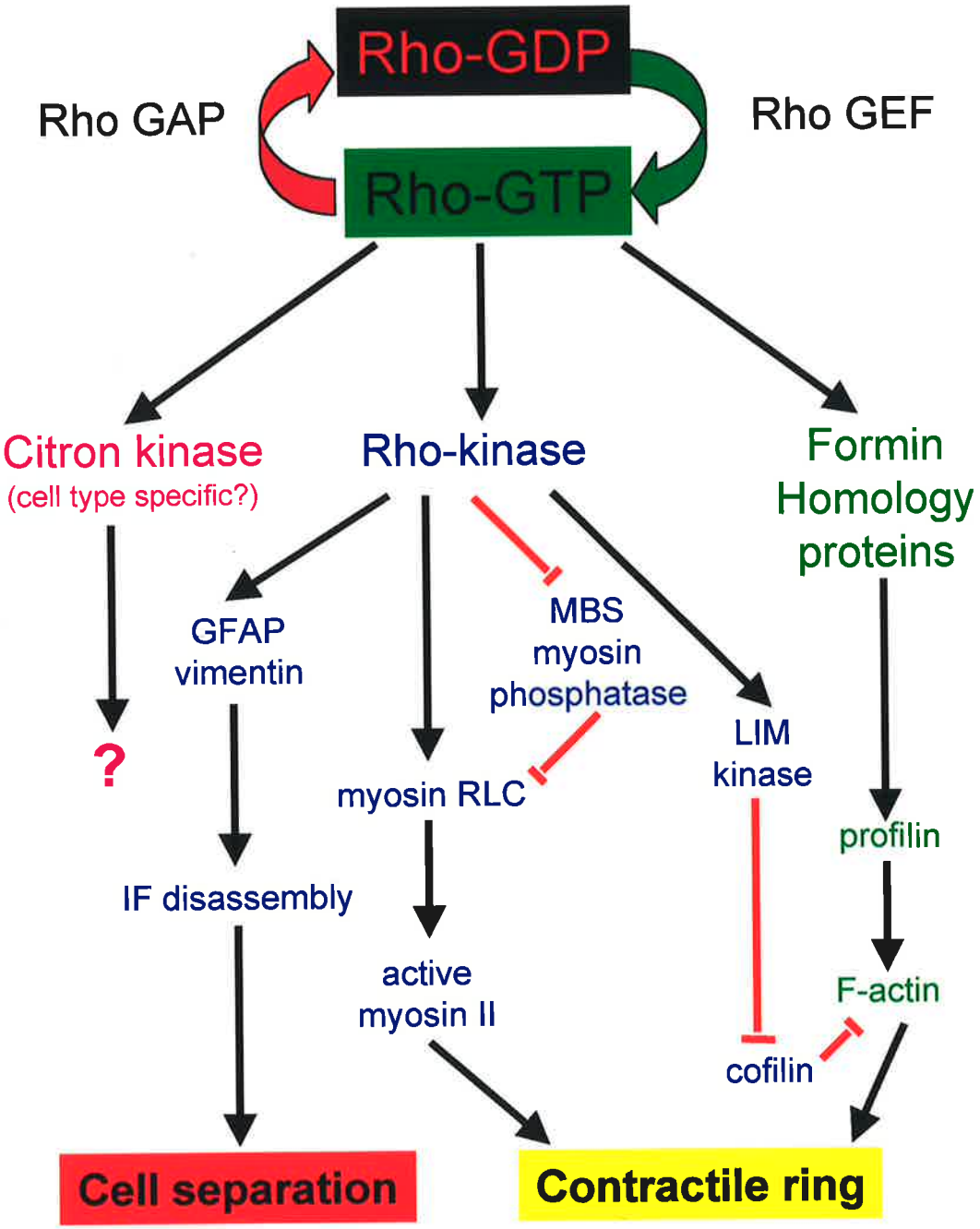
Rho-GDP
Rho GAP
Rho GEF
Rho-GTP
Citron kinase
(cell type specific?)
Rho-kinase
Formin
Homology
proteins
GFAP
vimentin
MBS
myosin
phosphatase
LIM
kinase
?
myosin RLC
profilin
IF disassembly
active
myosin II
F-actin
cofilin
Cell separation
Contractile ring

1:12 Rho GTPases and their regulators in *Drosophila*

Six Rho-family GTPases have so far been identified in the *Drosophila* genome; Rac1, Rac2, Mtl, RhoA, RhoL and Cdc42 (Dickson, 2001). As discussed previously, mutants were originally not available in *Drosophila* for Rac1, Rac2, RhoL or Cdc42. Although ectopic expression of modified forms of these proteins demonstrated an affect on actin cytoskeletal structures, no specific role in cytokinesis was identified for these proteins (Luo *et al.*, 1994; Harden *et al.*, 1995; Murphy and Montell, 1996). Subsequently, lethal mutations in *cdc42* were isolated by a reverse genetic screen (Fehon *et al.*, 1997). Further analysis demonstrated a role for Cdc42 in actin filament assembly, epithelial cell morphogenesis and cell signalling during *Drosophila* development. However, no role in cytokinesis was identified. (Genova *et al.*, 2000). Similarly, the three *Drosophila* Rac proteins Rac1, Rac2, and Mtl have very recently been shown, through the use of newly identified loss-of-function mutations, to play overlapping roles in the control of epithelial morphogenesis, myoblast fusion, axon growth, and axon guidance, processes which involve changes to the actin cytoskeleton. However, like Cdc42, no role in cytokinesis has been observed for these proteins (Hakeda-Suzuki *et al.*, 2002; Ng *et al.*, 2002).

RhoA on the other hand, has been clearly implicated in cytokinesis. *RhoA* null mutant clones fail to proliferate (Strutt *et al.*, 1997), *RhoA* homozygous mutant embryos contain multinucleate cells, and overexpression of a dominant negative form of RhoA leads to a complete block of cytokinesis (Prokopenko *et al.*, 1999). Thus RhoA appears to be the major Rho family member involved in cytokinesis in *Drosophila*.

In addition to its cytokinetic role, Rho also plays many other roles in *Drosophila* development. These include early developmental roles in cellularization (Crawford *et al.*, 1998), gastrulation (Barrett *et al.*, 1997; Hacker and Perrimon, 1998), segmentation (Magie *et al.*, 1999), and dorsal closure (Harden *et al.*, 1999), as well as later roles in the regulation of tissue polarity (Strutt *et al.*, 1997) and dendritic morphogenesis (Lee, T. *et al.*, 2000b). Given this large diversity of functions for Rho, one would assume that there exists a complex hierarchy of regulatory molecules controlling its activity. One possible mechanism for the regulation of Rho function could be the tissue, stage or cell cycle-specific expression of regulatory molecules such as GAPs and GEFs. Those that have been identified as playing such roles in *Drosophila* are discussed below.

1:12.1 Rho GEFs in *Drosophila*

Genome sequence analysis has revealed that there are at least 23 GEFs specific for Rho family GTPases in *Drosophila*. Further characterisation has begun on a few of these, including Pebble (PBL), DRhoGEF1, DRhoGEF2, DrhoGEF3, Still Life, Trio, dPIX, and GEF64C. PBL is a GEF that appears to target RhoA, and is the subject of this thesis. As such, it will be discussed in detail in a following section. DRhoGEF1 is expressed throughout oogenesis and embryogenesis, and is most abundant in regions of the embryo where cell shape change is occurring and the cytoskeleton is reorganising (Werner and Manseau, 1997). *DRhoGEF2* was originally identified in a screen for Rho signalling pathway components as a suppressor of the rough eye phenotype caused by ectopic expression of Rho1. Embryos lacking *DRhoGEF2* were found to fail to gastrulate owing to a defect in the cell shape changes required for tissue invagination (Barrett *et al.*, 1997). *DRhoGEF2* was also subsequently isolated as a maternal effect mutation that affected cell shape changes during gastrulation. A lack of maternal DRhoGEF2 product was found to result in the failure of mesodermal and endodermal primordia to invaginate (Hacker and Perrimon, 1998). DrhoGEF3 was found to have a dynamic expression pattern, being found in a segmented pattern during gastrulation and germ band extension, and at later developmental stages, being expressed in the visceral mesoderm, at the sites of muscle attachment and in groups of sub-epidermal cells (Hicks *et al.*, 2001). Still Life localises to the plasma membrane of synaptic terminals, and the expression of a truncated form of this protein resulted in defects in neuronal morphology (Sone *et al.*, 1997). Trio is unusual in that it contains two GEF domains, one of which has been shown in *Drosophila* to regulate axon guidance through its interaction with Rac (Newsome *et al.*, 2000). dPIX is another Rho family GEF in *Drosophila* which is required for the regulation of the postsynaptic structure of neuromuscular junctions (Parnas *et al.*, 2001). Finally, the Rho GEF, GEF64C, has been found to promote axon attraction to the central nervous system midline in the *Drosophila* embryo (Bashaw *et al.*, 2001).

1:12.2 Rho GAPs in *Drosophila*

Three Rho-family GAPs have also been characterised in *Drosophila*. DRacGAP negatively regulates both Rac1 and Cdc42 and has been shown to inhibit EGFR/Ras signalling in the imaginal wing disc (Sotillos and Campuzano, 2000). The function of another RacGAP, Rotund RacGAP, has been shown to be critical to both spermatid and retinal

differentiation (Bergeret *et al.*, 2001). Finally, p190 RhoGAP has been shown to regulate axon branch stability (Billuart *et al.*, 2001).

1:13 PBL is a Rho GEF required for cytokinesis in *Drosophila*

1:13.1 Embryonic development and the *pbl* mutant phenotype

The *pbl* gene was initially identified in a screen for zygotic embryonic lethal mutations affecting the pattern of the cuticle in the *Drosophila* larva (Jurgens *et al.*, 1984). Subsequent analysis of this gene revealed that homozygous *pbl* mutant embryos fail to undergo cytokinesis during cycle 14 (Hime and Saint, 1992; Lehner, 1992). During *Drosophila* development, the first 13 cell division cycles are rapid nuclear divisions that are near synchronous and occur in a common cytoplasm in the absence of cytokinesis. These nuclear cycles alternate between S phase and mitosis without any intervening gap phases. The first 8 of these nuclear divisions occur in the interior of the embryo before the majority of the nuclei migrate to the embryo cortex during cycles 8, 9 and 10. After 13 of these mitoses, which are known to rely on maternally provided products, a process called cellularisation occurs which involves the growth of membranes from the periphery of the embryo to encapsulate the nuclei, resulting in the formation of the cellular blastoderm. Subsequent division cycles include cytokinesis, and occur in a complex spatial pattern of mitotic domains, each domain comprised of cells that will ultimately differentiate into the same tissue type (Foe, 1989). The zygotic transcription of the mitotic activator *string* (*stg*) is known to regulate the timing and spatial occurrence of these mitoses (Edgar and O'Farrell, 1990). Once the process of cellularisation is complete, the embryo begins gastrulation.

The 14th division cycle is therefore the first *Drosophila* embryonic cycle to include cytokinesis. In homozygous *pbl* mutant embryos, the contractile ring fails in its attempt to divide the cytoplasm and its contents into two daughter cells. Despite the failure of cytokinesis, the nuclear events of mitosis continue, resulting in the formation of large, multinucleate cells after several rounds of failed cytoplasmic division (Hime and Saint, 1992; Lehner, 1992; Prokopenko *et al.*, 1999) (**Figure 1.4**). Interestingly, although the products of many genes are required for cytokinesis, *pbl* is the only gene that must be zygotically

expressed at cycle 14 for cytokinesis to proceed. All of the other products required for cytokinesis must be maternally deposited in sufficient quantities to drive cytokinesis in the earliest cellular divisions. Perhaps PBL needs to be absent during cellularisation and so is specifically degraded before being re-expressed in time for the cytokinesis of cycle 14. However, the pre-cellularisation role of PBL has not been determined due to an inability to generate germline mutant clones (O'Keefe and Saint, unpublished observations).

1:13.2 Characterisation of the *pbl* gene: *pbl* encodes a Rho GEF

The identification of P element mutations affecting PNS development in the *Drosophila* embryo enabled the cloning of the *pebble* gene (Salzberg *et al.*, 1997; Prokopenko *et al.*, 1999). Subsequent sequence analysis revealed that PBL contains Dbl Homology (DH) and Pleckstrin Homology (PH) domains which, as discussed previously, are characteristic of Rho GEFs (**Figure 1.5**). In accordance with this predicted role as an activator of Rho family G proteins, yeast 2-hybrid and genetic interactions confirmed that PBL specifically interacts with RhoA (Prokopenko *et al.*, 1999). Thus PBL appears to be a GEF specific for RhoA, which is known to be essential for the formation and function of the contractile ring during cytokinesis. Such a role would explain why *pbl* mutant embryos fail to undergo cytokinesis.

As discussed previously, given the wide diversity of functions for Rho, its individual roles are thought to be controlled by the specific spatial or temporal expression of its regulators. The Rho GEF activity of PBL could therefore be involved in the specific regulation of Rho activity during cytokinesis. Support for this comes from the localisation of PBL during the cell cycle. In late anaphase, PBL initially localises to the cell cortex at the time that the reorganisation of cortical actin begins (**Figure 1.6a**), before concentrating at the cleavage furrow (**Figure 1.6b**) (Prokopenko *et al.*, 1999). PBL is therefore thought to specifically activate Rho at the cleavage furrow, initiating the downstream signalling cascade required for the correct formation and constriction of the contractile ring. However, although the contractile ring was originally reported to fail to form in *pbl* mutant fixed tissue (Prokopenko *et al.*, 1999), subsequent real-time video microscopy revealed that the contractile ring partially forms, but collapses, resulting in the failure of cytokinesis (O'Keefe, pers comm). Thus the activation of Rho by PBL could be required at a later stage in cytokinesis than originally thought, and may be essential for the complete formation and continued stability of the contractile ring structure. However, it is also possible that there

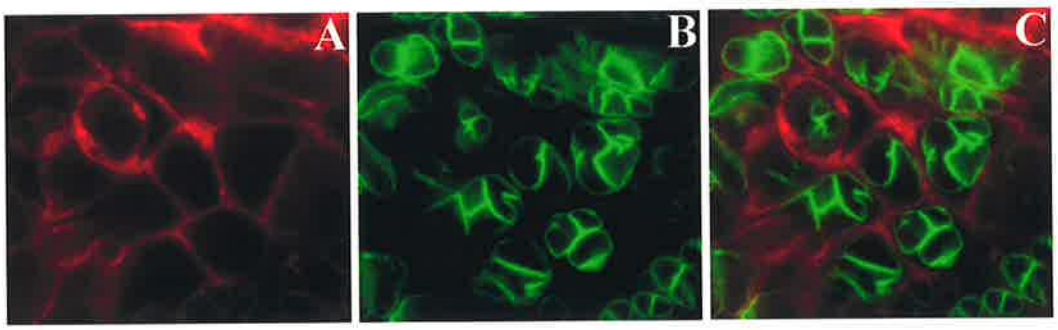

Figure 1.4 *pbl* mutant embryonic phenotype.

pbl mutant *Drosophila* embryos were fixed and stained with α- spectrin highlighting the cell membrane (shown in red), and α-lamin highlighting the nuclear envelope (shown in green). Images were taken at 100x magnification.

A. α- spectrin stain shows cells are large and irregular in *pbl* mutant embryos.

B. The same embryo stained with α-lamin. *pbl* mutant cells are multinucleate.

C. Merge of the two stains shown in A and B. In *pbl* mutant embryos, cytokinesis fails but nuclear division proceeds, resulting in the formation of multinucleate cells.

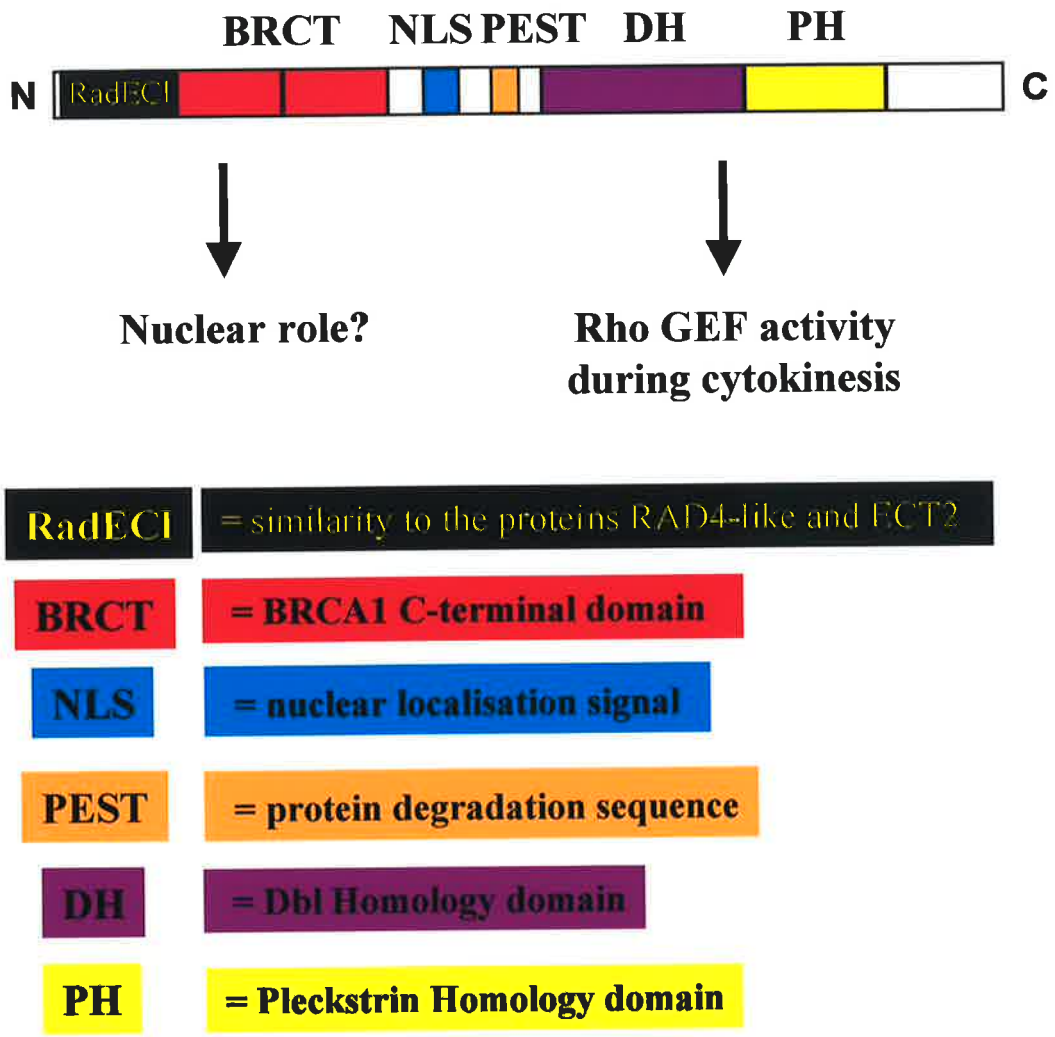

Figure 1.5 PBL encodes a Rho GEF with BRCT domains.

A schematic diagram of the structure of the PBL protein. The RadECl region is boxed in black and is so called because of the similarity between this region and regions of the proteins RAD4-like and ECT2 (RAD4-like ECT2 like region). The two consensus BRCA1 C-terminal domains (BRCT) are boxed in red, the consensus bipartite nuclear localisation signal (NLS) in blue, the PEST protein degradation sequence in orange, the Dbl homology domain (DH) in purple, and the Pleckstrin homology domain (PH) in yellow.

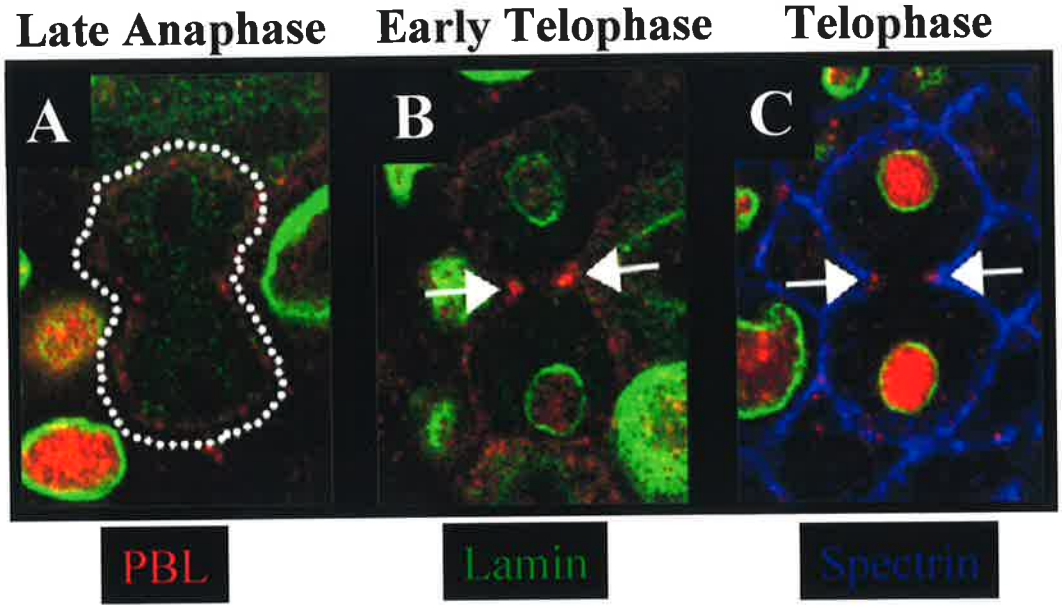

Figure 1.6 The mitotic localisation of PBL.

Wild type *Drosophila* embryos were fixed and stained with α-PBL (shown in red), α-lamin highlighting the nuclear envelope (shown in green) and α-spectrin highlighting the cell membrane (shown in blue). In A, where the PBL stain is weak, dashed white lines have been used to highlight the cortical stain. The arrows in B and C indicate the concentration of PBL at the cleavage furrow. Figure was adapted from (Prokopenko *et al.*, 1999).

A. During late anaphase, PBL is observed to localise to the cellular cortex.
B. In early telophase, PBL concentrates at the cleavage furrow, consistent with its activation of Rho and stimulation of cytokinesis.
C. By mid telophase and throughout interphase, PBL is observed to strongly relocalise to the nucleus.

may be some maternally deposited PBL present that is sufficient to initiate the formation of the contractile ring. Although this possibility remains to be resolved, it is clear that PBL functions as a Rho GEF that is essential for cytokinesis in *Drosophila*.

PBL also contains a predicted PEST sequence that could regulate its stability and thus the activity of Rho, at specific points in the cell cycle (**Figure 1.5**) (Rechsteiner and Rogers, 1996).

1:14 PBL is a Rho GEF that also contains nuclear BRCT domains

In addition to the DH and PH domains responsible for its Rho GEF activity, PBL is highly unusual in that it also contains a nuclear localisation signal, and two BRCA1 C-terminal (BRCT) domains (Prokopenko *et al.*, 1999) (**Figure 1.5**). The presence of a nuclear localisation signal within PBL could provide a means of regulating cytoplasmic Rho GEF activity. However, the presence of BRCT domains within a Rho GEF is unexpected and unique for Rho family GEFs. These domains were first identified in the breast cancer tumour suppressor protein BRCA1 (Koonin *et al.*, 1996), and have since been found in a multitude of other proteins, their unifying feature being an involvement in DNA damage sensing and repair (Bork *et al.*, 1997; Callebaut and Mornon, 1997). The presence of such domains in a Rho GEF poses an interesting and perplexing question for the function of PBL. While the DH and PH domains regulate Rho in the cytoplasm, BRCT domains have been implicated in the process of DNA repair, which is a nuclear event. In addition, all other known BRCT domains lie within nuclear proteins. So what are nuclear BRCT domains doing in a cytoplasmic Rho GEF protein? In addition to two BRCT domains, PBL also contains a third, as yet uncharacterised region, here named the RadECl region (**Figure 1.5**). This region lies immediately N-terminal to the first BRCT domain and contains several, but not all of the characteristic residues of a BRCT domain (**Figure 1.7a**). Sequence analysis showed that it shares a greater similarity with the proteins RAD4-like and ECT2 across this region (**Figure 1.7b**) and was thus named "RadECl" (for RAD4-like ECT2 like region). It seems to be conserved as a unit with an adjacent BRCT domain, and may have evolved from a BRCT

domain itself (R. Saint, pers comm). The possible role of this domain will be discussed in more detail in a following section.

Support for a nuclear role for PBL, other than the fact that it contains several known nuclear domains, comes from the subcellular localisation of PBL. As discussed previously, PBL localises initially to the cell cortex during late anaphase (**Figure 1.6a**) before concentrating at the cleavage furrow (**Figure 1.6b**), presumably to activate Rho and stimulate cytokinesis. By late telophase however, PBL is observed to strongly localise to the nucleus where it remains throughout interphase until the following prophase/metaphase when the nuclear envelope breaks down (**Figure 1.6c**).

Therefore there are three possible reasons why PBL localises to the nucleus. Firstly, nuclear localisation may simply be a sequestering mechanism to remove PBL Rho GEF activity from the cytoplasm once its role in cytokinesis has been completed. Secondly, PBL may perform a completely separate Rho-independent nuclear function. Thirdly, PBL may perform a novel Rho-mediated nuclear function. This thesis aims to examine these possibilities, and analyse the potential nuclear role that PBL may play.

1:15 *pbl* is orthologous to the proto-oncogene *ect2*

Initial database searches also revealed that *pbl* is orthologous to the mouse proto-oncogene *ect2*. Murine *ect2* was originally identified by the ability of an N-terminally truncated form of the encoded protein to transform NIH3T3 cells (Miki *et al.*, 1993). Like PBL, ECT2 contains two BRCT domains and a DH and PH domain indicative of Rho GEF activity. Interestingly, the truncated oncogenic form was missing the BRCT domains, suggesting that these domains are important for the regulation of ECT2 activity.

Human ECT2 was subsequently shown to act as a GEF for Rho, Rac and Cdc42 *in vitro*. A phosphorylated form of ECT2 was detected *in vivo* and shown to be required for its exchange activity *in vitro* (Tatsumoto *et al.*, 1999). Inhibition of human ECT2 by the expression of a dominant negative mutant, or by the injection of anti-ECT2 antibodies, was also found to block the completion of cytokinesis. Examination of the localisation of ECT2 throughout the cell cycle revealed that it is cytoplasmic in pro-metaphase, before concentrating at the midbody during cytokinesis. Like PBL, ECT2 then relocalises to the nucleus during interphase (Tatsumoto *et al.*, 1999). ECT2 was also shown to be critical for

the accumulation of GTP-bound RhoA during cytokinesis (Kimura *et al.*, 2000). Thus, like PBL, ECT2 Rho GEF function is also required during cytokinesis. Interestingly, the PBL/ ECT2 group of orthologues is the only Rho GEF sub-family to contain BRCT domains.

1:16 BRCT domains are involved in DNA damage sensing and repair

The BRCT domain was first defined within the human breast cancer tumour suppressor protein BRCA1 (Koonin *et al.*, 1996). Inherited mutations in BRCA1 predispose patients to breast and ovarian cancer. In particular, patients inheriting a mutation at the C-terminal end of BRCA1 were shown to develop very early-onset breast cancer (Friedman *et al.*, 1994). Subsequently, truncations of the BRCA1 C-terminal region were shown to prevent the ability of BRCA1 to inhibit breast cancer cell growth (Holt *et al.*, 1996). Sequence analysis of the C-terminal region of BRCA1 revealed a domain, which was named BRCT (BRCA1 C-terminus), which showed similarities to the yeast DNA repair protein RAD9 and a p53 binding protein 53BP1 (Koonin *et al.*, 1996). Subsequent hydrophobic cluster and sequence analysis revealed that this BRCT domain is found within numerous nuclear proteins, their unifying feature being their involvement in cell cycle checkpoint functions responsive to DNA damage. This BRCT domain superfamily includes over 40 nonorthologous proteins from a range of organisms, including PBL/ECT2, the human DNA repair protein XRCC1, the yeast replication checkpoint protein RAD4, and DNA-ligases III and IV (Bork *et al.*, 1997; Callebaut and Mornon, 1997). A summary of some of these proteins and their identified functions is shown in **table 1.1**.

Table 1.1 A summary of some of the characterised BRCT domain-containing proteins and their predicted functions.

A small selection of the over 40 identified proteins containing BRCT domains is shown, along with the species in which they were identified and a short summary of their identified functions. Their unifying feature is their involvement in DNA damage response and repair type processes. However, a specific role in DNA damage response or repair is yet to be demonstrated for PBL and its human and mouse homologue ECT2.

BRCT domain containing protein	Species	Identified function
BRCA1	human, mouse	Tumour suppressor- regulates multiple nuclear processes including DNA repair and transcription (Zhang *et al.*, 1998b; Scully and Livingston, 2000; Kerr and Ashworth, 2001) e.g. interacts with and is phosphorylated by protein kinases involved in damage checkpoint control, including ATM and ATR (Cortez *et al.*, 1999; Tibbetts *et al.*, 2000), activates Chk1 kinase that regulates DNA damage-induced G2/M arrest (Yarden *et al.*, 2002), binds to CtIP/CtBP to mediate transcriptional regulation of p21 in response to DNA damage (Li *et al.*, 1999).
53BP1	human	Binds to tumour suppressor p53 and enhances p53 mediated transcriptional activation (Iwabuchi *et al.*, 1998). Is hyperphosphorylated in response to DNA damage and localises to sites of DNA strand breaks (Rappold *et al.*, 2001).
RAD9	yeast (*S. cerevisiae*)	Checkpoint protein required for cell cycle arrest and transcriptional induction of DNA repair genes in response to DNA damage (Elledge, 1996).
RAD4/CUT5	yeast (*S. pombe*)	Required for DNA damage and replication checkpoints- prevents damaged or incompletely replicated chromosomes from being segregated (Saka and Yanagida, 1993; Saka *et al.*, 1994; McFarlane *et al.*, 1997; Verkade and O'Connell, 1998).
CRB2	yeast (*S. pombe*)	Damage and replication checkpoint protein- interacts with CUT5 and CHK1 kinase (Saka *et al.*, 1997).
DNA ligase III and IV	human	Involved in DNA repair- DNA ligase III interacts with DNA repair protein XRCC1 (Taylor *et al.*, 1998; Dulic *et al.*, 2001), DNA ligase IV interacts with DNA repair protein XRCC4 (Critchlow *et al.*, 1997),
ECT2	human, mouse	Oncogenic form lacks the BRCT domains- they are important for regulation of ECT2 activity (Miki *et al.*, 1993). A Rho GEF in cytokinesis (Tatsumoto *et al.*, 1999).
PBL	*Drosophila*	Functions as a Rho GEF in cytokinesis (Prokopenko *et al.*, 1999). Nuclear role?
Mus 101	*Drosophila*	Links DNA repair, replication and condensation of heterochromatin in mitosis (Yamamoto *et al.*, 2000).
TopBP1	human	Involved in DNA replication and DNA damage response - interacts with DNA pol ε and hRad9 (Makiniemi *et al.*, 2001).
DPB11	yeast (*S. cerevisiae*)	Required for DNA replication, replication checkpoint, and interacts with pol ε complex (Araki *et al.*, 1995).
XRCC1	human, mouse	Has 2 BRCT domains which interact independently with DNA ligase III and poly (ADP-ribose) polymerase to repair DNA (Cappelli *et al.*, 1997; Nash *et al.*, 1997; Masson *et al.*, 1998; Taylor *et al.*, 1998).

The BRCT domain itself is approximately 95 amino acids long and is made up of 5 conserved regions, or motifs, designated *A-E*. Motif *D* is the most highly conserved of these, and is organised around a conserved aromatic residue (tryptophan, phenylalanine or tyrosine). The residue following it is always hydrophobic, and the fourth and fifth residues preceding it are usually hydrophobic. Also, the fourth residue following it is usually a cysteine or a serine.

Motif *B* is the second most highly conserved region. It is made up of two consecutive glycines which are preceded in positions –4 and –8 by hydrophobic residues. Motif *C* contains a continuous stretch of three or four hydrophobic residues, or the sequence THΦΦ where Φ is a hydrophobic amino acid. BRCT domains can be found as tandem repeats at either end of the protein concerned, but are also found as a single copy. The number of residues between the motifs can also vary, and the domain appears to tolerate insertions of considerable length, particularly between motifs *A* and *B* and *B* and *C* (Bork *et al.*, 1997; Callebaut and Mornon, 1997).

X-ray crystallography has been used to determine the three-dimensional structure and fold of the BRCT domain within the human DNA repair protein XRCC1. The BRCT domain was found to consist of a four-stranded parallel β-sheet surrounded by three α-helices, which together form an autonomously folded domain (Zhang *et al.*, 1998c).

1:16.1 BRCA1, the founding member of the BRCT domain family

The founding member of the BRCT domain superfamily, BRCA1, has been implicated in an array of biological processes. BRCA1 contains a highly conserved ring finger motif (RING) at the N-terminus, and two BRCT domains at the extreme C-terminus. Most of the disease-associated mutations of *BRCA1* are frameshift or nonsense mutations that are predicted to cause large truncations of the protein. However, 5-10% of the cancer predisposing mutations cause single amino acid substitutions. Many of these substitutions are located within the RING or BRCT domains, highlighting the importance of these two domains to normal BRCA1 function in tumour suppression (Couch and Weber, 1996). In support of these findings in humans, mice carrying a *BRCA1* mutation that eliminates the C-terminal half of the protein survive, but exhibit a high level of tumours (Ludwig *et al.*, 2001). The results of numerous other studies have highlighted the importance of BRCA1 to tumour suppression. The fact that overexpression of BRCA1 leads to growth retardation of tumour cells in nude mice (Holt *et al.*, 1996), that transfection of wild type human *BRCA1* into breast

and ovarian cancer cells results in tumour suppression (Shao *et al.*, 1996) and that the inhibition of *BRCA1* expression confers tumourigenic properties to NIH3T3 cells (Rao *et al.*, 1996), all support the theory that BRCA1 acts as a tumour-suppressor protein. However the exact molecular mechanism of the BRCA1 tumour-suppressor is not yet known. Numerous studies have pointed to an extremely complex role for BRCA1 in aspects of DNA repair, the regulation of transcription and chromatin remodelling (Kerr and Ashworth, 2001).

1:16.2 A role for BRCA1 in the response to and repair of DNA damage

A role for BRCA1 in DNA repair processes is indicated by the fact that BRCA1 deficient cells contain spontaneous chromosomal abnormalities and are hypersensitive to ionising radiation due to defects in both double-strand break-induced homologous recombination, and transcription-coupled repair of oxidative DNA damage (Gowen *et al.*, 1998; Abbott *et al.*, 1999; Moynahan *et al.*, 1999; Scully *et al.*, 1999; Xu, *et al.*, 1999). BRCA1 has been shown to physically associate with numerous proteins involved in repair and recombination, including RAD51 (Scully *et al.*, 1997c), BACH1 (Cantor *et al.*, 2001) and the DNA repair complex RAD50/MRE11/NBS1 (Zhong *et al.*, 1999; Wang *et al.*, 2000). BRCA1 and RAD51 have been shown to colocalise to nuclear foci induced by ionising radiation, some of which are sites of DNA synthesis (Scully *et al.*, 1997b). RAD51 is also known to catalyse strand exchange during homology-directed repair of DNA double strand breaks (reviewed in Kerr and Ashworth, 2001). BACH1 is a DNA helicase that interacts with the BRCT domains of BRCA1 and is also thought to contribute to its DNA repair function (Cantor *et al.*, 2001). BRCA1 has also been shown to directly associate with the RAD50/MRE11/NBS1 complex which is responsible for end-processing of double-strand breaks during DNA repair (Tsubouchi and Ogawa, 1998; Zhong *et al.*, 1999).

BRCA1 has also been shown to associate with other large protein complexes known to be involved in DNA repair and chromatin remodelling. The BRCA1-associated genome surveillance complex, or BASC, contains at least 15 subunits including BRCA1, the ataxia telangiectasia mutated gene product (ATM), as well as 4 subcomplexes implicated in DNA repair; the RAD50/MRE11/NBS1 complex discussed previously, the MSH2/MSH6 heterodimer, the MLH1/PMS2 heterodimer and DNA replication factor C (Wang *et al.*, 2000). Many of the proteins that constitute BASC can bind to abnormal DNA structures such as double strand breaks. As such, it has been suggested that the complex may act as a DNA structure surveillance unit, consisting of both DNA damage sensor proteins and proteins such

as ATM, which is known to signal DNA damage (reviewed in Kerr and Ashworth, 2001). In support of this, BRCA1 itself is also known to be phosphorylated, in response to DNA damage, by ATM and other protein kinases that play important roles in DNA damage checkpoint control including ATR and CHK2 (Cortez *et al.*, 1999; Lee *et al.*, 2000a; Tibbetts *et al.*, 2000). As such, the phosphorylation of BRCA1 by these proteins is thought to be important for the function of BRCA1 in both double stranded break repair and cell cycle checkpoint control (Cortez *et al.*, 1999; Tibbetts *et al.*, 2000; Xu *et al.*, 2001). A direct role for BRCA1 in checkpoint control has also recently been identified. BRCA1 was shown to be essential for activating the CHK1 kinase that regulates DNA damage-induced G2/M arrest (Yarden *et al.*, 2002). Thus through its interaction with a multitude of different proteins, BRCA1 is directly involved in the response to and repair of DNA damage.

1:16.3 A role for BRCA1 in transcription regulation

BRCA1 has also been implicated in the regulation of transcription. The C-terminal region of BRCA1 containing the BRCT domains was initially found to act as a *trans*-activation domain when tethered to a transcriptional promoter via a heterologous DNA binding domain (Chapman and Verma, 1996; Monteiro *et al.*, 1996). The same region of BRCA1 was subsequently shown to remodel chromatin when tethered to chromosomal DNA (Hu *et al.*, 1999). Consistent with a role in the regulation of transcription, BRCA1 was found to associate with the RNA polymerase II holoenzyme via an interaction of its BRCT domains with RNA helicase A (Scully *et al.*, 1997a; Anderson *et al.*, 1998; Neish *et al.*, 1998).

In addition to this, BRCA1 has been shown to interact with and regulate the function of a number of different transcription factors. p53 is a tumour suppressor protein that is involved in a variety of different human cancers, and BRCA1 has been shown to enhance p53-dependent gene expression (Ouchi *et al.*, 1998; Zhang *et al.*, 1998a). BRCA1 also interacts with the signal transduction and activator of transcription protein STAT1. BRCA1 binds to the STAT1a transcriptional activation domain which leads to the induction of a family of interferon-gamma regulated genes. Interferons are important regulators of cell growth and apoptosis (Ouchi *et al.*, 2000), and thus the interaction of BRCA1 with STAT1 could be important in tumour suppression (reviewed in Kerr and Ashworth, 2001). BRCA1 has also been shown to transactivate the expression of p21 and inhibit cell cycle progression from G1 to S phase in human cells (Somasundaram *et al.*, 1997). p21 is a known target for p53 transcriptional activation, and more recently, the binding of the BRCT domains of

BRCA1 to another protein CtIP, has been shown to be critical in mediating the transcriptional regulation of p21 in response to DNA damage (Li *et al.*, 1999). Thus through seemingly complex interactions, BRCA1 is also capable of regulating the transcription and activity of a wide variety of important cellular regulators.

Given the fact that BRCA1 seems to have many varied functions, it was suggested that the protein may employ a common mechanism in these different functions, such as chromatin remodelling. BRCA1 was shown to induce large-scale chromatin decondensation, an activity that was conferred independently by three subdomains within BRCA1, the activation domain and the two BRCT domains. A novel cofactor of BRCA1 was identified (COBRA1), and was found to be recruited to the chromosome by the first BRCT domain, and was itself sufficient to induce chromatin unfolding (Ye *et al.*, 2001).

It remains to be seen whether chromatin remodelling is widely used by BRCA1 to control the multitude of genes it regulates, however it has been shown that chromatin remodelling is not a common feature of all BRCT domain-containing proteins. (Miyake *et al.*, 2000).

1:16.4 BRCT domain-containing proteins and their roles in DNA damage signalling

1:16.4.1 53BP1

p53 binding protein 1 (53BP1) is another BRCT domain-containing protein which has been implicated in the response to DNA damage. 53BP1 is a transcriptional coactivator of the tumour suppressor p53, binding to the DNA binding domain of p53 and enhancing p53-mediated transcriptional activation (Iwabuchi *et al.*, 1994; Iwabuchi *et al.*, 1998). Similar to BRCA1, human 53BP1 and its *Xenopus* homologue are hyperphosphorylated in response to ionising radiation and localise to the sites of DNA strand breaks, forming distinct nuclear foci (Schultz *et al.*, 2000; Anderson *et al.*, 2001; Rappold *et al.*, 2001; Xia *et al.*, 2001). Several observations also suggest that, like BRCA1, ATM is responsible for this phosphorylation. In the case of human 53BP1, ATM deficient cells show no 53BP1 hyperphosphorylation and reduced 53BP1 focus formation in response to irradiation. Treatment of cells with wortmannin, a potent inhibitor of ATM, was also found to strongly inhibit both the radiation induced hyperphosphorylation and focus formation of 53BP1. Thirdly, ATM was demonstrated to phosphorylate 53BP1 *in vitro* (Rappold *et al.*, 2001). In the case of the *Xenopus* 53BP1 (XL53BP1), inhibition of ATM was also found to reduce focus formation and the phosphorylation of XL53BP1 in response to irradiation (Anderson *et al.*, 2001).

XL53BP1 and human 53BP1 were also shown to act both *in vitro* and *in vivo*, as substrates for the ATM kinase (Xia *et al.*, 2001). Thus collectively these results indicate that the BRCT domain containing 53BP1 protein plays an important role in the response to DNA damage, probably in collaboration with ATM, and also possibly involving the signalling of damage to p53.

1:16.4.2 RAD9

The yeast checkpoint protein RAD9 is another BRCT domain-containing protein with well defined roles in the response to DNA damage. The results of numerous studies have indicated that RAD9 is required for both cell cycle arrest and the transcriptional induction of DNA repair genes in response to DNA damage (reviewed in Elledge, 1996). However, a more recent study has indicated that it is the BRCT domain that is important for this function. Yeast strains expressing mutant RAD9 lacking the BRCT domain or carrying mutations in its highly conserved residues, were found to be equivalent to *rad9* null cells in terms of rates of survival and checkpoint induced delay after irradiation. RAD9 hyperphosphorylation in response to DNA damage, and the RAD9-dependent phosphorylation of RAD53 were also both absent in the BRCT domain mutants, proving that the BRCT domain is essential for the function of RAD9. Yeast 2 hybrid analysis also indicated that the BRCT domain of RAD9 is required for the interaction of RAD9 with itself. This interaction was found to be eliminated by the same BRCT domain mutations that caused the null phenotypes described above, suggesting that RAD9 oligomerization is important for its function in the response to DNA damage (Soulier and Lowndes, 1999).

1:16.4.3 XRCC1 and PARP

The human DNA repair protein XRCC1 provides yet another striking example of BRCT domains acting as protein-protein interaction modules to signal the response to DNA damage. Poly(ADP-ribose) polymerase, or PARP, is a BRCT domain-containing DNA binding protein that detects and signals DNA strand breaks. At the site of breakage, PARP catalyses the poly(ADP-ribosylation) of nuclear proteins involved in chromatin structure and DNA metabolism, which converts the damage into an intracellular signalling cascade that can activate DNA repair (Althaus and Richter, 1987; De Murcia and Menissier-De Murcia, 1994; Oei *et al.*, 1997). The DNA repair protein XRCC1, which itself contains 2 BRCT domains, was found to interact with PARP, and this interaction occurs via BRCT domain 1 of XRCC1

and the BRCT domain and N-terminal zinc finger domain of PARP (Masson *et al.*, 1998). In addition to its interaction with PARP, XRCC1 has also been shown to interact with DNA ligase III through its second BRCT domain (Caldecott *et al.*, 1994; Caldecott *et al.*, 1995; Nash *et al.*, 1997; Taylor *et al.*, 1998). The C-terminal BRCT domain of DNA ligase III was responsible for this interaction (Nash *et al.*, 1997). Thus XRCC1 interacts with PARP via a BRCT-BRCT domain-mediated interaction, as well as DNA ligase III through a second BRCT-BRCT domain-mediated interaction. XRCC1 also interacts via a third separate domain with DNA polymerase β (Kubota *et al.*, 1996; Marintchev *et al.*, 2000). While XRCC1 itself has no known enzymatic activity (Thompson *et al.*, 1990), it is thought to function as a scaffold protein in the base excision repair pathway, bringing together DNA polymerase β, DNA ligase III, and PARP to form a DNA repair complex (Caldecott *et al.*, 1996; Kubota *et al.*, 1996; Cappelli *et al.*, 1997; Masson *et al.*, 1998).

1:16.4.4 TopBP1

Topoisomerase IIβ-binding protein (TopBP1), a human protein with 8 BRCT domains, has also been implicated in the response to DNA damage. TopBP1 interacts with DNA polymerase ε and is required for DNA replication. Inhibition of DNA synthesis has been shown to cause the relocalisation of TopBP1 together with BRCA1 to replication forks, suggesting that both of these may be involved in the rescue of stalled forks. In addition to this, DNA damage causes the formation of distinct TopBP1 nuclear foci that have been shown to colocalise with BRCA1 in S phase, suggestive of a role in the DNA damage response pathway. In support of this, TopBP1 was also shown to interact with human RAD9, a known DNA damage checkpoint protein. The interaction of TopBP1 with RAD9 was shown to occur via 2 of its BRCT domains, providing yet another example of a BRCT domain mediating a potentially important interaction in the DNA damage response pathway (Makiniemi *et al.*, 2001). A clue to this potential role could lie in the fact that the BRCT domains of TopBP1 and BRCA1 have also been shown to bind DNA strand breaks and termini of DNA (Yamane and Tsuruo, 1999). Thus the fact that TopBP1 can interact with hRAD9 and DNA polymerase ε and is also able to bind DNA strand breaks, suggests that it may act as a DNA damage sensor (Makiniemi *et al.*, 2001).

The BRCT domains of TopBP1 have recently been implicated in the regulation of TopBP1 levels in response to DNA damage. A yeast 2 hybrid screen showed that TopBP1 interacts with hHYD, a HECT domain ubiquitin ligase known to be involved in protein

ubiquitination and subsequent degradation. This interaction, which is mediated by the 5th and 6th BRCT domains of TopBP1, leads to the ubiquitination and degradation of TopBP1. However, x-irradiation was observed to diminish the ubiquitination of TopBP1, resulting in the localisation of stabilised TopBP1 to nuclear foci corresponding to DNA breaks (Honda *et al.*, 2002). Thus BRCT domains seem to be important for mediating complex and varied protein-protein interactions responsible for the recognition of and response to DNA damage.

1:16.4.5 Mus 101

Mus 101, the apparent *Drosophila* homologue of TopBP1, was first identified more than 25 years ago due to the larval hypersensitivity of mutants in this gene to DNA damaging agents (Boyd *et al.*, 1976; Makiniemi *et al.*, 2001). Mus101 contains 7 BRCT domains and has been shown to be involved in DNA synthesis (Boyd and Setlow, 1976; Calvi and Spradling, 1999), DNA repair (Boyd and Setlow, 1976; Brown and Boyd, 1981) and chromosome condensation at mitosis (Gatti *et al.*, 1983; Smith *et al.*, 1985; Yamamoto *et al.*, 2000). The nature of the roles of the BRCT domains has yet to be defined for this protein. However, the relatively recent cloning of the *mus101* gene (Yamamoto *et al.*, 2000) will enable the precise function of each of its 7 BRCT domains to be determined.

In conclusion, the BRCT domain is present in a wide range of proteins from a variety of organisms, its unifying feature being its involvement in the detection and repair of DNA damage. The founding member of this superfamily, BRCA1, interacts with numerous DNA repair proteins, is phosphorylated by checkpoint kinases, and has itself been shown to activate an essential DNA damage checkpoint kinase. It plays a role in the regulation of transcription of many important cellular regulators, and has the ability to remodel chromatin. The BRCT domain-containing RAD9 is required for cell cycle arrest and the transcriptional induction of DNA repair genes in response to DNA damage, while the BRCT protein 53BP1 is phosphorylated in response to DNA damage and localises to DNA strand breaks. XRCC1 interacts with both PARP and DNA ligase III through its two BRCT domains, and TopBP1 uses its BRCT domains to interact with hRAD9. The ability of TopBP1 to also bind DNA strand breaks through its BRCT domains and interact with DNA polymerase ε suggests that it may play a role in the sensing of DNA damage. Thus the roles of BRCT domains in the DNA damage response pathway are well established.

1:17 The RadECl region: a novel nuclear domain?

As discussed previously, PBL also contains a third, as yet uncharacterised region immediately N-terminal to the first BRCT domain (**Figure 1.5**). This region contains several, but not all of the characteristic residues of a BRCT domain (**Figure 1.7a**). However, sequence analysis revealed that it shares greater similarity with the proteins RAD4-like and ECT2, and hence was named the "RadECl" region in this study (**Figure 1.7b**). As can be seen from the sequence analysis shown in Figure 1.7b, it seems to be conserved as a unit with an adjacent BRCT domain and, as it contains several of the characteristic residues of a BRCT domain, it may have evolved from a BRCT domain itself. It is therefore likely that the RadECl region may function in tandem with the BRCT domain with which it is associated. Although its precise function, if any, remains unknown, the identified role for RAD4-like suggests a potentially nuclear role for this region. Human RAD4-like, is also known as Topoisomerase IIβ–Binding Protein (TopBP1) (Nagase *et al.*, 1996; Yamane *et al.*, 1997). As discussed in the previous section, TopBP1 is a protein with 8 BRCT domains which has been implicated in the response to DNA damage. It has been shown to interact with both hRAD9 and DNA polymerase ε and is also able to bind DNA strand breaks, suggesting that it might act as a DNA damage sensor (Yamane and Tsuruo, 1999; Makiniemi *et al.*, 2001). The *Drosophila* homologue of this gene, *mus 101*, contains 7 BRCT domains and has been shown to be involved in DNA synthesis (Boyd and Setlow, 1976; Calvi and Spradling, 1999), DNA repair (Boyd and Setlow, 1976; Brown and Boyd, 1981) and chromosome condensation at mitosis (Gatti *et al.*, 1983; Smith *et al.*, 1985; Yamamoto *et al.*, 2000). Given the well defined nuclear roles for both RAD4-like and Mus 101, and the nuclear localisation of PBL and ECT2, the RadECl region may be important for some as yet undefined nuclear role of PBL.

Figure 1.7 RadECl and BRCT domain sequence alignment of PBL.

A. The N-terminal sequence of PBL including part of the RadECl region (top) is aligned with the two identified BRCT domains of PBL (below- BRCT domain 1 is on top of BRCT domain 2). The 5 motifs that define the BRCT domain (A-E) are boxed. This N-terminal RadECl region of PBL contains some, but not all of, the characteristic conserved residues of a BRCT domain. These conserved residues are coloured as follows; motif A conserved residues are in red, motif B residues are in green, motif C residues are in blue, motif D residues are in purple, and motif E residues are in pink (Callebaut and Mornon, 1997).

B. The N-terminal protein sequences of *Drosophila melanogaster* PBL (accession # NP_523965), *Mus musculus* ECT2 (accession # AAH 25565), *Homo sapiens* ECT2 (accession # Q9H 8V3), *Drosophila melanogaster* Mus 101 (accession # NP_524909), and *Homo sapiens* RAD4-like (accession # BAA 13389) were obtained using an NCBI blast search, and aligned using the CLUSTAL W program (Thompson *et al.*, 1994). The GeneDoc program was used to present the alignment (Nicholas *et al.*, 1997). The residues boxed in red represent 100% conservation between the 5 sequences, the residues in green represent 80% conservation, and the residues in blue represent 60% conservation. The "RadECl" region (RAD4-like, ECT2 like region) is a region of extended homology immediately N-terminal to the first BRCT domain of each of these proteins. This "RadECl" region is highlighted by the black bar above the sequence alignment. The BRCT domain sequence is underlined and is highlighted by the yellow bar above the alignment. Human RAD4-like is also known as TopBP1, and Mus 101 is the *Drosophila* homologue of this gene (Nagase *et al.*, 1996; Yamane *et al.*, 1997; Yamamoto *et al.*, 2000).

A

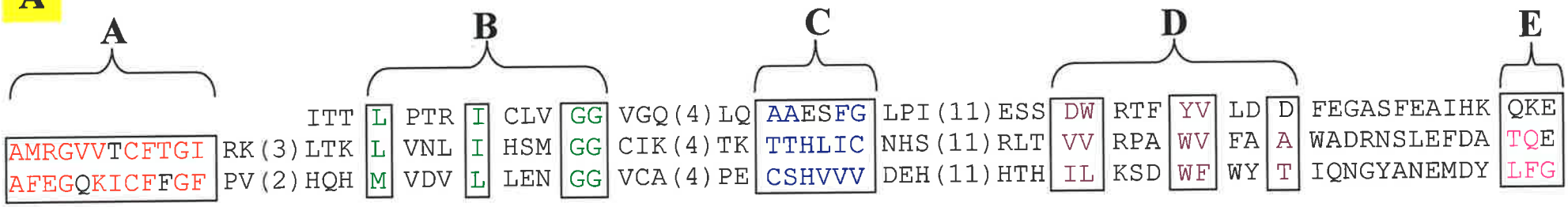
A
B
C
D
E
AMRGVVTCFTGI RK(3)LTK PV(2)HQH
ITT L PTR I CLV GG VGQ(4)LQ
L VNL I HSM GG CIK(4)TK
M VDV L LEN GG VCA(4)PE
AAESFG LPI(11)ESS
TTHLIC NHS(11)RLT
CSHVVV DEH(11)HTH
DW RTF YV LD D FEGASFEAIHK QKE
VV RPA WV FA A WADRNSLEFDA TQE
IL KSD WF WY T IQNGYANEMDY LFG

B

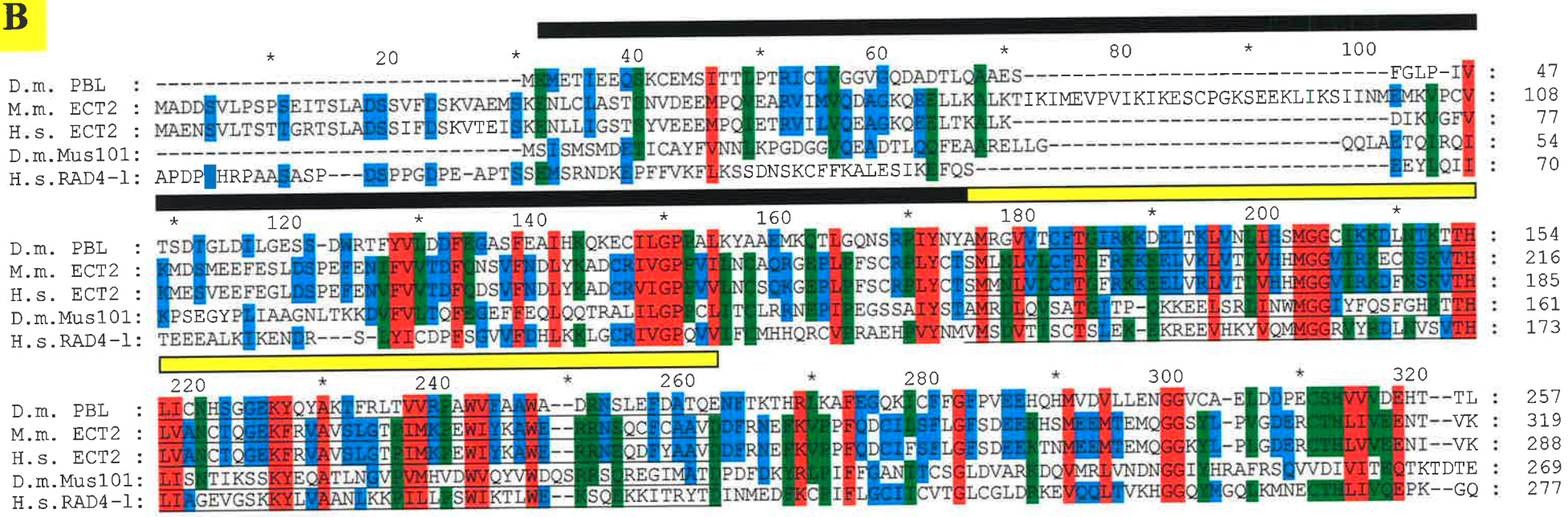
D.m. PBL
M.m. ECT2
H.s. ECT2
D.m.Mus101:
H.s.RAD4-1:

1:18 The mystery of PBL nuclear localisation

As discussed previously, the presence of the RadECl/BRCT domains in PBL poses an interesting yet perplexing question for the function of PBL. While the DH and PH domains have been shown to regulate Rho in the cytoplasm (Prokopenko *et al.*, 1999), BRCT domains have been implicated in the process of DNA damage sensing and repair, which is a nuclear event (Bork *et al.*, 1997; Callebaut and Mornon, 1997). In addition, all other known BRCT domains are within nuclear proteins. What are nuclear BRCT domains doing in a cytoplasmic Rho GEF protein and why does PBL localise to the nucleus?

1:18.1 Cdc24p is a GEF which is regulated by nuclear sequestration

Cdc24p is a GEF for Cdc42p in yeast that shows a very similar pattern of localisation to PBL. Cdc24p localises to the plasma membrane at sites of polarised growth, to mother bud necks during cytokinesis, and to the nucleus during G1 (Toenjes *et al.*, 1999). Cdc24p is actively sequestered in the nucleus through its binding to the cyclin dependent kinase inhibitor Far1p. Nuclear export is triggered either by entry into mitosis, which causes the degradation of Far1p, or by exposure to mating pheromone, which stimulates the export of the whole Far1p/Cdc24p complex (Nern and Arkowitz, 2000; O'Shea and Herskowitz, 2000; Shimada *et al.*, 2000). Thus in the case of Cdc24p, nuclear-cytoplasmic localisation appears to be important in the regulation of its function.

1:18.2 Net1 is a Rho GEF that is regulated by nuclear sequestration

Net1 is a mammalian Rho GEF which also appears to be regulated by nuclear sequestration. Like ECT2, the murine homologue of PBL (Miki *et al.*, 1993), oncogenic activation of Net1 occurs by truncation of the N-terminal part of the protein. Unlike ECT2 however, Net1 does not have BRCT domains at its N-terminal end. The nuclear import of Net1 is mediated by two nuclear localisation signals in its N-terminus, and thus the oncogenic form lacking these domains localises to the cytoplasm where it can activate Rho. Interestingly, in addition to its GEF-associated function, the pleckstrin homology domain of Net1 acts as a nuclear export signal, suggesting that this domain could also play such a role in PBL. However, the exit of PBL and of ECT2 from the nucleus corresponds with the

breakdown of the nuclear envelope in prophase/metaphase (Prokopenko *et al.*, 1999; Tatsumoto *et al.*, 1999; Kimura *et al.*, 2000), suggesting that this is unlikely to be an active process. Net1 has also been shown to shuttle into and out of the nucleus, and thus it has been suggested that activation of Rho by Net1 is controlled by changes in its subcellular localisation (Schmidt and Hall, 2002).

1:19 Thesis aims

Could the Rho GEF activity of PBL also be regulated by nuclear sequestration like both yeast Cdc24p and mammalian Net1? Does PBL move into the nucleus to remove Rho GEF function from the cytoplasm at the appropriate time, or does PBL have a separate nuclear role? Unlike Net1 and Cdc24p, PBL also contains BRCT domains, domains that have been proven to play important nuclear roles. Thus it is possible that PBL moves into the nucleus to carry out a separate nuclear function. Perhaps PBL localises to the nucleus for both reasons, to remove Rho GEF function from the cytoplasm, and to perform a separate nuclear role. Perhaps these two processes are intricately linked, and PBL performs some Rho dependent nuclear role, which would be completely novel. Perhaps PBL is capable, through its BRCT domains, of sensing and responding to DNA damage. It is possible that such an interaction with damage sensor or repair proteins prevents PBL from activating cytokinesis, providing an extra level of control where cell division is put on hold while DNA damage is repaired. Such an ability would not only contribute to the maintenance of genomic integrity, but would constitute an elegant mechanism of cell cycle control.

This thesis therefore aims to examine these possibilities and answer some of the questions that remain concerning the function of the PBL protein. Through the use of a variety of techniques including *in vitro* mutagenesis, transgenic analysis, genetic screening, and larval hypersensitivity assays, the nuclear role of PBL is examined, and the functions of its RadECl/BRCT domains are explored.

Chapter 2: Materials and Methods

2:1 Abbreviations

A_{600}: absorbance at 600nm

APS: ammonium persulfate

blotto: skim milk powder

bp: base pairs

BSA: bovine serum albumin

DNA: deoxyribonucleic acid

dNTP: deoxyribonucleoside triphosphate

EDTA: ethylene diamine tetraacetic acid

kb: kilobase pairs

kD: kilodalton

l: litre

PAGE: polyacrylamide gel electrophoresis

PBS: Phosphate buffered saline

PBT: Phosphate buffered saline + 0.1% Tween 20

RNA: ribonucleic acid

RNase A: ribonuclease A

r.p.m: revolutions per minute

SDS: sodium dodecyl sulphate

TEMED: N,N,N',N-tetramethylenediamine

UV: ultraviolet light

v: volts

2:2 Materials

2:2.1 Chemical reagents

All reagents were of analytical grade or the highest grade obtainable.

2:2.2 Enzymes

Restriction endonucleases were obtained from a variety of sources including Boehringer Mannheim, New England Biolabs (NEB), and Pharmacia.

Other enzymes were obtained from the following sources:

T4 DNA ligase: Boehringer Mannheim, NEB.

Calf Intestinal Phosphatase (CIP): Boehringer Mannheim.

RNase A and Lysozyme: Sigma.

Pfu Turbo DNA polymerase: Stratagene.

2:2.3 Kits

QIAquick gel extraction kit: Qiagen.

QIAprep spin miniprep kit: Qiagen.

Enhanced Chemiluminescence (ECL) kit: Amersham.

BRESAspin plasmid mini kit: Geneworks.

Western blot recycling kit: Alpha Diagnostics.

2:2.4 Antibiotics

Ampicillin: Sigma.

2:2.5 Molecular weight markers

DNA

λDNA was digested with *BstEII* and *SalI* to produce fragments of the following sizes (in kb) 14.14, 8.45, 7.24, 5.70, 4.82, 4.32, 3.68, 3.13, 2.74, 2.32, 1.93, 1.37, 1.26, 0.70, 0.50, 0.22 and 0.12.

Protein

Prestained molecular weight markers (NEB) sizes (in kD) 175, 83, 62, 47.5, 32.5, 25, 16.5 and 6.5.

2:2.6 Oligonucleotides

Oligonucleotides designed for *in vitro* mutagenesis were obtained from Geneworks. The primers for mutating the NLS and deleting the RadECl/BRCT domains were purchased as a 40nmole crude fraction and purified by SDS polyacrylamide gel electrophoresis. The primers for the addition of a FLAG tag were purified by high performance liquid chromatography.

Primers for mutating the consensus bipartite nuclear localisation signal

NLS1: 5' gcg ttg cga aaa acg gtt gtt gtt cct ttt gtt aaa gct aat ggg 3'

NLS2: 5' ccc att agc ttt aac aaa agg aac aac aac cgt ttt tcg caa cgc 3'

Primers for deleting the RadECl region and BRCT domains

ΔBRCTs1: 5' cgt aat gct atc caa ata gtc aat ggt ctc cat ttc c 3'

ΔBRCTs 2: 5' g gaa atg gag acc att gac tat ttg gat agc att acg 3'

Primers for FLAG tagging PBL constructs

FLAG 1: 5' ggt ctc cat ttc ctt gtc atc gtc gtc ctt gta gtc cat gga tct tct gc 3'

FLAG 2: 5' gc aga aga tcc atg gac tac aag gac gac gat gac aag gaa atg gag acc 3'

2:2.7 Antibodies

All secondary and tertiary antibodies were reconstituted according to the manufacturer's instructions.

Primary antibodies:

Alpha-tubulin: mouse monoclonal (Sigma), used at 1:1,000 on embryos and 1:10,000 on western blots.

Armadillo (N27A1): mouse monoclonal (Developmental Studies Hybridoma Bank), used at 1:1 on tissues.

FLAG: mouse M2 monoclonal (Amrad), used at 1:300 on cells.

PBL: rat polyclonal, crude sera (S. Prokopenko), used at 1:500 on tissues.

PBL: rat polyclonal, IgG purified sera, used at 1:200 on tissues and 1:2,000 on western blots.

Phalloidin-FITC (Sigma): used at 1:200 on tissues.

Spectrin (3A9): rabbit polyclonal (D. Branton), used at 1:50 on tissues.

Lamin: mouse monoclonal (Y. Gruenbaum), used at 1:10 on tissues.

Myc (9E10): mouse monoclonal (Developmental Studies Hybridoma Bank, purified by the Institute of Medical and Veterinary Science (IMVS), Adelaide, SA.), used at 1:250 on tissues.

Phosphorylated histone H3: rabbit polyclonal (Upstate Biotechnology), used at 1:300 on tissues, and 1:3,000 on western blots.

Phosphorylated H2AX (γ-H2AX): rabbit polyclonal (Upstate Biotechnology), used at 1:1,000 on western blots.

ELAV (7E8A10): rat polyclonal (Developmental Studies Hybridoma Bank), used at 1:500 on tissues.

Secondary antibodies:

α-mouse-biotin (Jackson Laboratories): used at 1:200 on tissues.

α-rat-biotin (Jackson Laboratories): used at 1:200 on tissues.

α-rabbit-biotin (Jackson Laboratories): used at 1:200 on tissues.

α-rabbit-Cy5, (Jackson Laboratories): used at 1:200 on tissues.

α-mouse-HRP (Jackson Laboratories): used at 1:3,000 on western blots.

α-rat-HRP (Jackson Laboratories): used at 1:3,000 on western blots.

α- rabbit-HRP (Jackson Laboratories): used at 1:3,000 on western blots.

α-mouse-Alexa 594 (Molecular Probes): used at a final concentration of 5-20μg/ml on cells.

Tertiary complexes:

Strepavidin-Alexa 488 (Molecular Probes): used at 1:200 on tissues.

Strepavidin-Cy5 (Jackson Laboratories): used at 1:200 on tissues.

2:2.8 DNA stains

10mg/ml Hoechst 33258 (Sigma) was used at 1:1,000 on tissues for 5 mins.

1mg/ml propidium iodide (Sigma) stain was performed on RNase treated tissues at 1:100 for 2 hours.

2:2.9 Media, Buffers and Solutions

2:2.9.1 *Drosophila* media

Fortified (F1) *Drosophila* medium: 1% (w/v) agar, 18.75% compressed yeast, 10% treacle, 10% polenta, 1.5% acid mix (47% propionic acid, 4.7% orthophosphoric acid), 2.5% tegosept (10% para-hydroxybenzoate in ethanol).

Grape juice agar plates: 0.3% agar, 25% grape juice, 0.3% sucrose, 0.03% tegosept mix.

2:2.9.2 Bacterial media

All media were prepared with distilled and deionised water and sterilised by autoclaving, except heat labile reagents, which were filter sterilised. Antibiotics were added from sterile stock solutions to the media after it had been autoclaved.

L-Broth: 1% (w/v) amine A, 0.5% yeast extract, 1% NaCl, pH 7.0.

Plates: L-Broth with 1.5% (w/v) bactoagar supplemented with ampicillin (50mg/ml) where appropriate.

2:2.9.3 Buffers and solutions

Agarose gel loading buffer:	50% (w/v) glycerol, 50 mM EDTA, 0.1% (w/v) bromophenol blue.
Blotto solution:	5% (w/v) skim milk powder in 1x PBT.
1.5x Brower's solution:	0.15M PIPES, 3mM $MgSO_4$, 1.5mM EGTA, 1.5% NP-40 pH6.9.
Embryo injecting buffer (1x):	5mM KCl, 0.1mM $NaPO_4$ pH 6.8.
10X HEN buffer:	1M HEPES, O.5M EGTA, 0.1% NP-40, pH to 6.9 and filter sterilised.
Homogenisation buffer:	1M Tris pH 7.5, 1M $MgCl_2$.
PBS:	7.5mM Na_2HPO_4, 2.5 mM NaH_2PO_4, 145mM NaCl.
1 X PBT:	1 x PBS, 0.1% Tween 20 or Triton X-100.
Protein gel transfer buffer:	48mM Tris-base, 39mM Glycine, 0.037% (w/v) SDS, 20% methanol.
3 X sample buffer:	10% glycerol, 2% SDS, 5% β-mercaptoethanol, 0.05% bromophenol blue, 12.5% 0.5M Tris-HCl pH6.8.
Protein gel running buffer:	1.5% Tris-base, 7.2% Glycine, 0.5% SDS.

STET:	50mM Tris-HCl pH8.0, 50mM EDTA, 8%w/v sucrose and 0.05% Triton X-100.
TAE:	40mM Tris-acetate, 20mM sodium acetate, 1mM EDTA, pH 8.2.

2:2.10 Plasmids

pBluescript KS+ (Statagene).

pUAST - UAS promoter (obtained from H. Richardson).

pACT- chicken β-actin promoter (obtained from L. MacMillan).

PCS2- MYC tag vector (obtained from S. Prokopenko).

2:2.11 Bacterial strains

E. coli DH5α: F' f80 lacZΔM15 recA1 endA1 gyrA96 thi-1 hsdR17 (rK- mK+) supE44 relA1 deoR Δ(lacZYA-argF) U169.

2:2.12 *Drosophila* strains

2:2.12.1 Wild-type

w^{1118} was used as the wild-type strain in immunohistological stains and for the generation of transgenic lines.

2:2.12.2 *pbl* mutants

pbl^{2} and pbl^{3} alleles (originally referred to as pbl^{5D} and pbl^{7O} respectively in Jurgens *et al.*, 1984) correspond to nonsense mutations that result in truncated protein products of 37 and 185 amino acids respectively (Prokopenko *et al.*, 1999).

pbl^{p3} is an EMS induced allele with a point mutation in the PH domain obtained from J. Skeath.

2:2.12.3 GAL4/UAS stocks

GMR-GAL4, *prd-GAL4* and *UAS-GFP* were obtained from the Bloomington Stock centre.

elav -GAL4 and GUT/SAV 109.88-*GAL4* were obtained from H. Richardson.

71B-GAL4 was obtained from M. Fictz.

2:2.12.4 Cell cycle and apoptosis stocks

RBF^{14} null allele, *GMR-p35* and *Df(3)H99* were obtained from H. Richardson.

2:2.12.5 Rho family members

RhoA^{72R} and *RhoA*^{72O} null alleles were obtained from M. Mlodzik. *Cdc42*^{3} lethal allele was obtained from R. Fehon. The deficiency stock *Df(3L)Ar14-8* was used as an allele of *Rac1*. The deficiency stock *Df(3L)RM5-2* was used as an allele of *Rac2*. Since this stock also removes *pbl*, a recombinant chromosome was generated with the *cos34* transposon, one copy of which is sufficient to rescue *pbl* mutant embryos to adulthood (J. Wong and R. Saint, unpublished observations). *ΔMtl* is a deletion generated by imprecise excision of a P-element that removes the entire *Mtl* open reading frame and was obtained from B. Dickson (Hakeda-Suzuki *et al.*, 2002).

2:2.12.6 Downstream Rho effectors and genes required for cytokinesis

dia^{2} was provided by S. Wasserman. *chic*^{221} was provided by L. Jones, and *acu*^{E636} was provided by J. Treismann.

2:2.12.7 Checkpoint genes

grp^{1} maternal-effect lethal mutation was obtained from W. Sullivan (Fogarty *et al.*, 1994).

2:2.13 X-irradiation source

A Biointernational ^{137}Cs x-ray machine (activity 3400 Ci) was used to irradiate all samples.

2:3 Methods

Standard molecular genetic techniques were performed as described in (Sambrook *et al.*, 1989) or (Ausubel *et al.*, 1994).

2:3.1 Restriction endonuclease digestion of DNA

All restriction digestions were performed using the buffers recommended by the manufacturer at 1x concentration. For complete digestion, 3-5 units of enzyme were added per µg of DNA and incubated at 37°C for 2 hours.

To end fill restriction digestions samples were firstly phenol/chloroform extracted and ethanol precipitated. The resultant pellets were then resuspended in 34 µl of Milli Q water (MQ H_2O) before the addition of 5 µl of 2.5mM dNTPs, 10 µl of 5x T4 buffer, and 1 µl of

T4 DNA polymerase to make the volume up to 50 µl. The tubes were then incubated at 37°C for 30 mins.

2:3.2 Agarose gel electrophoresis

Molten 1% agarose in TAE was poured onto a glass slide using a plastic comb to form the well slots. The gel was then placed in an electrophoresis tank and submerged in TAE. The DNA samples containing a suitable amount of loading buffer were then loaded into the gel slots and 40-80V were applied to the tank until the bromophenol blue dye had migrated the required distance. The DNA was then stained with ethidium bromide in order to be visualised by illumination with long wave UV light.

2:3.3 Phenol/chloroform extraction of DNA

Sterile water was firstly added to the sample to make the volume up to 200µl. 200µl of phenol/ chloroform/ isoamylalcohol was added and the tube was vortexed briefly and spun down for 5 minutes at 14000 rpm in a microcentrifuge. The top layer was then removed to a clean tube and the process of making the volume up to 200µl with water, adding phenol/ chloroform/ isoamylalcohol, vortexing and spinning down was repeated. The sample was then ethanol precipitated as described below.

2:3.4 Ethanol precipitation of DNA

2µl of glycogen, 1/10th the volume of 3M NaAc (pH4.6) and 21/2 volumes of chilled absolute ethanol were added and the tube was incubated at -20°C for at least 30 mins. The tube was then spun down in a microcentrifuge at 14000 rpm for 10 mins and the resultant pellet was washed in 70% ethanol before being vacuum dried in a speedivac and resuspended in an appropriate volume of sterile water.

2:3.5 Generation of recombinant plasmids

Dephosphorylation of vector DNA

After the vector DNA was linearized by restriction enzyme digestion, 1-2 units (U) of CIP was added to the reaction and incubated at 37°C for 1 hour.

Purification of DNA from agarose gels

QIAquick gel extraction kit was used to purify DNA bands from agarose gels, using the manufacturer's protocol.

Ligation

DNA fragments to be ligated were placed in a mix (total volume 20µl) containing 1U of T4 DNA ligase, and 1x ligation buffer and incubated at 18°C overnight. 15% PEG was included in the ligation mix when DNA fragments to be ligated had blunt ends. For transformation by electroporation, the ligation was phenol/chloroform extracted and ethanol precipitated prior to resuspension in 10µl MQ H_2O.

2:3.6 Transformation of bacteria

500ml of L-broth was inoculated with 5ml of an overnight culture of *E. coli DH5α* cells and grown to an OD_{A600} of 0.5-0.6. The culture was then chilled on ice for 15 to 30 minutes and the cells harvested by centrifugation at 4000g for 15 minutes. The cells were then resuspended in 500ml of ice-cold MQ H_2O, pelleted at 5000g, resuspended in 250ml of ice-cold MQ H_2O, pelleted at 4000g, resuspended in 10ml of ice-cold 10% glycerol, re-pelleted at 3000g and finally resuspended in 1ml of ice-cold 10% glycerol. The competent cells were then snap frozen in liquid nitrogen and stored as 42µl aliquots at -80°C.

For transformation, 40µl of cells were thawed on ice and then transferred to an ice-cold 2mm electroporation cuvette. The DNA to be transformed was added to the cells and electroporated in a Bio-Rad Gene Pulser set to 2500V, 25 µFD capacitance and Capacitance Extender set to 500 µFD. The cuvette was immediately washed out with 960µl of L-Broth, and the suspension incubated at 37°C for 1 hour. Cells were then pelleted for 8 seconds at 14 000rpm, then 800µl of the supernatant was removed, and the cells gently resuspended in the remaining L-Broth. The cell suspension was plated onto L-agar plates supplemented with 50µg/ml ampicillin and incubated at 37°C overnight.

2:3.7 Isolation of plasmid DNA

Small scale preparation- Rapid boiling lysis method:

A 2ml culture supplemented with the appropriate antibiotics, was incubated overnight at 37°C, with shaking. Cells were harvested by centrifugation at 14,000 rpm in a microcentrifuge for 15 seconds. The bacterial pellet was resuspended in 200µl of STET, followed by addition of 10µl of lysozyme (10mg/ml). The suspension was heated at 100°C for 45 seconds and centrifuged at 14,000 rpm for 15 min. The pellet was removed with a toothpick. Plasmid DNA was then precipitated with 240µl of isopropanol, centrifuged, and washed with 70% ethanol. The pellet was then dried and resuspended in 20µl MQ H_2O.

Large scale preparation:

Alkaline lysis midi-preps were prepared from 10 ml cultures following standard protocols (Sambrook *et al.*, 1989).

High quality plasmid DNA, for microinjection of *Drosophila* embryos and for automated sequencing reactions, was prepared using either Qiagen midi columns or Bresaspin mini columns according to manufacturer's instructions.

2:3.8 *In vitro* site-directed mutagenesis

The design of the primers used in the site directed mutagenesis followed the instructions provided in Stratagene's QuikChange Site-Directed Mutagenesis kit. The reaction was carried out in a 20µl volume. To each reaction the following was added

2µl of 10x reaction buffer
50ng of dsDNA template (pBS-*pbl1A*)
125ng of the forward primer
125ng of the reverse primer
1µl of 10mM dNTP mix (2.5mM each dNTP)
Sterile MQ H_2O to a final volume of 19µl
1µl of *Pfu* Turbo DNA polymerase (2.5U/µl) was added last

The reaction was cycled according to the manufacturers instructions in a MJ Research, PTC-200 peltier, thermal cycler. The reaction was transferred to a new microfuge tube, 1µl of *DpnI* (10U/µl) added to the reaction, mixed and allowed to incubate at 37°C for 1 hour to digest the parental (nonmutated) dsDNA. The reaction was phenol/$CHCl_3$ extracted, ethanol precipitated and resuspended in 10µl of MQ H_2O. 5µl were then transformed into *DH5α* using electroporation. Restriction analysis was used to identify mutated clones where possible but all mutations were confirmed by sequence analysis before use in subsequent experiments.

2:3.9 Automated sequencing

DNA was sequenced using the ABI Prism™ Dye Terminator Cycle Sequencing Ready Reaction Kit (Perkin-Elmer), essentially as described in the manufacturer's protocol with the modification of using half the described amount of reaction mix. Double-stranded DNA was used as a template and, in general, primers were de-salted. Reactions were performed on a Corbett Research FTS-1S Capillary Thermal Sequencer, with the following conditions: 25

cycles of 96°C for 10 seconds, 50°C for 5 seconds and 60°C for 4 minutes with a temperature ramp setting of 2.

Running and analysis of Dye Terminator gels was conducted by the Sequencing Centre at the IMVS.

2:3.10 SDS polyacrylamide gel electrophoresis

All protein samples were run on a 10% separating gel with a 4% stacking gel using the Mini-PROTEAN II Duel Slab Cell (Bio-Rad) according to the manufacturers instructions. The gels were prepared as follows:

	10%	4%
H_2O	4.02ml	3ml
1.5M Tris-HCl pH 8.8	2.5ml	
0.5M Tris-HCl pH 6.8		1.25ml
10% SDS	100µl	50µl
30% Acrylamide/Bis	3.33ml	0.67ml
TEMED	10µl	10µl
25% APS	50µl	25µl
	10ml	5ml

The separating gel mixture was poured into the gel mould and a layer of water was added before the gel was allowed to set. The water was then removed and the stacking gel was poured. A plastic comb was inserted to create the wells and the gel was allowed to polymerise. The vertical gel running apparatus was then set up and 1 x protein gel running buffer added before the protein samples were loaded and the gel was run at 150 volts for 1-1.5 hours.

2:3.11 Western blotting

Western blotting of proteins onto nitrocellulose membrane was performed using a Bio-Rad Transblot Semi-dri transfer cell according to manufacturer's guidelines. In general, a current of 3 mA per cm^2 of gel was applied for 30 min. Nitrocellulose blots were washed thoroughly with 1 X PBT and then blocked for 1 hour in 5% Blotto. Primary antibody incubations were carried out overnight at 4°C and secondary antibody incubations for 2hr at RT, with the

appropriate dilutions of antibody in Blotto. The secondary antibodies were HRP conjugated and detected by ECL.

2:3.12 *P*-element mediated transformation of *Drosophila*

Micro-injection: DNA for injection was prepared using the Qiagen or Bresaspin kit according to the supplier's protocol. An injection mix was prepared to a concentration of 0.5-1μg/μl transformation vector plasmid DNA and 0.3μg/μl of pπ25.7wc (Δ2-3 transposase) plasmid in 1x Embryo injecting buffer. The injection needle was back filled using a drawn out capillary containing 2μl of the injection mix that had been centrifuged briefly to remove any particulate matter. w^{1118} embryos to be injected were collected from 30 min lays on grape juice agar plates at 25°C, dechorionated in 50% bleach for 3 min, and rinsed thoroughly in MQ H_20. Embryos were then aligned along a strip of non-toxic rubber glue such that their posterior ends would face the needle. A drop of liquid parafin was placed over the embryos and the slide placed on the stage of an inverted microscope. A micromanipulator was used to position the needle, with injection carried out by moving the microscope stage to bring the embryos to the needle, such that a very small amount of DNA was injected into the posterior cytoplasm.

Identification of transformants: The slides of microinjected embryos were then placed in a petri dish containing moist tissue paper with a small amount of yeast paste surrounding the embryos and kept at 18°C to allow the embryos to hatch. Larvae were collected after 2 days using strips of Whatman paper and placed in a fly food vial where they developed into adult flies. The flies were then crossed to w^{1118} flies to identify transformants on the basis of the *mini-white*$^{+}$ eye pigmentation phenotype. Numerous independent transformants were mapped to determine the chromosome of insertion, using the dominantly-marked balancer chromosomes CyO and TM6B in the stocks *w ; Sco / CyO* and *w ; Df(3R)roXB3 / TM6B Hu.* Homozygous lines were then generated using these balancers.

2:3.13 Clones and stocks generated

UAS-ΔNLSpbl

UAS-ΔNLSpbl was generated by site-directed mutagenesis using NLS primer 1 and 2 with *pbl1A* as the template, then subcloned into pUAST and used to generate multiple *UAS-ΔNLSpbl* transgenic lines.

UAS-ΔBRCTpbl

UAS-ΔBRCTpbl was generated by site-directed mutagenesis using BRCTs primer 1 and 2 with *pbl1A* as the template, then subcloned into pUAST and used to generate multiple *UAS-ΔBRCTpbl* transgenic lines.

UAS-myc-ΔBRCTpbl

To generate a MYC tagged ΔBRCT PBL, *ΔBRCTpbl* in pBluescript was digested with *NcoI* and end-filled prior to ligation with 6 myc epitope tag as a *DraI-XhoI* end-filled fragment from pCS2. The *myc-ΔBRCTpbl* construct was then subcloned into pUAST and used to generate multiple *UAS-myc-ΔBRCTpbl* transgenic lines.

UAS-ΔNLSΔBRCTpbl

UAS-ΔNLSΔBRCTpbl was generated by site-directed mutagenesis using NLS primer 1 and 2 with *ΔBRCTpbl* in pBluescript as the template, then subcloned into pUAST and used to generate multiple *UAS-ΔNLSΔBRCTpbl* transgenic lines.

UAS-myc-ΔNLSΔBRCTpbl

To generate a MYC tagged ΔNLSΔBRCT PBL, *ΔNLSΔBRCTpbl* in pBluescript was digested with *NcoI* and end-filled prior to ligation with 6 myc epitope tag as a *DraI-XhoI* end-filled fragment from pCS2. The *myc-ΔNLSΔBRCTpbl* construct was then subcloned into pUAST and used to generate multiple *UAS-myc-ΔNLSΔBRCTpbl* transgenic lines.

GMR>ΔNLSpbl

A recombinant was generated between *GMR-GAL4* and the *UAS-ΔNLSpbl* transgenic line *14-1* on the second chromosome. This was then balanced with *CyO*, generating the *GMR>ΔNLSpbl/CyO* stock. This stock was semi-lethal at 25°C and was therefore maintained at 18°C.

GMR>ΔBRCTpbl

A recombinant was generated between *GMR-GAL4* and the *UAS-ΔBRCTpbl* transgenic line *M2* on the second chromosome. This was then balanced with *CyO*, generating the *GMR>ΔBRCTpbl/CyO* stock. This was semi-lethal at 25°C and was therefore maintained at 18°C.

GMR>ΔNLSΔBRCTpbl

A recombinant was generated between *GMR-GAL4* and the *UAS-ΔNLSΔBRCTpbl* transgenic line *M10* on the second chromosome. This was then balanced with *CyO*, generating the *GMR>ΔNLSΔBRCTpbl/CyO* stock. This stock was lethal at 25°C and was therefore maintained at 18°C.

GMR>pbl

The cloning of the *pbl1A* cDNA into pUAST and subsequent generation of three *UAS-pbl* transgenic lines was performed by L. Prior. *UAS-pbl3.2* was the only one of these lines that resulted in a rough eye phenotype when expressed with *GMR-GAL4*. A recombinant chromosome was generated between *UAS-pbl3.2* and *GMR-GAL4* and balanced with CyO, thus generating the *GMR>pbl/CyO* stock.

GMR>ΔDH pbl

The *GMR>ΔDH pbl/CyO* stock was generated by A. Brumby. The *pbl1A* cDNA was digested with *ScaI* and *SpeI*. The *SpeI* site was end-filled and re-ligated with *ScaI* which resulted in a 53 amino acid deletion in the catalytic portion of translated product of the *pbl1A* cDNA. This mutant form of PBL (ΔDH PBL) would be unable to catalyse the exchange of GDP for GTP. This was cloned into pUAST and used to generate multiple *UAS-ΔDH pbl* transgenic lines. A recombinant chromosome was generated between two of these lines resulting in the *UAS-ΔDHpbl5B, UAS-ΔDHpbl6A/CyO* stock. A triple recombinant was then generated between *GMR-GAL4* and these two copies of *UAS-ΔDHpbl* resulting in a stock referred to as *GMR>ΔDH pbl /CyO*. This stock resulted in a temperature dependent rough eye phenotype that was visible at 25°C but not at 18°C.

UAS-pbl,RhoA^{720}

A recombinant was generated between the null *RhoA^{720}* mutant allele and the *UAS-pbl3.2* transgenic line on the second chromosome. This was balanced with *CyO*, generating the stock *UAS-pbl,RhoA^{720}/CyO*.

UAS-ΔNLSpbl,RhoA^{720}

A recombinant was generated between the null *RhoA^{720}* mutant allele and the *UAS-ΔNLSpbl* transgenic line *14-1* on the second chromosome. This was balanced with *CyO*, generating the stock *UAS-ΔNLSpbl,RhoA^{720}/CyO*.

UAS-ΔBRCTpbl,RhoA^{720}

A recombinant was generated between the null *RhoA^{720}* mutant allele and the *UAS-ΔBRCTpbl* transgenic line *M2* on the second chromosome. This was balanced with *CyO*, generating the stock *UAS-ΔBRCTpbl,RhoA^{720}/CyO*.

UAS-ΔNLSΔBRCTpbl,RhoA^{720}

A recombinant was generated between the null *RhoA^{720}* mutant allele and the *UAS-ΔNLSΔBRCTpbl* transgenic line *M10* on the second chromosome. This was balanced with *CyO*, generating the stock *UAS-ΔNLSΔBRCTpbl,RhoA^{720}/CyO*.

Stocks generated for rescue assays

A recombinant chromosome was generated by L. O'Keefe between *prd-GAL4* and *pbl^{2}* and balanced with *TM3Sb*. This *prd-GAL4,pbl2/TM3Sb* stock was used in all rescue experiments. Recombinant chromosomes were also generated between *pbl^{3}* and various *UAS-pbl* lines on the third chromosome and balanced with *TM3Sb*. The stocks generated are;

- *UAS-pbl3.2,pbl^{3}/TM3Sb* (L. O'Keefe)
- *UAS-ΔNLSpbl,pbl^{3}/TM3Sb*
- *UAS-ΔBRCTpbl,pbl^{3}/TM3Sb*
- *UAS-myc-ΔBRCTpbl,pbl^{3}/TM3Sb*
- *UAS-ΔNLSΔBRCTpbl,pbl^{3}/TM3Sb*
- *UAS-myc-ΔNLSΔBRCTpbl,pbl^{3}/TM3Sb*.

2:3.14 Growth conditions

Fly stocks were maintained on standard media at 18°C with 70% humidity. Experimental fly crosses were performed at 25°C, 18°C and 13°C depending on the transgenic construct and *GAL4* driver used. All *GMR>ΔNLSpbl* crosses were performed at 25 and 18°C. All *GMR>ΔBRCTpbl* crosses were performed at 25 and 18°C. All *GMR>ΔNLSΔBRCTpbl* crosses were performed at 18 and 13°C. All crosses with other *GAL4* drivers were performed at 25°C unless otherwise indicated in the text. Egg lays were performed at 25°C on grape juice agar plates.

2:3.15 *Drosophila* protein extracts

For western analysis of protein expression levels in *Drosophila* larval tissues, extracts were prepared. Tissues were dissected in 1xPBS, this solution was removed and 10µl of homogenisation buffer plus 10µl of 3x sample buffer was added. Samples were spun for 5 seconds at 14,000 rpm and stored at -80°C. To prepare the samples for western analysis they were boiled at 100°C for 10 mins and spun at 14,000 rpm for 10 mins at room temperature before being loaded onto a SDS-polyacrylamide gel and subsequently analysed by western blot.

2:3.16 Collection and fixation of *Drosophila* embryos

Embryos were collected on grape juice agar plates smeared with yeast, harvested and washed thoroughly in a basket using 0.7%NaCl, 0.3%Triton X-100. The embryos were then dechorionated by soaking for 2.5 mins in 50% commercially available bleach (2% sodium hypochlorite) before again being washed thoroughly in 0.7%NaCl, 0.3%Triton X-100. They were then transferred to a glass scintillation vial containing a two-phase mixture of 4 ml of 4% formaldehyde in 1 x HEN and 4 ml of heptane. The vial was then shaken on an orbiting platform such that the interface between the liquid phases was disrupted and the embryos were bathing in an emulsion, for 25 minutes to 'fix' the embryos. The bottom phase (aqueous) was drawn off and replaced with 4 ml of methanol and the vial was shaken vigorously for 30 seconds to de-vitellinise the embryos. De-vitellinised embryos sink from the interface and were collected from the bottom methanol phase. Embryos were rinsed thoroughly in methanol and then several times in ethanol before being stored under ethanol at -20°C until required.

2:3.17 Whole mount immunostaining of *Drosophila* embryos

Embryos stored under ethanol were firstly rinsed in methanol and then re-hydrated by rinsing in 50% methanol/50% 1X PBT, several times in 1 x PBT, and then a single wash for 30 minutes in 1x PBT. The embryos were then 'blocked' in 200µl of 1 x PBT containing 0.1% bovine serum albumin (BSA) and 5% normal goat serum (NGS) for at least 1 hour at room temperature with gentle agitation. The blocking solution was removed and primary antibody diluted in fresh blocking solution was added (usually 50-200µl). The embryos were routinely incubated in primary antibody with gentle rocking at 4°C overnight. The next day, the antibody solution was removed and the embryos were washed extensively in 1 x PBT over the course of at least an hour. The embryos were then re-blocked in PBT containing 0.1% BSA for at least 30 mins before being incubated with secondary antibody diluted in PBT for 2 hours at room temperature with gentle rocking. Following a period of washing, the embryos were incubated with a tertiary complex for two hours and then washed extensively in 1 x PBT. Embryos were then stained for 5 mins with Hoechst 33258 and washed in 1 x PBT on the nutator overnight. The embryos were mounted in PBS/80% glycerol onto a slide under a coverslip supported by two pieces of double-sided tape and coverslips were sealed to the glass using commercially available clear nail varnish.

2:3.18 Immunostaining of *Drosophila* larval tissues

Larval tissues were dissected in 1 x PBS and fixed in a mixture of 3 parts 1.5 x Brower's solution, 0.5 part 16% Formaldehyde and 0.5 parts water for 30 minutes on ice. Tissues were washed in 1 x PBT-BSA (1 x PBS, 0.3% triton-X100, 1mg/ml BSA) and blocked with a solution of 1 x PBS, 0.1% Tween-20 and 5mg/ml BSA for at least 1 hour on ice. The primary antibody diluted in blocking solution was incubated at 4°C overnight with gentle rocking. The next day, the tissues were washed extensively in 1 x PBT before being re-blocked for 30 mins in 1xPBT-BSA. The secondary antibody conjugated to biotin was diluted in 1 x PBT and incubated for 2 hours at room temperature with gentle rocking. After several washes in 1x PBT, the tertiary complex was added and incubated for 2 hours at room temperature on the nutator. After further washes, the tissues were then stained for 5 mins with Hoechst 33258 and washed in 1 x PBT on the nutator overnight at 4°C. For microscopy the tissue samples were dissected in 80% glycerol, flattened and mounted directly on the slide with a coverslip carefully placed on top.

2:3.19 Immunostaining of *Drosophila* pupal retinas

White pre-pupae were picked and aged to the appropriate stage. Retinas were dissected in 1 x PBS and fixed in 4% formaldehyde in 1 x HEN for 30 mins at room temp. All fixation and washing steps were performed in a cut off eppendorf lid, using a drawn out pasteur pipette whilst looking down a dissecting microscope. Retinas were washed in 1 x PBS + 0.1% Saponin and blocked for 1hr with 5% normal goat serum. Incubations with primary antibodies were performed overnight at 4°C, while secondary antibodies and tertiary complexes were incubated for 2hr at room temp.

2:3.20 Acridine orange staining of larval discs

Larval discs were dissected in 1 x PBS and stained for 5 mins in a drop of 1.6 x 10-6 M acridine orange in 1 x PBS (1.6 x 10^{-3} M stock of AO was made up in ethanol and stored at -20°C for convenience). The discs were mounted directly in this drop of AO by flattening out the sample and carefully lowering a coverslip. Each sample was analysed, within 5 mins of staining, by fluorescence microscopy.

2:3.21 Dissociation of eye disc cells

Eye discs were dissected in 1 x PBS and incubated in 200µl of PBTH (55µl 10 x PBS, 100µl 2.5% trypsin, 0.5µl Hoechst, 395µl MQ H_2O) for 3 hr at room temp with gentle rocking. Approx 30µl of this solution was mounted directly onto a slide for fluorescent microscopic analysis.

2:3.22 Transverse sections

Adult eyes were incubated in periodate/lysine/paraformaldehyde for 30 mins, fixed in 2.5% gluteraldehyde/0.1M sodium phosphate (pH7.2) overnight, post-fixed in 2% osmium tetroxide, washed in water, and dehydrated in acetone. Specimens were mounted in epoxy resin, sectioned at 2µm, and stained with methylene blue.

2:3.23 Tissue culture and heterokaryon formation

All heterokaryon experiments were performed in collaboration with L. MacMillan.

Tissue culture

HEK 293T and NIH-3T3 cells were maintained in Dulbecco's modified Eagle's medium (DMEM, CSL) supplemented with 10% foetal calf serum and 1% penicillin-streptomycin (CSL) in a 37°C, 5% CO_2 incubator. HEK 293T cells were seeded at 6x 10^5-10^6 cells/6cm

dish. At subconfluence HEK 293T cells were transfected following the standard Ca phosphate protocol using 10μg DNA/6cm dish. After 5 hours incubation, medium containing the DNA precipitate was replaced with fresh medium and the cells were left to recover overnight.

Heterokaryon formation

At 24 hours post transfection HEK 293T cells were trypsinized and seeded in equal number with trypsinized NIH-3T3 cells in a culture tube with addition of the required medium. Cells were well mixed and the cell suspension (4x 10^4 cells/chamber) was placed into fibronectin (Boehringer Mannheim) treated chamber slides (50 μg/ml fibronectin, 200μl/well for 45 mins at room temp). Co-cultures were incubated for 3.5 hours to allow the cells to attach to the slides.

Cycloheximide (Calbiochem) was added at a concentration of 100μg/ml and the cultures were then incubated for another 30 mins to inhibit further protein synthesis.

At 4 hours, the medium was removed from the cells and 5 drops of 50% PEG solution (in 0.1M HEPES pH 7-7.4 with 10% DMSO) was added to the wells for 1-2 mins with gentle rocking. 300μl of complete medium was then added to dilute the PEG solution, before the wells were drained and another 300μl of complete medium was added to wash the cells. This washing step was repeated twice before 250μl of complete medium with 100μg/ml of cycloheximide was added to the wells. The cells were then incubated at 37°C in a 5% CO_2 incubator for 4 hours. The medium was finally removed and the cells were washed with PBS before fixation.

Fixation and immunostaining

A -20°C fixation solution (47.5% methanol: 47.5% acetone: 5% formaldehyde) was used to fix the cells for 1 min on ice. The fixative was removed and the cells were washed with ice cold PBS+ 1% BSA. The primary antibody (anti-FLAG) was diluted 1/300 in PBS+ 1% BSA and incubated for 1 hour at 4°C on ice. The cells were then washed twice with PBS+ 1% BSA before the secondary antibody (anti-mouse Alexa 594) was added at a final concentration of 5-20 μg/ml together with Hoechst 33258 at a final concentration of 1μg/ml for 45 mins at 4°C on ice. After staining the cells were washed twice with PBS+ 1% BSA before mounting in glycerol+ 2% propylgalate.

2:3.24 Light and fluorescence microscopy

Light microscopy was performed on a Zeiss Axiophot light microscope with DIC optics. Images were collected digitally with Photograb and Adobe Photoshop 6.0 was used for image preparation. Fluorescence microscopy was performed on an Olympus AX70. Digital images were collected with a cooled CCD camera and Adobe Photoshop 6.0 was used for image preparation. Confocal images were obtained with a BioRad MRC1000 scanhead confocal microscope equipped with a krypton/argon laser and images were collected and analysed using Confocal Assistant. Images of adult eyes were obtained using an Olympus SZH10 microscope and Polaroid digital camera.

2:3.25 Regulatory considerations

All manipulations involving recombinant DNA were carried out in accordance with the regulations and approval of the Genetic Manipulation Advisory Committee and the University Council of Adelaide University.

All manipulations involving animals were carried out in accordance with the regulations and approval of the Animal Ethics Committee and the University Council of Adelaide University.

Chapter 3: The importance of sequestering PBL to the nucleus

3:1 Introduction

As discussed in chapter 1, the *pbl* gene is required for cytokinesis in *Drosophila.* In *pbl* mutant embryos, the contractile ring partially forms but ultimately fails in its attempt to divide the cytoplasm and its contents into two daughter cells. Despite the failure of cytokinesis, the nuclear events of mitosis continue, resulting in the formation of large, multinucleate cells after several rounds of failed cytoplasmic division (Hime and Saint, 1992; Lehner, 1992; Prokopenko *et al.*, 1999) (see chapter 1, **Figure 1.4**).

The initial clue to the role of PBL in cytokinesis came with the determination of its protein sequence. The PBL protein contains Dbl Homology (DH) and Pleckstrin Homology (PH) domains, characteristic of the GTP exchange factors (GEFs) that activate the Rho family of small GTPases (chapter 1, **Figure 1.5**). In their active form, these Rho family GTPases mediate reorganisation of the actin cytoskeleton, which is an essential event during cytokinesis. PBL, through its DH/PH domains is therefore responsible for the activation of Rho and stimulation of cytokinesis (Prokopenko *et al.*, 1999). In addition to these cytoplasmic domains, PBL also contains a consensus bipartite nuclear localisation signal (NLS), two characteristic BRCT domains, and a third as yet uncharacterised region, here termed the RadECl region (chapter 1, **Figure 1.5**). This region contains several, but not all of the characteristic residues of a BRCT domain and was found to share a greater similarity with the proteins RAD4-like and ECT2 (chapter 1, **Figure 1.7**). As discussed in the introduction, this RadECl region seems to be conserved as a unit with an adjacent BRCT domain, and may have evolved from a BRCT domain itself. It was therefore proposed that the RadECl region may function in tandem with the BRCT domain with which it is associated.

BRCT domains were originally identified in the BRCA1 breast cancer tumour suppressor protein (Koonin *et al.*, 1996), and have since been found in a multitude of other proteins, their unifying feature being their involvement in maintaining the integrity of the genome (Bork *et al.*, 1997; Callebaut and Mornon, 1997). The presence of such domains in a Rho GEF poses an interesting and perplexing question for the function of PBL. While the

DH and PH domains regulate Rho in the cytoplasm, BRCT domains have been implicated in the process of DNA repair, which is a nuclear event. In addition, all other known BRCT domains are within nuclear proteins. Evidence for a nuclear role for PBL, other than the fact that it contains several known nuclear domains, can be obtained from examining the localisation of PBL throughout the cell cycle. During late anaphase, PBL localises initially to the cell cortex (chapter 1, **Figure 1.6a**) before concentrating at the cleavage furrow (**Figure 1.6b**), presumably to activate Rho and stimulate cytokinesis. By late telophase, PBL is observed to strongly localise to the nucleus where it remains throughout interphase until the following prophase/metaphase when the nuclear envelope breaks down (**Figure 1.6c**).

There are three possible reasons why PBL localises to the nucleus. Firstly, nuclear localisation may simply be a means to remove PBL Rho GEF activity from the cytoplasm once its role in cytokinesis has been completed. Secondly, PBL may perform a completely separate Rho-independent nuclear function. Thirdly, PBL may perform a Rho-dependent nuclear function, which would be completely novel.

In an attempt to differentiate between these possibilities, the importance of sequestering the protein to the nucleus was first examined. Site-directed mutagenesis was used to mutate the consensus bipartite NLS of PBL, and the mutant protein was then expressed in various tissues to answer the following questions:

1) Does the consensus bipartite NLS act as the nuclear targeting signal for PBL?

2) What are the phenotypic consequences of expression of a cytoplasmic form of PBL in different tissues?

3) Is nuclear sequestration important for PBL function in cytokinesis?

3:2 Site directed mutation of the consensus bipartite nuclear localisation signal

Bipartite nuclear localisation signals are defined by two basic residues, followed by a spacer of 10 non-specific residues, before a second basic cluster containing at least 3 out of 5 basic residues (Robbins *et al.*, 1991). The program PSORT (Prediction of Protein Localisation Sites) was used to scan for a PBL sequence matching this description. A match was found, with an estimate of 97% certainty that this would function as an NLS (**Figure 3.1a**).

Site directed mutagenesis was used to test the importance of this sequence to the nuclear localisation of PBL. Robbins *et al.* (1991) had shown that mutation of three lysine residues to asparagines in the bipartite NLS of nucleoplasmin completely abolishes nuclear localisation of the protein. Therefore the codons for the equivalent lysine/arginine/lysine residues at position 318-320 of PBL were specifically mutated to asparagine codons. This was accomplished by designing two complementary primers containing the mutated bases ($A^{1404} \rightarrow C$, $C^{1405} \rightarrow A$, $G^{1406} \rightarrow A$, $G^{1410} \rightarrow C$) flanked on either side by 15 and 23 bp of non-mutated sequence (**Figure 3.1b**). *In vitro* site directed mutagenesis was then performed with these primers on the *pbl1A* cDNA sequence using the Stratagene *in vitro* mutagenesis kit. Sequences of the resulting potential mutant clones were then determined to ensure they had the specific NLS mutation (referred to hereafter as ΔNLS), but no other mutations.

A ΔNLS mutant *pbl* cDNA sequence was then cloned into the multiple cloning site of the pUAST vector using the enzymes XhoI/XbaI. This vector places the gene of interest under the direct control of a *S. cerevisiae GAL4* upstream activator sequence (UAS). Upon introduction into the germline of *Drosophila* by genetic transformation, expression of the gene can be induced by the presence of the yeast GAL4 protein (Brand and Perrimon, 1993). The pUAST vector carries P-element inverted repeats which allow insertion of the construct into the *Drosophila* germline in the presence of P transposase (Rubin and Spradling, 1982; Spradling and Rubin, 1982). The Δ*NLSpbl* cDNA pUAST construct was therefore injected into the pole cells of *Drosophila* embryos and after subsequent crosses, 8 separate transgenic lines were established. The position of the insert in these lines was then determined by genetic mapping. One line mapped to the X chromosome, two mapped to the second

chromosome, and five mapped to the third chromosome. All except one of these inserts were homozygous viable.

3:3 Expression of ΔNLS PBL in the *Drosophila* eye disc causes a severe rough eye

To determine whether mutation of the NLS sequence generated a cytoplasmic form of PBL, and to analyse the effect of such subcellular mislocalisation, the eye specific enhancer construct *GMR-GAL4* was used to drive expression of GAL4, and hence the ΔNLS mutant PBL protein, in the developing eye disc. The *glass* minimal promoter region (*GMR*) drives the expression of GAL4 in all cells posterior to the morphogenetic furrow of the eye disc during larval development (Ellis *et al.*, 1993). When this system was used to drive the expression of full-length wild type PBL, the protein was observed to be nuclear in all cells, apart from those undergoing mitosis (**Figure 3.2a**). Upon nuclear envelope breakdown during prophase/metaphase, PBL becomes redistributed throughout the cytoplasm (**Figure 3.2a'**). However, when ΔNLS PBL is expressed in the eye disc using *GMR,* the mutant protein was found to be cytoplasmic throughout the cell cycle (**Figure 3.2b**). Thus the consensus bipartite NLS identified in this study functions as the PBL nuclear localisation signal.

GMR-driven expression of full-length wild type PBL results in a mild rough eye phenotype (**Figure 3.3b**). The eye maintains its pigment, but has an increased number of bristle cells (Prokopenko *et al.*, 1999). Expression of ΔNLS PBL on the other hand resulted in extreme roughening of the eye. Of the 7 transgenic lines tested, 2 were lethal when expressed under the control of the *GMR* promoter at 25°C. As the eye is a non essential organ for flies raised in laboratory conditions, the lethality was presumably due to the leaky expression of this driver in other tissues. 4 lines gave extreme eye phenotypes, and one gave a medium rough eye phenotype. The *GMR>ΔNLSpbl* eyes were characteristically smaller than those of *GMR>pbl* flies, had lost most of their pigment, and had a severely blistered appearance. Large areas of necrosis were also often observed (**Figure 3.3c**). Sections of these eyes confirmed the extreme nature of the phenotype, revealing a severe disruption of the eye

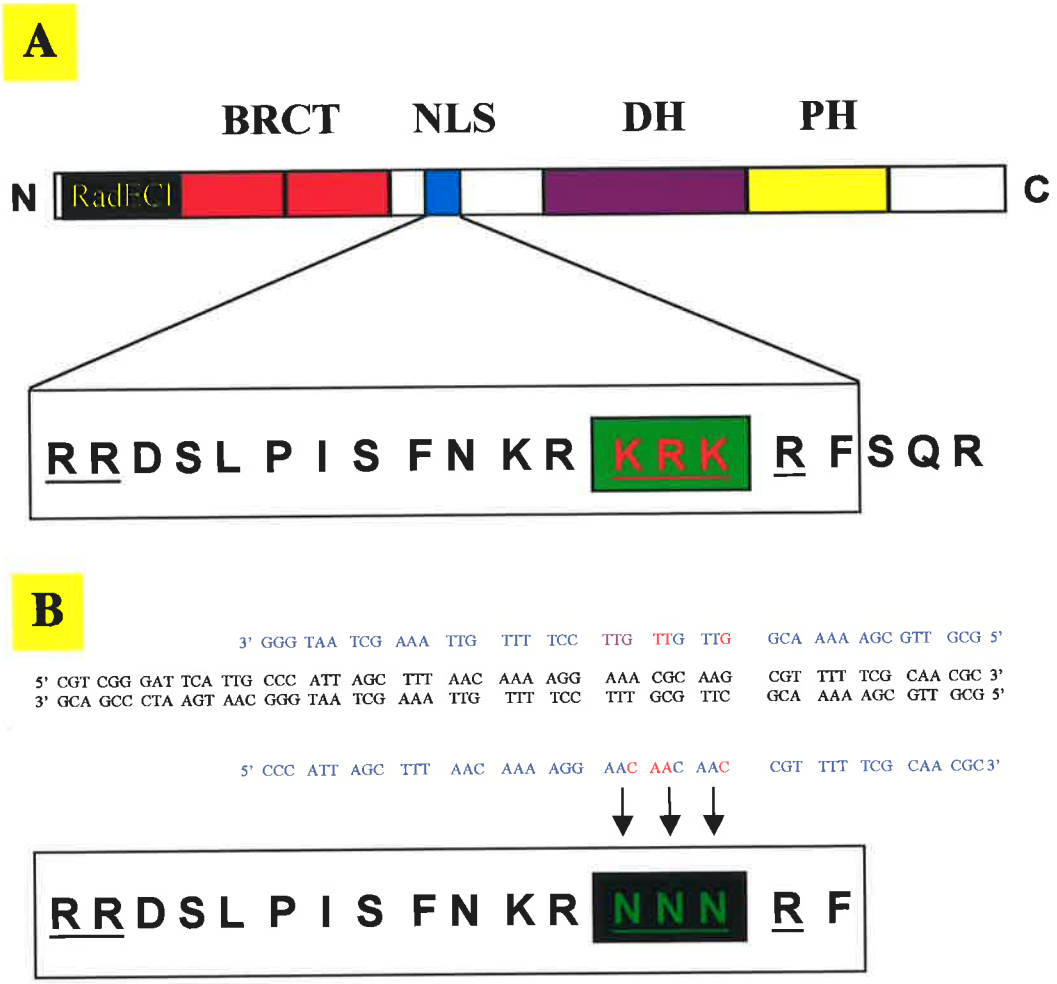

Figure 3.1 Site directed mutagenesis of the consensus bipartite nuclear localisation signal of PBL.

A. A schematic diagram of the structure of the PBL protein, with the RadECl region boxed in black, the 2 consensus BRCT domains in red, the Dbl homology domain (DH) in purple, and the Pleckstrin homology domain (PH) in yellow. The consensus bipartite nuclear localisation signal is boxed in blue. Underneath is the PBL amino acid sequence in this region with the consensus bipartite nuclear localisation signal boxed. The critical basic residues of this signal are underlined, and the lysine (K) and arginine (R) residues, which were targeted for mutation, are shown in red highlighted by a green box.
B. The DNA sequence from this region is shown. The primers designed to mutate 4 base pairs of the sequence are shown in blue, with the 4 mutant base pairs shown in red. Beneath is the amino acid sequence of the mutated nuclear localisation signal. The lysine/arginine/lysine (K/R/K) residues were changed to asparagine residues (N) and are shown in green, highlighted by a black box.

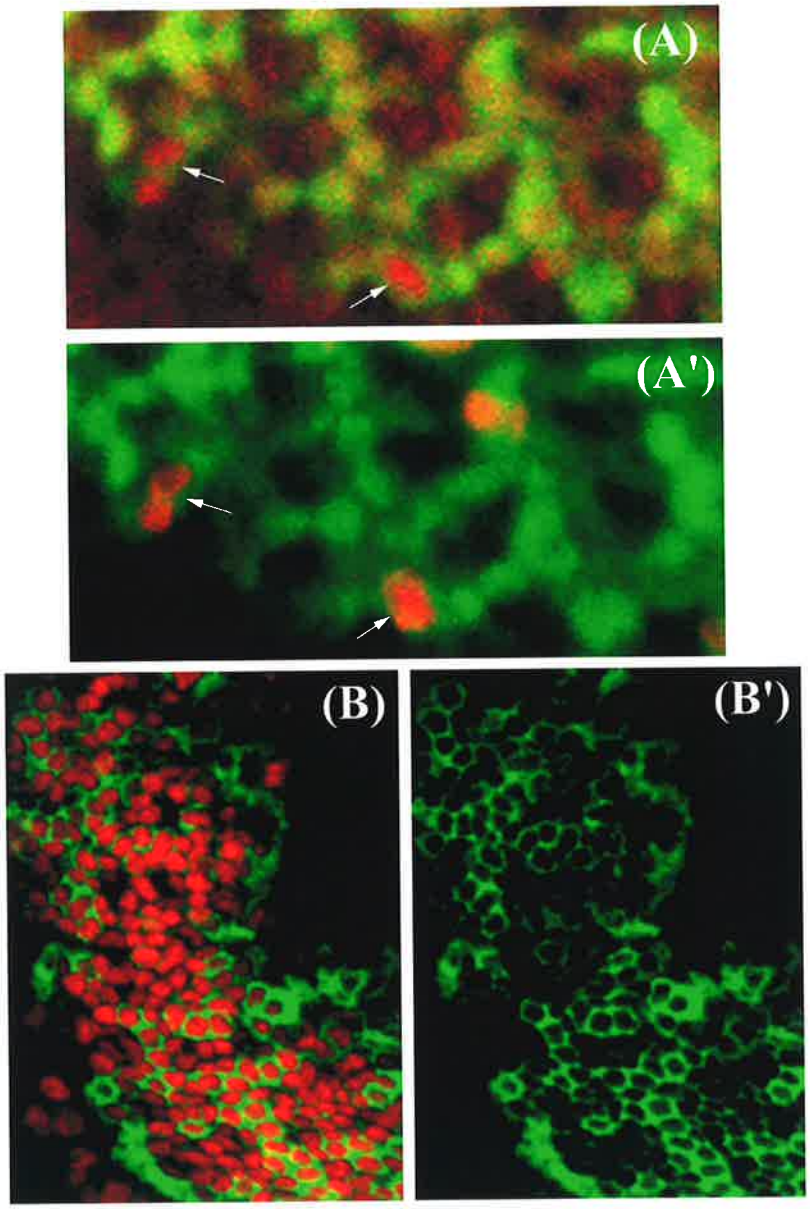

Figure 3.2 ΔNLS PBL is cytoplasmic throughout the cell cycle.

GMR GAL4::UAS pbl and *ΔNLSpbl* eye discs were dissected, fixed and stained with anti-PBL antibody (shown in green), anti-phosphorylated histone H3 which stains mitotic figures, and propidium iodide which stains the DNA (both shown in red, as indicated).

A. *GMR GAL4::UAS pbl* eye disc stained with PBL (green) and propidium iodide (red). Wild type PBL is observed to localise to the nucleus in interphase cells, and is cytoplasmic in cells undergoing mitosis (white arrows). The mitotic figures are shown in A' where anti-phosphorylated histone H3 is in red and PBL is in green.

B. *GMR GAL4::UAS ΔNLSpbl* eye disc stained with PBL (green) and propidium iodide (red). PBL is completely cytoplasmic. The PBL stain alone is shown in B'.

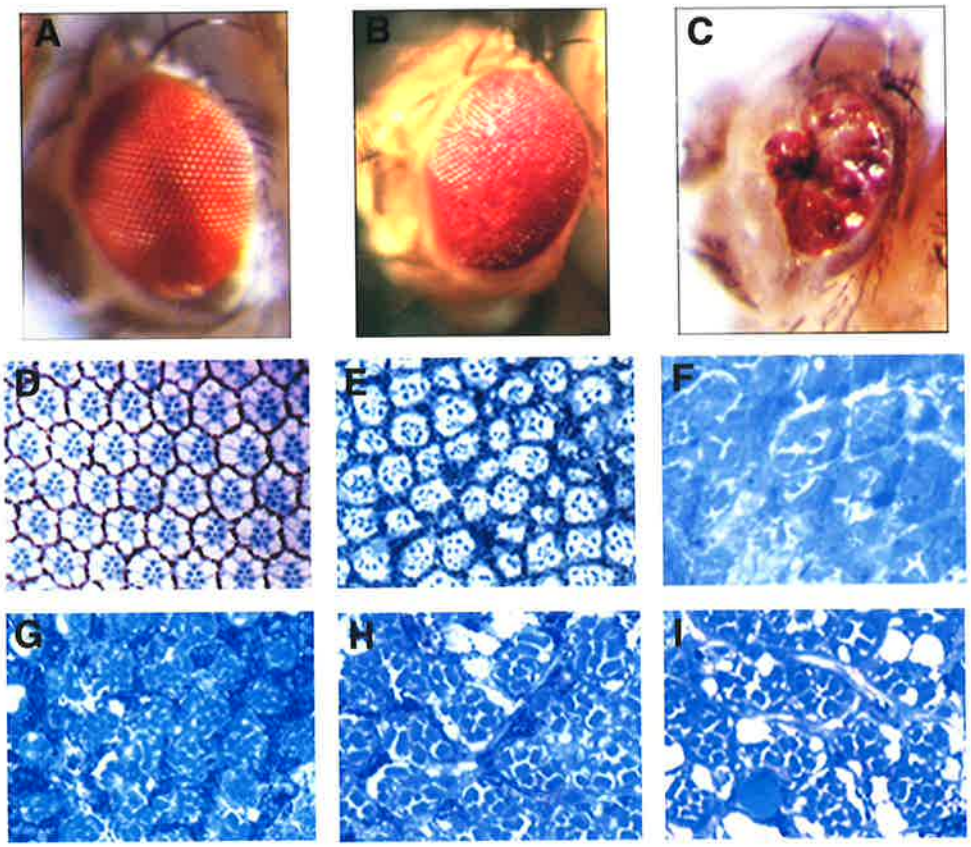

Figure 3.3 Rough eye phenotypes caused by overexpression of PBL.

A. A wild type *Drosophila* adult eye.
B. A *GMR GAL4::UAS pbl* adult eye. A mild rough eye phenotype is caused by the overexpression of PBL posterior to the morphogenetic furrow in the developing eye disc at 25 degrees C.
C. A *GMR GAL4::UAS ΔNLSpbl* adult eye. An extreme rough eye phenotype is caused by the overexpression of ΔNLS PBL posterior to the morphogenetic furrow in the developing eye disc at 25 degrees C.
D - I. Tangential sections through adult eyes of the following genotypes. All sections were stained with methylene blue to visualise the structure.
D. A wild type adult eye.
E. A *GMR GAL4::UAS pbl* adult eye at 25 degrees C.
F. A *GMR GAL4::UAS ΔNLSpbl* adult eye at 25 degrees C. The structure of the eye is destroyed.
G- I. *GMR GAL4::UAS ΔNLSpbl* adult eyes at 18 degrees C.
G. An apical section.
H. A section through the middle of the eye.
I. A basal section.

structure (**Figure 3.3f -i**). In *GMR>ΔNLSpbl* adult eyes raised at 25°C, the disruption was so severe, that it was impossible to identify any cell types (**Figure 3.3f**). At 18°C, the expression of *GMR* is not as strong, resulting in a milder phenotype. Sections of these eyes were still severely disrupted, making it difficult to identify the exact nature of the disruption (**Figure 3.3g-i**).

To discount the possibility that the severity of the *ΔNLSpbl* phenotype is simply due to this construct being expressed at a much higher level than the *UAS pbl* construct, western analysis was performed. Wild type, *GMR>pbl* and *GMR>ΔNLSpbl* eye discs were dissected, boiled and run on a 10% SDS polyacrylamide gel, which was then transferred to nitrocellulose and probed with an anti-PBL antibody. As can be seen from **Figure 3.4**, wild type PBL was present at higher levels than ΔNLS PBL, despite the phenotypic effect being much milder, showing that the *ΔNLSpbl* phenotype was not due to increased expression levels. Thus nuclear localisation is important for normal PBL function.

3:4 Characterisation of the ΔNLS PBL phenotype in the eye

As can be seen from the adult eye and the sections through the adult eye, expression of an NLS mutant form of PBL causes a severe disruption of eye structure. But at what stage of development do things start to go wrong? As a first step in the characterisation of the mutant phenotype, larval eye disc cells were examined. Due to the compact columnar epithelial structure of the larval eye disc, it was decided to dissociate the cells in order to examine individual cells. *GMR>ΔNLSpbl* flies were crossed to a *UAS-GFP* line, so that those cells overexpressing ΔNLS PBL would also be expressing GFP, allowing identification of the cells without fixation and antibody staining. GFP also enables visualisation of the individual cells, and when combined with Hoechst stain for the DNA, the basic cellular phenotype can be determined. *GMR>ΔNLSpbl* eye disc cells were found to show a range of basic phenotypes. Some cells were multinucleate, and some anucleate, suggesting a disruption of cytokinesis (**Figure 3.5a and b**). In addition, some cells were also observed to have a disrupted shape (**Figure 3.5b**). This is in direct contrast to the *GMR>pbl* eye disc phenotype,

where no obvious effect was observed (**Figure 3.5d and e**). Interestingly, the *GMR>ΔNLSpbl* phenotype in eye disc cells was similar to that found in *GMR>ΔDHpbl* eye disc cells. The ΔDH mutant form of PBL, where a portion of the DH domain responsible for GEF activity had been deleted, was previously shown to be acting as a dominant negative form of the PBL protein. In these cells, multiple nuclei were often observed (**Figure 3.5f**) as well as a similar disruption of cell shape (**Figure 3.5g**).

Expression of ΔNLS PBL was therefore shown to disrupt both cytokinesis and cell shape in the larval eye disc. However, what effect does this disruption have on the further development of the eye disc? To answer this question and to gain further insight into the basis of the severe adult eye phenotype, pupal eye discs were examined. The structure and composition of the pupal eye disc of *Drosophila* has been extensively characterised, with the types of cells, their number and fate having been completely mapped out (Wolff and Ready, 1993). To examine the pupal phenotype, *GMR>ΔNLSpbl* pupal discs were dissected out, fixed and stained for the epithelial cell contact marker Armadillo. Hoechst 33258 stain was used to visualise the DNA. When raised at 25°C, the pupal discs were severely necrotic, making it impossible to analyse their phenotype. At 18°C, the expression of *GMR* is not as strong, resulting in a milder phenotype that is easier to analyse.

As can be seen from **Figure 3.6c,** *GMR>ΔNLSpbl* pupal eye discs at 18°C have too many bristle cells, too many interommatidial cells, and some ommatidia have too few cone cells. This is similar to, but more severe than the *GMR>pbl* pupal disc phenotype at 25°C, in which there are too many bristle and interommatidial cells (**Fig 3.6b**). The occasional ommatidium has too few cone cells (**Fig 3.6b'**).

Given the effect on the patterning of the pupal disc cells, the next question was at what stage does the patterning process begin to fail. To answer this question, *GMR>ΔNLSpbl* larval eye discs were fixed and stained with anti-ELAV. ELAV is expressed specifically in those cells of the eye disc that have adopted a neural fate (Campos *et al.*, 1987; Robinow and White, 1988). Analysis of the pattern of ELAV in the larval eye disc therefore reveals whether this initial patterning event is disrupted. While the pattern of ELAV expression was only mildly disrupted in *GMR>pbl* eye discs (**Figure 3.7d-f**), *GMR>ΔNLSpbl* eye discs were found to have a massive reduction in the number of ELAV expressing cells (**Figure 3.7g-i**). The furrow still progresses (**Fig 3.7i**), but the adoption of a neural cell fate seems to be delayed. Despite the smaller number of ELAV expressing cells, their organisation into clusters remains.

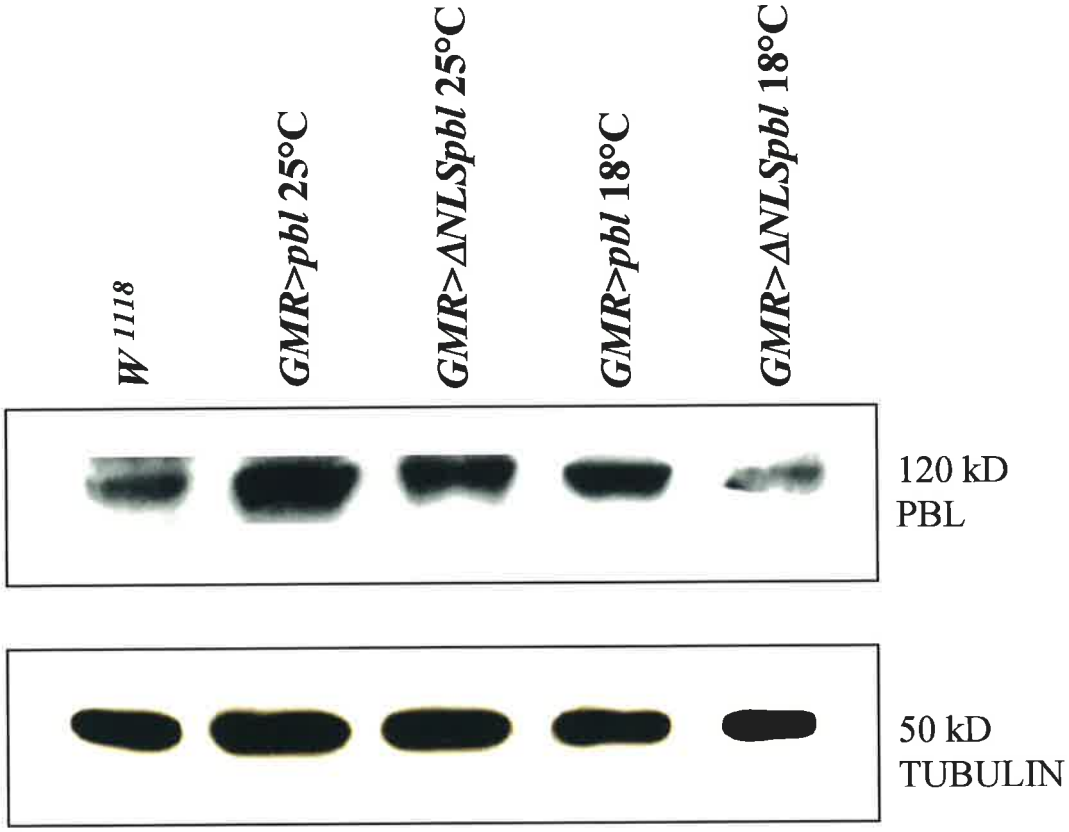

Figure 3.4 Western analysis of *GMR GAL4* expression levels in the eye.

w^{1118}, *GMR GAL4::UAS pbl*, and *GMR GAL4::UAS ΔNLSpbl* eye discs were dissected at 25°C or 18 °C as indicated, boiled and run on a 10% SDS polyacrylamide gel, which was then transferred to a nitrocellulose filter. The filter was then probed with an anti-PBL antibody, producing a band of approximately 120 kD in size in each lane.
The filter was then stripped and reprobed with an alpha-tubulin antibody, which served as a loading control. This produced a band of approximately 50 kD in size.
As can be seen from the filter, ΔNLS PBL is expressed at a slightly lower level in the eye than full length PBL.

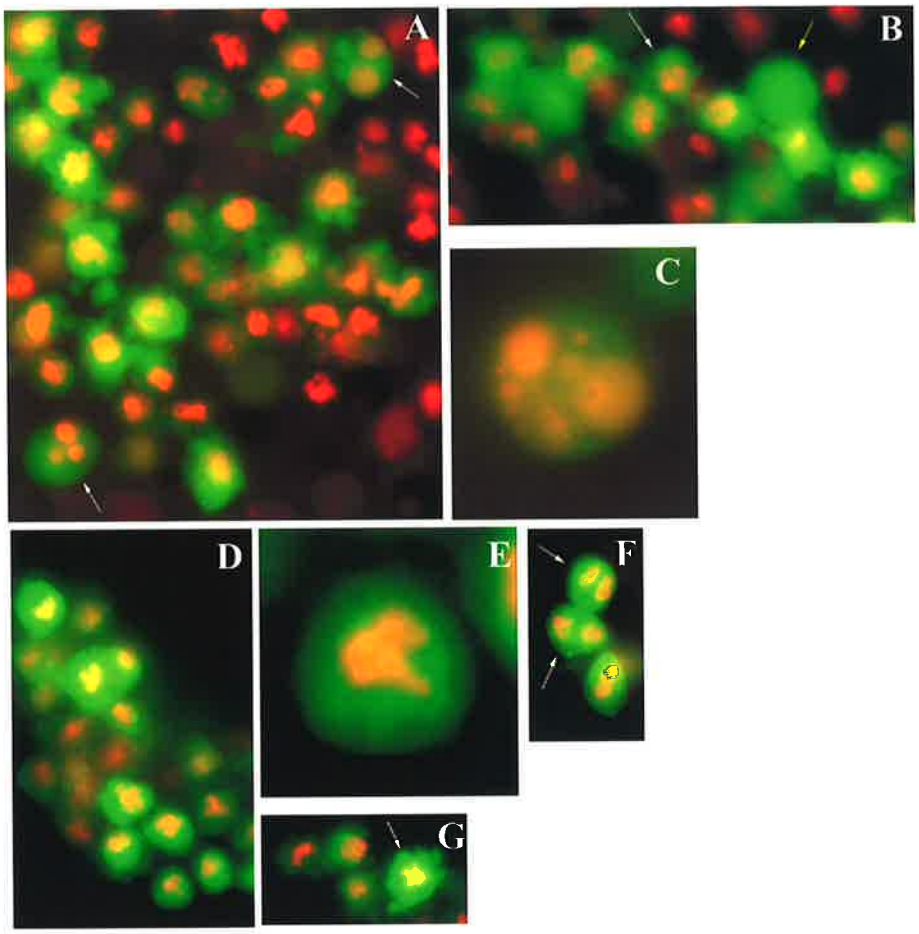

Figure 3.5 Dissociation of eye disc cells and visualisation by epifluorescence. *GMR GAL4::UAS pbl,* Δ*NLSpbl* and Δ*DHpbl* eye discs were dissociated and stained with hoechst to visualise the DNA (shown in red). *UAS GFP* was co-expressed to enable visualisation of the cells overexpressing the *pbl* constructs (shown in green).

A. *GMR GAL4::UAS* Δ*NLSpbl* dissociated eye disc cells (100x mag). Some cells are multinucleate, as indicated by the white arrows.

B. *GMR GAL4::UAS* Δ*NLSpbl* dissociated eye disc cells (100x mag). Some cells have disrupted shape (white arrow), and some appear to be anucleate (yellow arrow).

C. Close up view of a multinucleate *GMR GAL4::UAS* Δ*NLSpbl* eye disc cell. There are at least two large nuclei, surrounded by multiple micronuclei.

D. *GMR GAL4::UAS pbl* dissociated eye disc cells (100x mag). Cells are mononucleate.

E. Close up view of a normal *GMR GAL4::UAS pbl* eye disc cell.

F. *GMR GAL4::UAS* Δ*DHpbl* dissociated eye disc cells (100x mag). Some of these cells are multinucleate as indicated by the white arrows.

G. *GMR GAL4::UAS* Δ*DHpbl* dissociated eye disc cells (100x mag). Some cells have disrupted shape (white arrow).

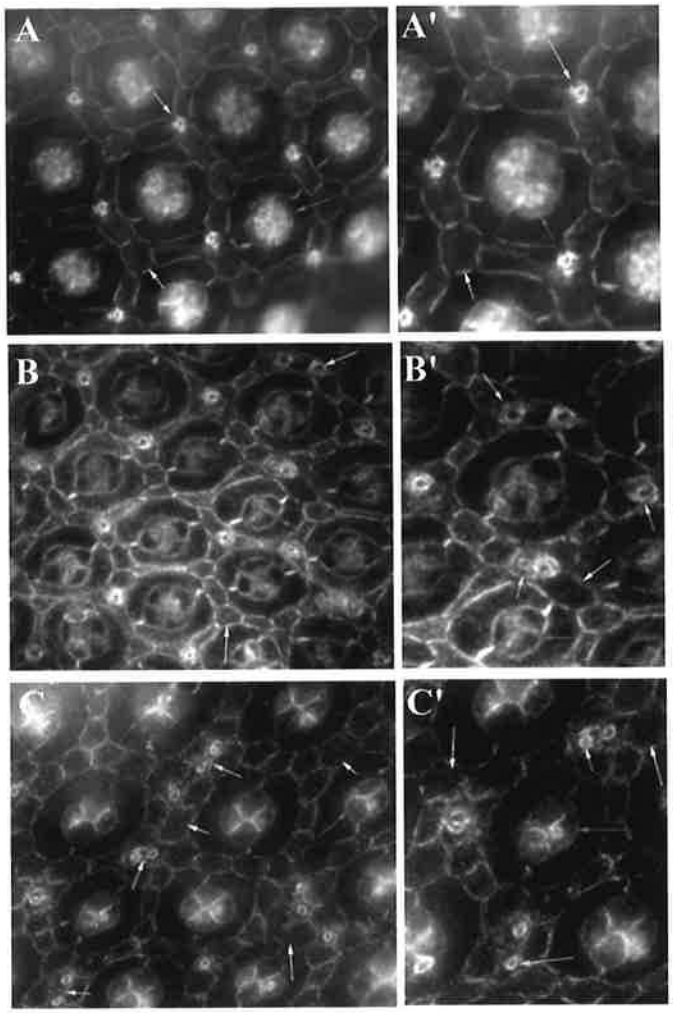

Figure 3.6 Disruption of pupal eye disc structure in *GMR GAL4::UAS ΔNLSpbl* eye discs.

All pupal discs were stained with antibodies against the cell contact marker Armadillo.

A. Wild type pupal eye disc at 42 hr APF at 25 degrees C (100x mag). The white arrow indicates an interommatidial cell, the yellow arrow a bristle cell, and the red arrow points to a group of cone cells. A'. Close up view of a wt pupal ommatidium.

B. *GMR GAL4::UAS pbl* eye disc 42 hr APF at 25 degrees C (100x mag). The pupal disc has more interommatidial cells than wild type (white arrow), more bristle cells (yellow arrow), and the occasional ommatidium has too few cone cells (red arrow). B'. Close up view of a *GMR>pbl* ommatidium.

C. *GMR GAL4::UAS ΔNLSpbl* eye disc at 84 hr APF at 18 degrees C (100x mag). The pupal disc has more interommatidial cells than wild type (white arrows), more bristle cells (yellow arrows), and some ommatidia have too few cone cells (red arrows). C'. Close up view of a *GMR>ΔNLSpbl* ommatidium.

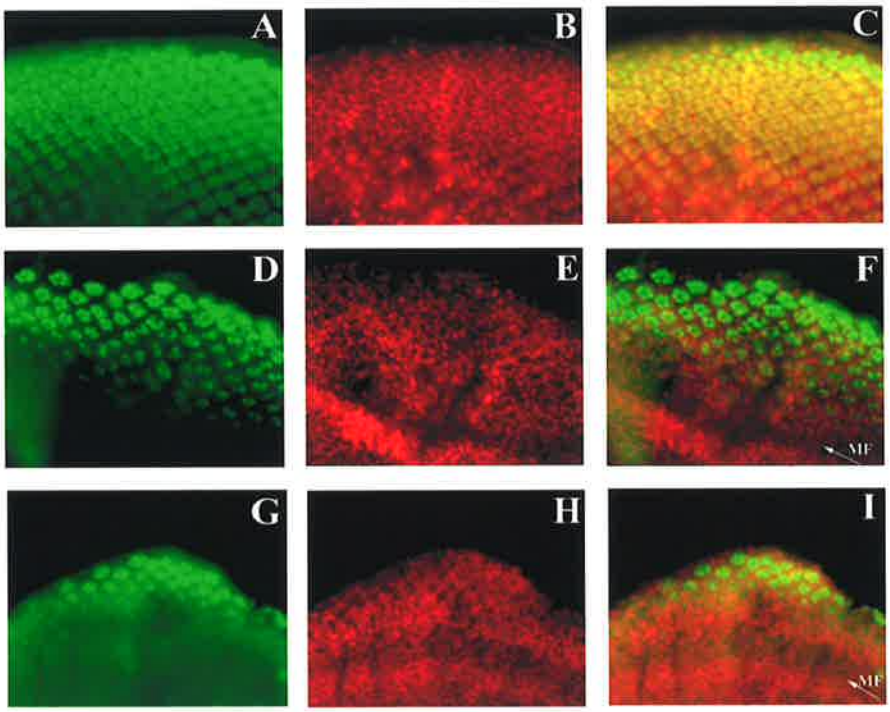

Figure 3.7 Adoption of neural cell fate is delayed in *GMR GAL4::UAS ΔNLSpbl* eye discs.
Third larval instar eye discs were stained with the neural specific antibody ELAV. ELAV is normally expressed in all cells posterior to the morphogenetic furrow which have adopted a neural fate.

A - C. Wild type eye disc stained with α–ELAV in green (A), and hoechst 33258 DNA stain in red (B). The merge of these two images is shown in C.

D - F. *GMR GAL4::UAS pbl* eye disc stained with α–ELAV in green (D), and hoechst 33258 DNA stain in red (E). The pattern of ELAV staining cells is mildly disrupted. The merge of these two images is shown in (F), with the position of the morphogenetic furrow indicated by a white arrow.

G - I. *GMR GAL4::UAS ΔNLSpbl* eye disc stained with α–ELAV in green (G), and hoechst 33258 DNA stain in red (H). A large reduction in the number of ELAV-staining cells is observed posterior to the morphogenetic furrow. However the clustered organisation of the ELAV-expressing cells remains. The merge of these two images is shown in I. The furrow still progresses (white arrow), but only those cells furthest from the furrow are expressing ELAV.

3:5 The effect of ΔNLS PBL expression in the wing disc

As previously discussed, expression of ΔNLS PBL in the proliferating and differentiating cells of the eye disc using the enhancer *GMR* was shown to cause disruptions in cytokinesis, cell shape, and the resultant patterning of the eye disc. Does expression of this construct affect other proliferating tissues? To answer this question, the *ΔNLSpbl* construct was expressed in the developing wing disc using the driver *71B*. When the *UAS pbl* construct is expressed, PBL is observed to localise to the nucleus (**Figure 3.8a**). Surprisingly however, there seems to be no effect of overexpressing PBL on wing development. Adult wings of normal size are produced, with normal venation (**Figure 3.8c**). Expression of *ΔNLSpbl* on the other hand resulted in blistered wings which frequently lacked the two cross veins (**Figure 3.8d**). Ectopic vein tissue was also observed, suggestive of a patterning defect (**Figure 3.8e-f**). The ΔNLS PBL protein was completely cytoplasmic as expected (**Figure 3.8b**).

3:6 The effect of ΔNLS PBL expression in differentiating cells of the eye disc

As described in the previous section, *ΔNLSpbl* causes a severe phenotype when expressed in both the proliferating cells of the eye disc using *GMR* and the proliferating cells of the wing disc using the driver *71B*. To investigate whether the effect of *ΔNLSpbl* was restricted to proliferating cells, the ΔNLS mutant form of the protein was expressed under the control of the *elav GAL4* driver, specific for differentiating cells of the eye (Campos *et al.*, 1987; Robinow and White, 1988). When wild type PBL was expressed under the control of *elav GAL4*, no disruption to eye development was observed (**Figure 3.9a**). However, when ΔNLS PBL was expressed using this driver, a severe rough eye phenotype was observed (**Figure 3.9b**). Eyes were characteristically small and glassy in appearance, with a ring of necrosis in the middle of the eye. As ELAV is expressed in cells that have adopted a neural fate, this indicates that the ΔNLS PBL protein can affect cells that are differentiating, and not just those that are proliferating. These flies were also approximately half the size of their wild type siblings, presumably due to the expression of this driver in other neural tissues.

3:7 The effect of ΔNLS PBL expression in salivary glands

The effect of ΔNLS PBL on non-proliferating tissues was examined further using the salivary gland. The salivary gland of a wild type *Drosophila* is initially formed from a primordium during embryogenesis, in G2 phase of cell cycle 15. Following the 15th division, multiple rounds of endoreplication follow in the absence of mitosis, resulting in the production of large, highly polyploid cells (**Figure 3.10a**). These cells have characteristic regular hexagonal and pentagonal shapes and are conducive to microscopic analysis owing to their large size. To analyse the effect of ΔNLS PBL expression in this tissue, the gut and salivary gland specific driver 109.88 GAL4 (referred to hereafter as sav *GAL4*) was used. The sav *GAL4* construct drives expression in these cells after formation of the primordium, following the terminal cytokinesis of mitosis 15. Endogenous PBL is expressed in this tissue and is found to localise to the nucleus (**Figure 3.10b**). When the full length *pbl* construct is expressed in these cells, the resulting glands are much smaller than wild type, and their cells are significantly rounded (**Figure 3.10c**). PBL retains its nuclear localisation. When *ΔNLSpbl* is expressed, a similar but more severe phenotype is obtained. The glands are even smaller still, and the cells are severely rounded. The ΔNLS PBL is cytoplasmic as expected (**Figure 3.10d**). Therefore ΔNLS PBL, despite being completely cytoplasmic, gives a similar, but more severe phenotype than full length PBL, which is nuclear when expressed in the salivary gland. To compare the expression levels of these two constructs, western analysis was performed using wild type, sav>*pbl* and sav>*ΔNLSpbl* salivary gland samples. As can be seen from **Figure 3.10e**, *UAS pbl* is expressed at a much higher level than *UAS ΔNLSpbl*. Therefore, the severity of the *ΔNLSpbl* phenotype is due to the presence of PBL in the cytoplasm, and not simply an increased expression level.

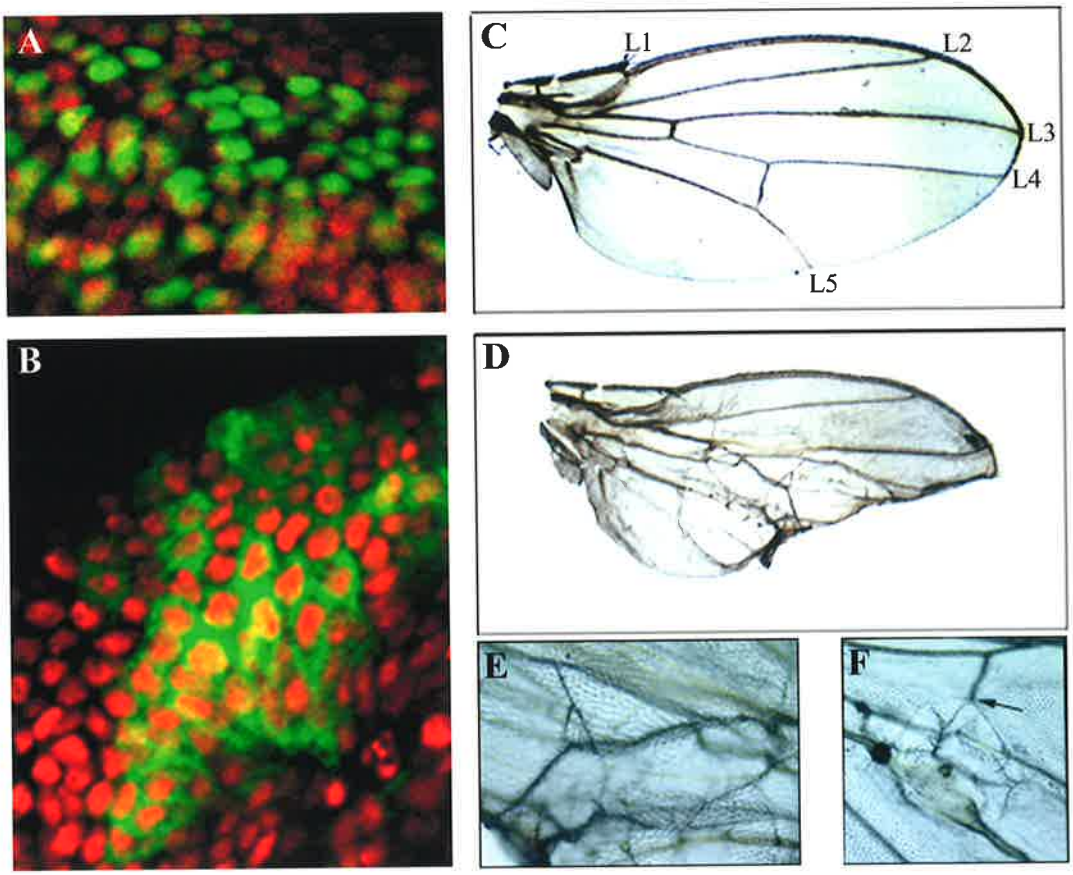

Figure 3.8 ΔNLS PBL disrupts wing development.

A and **B**. *71B GAL4::UAS pbl* and *ΔNLSpbl* third larval instar wing discs were dissected, fixed and stained with anti-PBL antibody (shown in green) and propidium iodide which stains the DNA (shown in red). Confocal images are shown taken with a 40x water lens with 3x zoom. Wild type PBL is observed to localise to the nucleus (A), while ΔNLS PBL is completely cytoplasmic (B).
C. *71B GAL4::UAS pbl* adult wing (5x mag). Overexpressing PBL has no effect on wing development. Adult wings of normal size are produced, with normal venation.
D. *71B GAL4::UAS ΔNLSpbl* adult wing (5x mag). Overexpression of ΔNLS PBL disrupts wing development, producing blistered wings which frequently lack the two cross veins. Ectopic vein tissue is also observed.
E. Close up view of the wing in (D) showing ectopic vein tissue.
F. Close up view of another *71B GAL4::UAS ΔNLSpbl* wing. The venation pattern is disrupted, with cross vein number 2 failing to traverse the distance between L4 and L5 (highlighted by the black arrow). Ectopic veins are also observed.

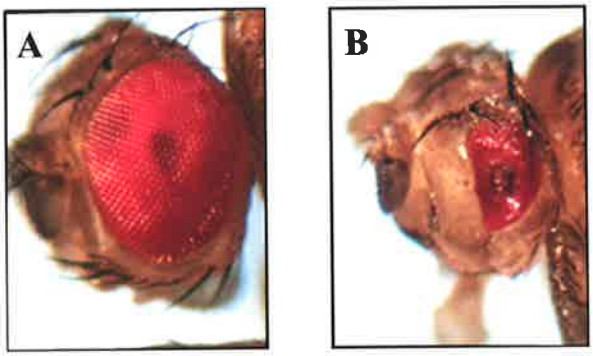

Figure 3.9 Expression of ΔNLS PBL in differentiating cells of the developing larval eye disc.

A. An *elav GAL4::UAS pbl* adult eye at 25 degrees C (5x mag). Expression of PBL in differentiating neural cells of the developing larval eye disc has no effect on the development of the adult eye.

B. An *elav GAL4::UAS ΔNLSpbl* adult eye at 25 degrees C (5x mag). Expression of ΔNLS PBL in differentiating neural cells of the developing larval eye disc causes a severe disruption to eye development. Eyes are reduced in size, and are glassy in appearance with a characteristic ring of necrosis in the middle of the eye. Adult flies are also approximately half the size of their wild type siblings.

While the severity of the ΔNLS PBL phenotype is consistent with that seen in other tissues, the severity of the full-length wild type PBL salivary phenotype is surprising. As discussed in the previous sections, expression of full length PBL causes relatively mild disruptions compared to that of ΔNLS PBL when it is expressed in the eye and wing disc. These observations supported the notion that nuclear localisation is simply a sequestering mechanism to remove Rho GEF action from the cytoplasm. However, the effect of nuclear PBL on the cytoskeleton in the salivary gland challenged this notion and warranted further investigation.

Figure 3.10 ΔNLS PBL affects cell shape when overexpressed in salivary glands.

A- D. *UAS pbl* and *UAS ΔNLSpbl* flies were crossed to the gut and salivary gland specific driver, sav *GAL4*. Salivary glands were then dissected, fixed and stained with phalloidin which binds to filamentous actin (shown in red), and α–PBL (shown in green) unless otherwise indicated.

A. Wild type salivary gland stained with phalloidin in red and α–PBL shown in green. The cells of a wild type gland are a regular hexagonal or pentagonal shape (40x magnification).

B. Wild type salivary gland showing PBL in green and DNA in red. PBL localises to the nucleus (40x magnification).

C. sav *GAL4::UAS pbl* salivary gland stained with phalloidin (red) and PBL (green). PBL is nuclear and cells are rounded (40x magnification).

D. sav *GAL4::UAS ΔNLSpbl* salivary gland stained with phalloidin (red) and PBL (green). PBL is weakly cytoplasmic and cells are rounded (40x magnification). Endogenous PBL is observed to localise to the nucleus.

E. Western analysis of expression levels.
w^{1118}, sav *GAL4::UAS pbl* and sav *GAL4::UAS ΔNLSpbl* salivary glands were dissected at 25°C, boiled and run on a 10% SDS polyacrylamide gel which was then transferred to a nitrocellulose filter. The filter was then probed with an anti-PBL antibody which produced a band of approximately 120 kD in size in each lane. The filter was then stripped and re-probed with an anti-alpha tubulin antibody which served as a loading control. This produced a band of approximately 50 kD in size.
As can be seen from the gel, ΔNLS PBL is expressed at a lower level than full length PBL in the salivary gland.

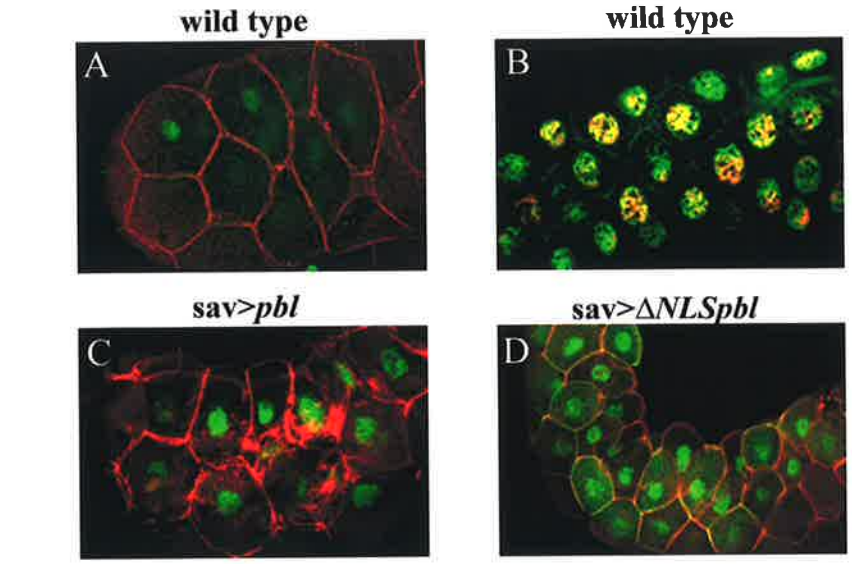
wild type
A
wild type
B
sav>pbl
C
sav>ΔNLSpbl
D

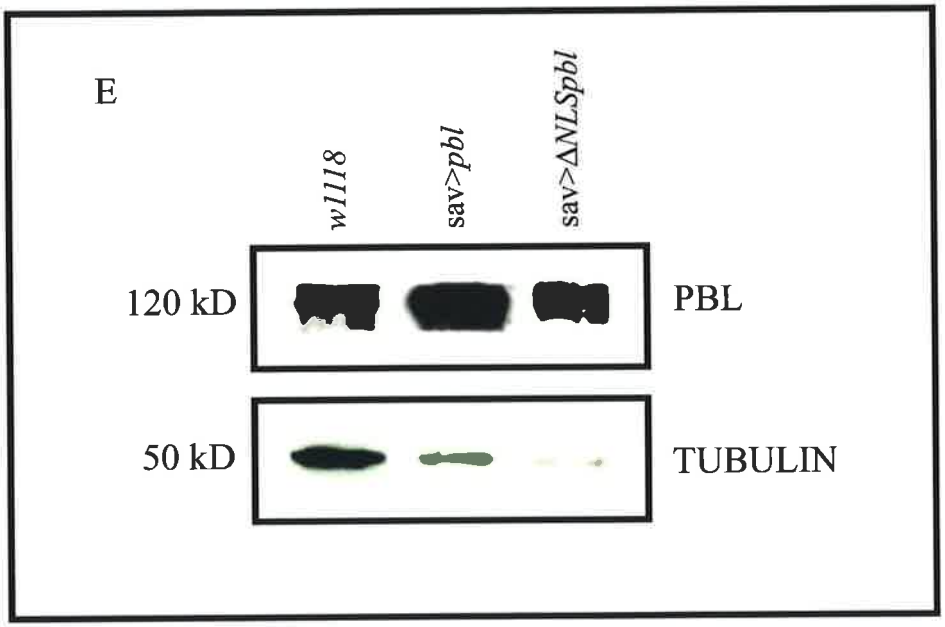
E
w1118
sav>pbl
sav>ΔNLSpbl
120 kD
PBL
50 kD
TUBULIN

3:8 Genetic analysis of the eye phenotype - the ΔNLS PBL eye phenotype is suppressed by a *Rho* mutation

Expression of ΔNLS PBL in a variety of tissues causes extreme phenotypes, regardless of whether expression is driven in proliferating or differentiating tissues. Initial analyses of these phenotypes indicated several defects. In the larval eye disc, both cytokinesis and cell shape was disrupted, a phenotype similar to that caused by the overexpression of a dominant negative form of PBL in the eye. In the pupal eye disc, disruption to the patterning of cells was observed. This disruption was similar to, but more severe than, that caused by the overexpression of full length PBL. In the salivary gland, a severe rounding of the cells was observed, a phenotype that was also similar to that caused by the overexpression of full length PBL. Given this complicated range of phenotypes, it was decided to utilise genetic analysis to further dissect the basis of these phenotypes. The adult eye of *Drosophila* provides an excellent system in which to look for genetic interactions. The rough eye phenotypes caused by overexpression of the various mutant forms of PBL can be used to screen for mutations in other genes that dominantly modify these phenotypes. Characterisation of the genes that are found to interact may provide insight into both PBL function and the basis of the phenotypes generated in the eye.

Two rough eye phenotypes caused by the *GMR*-driven overexpression of PBL and of the dominant negative form of PBL which lacks a portion of the DH domain essential for GTP/GDP exchange (ΔDH PBL), were previously used to screen for dominant modifiers. All of the known members of the Rho family of small GTPases in *Drosophila* were tested in this genetic assay in an attempt to define which member the PBL Rho GEF acts through. RhoA was the only member found to modify these phenotypes, showing a medium suppression of the *GMR>pbl* phenotype and a strong enhancement of the *GMR>ΔDHpbl* dominant negative phenotype (Prokopenko *et al.*, 1999). This indicated that RhoA is the target of PBL activity and that when overexpressed, PBL still acts through a Rho-mediated pathway. Yeast-2-hybrid experiments supported this result, showing that PBL specifically interacts with RhoA, and not other Rho family members, including Rac1 and Cdc42 (Prokopenko *et al.*, 1999).

To test whether the cytoplasmic NLS mutant form of PBL had maintained its specificity for RhoA, a $RhoA^{720}$ mutant allele was introduced into the *GMR>ΔNLSpbl* background. Reducing the amount of Rho in this way was shown to strongly suppress the *GMR>ΔNLSpbl* rough eye phenotype at both 18°C and 25°C, proving that a completely cytoplasmic form of the protein is capable of interacting with Rho (**Figure 3.11a-d**).

The reduction in the level of Rho also completely suppressed the semi-lethality associated with the *GMR>ΔNLSpbl* phenotype at 18°C. When males of the genotype *GMR>ΔNLSpbl / CyO* were crossed to $RhoA^{720}$ / *CyO* virgins to test for suppression, equal numbers of the genotypes *GMR>ΔNLSpbl / CyO*, $RhoA^{720}$ / *CyO* and *GMR>ΔNLSpbl /* $RhoA^{720}$ were expected (*CyO/ CyO* is embryonic lethal). However, at 18°C *GMR>ΔNLSpbl / CyO* flies made up only 15% of the total progeny, while 46% of the progeny were *GMR>ΔNLSpbl /* $RhoA^{720}$, and 39% were $RhoA^{720}$ / *CyO*. The suppression of *GMR>ΔNLSpbl* semi-lethality was strong, but not complete at 25°C. While only 1% of the total progeny were *GMR>ΔNLSpbl / CyO* at 25°C, 18% were *GMR>ΔNLSpbl /* $RhoA^{720}$, and 81% were $RhoA^{720}$ / *CyO*.

The *GMR>ΔNLSpbl* rough eye phenotype was then tested for genetic interactions with mutant alleles or deficiencies covering other characterised members of the Rho family of small GTPases, including Rac 1 and 2, Mtl and Cdc42. In all cases, loss of one copy of the gene did not result in suppression of the *GMR>ΔNLSpbl* rough eye phenotype, indicating that the ΔNLS PBL maintained its specificity for RhoA (**Table 3.1**).

As previously discussed, the ΔDH mutant form of the PBL protein, where a portion of the DH domain responsible for GEF activity had been deleted, was shown to act as a dominant negative. While deletion of this domain resulted in a comparatively moderate phenotype in the eye, reduction of the amount of PBL through the introduction of a *pbl* null mutant allele, was shown to strongly enhance this *GMR>ΔDHpbl* rough eye phenotype (L. O'Keefe, pers comm; Prokopenko *et al.*, 1999). To test whether the ΔNLS mutant form of the protein was acting as a dominant negative, two *pbl* null mutant alleles were tested for their ability to dominantly enhance this phenotype. Both were found to have no effect on the *GMR>ΔNLSpbl* rough eye phenotype. Thus the completely cytoplasmic ΔNLS PBL is not interfering with normal PBL function to cause the severe phenotypes observed, but is still functioning through its GEF domains to activate RhoA (**Table 3.1**).

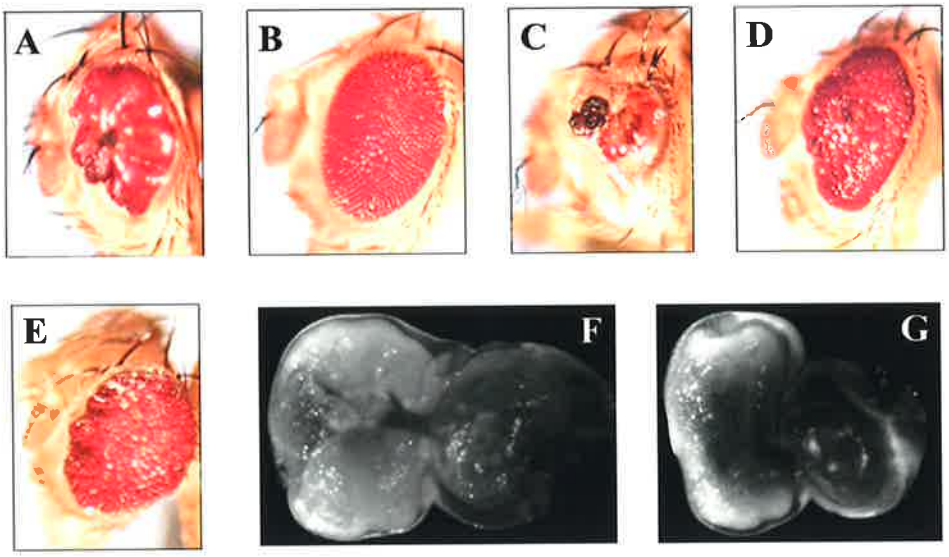

Figure 3.11 Suppression of the *GMR GAL4::UAS ΔNLSpbl* rough eye phenotype by *RhoA*.

A. A *GMR GAL4::UAS ΔNLSpbl* adult eye at 18 degrees C. Eye development is disrupted by the overexpression of ΔNLS PBL posterior to the morphogenetic furrow of the developing larval eye disc.

B. Suppression of the *GMR GAL4::UAS ΔNLSpbl* rough eye phenotype in $RhoA^{720}$ heterozygotes at 18 degrees C. The rough eye phenotype caused by the overexpression of ΔNLS PBL posterior to the morphogenetic furrow is strongly suppressed when a *RhoA* mutant allele is introduced into the genetic background of these flies.

C. A *GMR GAL4::UAS ΔNLSpbl* adult eye at 25 degrees C. A severe rough eye phenotype is produced by the overexpression of ΔNLS PBL posterior to the morphogenetic furrow.

D. Suppression of the *GMR GAL4::UAS ΔNLSpbl* rough eye phenotype in $RhoA^{720}$ heterozygotes at 25 degrees C. The rough eye phenotype caused by the overexpression of ΔNLS PBL posterior to the morphogenetic furrow is strongly suppressed when a *RhoA* mutant allele is introduced into the genetic background of these flies.

E. Suppression of the *GMR GAL4::UAS ΔNLSpbl* rough eye phenotype by *GMR>p35*. The rough eye phenotype can be suppressed at 18 degrees C by the overexpression of the cell death inhibitor, *p35* (compare to A).

F. Acridine orange stain of a *GMR GAL4::UAS pbl* larval eye disc.

G. Acridine orange stain of a *GMR GAL4::UAS ΔNLSpbl* larval eye disc. There is a slight increase in the number of staining cells.

This finding that ΔNLS PBL is not acting as a dominant negative form of the protein is quite perplexing, given the similar nature of the ΔNLS PBL and ΔDH PBL phenotypes in larval eye disc cells. As shown previously, *GMR>ΔNLSpbl* and *GMR>ΔDHpbl* gave very similar phenotypes in these cells, with a disruption in cytokinesis leading to multinucleate cells, in addition to a disruption in cell shape. Therefore, although these two constructs give similar phenotypes at the larval stage of development, it appears to be for different reasons. These reasons most likely explain the very different adult eye phenotypes that result from the overexpression of these two constructs.

The *GMR>ΔNLSpbl* rough eye phenotype was then tested against mutant alleles of numerous other genes including genes involved in cytokinesis, cell death, and DNA damage checkpoints (**Table 3.1**). The only gene found to have an effect on the eye phenotype, other than *RhoA*, was *p35*. P35 is an apoptosis inhibitor and *GMR>p35* results in the overexpression of this cell death inhibitor in the eye disc (Hay *et al.*, 1994). This was found to suppress the *GMR>ΔNLSpbl* rough eye phenotype (**Figure 3.11e**).

In contrast to this, *GMR>p35* has previously been shown to enhance the *GMR>pbl* rough eye phenotype. The *GMR>pbl* rough eye phenotype was shown to be due to an inhibition of some of the normal programmed cell death events in the pupal eye disc. Inhibiting this process further with the overexpression of P35 resulted in an enhancement of this phenotype in the eye (L. O'Keefe, pers comm). The opposite seems to be true for the *GMR>ΔNLSpbl* rough eye phenotype, implying that some of the phenotype results from programmed cell death. However, induction of cell death may be a secondary effect of disrupting cells in the eye disc and not an indication of a direct involvement of PBL in programmed cell death. Whatever damaging effect the expression of the ΔNLS mutant form of the protein has on the eye disc cells, apoptosis may be signalled to remove these damaged cells. Therefore inhibiting cell death in the eye may suppress the phenotype simply because damaged cells which would normally be removed by programmed cell death are being kept alive. Acridine orange staining for cell death in larval eye discs indicated that the levels of cell death are only slightly increased in *GMR>ΔNLSpbl* eye discs compared to that of *GMR>pbl* (**Figure 3.11f-g**). It is therefore likely that cell death is occurring later in development to remove cells damaged by the expression of the ΔNLS mutant form of PBL. This possibility was not examined here, as it would not necessarily shed any further light on PBL function, but could be confirmed by a detailed analysis of apoptosis during the later development of the eye discs.

Table 3.1 Screening for enhancement or suppression of the *GMR GAL4::UASΔNLSpbl* rough eye phenotype

Flies of the genotype *GMR GAL4::UASΔNLSpbl* were crossed to produce flies heterozygous for loss of function alleles or deficiencies covering the genes listed in the table.

RhoA, Rac1, Rac2, cdc42, and *Mtl* are all Rho family members. $RhoA^{720}$ is a null allele (Strutt *et al.*, 1997). $cdc42^{3}$ is a lethal allele (Fehon *et al.*, 1997) and *ΔMtl* is a deletion which removes the entire *Mtl* open reading frame (Hakeda-Suzuki *et al.*, 2002). There were no specific mutations available in *Rac1* and *Rac2* and so deficiency stocks were used. The deficiency *Df(3L)Ar14-8* removes *Rac1*. *Df(3L)RM5-2* is a large deficiency which deletes the *pbl* gene as well as *Rac2*. This stock was tested alone, as well as with a cosmid (*cos34*), which carries the entire *pbl* gene, recombined onto the same chromosome. This cosmid is known to completely rescue PBL function (J. Wong and R. Saint, unpublished observations). pbl^{2} and pbl^{3} are both null alleles of *pbl* (Prokopenko *et al.*, 1999). Dia^{2} has a specific mutation in *Diaphanous*, a *Drosophila* formin protein required for actin re-organisation and cytokinesis (Castrillon and Wasserman, 1994). $chic^{221}$ has a mutation in *chickadee* which encodes profilin and acts downstream of *Diaphanous* during actin re-organisation (Verheyen and Cooley, 1994). acu^{E636} has a specific mutation in *act-up* which controls actin polymerisation and acts in the opposite direction to *chickadee* (Benlali *et al.*, 2000). *Diaphanous*, *chickadee* and *act-up* are all Rho effectors. *Df(3R)H99* is a deficiency which takes out the cell death genes *Hid*, *Grim*, and *Reaper*. *GMR>p35* overexpresses the apoptosis inhibitor *p35* (Hay *et al.*, 1994). grp^{1} is a maternal-effect lethal mutation in the checkpoint gene *grapes* (Fogarty *et al.*, 1994). RBF^{14} is a null allele of the *Drosophila* retinoblastoma family protein (Du *et al.*, 1996; Du and Dyson, 1999).

Gene screened	Effect on phenotype of *GMR GAL4::UASΔNLSpbl*
RhoA^{720}	Strong suppression
Df(3L)Ar14-8 (*Rac1*)	No effect
Df(3L)RM5-2 (*Rac2* and *pbl*)	No effect
Df(3L)RM5-2,cos34 (*pbl*$^{+}$)	No effect
cdc 42^{3}	No effect
ΔMtl	No effect
pbl^{2}	No effect
pbl^{3}	No effect
Dia^{2}	No effect
chic^{221}	No effect
acu^{E636}	No effect
Df(3R)H99	No effect
GMR>p35	Medium suppression
grp^{1}	No effect
RBF^{14}	No effect

3:9 Genetic analysis of the salivary gland phenotype - ΔNLS PBL does not interact with Rho

In the eye system, expression of both PBL and ΔNLS PBL were shown to act predominantly through RhoA. To test if this action of PBL was also true in the salivary gland, the *RhoA*^{720} null mutant allele was recombined onto both the *UAS pbl* chromosome and the *UAS ΔNLSpbl* chromosome, and each stock was crossed to the sav *GAL4* driver. Reduction of RhoA in the sav *GAL4:UAS pbl* salivary gland leads to a strong suppression of the phenotype (**Figure 3.12b**). The resultant glands are much larger, and the cells are less round and more wild type in shape. Reduction of RhoA in the sav *GAL4:UAS ΔNLSpbl* salivary glands on the other hand, does not appear to be able to suppress this phenotype (**Figure 3.12d**). Given the possibility that this phenotype is just too severe to be rescued merely by reducing the amount of Rho by half, the cross was repeated at 18°C. At this lower temperature, sav *GAL4* is not as highly expressed, leading to a less severe effect on salivary gland structure (**Figure 3.12e**). However, reducing the amount of RhoA still cannot rescue the *ΔNLSpbl* salivary gland phenotype (**Figure 3.12f**). Therefore, while RhoA can suppress the severe ΔNLS PBL phenotype in the eye, it appears to be unable to do so in the salivary gland. This difference indicates either differing roles for PBL in these tissues, or differing modes of regulation.

Figure 3.12 Removal of one copy of *RhoA* does not suppress the ΔNLS PBL salivary gland phenotype.

UAS pbl and *UAS ΔNLSpbl* flies were crossed to the gut and salivary gland specific driver sav::*GAL4* at the temperatures indicated. Salivary glands were then dissected, fixed and stained with phalloidin which binds to filamentous actin (shown uncoloured and in red), and α–PBL (shown in green).

A- B. A sav *GAL4::UAS pbl* salivary gland (A) and a sav *GAL4::UAS pbl* salivary gland heterozygous for a null *RhoA* mutant allele (B) at 25°C. Phalloidin staining is shown uncoloured in (A) and (B) and false coloured red along with PBL staining in green in (A') and (B'). Removal of one copy of *RhoA* suppresses the salivary gland phenotype (10x mag).

C- D. A sav *GAL4::UAS ΔNLSpbl* salivary gland (C) and a sav *GAL4::UAS ΔNLSpbl* salivary gland heterozygous for a null *RhoA* mutant allele (D) at 25°C. Phalloidin staining is shown uncoloured in (C) and (D) and false coloured red along with PBL staining in green in (C') and (D'). Removal of one copy of *RhoA* does not suppress the phenotype at 25°C (10x mag).

E- F. A sav *GAL4::UAS ΔNLSpbl* salivary gland (E) and a sav *GAL4::UAS ΔNLSpbl* salivary gland heterozygous for a null *RhoA* mutant allele (F) at 18°C. Phalloidin staining is shown uncoloured in (E) and (F) and false coloured red along with PBL staining in green in (E') and (F'). Removal of one copy of *RhoA* does not suppress the phenotype at 18°C (10x mag).

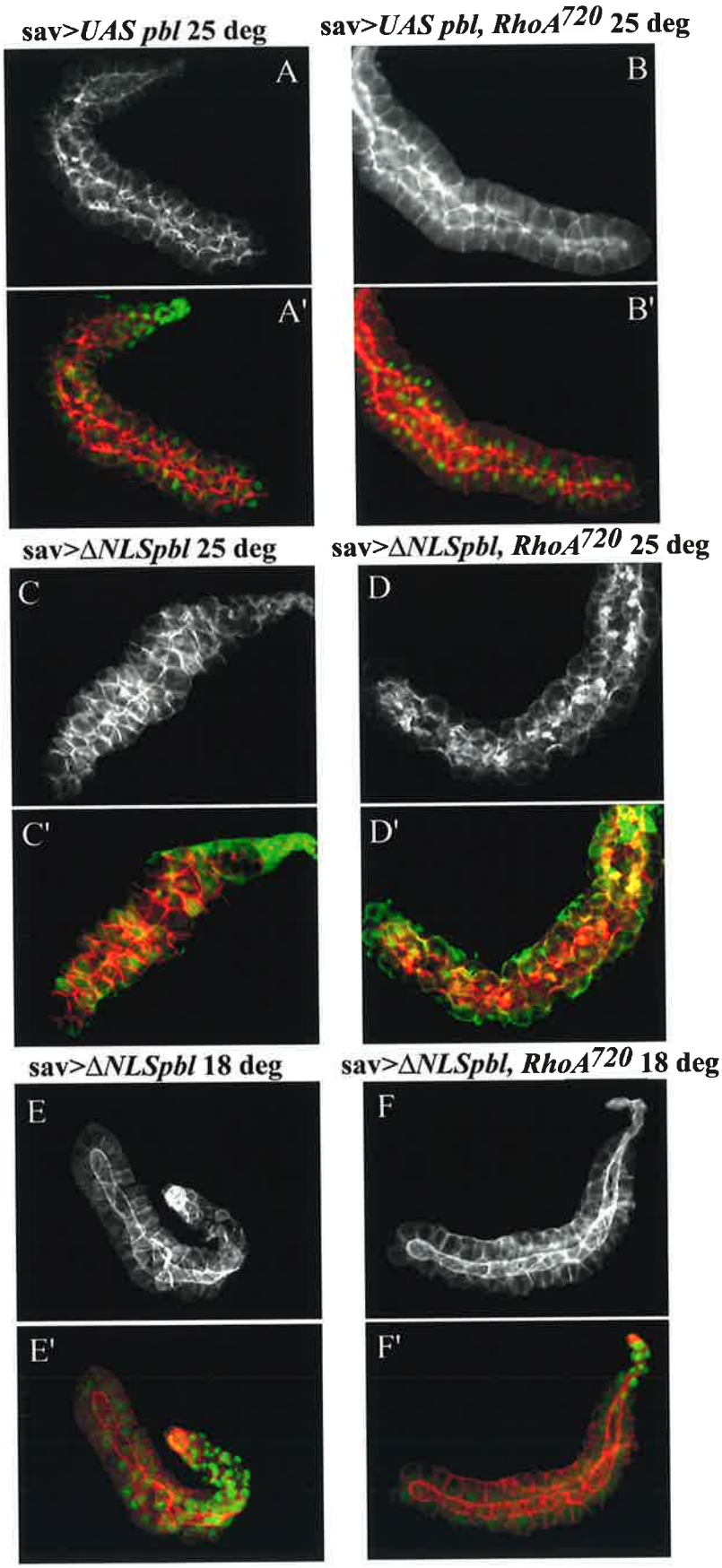
sav>UAS pbl 25 deg
sav>UAS pbl, RhoA720 25 deg
A
B
A'
B'
sav>ΔNLSpbl 25 deg
sav>ΔNLSpbl, RhoA720 25 deg
C
D
C'
D'
sav>ΔNLSpbl 18 deg
sav>ΔNLSpbl, RhoA720 18 deg
E
F
E'
F'

3:10 ΔNLS PBL can still activate cytokinesis

As discussed in the previous sections, expression of ΔNLS PBL causes extreme phenotypes in both proliferating and differentiating tissues. Localisation of the protein to the nucleus is therefore highly important for the maintenance of normal cellular processes. However, is localisation of PBL to the nucleus essential for its role in cytokinesis? To answer this question, ΔNLS PBL was expressed in a *pbl* mutant background using the embryonic driver *prd GAL4* (Yoffe *et al.*, 1995). When full length PBL is expressed in stripes along the *pbl* mutant embryo using this driver, the cytokinetic defect of the *pbl* mutant is completely rescued within those stripes (**Figure 3.13a-c**). This provides an excellent system in which to test the importance of the individual domains of the protein for cytokinesis. As *prd GAL4* expresses in alternate segments along the embryo, the intervening segments where no protein is expressed also provides an internal negative control. When ΔNLS PBL was expressed in a *pbl* mutant background in alternate segments using this driver, the cytokinetic defect was completely rescued within those stripes (**Figure 3.13d-f**). Thus localisation of the protein to the nucleus is not essential for the process of cytokinesis. ΔNLS PBL was observed to be completely cytoplasmic as expected (**Figure 3.13g**).

3:11 Discussion

The *pebble* (*pbl*) gene is required for cytokinesis in *Drosophila*. The PBL protein contains Dbl Homology (DH), and Pleckstrin Homology (PH) domains, characteristic of GTP exchange factors that activate the Rho family of small GTPases (RhoGEFs). In their active form, these Rho family GTPases mediate reorganisation of the actin cytoskeleton, which is an essential event during cytokinesis. PBL also contains BRCT (BRCA1 C-Terminal) domains, which are found in a number of proteins involved in DNA repair. The presence of domains within a Rho GEF that normally function in the nucleus is both unique and intriguing. In accordance with a potential nuclear role for PBL, PBL contains a consensus bipartite nuclear localisation signal (NLS) and is observed to localise to the nucleus after its transient cortical and cleavage furrow localisation late in mitosis.

Nuclear localisation of PBL could simply be a means of removing the PBL Rho GEF activity from the cytoplasm during interphase, or could be indicative of a separate nuclear function. In an attempt to examine the importance of nuclear sequestration, the consensus bipartite NLS was specifically mutated and the altered protein was expressed in a variety of tissues. Mutation of $lys^{318}/arg^{319}/lys^{320}$ to $asn^{318-320}$ was found to completely abolish the nuclear localisation of the protein, proving that the predicted bipartite NLS functions as a nuclear localisation signal *in vivo*.

The ΔNLS cytoplasmic form of the protein was then found to cause a range of severe phenotypes when overexpressed in a variety of different tissues. Compared to full length PBL, which causes a mild roughening of the eye when overexpressed in the developing larval eye disc, ΔNLS PBL causes a severe roughening of the eye. The *GMR>ΔNLSpbl* adult eye is significantly smaller and blistered in appearance, with large areas of necrosis. Initial analysis of this phenotype indicated that cytokinesis is disrupted in the larval eye disc cells, resulting in both multinucleate and anucleate cells, a phenotype which is similar to that caused by the overexpression of a dominant negative form of the PBL protein. However, owing to the compact structure of the eye disc itself, it is difficult to determine the precise behaviour of cells in this tissue.

Later in development, the patterning of the pupal disc is also affected. Even the weaker expression of *ΔNLSpbl* at 18°C caused a disruption in the number of bristle, interommatidial and cone cells. This phenotype was similar to, but more severe than, that observed when the full-length PBL protein is expressed in the developing eye. Defects in pattering occurred early in the development of eye cells, with the number of ELAV-expressing neural cells severely reduced posterior to the morphogenetic furrow of the developing larval eye disc. As the morphogenetic furrow progresses, the differentiation of neural cells posterior to the furrow seems to be delayed, but not prevented, by expression of ΔNLS PBL, as some neural cell clusters are observed. Indeed, later in the development of the adult eye, neural cell types are still observed.

The *ΔNLSpbl* construct was also shown to affect the proliferating cells of the wing disc, the differentiating cells of the eye disc when driven by the *elav GAL4* promoter, and the non-cytokinetic cells of the salivary gland. Thus expression of ΔNLS PBL in a variety of tissues causes extreme phenotypes, regardless of whether expression is driven in proliferating tissues or tissues that have ceased proliferation and are differentiating.

The phenotype generated by expression of the *ΔNLSpbl* construct in the eye was strongly suppressed by reducing the amount of RhoA, but not of other Rho family G proteins,

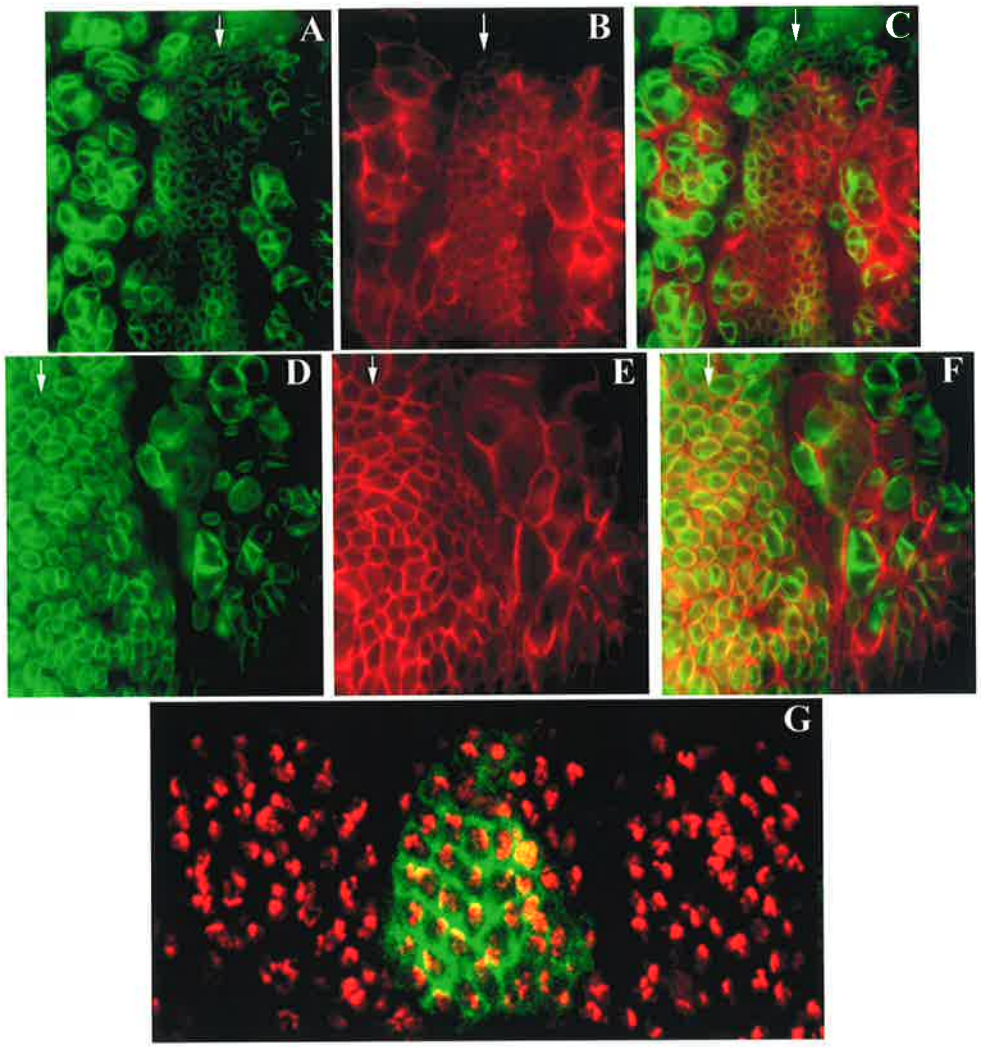

Figure 3.13 ΔNLS PBL can rescue cytokinesis in a *pbl* mutant background. **A- C**. A *prd GAL4, pbl^{2}/UAS pbl, pbl^{3}* embryo expressing wild type PBL in a *pbl* mutant background. The embryo was fixed and stained with anti-lamin which highlights the nuclear envelope, shown in green in (A), and anti-spectrin which stains the cell cortex, shown in red in (B). The merge of these two images is shown in (C). Expression of wild type PBL in alternate stripes along the embryo using *prd GAL4*, completely rescued the cytokinetic defect of the *pbl* mutant within those stripes. The rescue stripe is indicated by the white arrows. **D- F**. A *prd GAL4, pbl^{2}/UAS ΔNLSpbl, pbl^{3}* embryo expressing ΔNLS PBL in a *pbl* mutant background. The embryo was fixed and stained with lamin (D) and spectrin (E). The merge of these two images is shown in (F). Expression of ΔNLS PBL in stripes along the embryo using *prd GAL4*, completely rescued the cytokinetic defect of the *pbl* mutant within those stripes (white arrows). **G**. A *prd GAL4, pbl^{2}/UAS ΔNLSpbl, pbl^{3}* embryo expressing ΔNLS PBL in a *pbl* mutant background. The embryo was fixed and stained with anti-PBL (shown in green) and propidium iodide which stains the DNA (shown in red). PBL is completely cytoplasmic.

indicating that this cytoplasmic form of PBL continues to act through RhoA. However, in the case of Rac, the redundancy between the three *Drosophila* Rac proteins Rac1, Rac2 and Mtl (Hakeda-Suzuki *et al.*, 2002) poses a problem in that unless all three are removed at the same time, it cannot be concluded that PBL does not act through Rac. Also the fact that the only available Rac alleles were deficiencies that take out large regions of the chromosome, introduces the possibility that other genetic interactions may mask any potential interaction with Rac. In particular, *Rac2* lies within a deficiency that also removes *pbl*. To counteract this, a cosmid carrying the entire *pbl* gene and known to rescue *pbl* function (Wong and Saint, unpublished observations) was recombined onto the *Rac2, pbl* deficiency chromosome. This was also found to have no effect on the *GMR>pbl* or *GMR>ΔNLSpbl* rough eye phenotypes.

Reducing the amount of PBL through the introduction of a *pbl* null mutant allele had no effect on the *GMR>ΔNLSpbl* phenotype. This suggested that ΔNLS PBL is not acting as a dominant negative form of the PBL protein, despite the similarities in its larval eye phenotype to that of the ΔDH dominant negative form of the protein. The different action of these two forms is consistent with clear differences in the resultant adult eye phenotypes.

Overexpression of the cell death inhibitor P35 was found to moderately suppress the *GMR>ΔNLSpbl* rough eye phenotype. This was in contrast to the observed enhancement of the *GMR>pbl* phenotype by *GMR>p35*. No dramatic differences in larval eye disc apoptosis were observed, indicating that the suppression by *GMR>p35* is likely to be due to blocking a secondary apoptotic effect induced by the extreme disruption to cell function in *GMR>ΔNLSpbl* expressing cells.

Expression of the ΔNLS construct in the salivary gland was shown to cause a similar but more severe effect than the expression of full length PBL. Even though full length PBL is nuclear when expressed in the salivary gland, a surprisingly strong effect on the cytoskeleton was observed with a decrease in cell size and a rounding of the cell shape. When ΔNLS PBL was expressed, the cells were smaller still and showed extreme rounding. The dramatic effect of full length PBL in this tissue was surprising given its nuclear localisation. The similarity in the phenotypes between the nuclear PBL and the cytoplasmic ΔNLS PBL challenges the concept that the localisation of the wild type protein to the nucleus is simply a sequestering mechanism to remove Rho GEF action from the cytoplasm. Reduction of RhoA was then shown to suppress the PBL phenotype in the salivary gland. However, reducing Rho was unable to suppress the ΔNLS PBL phenotype. Whether the cytoplasmic form is acting through another pathway in this tissue, or whether the phenotype is just too severe to be

suppressed by reducing RhoA remains to be seen. One possibility is that expression driven by sav *GAL4* in the salivary gland is higher than that of *GMR GAL4* in the eye, allowing other G proteins to be activated in this tissue. Analysis of the ability of other Rho family members to suppress these phenotypes would resolve this question. A second possibility is that the effect could be GEF independent.

The primary conclusion from this work arises from the range of severe phenotypes caused by the cytoplasmic form of PBL. It is clear that the sequestration of the protein to the nucleus is essential for the maintenance of normal cellular processes during development. This finding supports the proposal that the purpose of nuclear localisation at the end of cytokinesis is removal of PBL Rho GEF activity from the cytoplasm following completion of cytokinesis. The phenotypes observed with ΔNLS PBL could be caused by unregulated Rho GEF activity in the cytoplasm. However, nuclear localisation is not the only possible way of removing PBL function from the cytoplasm at the appropriate time. Post translational modifications such as phosphorylation or degradation could be used to regulate PBL function in the cytoplasm, while nuclear localisation could be associated with a completely separate nuclear function. In support of this, and in contrast to previous results, was the severe effect on the actin structure caused by the overexpression of nuclear wild type PBL. The ability of a nuclear form of the protein to modify the cytoskeleton in such a way suggested that, at least in this tissue, nuclear sequestration is not sufficient.

In addition to this, the ability of the completely cytoplasmic form of PBL to activate cytokinesis showed that nuclear localisation is not essential for the role of the protein in cytokinesis. In the case of the yeast Cdc24p GEF, its correct localisation and function at the bud site requires its association with another factor in the nucleus (Toenjes *et al.*, 1999; Nern and Arkowitz, 2000; O'Shea and Herskowitz, 2000; Shimada *et al.*, 2000). Therefore in the case of PBL, either a nuclear co-factor is not needed, or it is able to interact with a co-factor in the cytoplasm.

So why does PBL localise to the nucleus? The results discussed so far cannot discount the possibility of a separate nuclear role, and the presence of nuclear acting BRCT domains within the protein also add further weight to this possibility. Why would highly conserved BRCT domains be present in a protein whose only action is in the cytoplasm? Do they play a separate nuclear function, or is their role to anchor the PBL protein in the nucleus during interphase? These questions are addressed in the next chapter, where *in vitro* mutagenesis was used to delete the potential nuclear functional domains of the protein, and the effect was analysed in transgenic flies.

Chapter 4: Analysis of a separate nuclear role for PBL

4:1 Introduction

As previously discussed, *pbl* encodes a Rho GEF protein whose predicted action in cytokinesis is to activate Rho in the cytoplasm, enabling both the correct formation and function of the contractile ring (Prokopenko *et al.*, 1999). However, in addition to the DH and PH domains deemed responsible for this action, PBL also notably contains several domains known to have nuclear functions. PBL contains a consensus bipartite nuclear localisation signal, and is observed to localise to the nucleus after its transient cortical and cleavage furrow localisation late in mitosis (Prokopenko *et al.*, 1999). As discussed in the previous chapter, mutation of this nuclear localisation signal results in a completely cytoplasmic form of the protein. Expression of this form in a variety of tissues causes a range of severe phenotypes, suggesting that the sequestration of the protein to the nucleus is highly important. The question that now remains is whether nuclear localisation is simply a sequestering mechanism, removing PBL Rho GEF activity from the cytoplasm once its role in cytokinesis has been completed, or whether PBL has a separate nuclear function.

In support of a separate nuclear function for PBL, the protein contains two consensus BRCT domains, domains that are known to be associated with the nuclear process of DNA repair (Bork *et al.*, 1997; Callebaut and Mornon, 1997). BRCT domains were initially identified in the human BRCA1 breast cancer tumour suppressor protein (Koonin *et al.*, 1996), and have since been found in numerous other proteins from yeast to man. Included within these is the human XRCC1 DNA repair protein. XRCC1 contains two BRCT domains which interact independently with DNA ligase III and poly (ADP-ribose) polymerase to repair DNA single-strand breaks (Cappelli *et al.*, 1997; Nash *et al.*, 1997; Masson *et al.*, 1998; Taylor *et al.*, 1998). A similar story is observed with many other BRCT domain-containing proteins, whose unifying feature seems to be their involvement in maintaining the integrity of the genome. **Table 1.1** in the introduction shows a summary of some of the characterised BRCT domain-containing proteins and their predicted functions.

The presence of such domains within PBL, a Rho GEF, poses an interesting, yet perplexing question for the function of the PBL protein. If the only role for PBL is in the cytoplasm to activate Rho, and movement into the nucleus is a means of regulating its action in the cytoplasm, then why does it contain two highly conserved nuclear acting domains? In addition to these two BRCT domains, PBL also contains a third as yet uncharacterised region termed the RadECl region. The RadECl region is a region of extended homology immediately N-terminal to the first BRCT domain, which shares a high level of similarity with the proteins RAD4-like and ECT2 (chapter 1, **Figure 1.7**). RAD4-like, also known as Topoisomerase IIβ–Binding Protein (TopBP1) is a human protein with 8 BRCT domains which has been implicated in the response to DNA damage. It has been shown to interact with both hRAD9 and DNA polymerase ε and is also able to bind DNA strand breaks, suggesting that it might act as a DNA damage sensor (Yamane and Tsuruo, 1999; Makiniemi *et al.*, 2001). ECT2 is the murine homologue of *pbl* which, like PBL, localises to the nucleus during interphase, and contains two BRCT domains (Miki *et al.*, 1993; Tatsumoto *et al.*, 1999). Therefore, considering the presence of known nuclear domains, and the nuclear localisation of the protein, a separate nuclear function for PBL, unrelated to Rho, is a distinct possibility. In addition to this, a third possibility is that PBL plays a separate Rho-dependent nuclear function, which would be completely novel. Considering the findings of the previous chapter, another possibility is that the RadECl/BRCT domains anchor PBL in the nucleus to keep it out of the cytoplasm during interphase.

In an attempt to differentiate between these possibilities, and to begin to understand the role PBL may play in the nucleus, a second *in vitro* mutagenesis construct was made. This construct was designed to delete the three possible nuclear acting domains of the protein; the RadECl region, and the two BRCT domains. Flies transgenic for this construct were obtained, and the mutant protein was expressed in a variety of tissues to answer the following questions:

1) Has the localisation of the protein been altered by this deletion?

2) What effect does this deletion have when expressed in different tissues?

3) Are these domains required for cytokinesis?

4) Or are these domains responsible for a separate nuclear function for PBL?

4:2 Site directed deletion of the potential nuclear functional domains of PBL

In an attempt to determine the role, if any, of the nuclear domains of PBL, *in vitro* mutagenesis was used to delete the sequence that encodes them from the *pbl1A cDNA* sequence. 858 base pairs were specifically deleted from the *pbl1A* cDNA sequence which, when translated, removes 286 amino acids (amino acids 7 through to 292). This deletion removes the two consensus BRCT domains as well as the majority of the RadECl region (**Figure 4.1a**). This deletion was obtained by designing a set of complementary primers that lack the sequence of the region to be deleted, but bind to either side of the region (**Figure 4.1b**). Upon binding to their complementary sequences, the primers cause the intervening sequence to loop out. After PCR amplification, the newly synthesised product will specifically lack the sequence between the two primer binding sites. Potential mutant clones were initially screened on the basis of their smaller size, before their sequence was determined to ensure that they lacked the specific base pairs desired, and that the sequence either side of the deletion was normal. This deletion construct, which removes the RadECl region and two BRCT domains, will hereafter be referred to as the ΔBRCT construct, although it should be noted that it removes the RadECl region as well.

A ΔBRCT mutant *pbl* cDNA sequence was then cloned into the multiple cloning site of the pUAST P element-mediated transformation vector using the enzymes XhoI and XbaI. As previously discussed, this vector places the gene of interest under the direct control of a *S. cerevisiae GAL4* upstream activator sequence (UAS), whose expression can be induced by the presence of the yeast GAL4 protein (Brand and Perrimon, 1993). The *ΔBRCTpbl* cDNA pUAST construct was transformed into *Drosophila* by microinjection, and after subsequent crosses, 10 separate transgenic lines were established. The position of the insert in these lines was then determined by genetic mapping. Two lines mapped to the X chromosome, three mapped to the second chromosome, and five mapped to the third chromosome. All but two of these inserts were homozygous viable.

4:3 Expression of ΔBRCT PBL in the *Drosophila* eye disc causes a severe rough eye

To determine whether deletion of the potential nuclear functioning domains had altered the localisation of the protein, and to analyse the effect of this deletion, the eye specific enhancer *GMR* was used, as before, to drive the expression of the ΔBRCT mutant protein in the developing eye disc. As shown previously, when this system was used to drive the expression of full length PBL, the protein was observed to localise to the nucleus (**Figure 4.2a**). Upon nuclear envelope breakdown during prophase/metaphase, *GMR*-driven PBL becomes redistributed throughout the cytoplasm (**Figure 4.2b**). When *UAS ΔBRCTpbl* was expressed using this driver, the mutant protein retained its nuclear localisation. ΔBRCT PBL was nuclear in all cells (**Figure 4.2c**) apart from those undergoing mitosis where it was observed in the cytoplasm (**Figure 4.2d**).

GMR-driven expression of ΔBRCT PBL results in a much more severe adult eye phenotype than that of full-length wild type PBL, despite maintaining its nuclear localisation (**Figure 4.3b**). Of the seven lines tested, two were lethal when expressed under the control of the *GMR* promoter at 25°C. As discussed previously, the eye is a non essential organ for flies raised under laboratory conditions, and the lethality of this construct is presumably due to the leaky expression of the driver in other tissues. Two lines gave extremely rough eye phenotypes, and three gave very rough eye phenotypes. All of the transgenic lines tested gave much more severe phenotypes than *GMR>pbl*. The eyes were characteristically much smaller than *GMR>pbl*, but, unlike the *GMR>ΔNLSpbl* rough eye phenotype, they maintained most of their pigment. The *GMR>ΔBRCTpbl* eyes were characteristically small and glassy in appearance, a very different phenotype to that of *GMR>pbl* and *GMR>ΔNLSpbl* flies. Sections of the *GMR>ΔBRCTpbl* eyes confirmed the extreme nature of the phenotype, revealing a severe disruption of the eye structure (**Figure 4.3d-f**). *GMR>ΔBRCTpbl* adult eyes raised at 25°C were so disrupted that it was deemed pointless to attempt to section them. Two separate *ΔBRCTpbl* transgenic lines, one which gave a relatively mild rough eye phenotype, and one which gave a medium rough eye phenotype when expressed under the control of *GMR*, were therefore sectioned at 18°C. Despite the comparatively milder phenotypes of these flies, the resultant sections were so severely disrupted that it was difficult to make any conclusions on the basis of the phenotype (**Figure 4.3d-f**).

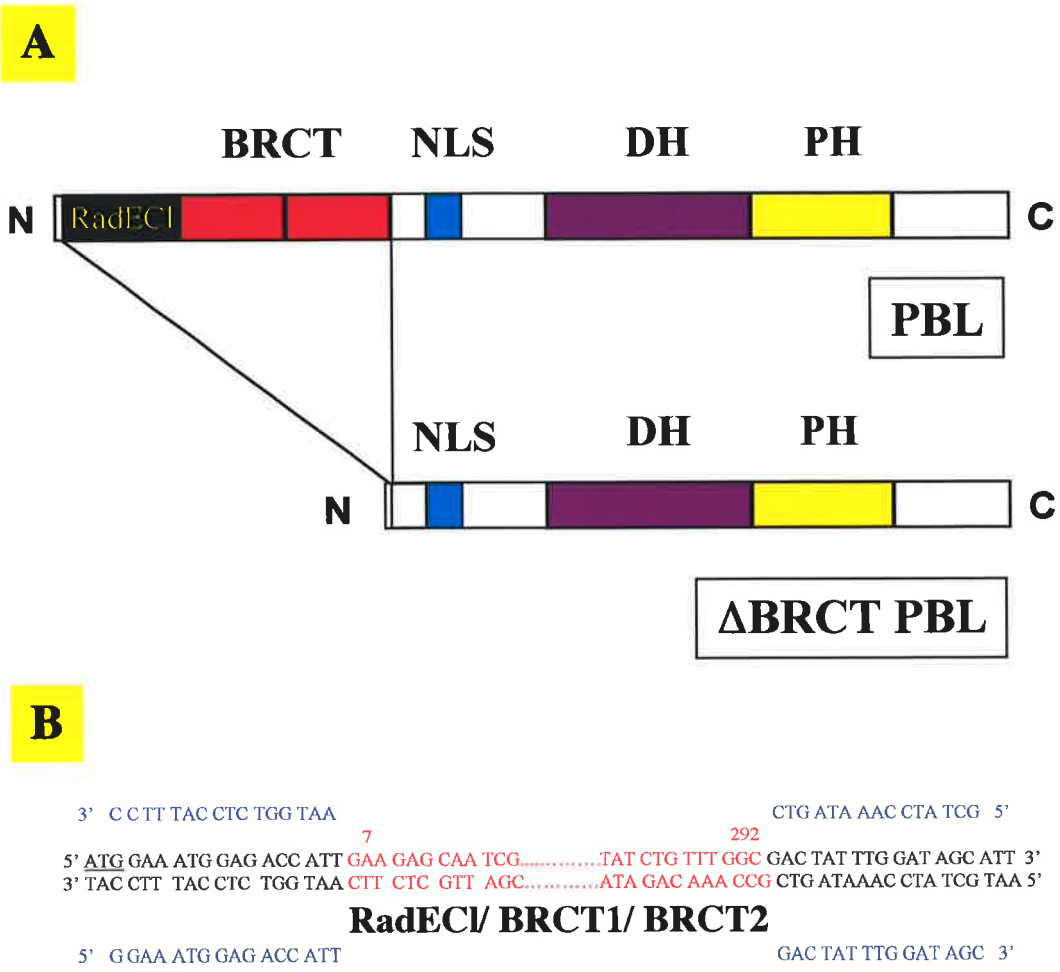

Figure 4.1 Site directed deletion of the potential nuclear domains of PBL.

A. A schematic diagram of the structure of the PBL protein, with the RadECl region boxed in black, the 2 consensus BRCT domains in red, the consensus bipartite nuclear localisation signal in blue, the Dbl homology domain (DH) in purple, and the Pleckstrin homology domain (PH) in yellow. Underneath is the ΔBRCT construct which specifically removes both the BRCT domains and the RadECl region, but contains the NLS and the DH/PH domains.

B. The DNA sequence covering this deletion is shown. Highlighted in red is the sequence of the RadECl region and BRCT domains which were specifically deleted using the primers shown above and below the sequence in blue. These primers specifically remove 286 amino acids, from amino acid 7 through to amino acid 292. The initiating ATG is underlined in black.

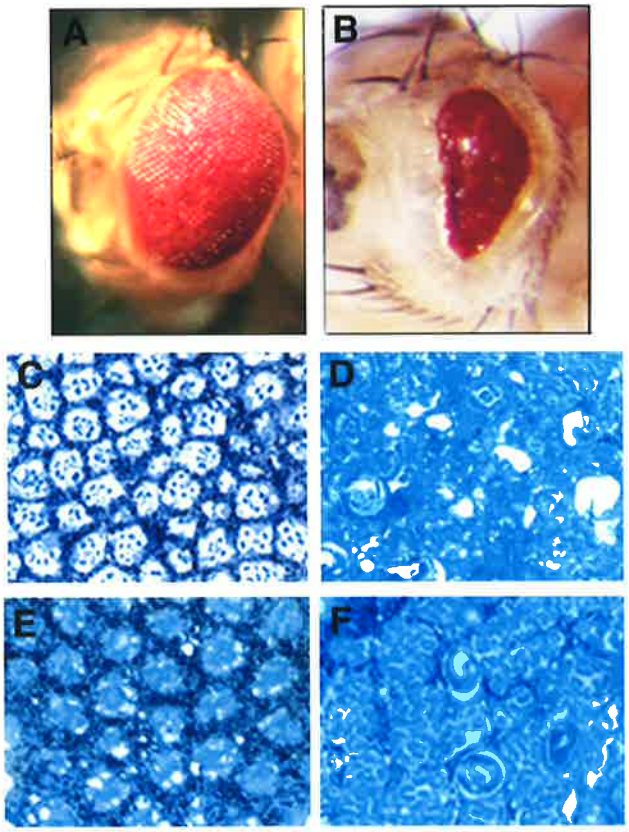

Figure 4.3 Rough eye phenotypes caused by overexpression of PBL and ΔBRCT PBL.

A. A *GMR GAL4::UAS pbl* adult eye. A mild rough eye phenotype is caused by the overexpression of PBL posterior to the morphogenetic furrow in the developing eye disc at 25 degrees C.

B. A *GMR GAL4::UAS ΔBRCTpbl* adult eye. An extreme rough eye phenotype is caused by the overexpression of ΔBRCT PBL posterior to the morphogenetic furrow in the developing eye disc at 25 degrees C.

C- F. Tangential sections through adult eyes of the following genotypes. All sections were stained with methylene blue to visualise the structure.

C. A *GMR GAL4::UAS pbl* adult eye at 25 degrees C.

D. A *GMR GAL4::UAS ΔBRCTpbl* medium rough adult eye at 18 degrees C. The structure of the eye is destroyed.

E- F. *GMR GAL4::UAS ΔBRCTpbl* mild rough adult eyes at 18 degrees C.

E. An apical section.

F. A basal section.

To discount the possibility that the severity of the *ΔBRCTpbl* phenotype is simply due to expression at a much higher level than the full length *pbl* construct, western analysis was performed. Wild type, *GMR>pbl*, *GMR>ΔNLSpbl* and *GMR>ΔBRCTpbl* eye discs were dissected at 25°C, boiled, and run on a 10% SDS polyacrylamide gel, which was then transferred to nitrocellulose and probed with an anti-PBL antibody. As can be seen from **Figure 4.4**, *ΔBRCTpbl* is expressed at a level similar to that of full-length *pbl*. For the *GMR>ΔBRCTpbl* sample two bands were observed, one representing the wild type protein, and the smaller band representing the truncated ΔBRCT form of PBL. The stronger single band in the *GMR>pbl* sample represents both the wild type background and overexpressed forms of the protein. The alpha-tubulin load control shows that a similar amount of protein was loaded for each of the samples. Therefore the more severe *ΔBRCTpbl* phenotype must be due to the absence of the RadECl/BRCT domains and not simply a higher expression level.

4:4 Characterisation of the ΔBRCT PBL phenotype in the eye

Expression of the ΔBRCT mutant form of PBL caused a severe disruption of adult eye structure, a disruption which appeared quite different to that caused by the expression of either full length wild type PBL or ΔNLS mutant PBL. As a first step in the characterisation of this mutant phenotype, larval eye disc cells were examined. As discussed in the previous chapter, the larval eye disc has a compact columnar epithelial structure, making dissociation necessary for the examination of individual cells. *GMR>ΔBRCTpbl* flies were crossed to a *UAS-GFP* line so that those cells overexpressing ΔBRCT PBL would also be expressing GFP, allowing identification and visualisation of the cells without fixation and antibody staining.

The most striking feature of the *ΔBRCTpbl* phenotype was the effect on nuclear morphology. Severe disruptions to both nuclear and cellular morphology were observed (**Figure 4.5a**), with the apparent failure to complete sister chromatid separation in several cells (**Figure 4.5b-d**), suggesting a block in mid-anaphase. As described in the previous chapter, no obvious phenotype was observed in *GMR>pbl* eye disc cells (**Figure 3.5d-e**). To determine whether the ΔBRCT cells are trapped in mitosis as they appear, western analysis

was performed on these eye discs using an antibody against the mitosis specific marker, phosphorylated-histone H3 (Hendzel *et al.*, 1997). Wild type, *GMR>pbl*, *GMR>ΔNLSpbl*, and *GMR>ΔBRCTpbl* eye discs were dissected, boiled and run on a 10% SDS polyacrylamide gel. The separated proteins were then transferred to nitrocellulose and probed with the anti-phosphorylated histone H3 antibody. As can be seen from **Figure 4.6**, there is no difference in the level of mitosis between any of the samples, suggesting that the fused sister chromatid phenotype observed in the *GMR>ΔBRCTpbl* cells is not a result of a block in mitosis. Therefore it seems that ΔBRCT PBL affects nuclear integrity, and not the process of mitosis itself. The ability of the nuclear ΔBRCT form of the protein to also affect cellular morphology suggests two possibilities. Either there is cross talk between the nucleus and the cytoplasm, or it may be that the ΔBRCT form is disrupting the cytoskeleton when it is redistributed throughout the cytoplasm upon the nuclear envelope breakdown of prophase/metaphase.

To analyse the effect of expression of this construct on the further development of the eye disc, pupal eye discs were examined. *GMR>ΔBRCTpbl* pupal discs were dissected, fixed and stained for the epithelial cell contact marker Armadillo. Hoechst 33258 stain was used to visualise the DNA. As was the case with the *GMR>ΔNLSpbl* pupal discs at 25°C, the *GMR>ΔBRCTpbl* pupal discs were severely necrotic, making phenotypic analysis impossible. At 18°C, the expression of *GMR* is not as strong, resulting in a milder phenotype that is easier to analyse. As can be seen from **Figure 4.7**, *GMR>ΔBRCTpbl* pupal eye discs at 18°C have too many interommatidial cells (**Figure 4.7c**) and occasionally too many bristle cells (**Figure 4.7e**). The cone cells appear quite disrupted, and the occasional ommatidium has too few cone cells (**Figure 4.7d**). Despite their very different phenotypic appearance, *GMR>ΔBRCTpbl* and *GMR>ΔNLSpbl* have surprisingly similar pupal disc phenotypes (**Figure 4.7f-g**). However the increase in interommatidial cells, and the disruption of cone cells is far more obvious in *GMR>ΔBRCTpbl* pupal discs. These differences, along with later developmental defects must explain the very different phenotypic appearances of these two adult eyes.

To determine when the patterning process of the eye disc begins to fail, *GMR>ΔBRCTpbl* larval eye discs were fixed and stained with anti-ELAV. ELAV is expressed in those cells of the eye disc that have adopted a neural fate (Campos *et al.*, 1987; Robinow and White, 1988). As discussed previously, while the pattern of ELAV expression was only mildly disrupted in *GMR>pbl* eye discs (**Figure 4.8d and f**), *GMR>ΔNLSpbl* eye

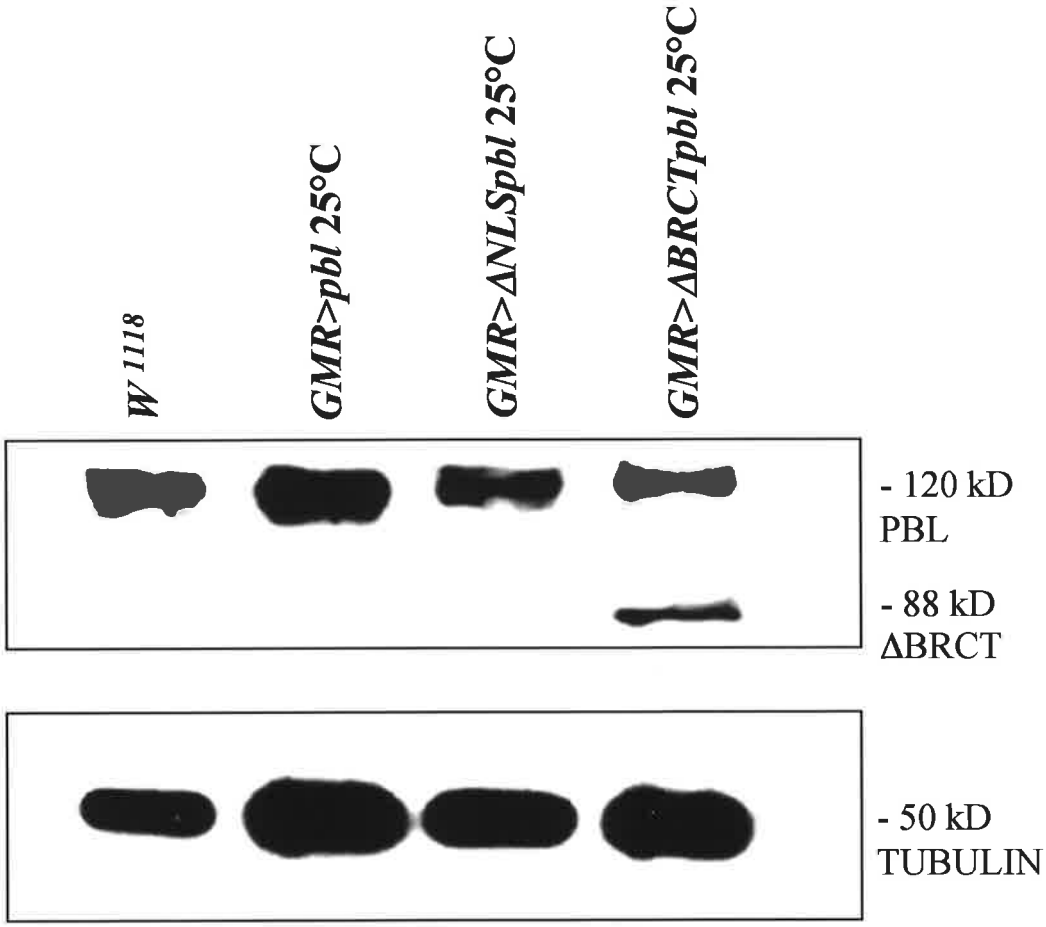

Figure 4.4 Western analysis of *GMR GAL4* expression levels in the eye.

w^{1118}, *GMR GAL4::UAS pbl*, *GMR GAL4::UAS ΔNLSpbl* and *GMR GAL4::UAS ΔBRCTpbl* eye discs were dissected at 25°C, boiled and run on a 10% SDS polyacrylamide gel, which was then transferred to a nitrocellulose filter.
The filter was then probed with an anti-PBL antibody, which produced a band of approximately 120 kD in size in each lane. The ΔBRCT form of PBL removes 286 amino acids, and is approximately 88 kD in size.
The filter was then stripped and reprobed with an alpha-tubulin antibody, which served as a loading control. This produced a band of approximately 50 kD in size.
As can be seen from the filter, ΔBRCT PBL is expressed at a lower level than full length PBL in the eye.

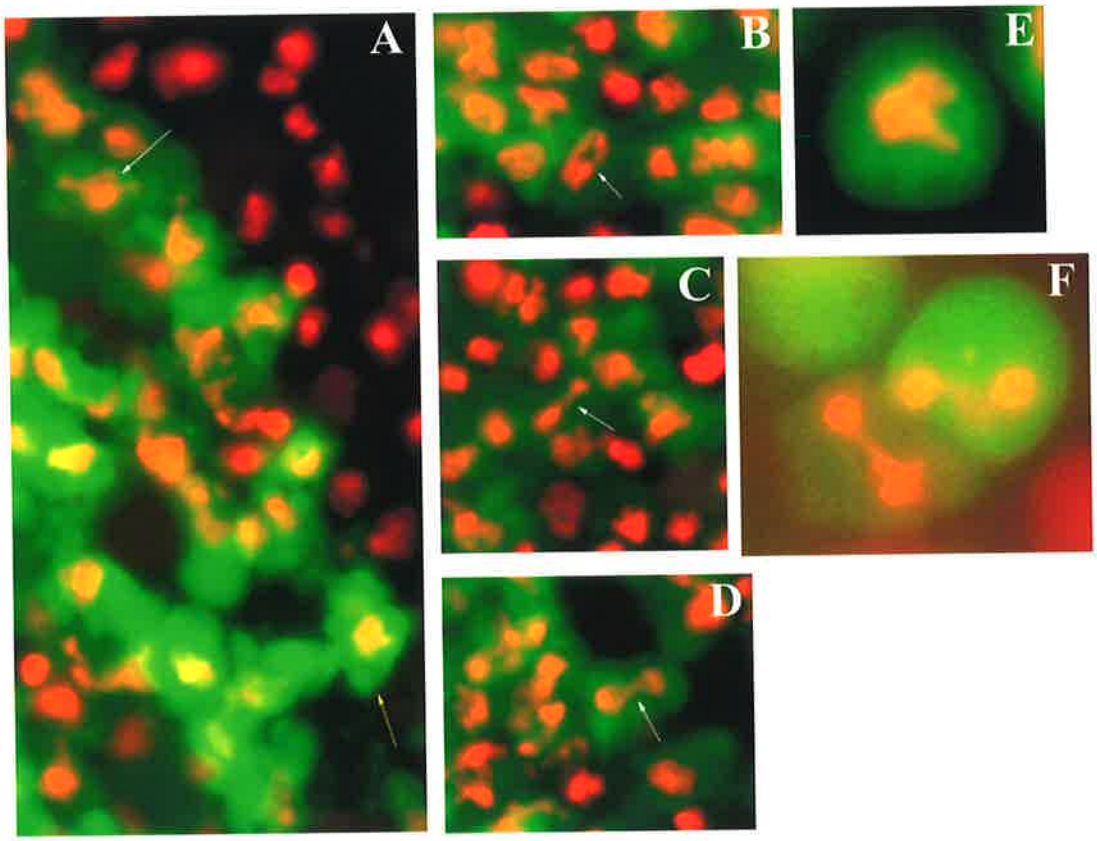

Figure 4.5 Dissociation of eye disc cells and visualisation by epifluorescence.

GMR GAL4::UAS pbl, and *GMR GAL4::UAS ΔBRCTpbl* eye discs were dissociated and stained with hoechst to visualise the DNA (shown in red). *UAS GFP* was co-expressed to enable visualisation of the cells overexpressing the *pbl* constructs (shown in green).

A. *GMR GAL4::UAS ΔBRCTpbl* dissociated eye disc cells (100x mag). Some cells have disrupted nuclear morphology, as indicated by the white arrow, and some cells have a disrupted shape (yellow arrow).

B- D. *GMR GAL4::UAS ΔBRCTpbl* dissociated eye disc cells (100x mag). The sister chromatids in some nuclei appear to have failed to segregate completely (white arrows).

E. Close up view of a *GMR GAL4::UAS pbl* eye disc cell. This cell contains one nucleus.

F. Close up view of two *GMR GAL4::UAS ΔBRCTpbl* eye disc cells. Both of these show incomplete sister chromatid separation.

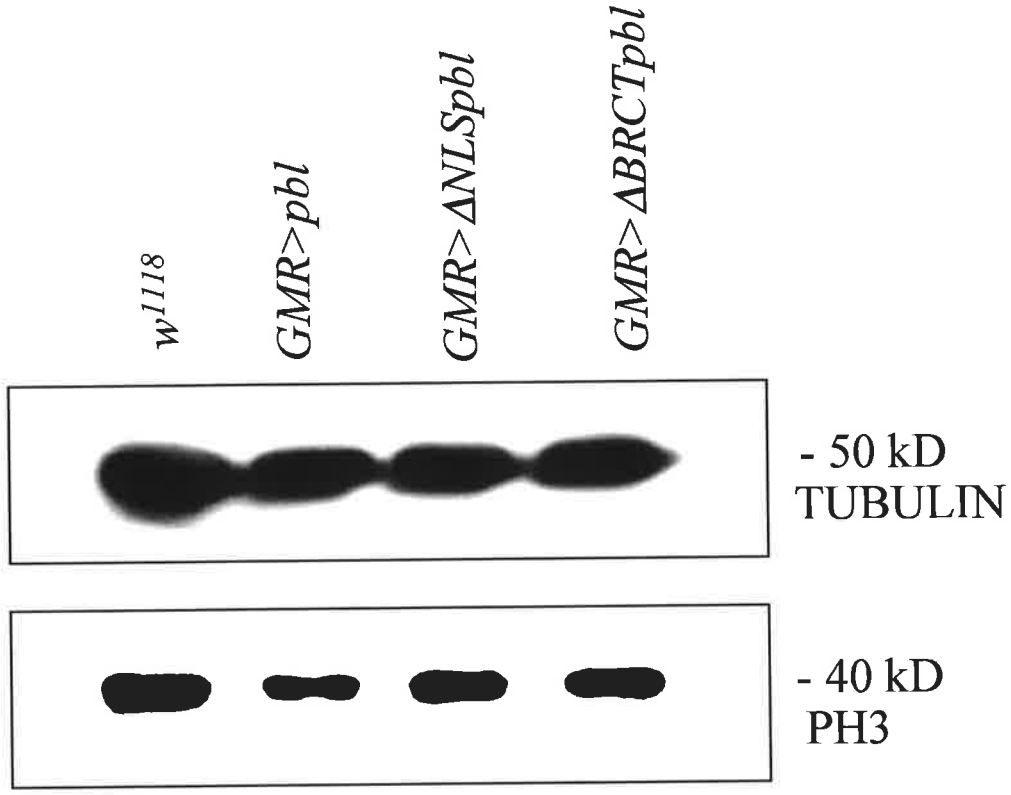

Figure 4.6 Overexpression of PBL in the eye disc does not block cells in mitosis.

w^{1118}, *GMR GAL4::UAS pbl*, *GMR GAL4::UAS ΔNLSpbl*, and *GMR GAL4::UAS ΔBRCTpbl* eye discs were dissected at 25°C, boiled and run on a 10% SDS polyacrylamide gel, which was then transferred to a nitrocellulose filter.
The filter was then probed with an antibody specific for mitotic cells (PH3= anti-phosphorylated histone H3) which produced a band of approximately 40 kD in size in each lane.
The filter was then stripped and reprobed with an alpha-tubulin antibody, which served as a loading control. This produced a band of approximately 50 kD in size.
As can be seen from the filter, overexpression of the various forms of PBL in the eye disc does not increase the number of cells in mitosis, as judged by the level of phosphorylated histone H3.

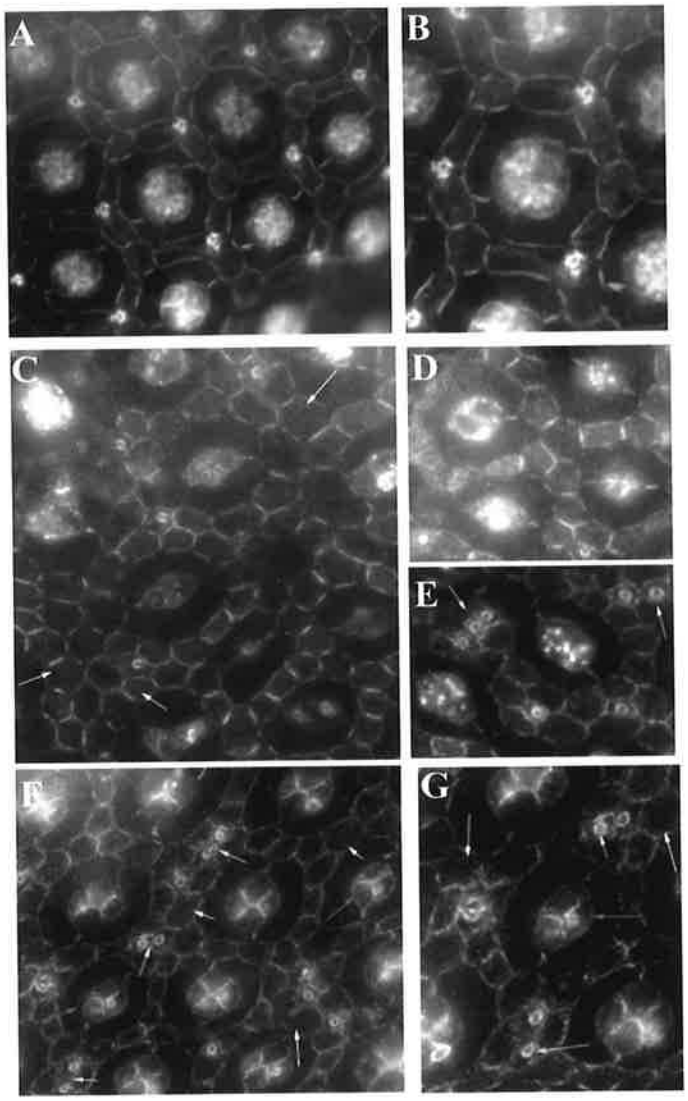

Figure 4.7 Disruption of pupal eye disc structure in *GMR GAL4::UAS ΔBRCTpbl* eye discs.

All pupal discs were stained with an antibody against the cell contact marker Armadillo.

A. Wild type pupal eye disc at 42hr APF at 25 degrees C (100x mag).

B. Close up view of a wild type pupal ommatidium.

C- E. *GMR GAL4::UAS ΔBRCTpbl* eye discs at 84 hr APF at 18 degrees C (100x mag).

- **C**. The pupal disc has an excessive number of interommatidial cells, as indicated by the white arrows.
- **D**. The occasional ommatidium has too few cone cells (red arrow).
- **E**. Extra bristle cells are occasionally observed (yellow arrows).

F. *GMR GAL4::UAS ΔNLSpbl* eye disc at 84 hr APF at 18 degrees C (100x mag). The pupal disc has more interommatidial cells than wild type (white arrows), more bristle cells (yellow arrows), and some ommatidia have too few cone cells (red arrows).

G. Close up view of a *GMR>ΔNLSpbl* ommatidium.

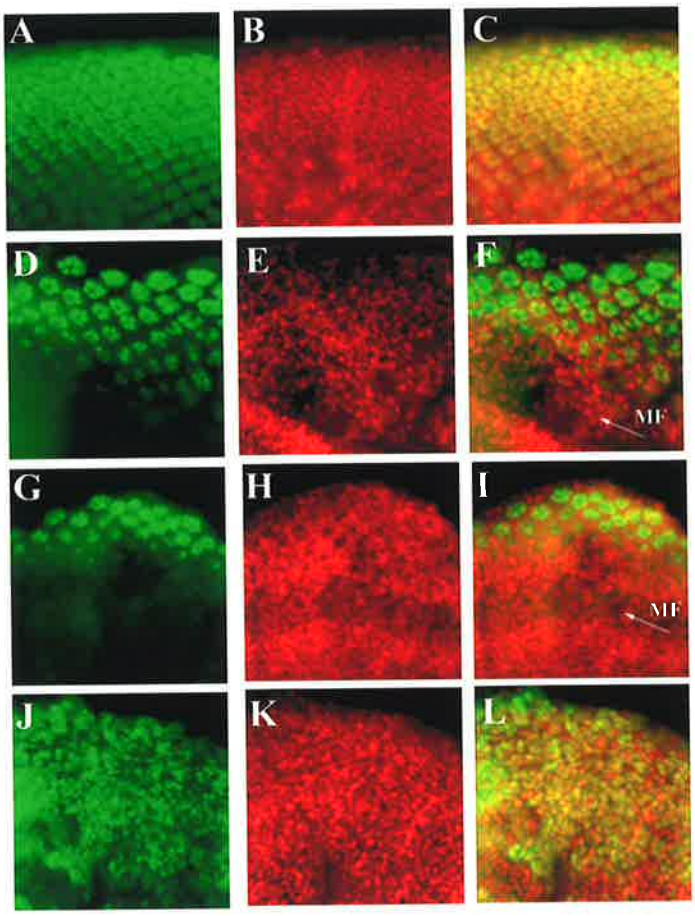

Figure 4.8 The clustered organisation of ELAV expressing cells is disrupted in *GMR GAL4::UAS ΔBRCTpbl* eye discs.

Third larval instar eye discs were stained with the neural specific antibody ELAV. ELAV is normally expressed in all cells posterior to the morphogenetic furrow which have adopted a neural fate.
A- C. Wild type eye disc stained with α–ELAV in green (A), and hoechst 33258 DNA stain in red (B). The merge of these two images is shown in C.
D- F. *GMR GAL4::UAS pbl* eye disc stained with α–ELAV in green (D), and hoechst 33258 DNA stain in red (E). The pattern of ELAV staining cells is mildly disrupted. The merge of these two images is shown in (F), with the position of the morphogenetic furrow indicated by a white arrow.
G- I. *GMR GAL4::UAS ΔNLSpbl* eye disc stained with α–ELAV in green (G), and hoechst 33258 DNA stain in red (H). A large reduction in the number of ELAV-staining cells is observed posterior to the morphogenetic furrow. However the clustered organisation of the ELAV-expressing cells remains. The merge of these two images is shown in I. The furrow still progresses (white arrow), but only those cells furthest from the furrow are expressing ELAV.
J- L. *GMR GAL4::UAS ΔBRCTpbl* eye disc stained with α–ELAV in green (J), and hoechst 33258 DNA stain in red (K). Cells continue to express ELAV, but the clustered organisation of these cells is completely lost. The merge of these two images is shown in L.

discs had a massive reduction in the number of ELAV expressing cell clusters (**Figure 4.8g and i**). In contrast, *GMR>ΔBRCTpbl* eye discs had numerous cells staining posterior to the morphogenetic furrow, but these had completely lost their organisation into clusters (**Figure 4.8j and l**).

4:5 The effect of ΔBRCT expression in the wing disc

As previously discussed, expression of ΔBRCT PBL in the proliferating and differentiating cells of the eye disc using the enhancer *GMR* was shown to cause disruptions in nuclear morphology, cellular morphology, and the resultant patterning of the eye disc. In an attempt to address the question of whether expression of this construct can affect other proliferating tissues, *ΔBRCTpbl* was also expressed in the developing wing disc using the driver *71B*. When the *UAS pbl* construct was expressed, PBL was observed to localise to the nucleus without affecting wing development (**Figure 4.9a** and **c**). When *ΔBRCTpbl* was expressed, PBL was observed to retain its nuclear localisation (**Figure 4.9b**). However, the development of the wing was severely disrupted. Adult wings were produced which were crumpled, blistered and fluid filled (**Figure 4.9d**). Wings also lacked the cross veins (**Figure 4.9f**), and ectopic vein tissue was also frequently observed (**Figure 4.9e**). Thus, expression of the ΔBRCT mutant form of PBL in the proliferating cells of both the eye and wing disc severely disrupted the development of these tissues.

4:6 The effect of ΔBRCT PBL expression in differentiating cells of the eye disc

To investigate whether the effect of ΔBRCT PBL was restricted to proliferating cells, this construct was then expressed under the control of the *elav GAL4* driver, specific for differentiating cells of the eye. As discussed in the previous chapter, when full-length wild type PBL was expressed under the control of *elav GAL4*, no disruption to eye development was observed (**Figure 4.10a**). When ΔBRCT PBL was expressed under the control of this driver, a severe rough eye phenotype was observed (**Figure 4.10b**). This phenotype was almost identical to that produced when ΔNLS PBL was expressed (**Figure 4.10c**). The eyes were small and glassy in appearance, with a ring of necrosis in the middle of the eye. As ELAV is expressed in cells that have adopted a neural fate, this indicates that the ΔBRCT protein can also affect cells that are differentiating, and not just those that are proliferating.

4:7 The effect of ΔBRCT PBL expression in salivary glands

The effect of ΔBRCT PBL on the non-proliferating tissues of the larva was examined further using the salivary gland. As discussed before, the salivary gland provides a set of large, regular shaped cells that have ceased cytokinesis, and are conducive to microscopic analysis owing to their large size. The sav *GAL4* construct drives expression in these cells after the terminal cytokinesis of mitosis 15 in embryogenesis. As described in the preceding chapter, when wild type PBL was expressed in these cells it was observed to localise to the nucleus (**Figure 4.11b**). Despite its nuclear localisation, it was observed to have a significant effect on both cell size and shape. The resultant glands were much smaller than wild type, and their cells were significantly rounded (**Figure 4.11b**). When *ΔBRCTpbl* was expressed, the resultant glands were also reduced in size, and cells were significantly rounded. However, in addition to this, a severe disruption of the actin cytoskeleton was observed (**Figure 4.11c**). The cortical actin structure was disturbed, and sheets of filamentous actin formed in the

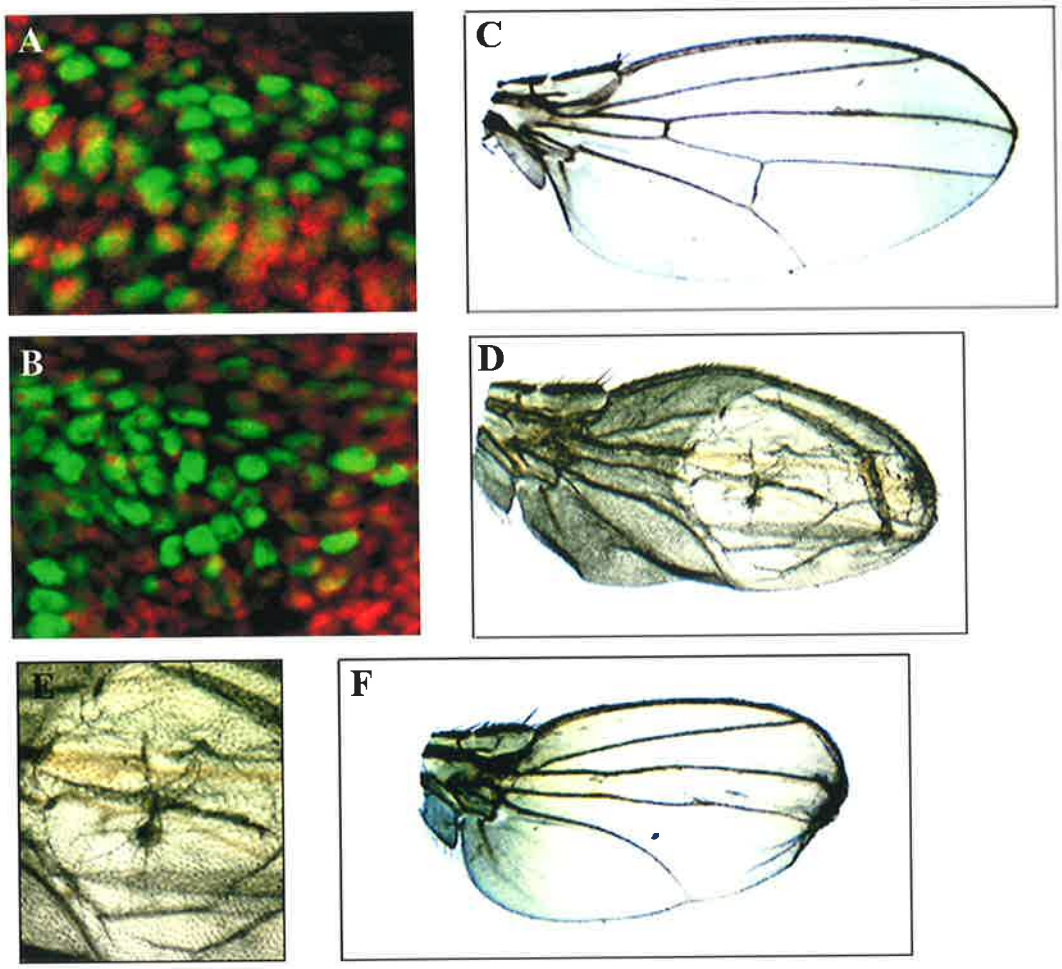

Figure 4.9 ΔBRCT PBL disrupts wing development.

A and **B**. *71B GAL4::UAS pbl* and ΔBRCT*pbl* third larval instar wing discs were dissected, fixed and stained with anti-PBL antibody (shown in green) and propidium iodide which stains the DNA (shown in red). Confocal images are shown taken with a 40x water lens with 3x zoom. Both wild type PBL (A) and ΔBRCT PBL (B) localise to the nucleus.
C. *71B GAL4::UAS pbl* adult wing (5x mag). Overexpressing PBL has no effect on wing development. Adult wings of normal size are produced, with normal venation.
D. *71B GAL4::UAS ΔBRCTpbl* adult wing (5x mag). Overexpression of ΔBRCT PBL disrupts wing development, producing crumpled, blistered wings which frequently lack the two cross veins. Ectopic vein tissue is also observed.
E. Close up view of the wing in (D) showing ectopic vein tissue.
F. *71B GAL4::UAS ΔBRCTpbl* adult wing with a weaker phenotype. Although non-blistered, the wing is smaller than wild type, and lacks both cross veins.

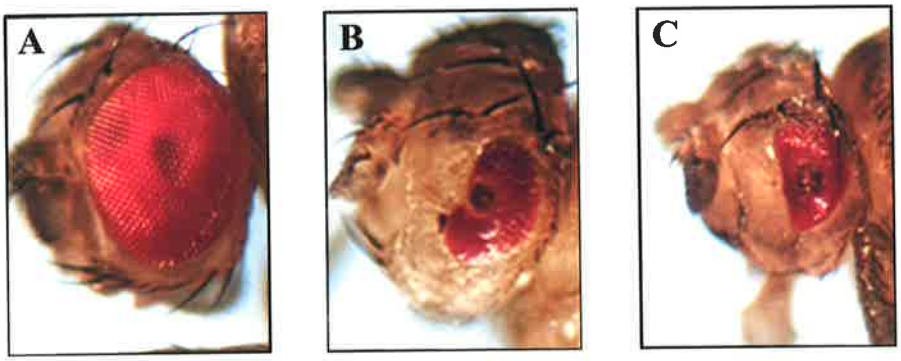

Figure 4.10 Expression of ΔBRCT PBL in differentiating cells of the developing larval eye disc.

A. An *elav GAL4::UAS pbl* adult eye at 25 degrees C (5x mag). Expression of PBL in differentiating neural cells of the developing larval eye disc has no effect on the development of the adult eye. A normal adult eye is produced.

B. An *elav GAL4::UAS ΔBRCTpbl* adult eye at 25 degrees C (5x mag). Expression of ΔBRCT PBL in differentiating neural cells of the developing larval eye disc causes a severe disruption to eye development. Eyes are small and glassy with a characteristic ring of necrosis in the middle of the eye.

C. An *elav GAL4::UAS ΔNLSpbl* adult eye at 25 degrees C (5x mag). Expression of ΔNLS PBL in differentiating neural cells of the larval eye disc produces a very similar phenotype to that of ΔBRCT PBL.

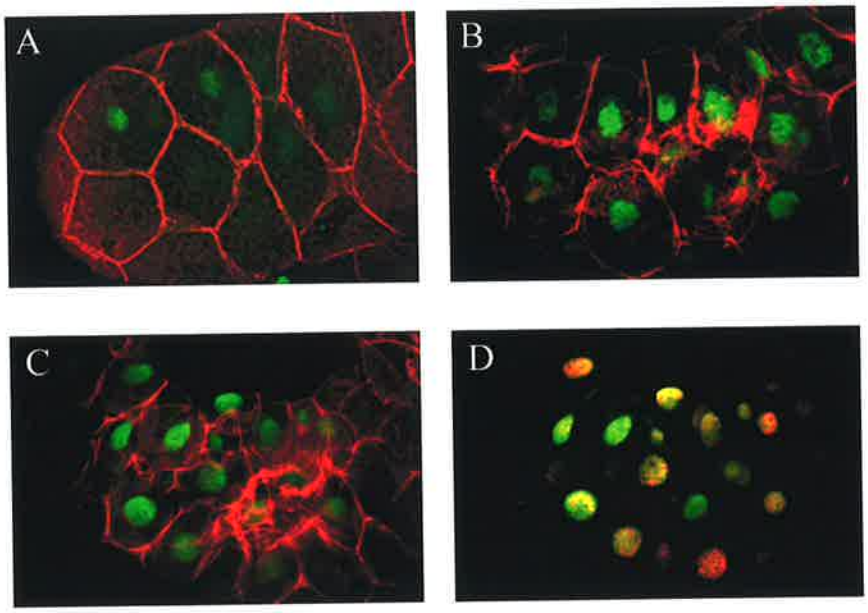

Figure 4.11 Expression of ΔBRCT PBL in salivary glands disrupts actin structure.

UAS pbl and *UAS ΔBRCTpbl* flies were crossed to the gut and salivary gland specific driver sav::*GAL4*. Salivary glands were then dissected from third instar larvae, and fixed and stained with phalloidin which binds to filamentous actin (shown in red), and α-PBL (shown in green) unless otherwise indicated. All images were taken at 40x magnification.

A. Wild type salivary gland stained with phalloidin in red, and α-PBL shown in green. The cells of a wild type gland are a regular hexagonal or pentagonal shape.

B. sav *GAL4::UAS pbl* salivary gland stained with phalloidin (red) and PBL (green). PBL is nuclear and cells are rounded.

C. sav *GAL4::UAS ΔBRCTpbl* salivary gland stained with phalloidin (red) and PBL (green). PBL is nuclear, cells are rounded, and actin structure is disrupted.

D. The same sav *GAL4::UAS ΔBRCTpbl* salivary gland as in (C), but PBL is in green and propidium iodide stain for the DNA is shown in red. PBL is nuclear and partially colocalises with DNA.

cytoplasm. Despite the severe effect on actin structure, ΔBRCT PBL retained its nuclear localisation (**Figure 4.11d**).

To discount the possibility that the severity of the *ΔBRCTpbl* phenotype is simply due to a higher expression level than that of *UAS pbl*, western analysis was performed. Wild type, sav>*pbl* and sav>*ΔBRCTpbl* salivary glands were dissected, boiled and run on a 10% SDS polyacrylamide gel, which was then transferred to nitrocellulose and probed with an anti-PBL antibody. As can be seen from **Figure 4.12**, *UAS pbl* is expressed at a similar or higher level than *UAS ΔBRCTpbl*. Therefore the severity of the *UAS ΔBRCTpbl* phenotype compared to that of *UAS pbl* must be due to the absence of these nuclear domains.

The ability of wild type and ΔBRCT PBL to have such a severe effect on the actin structure in the cytoplasm is quite surprising, considering that PBL antibody stains on fixed salivary gland tissue show both of these constructs to localise to the nucleus. As discussed previously, this observation challenges the notion that nuclear localisation is simply a sequestering mechanism, removing Rho GEF action from the cytoplasm at the appropriate time. A possible explanation for this dichotomy may be that the PBL protein shuttles between the nucleus and the cytoplasm. It is possible that the "in rate" is much higher than the "exit rate" from the nucleus, making the protein appear solely nuclear in fixed tissues. In support of this, a low level of fluorescence is observed in the cytoplasm of wild type, *UAS pbl* and *UAS ΔBRCT* salivary glands when they are fixed and stained with the PBL antibody. However, it is difficult to discriminate between cytoplasmic staining and autofluorescence of this tissue. The increase in severity of the *ΔBRCTpbl* construct compared to wild type PBL could be explained if the BRCT domains were required for anchoring the protein in the nucleus, making the "exit rate" of this mutant form into the cytoplasm higher than that of full length PBL. However, this cannot be the sole explanation for this phenotype, otherwise the *ΔNLSpbl* construct would give a similar, but more severe effect on cytoplasmic filamentous actin than the *ΔBRCTpbl* construct. A function for the BRCT domains in the cytoplasm could explain these observations. This possibility is explored in a following chapter.

4:8 Genetic analysis of the eye phenotype– the ΔBRCT PBL phenotype is suppressed by a *Rho* mutation

As discussed previously, expression of ΔBRCT PBL in a variety of tissues causes extreme phenotypes, regardless of the tissue type or its cell cycle profile. Initial analyses of these different phenotypes indicated several defects. In the larval eye disc, nuclear and cellular morphology was disrupted. In the pupal eye disc, disruption to the patterning of cells was observed. This disruption was similar to that caused by the overexpression of both wild type PBL and ΔNLS PBL. In the salivary gland, in addition to an effect on cell shape, actin structure in the cytoplasm was severely disrupted. It was possible that these phenotypes were caused by loss of specificity of the mutated forms for the Rho G protein. RhoA was the only *Drosophila* Rho family member found to dominantly modify both the *GMR>pbl* and *GMR>ΔNLSpbl* rough eye phenotypes. This indicated that RhoA is the target of PBL activity, even when PBL is completely cytoplasmic. To test whether the ΔBRCT mutant form of the PBL protein had maintained its specificity for RhoA, a $RhoA^{720}$ mutant allele was introduced into the *GMR>ΔBRCTpbl* background. The *GMR>ΔBRCTpbl* recombinant stock which was used to screen for modifiers was lethal at 25°C. Reducing the amount of Rho through the introduction of a $RhoA^{720}$ mutant allele at 25°C was not able to suppress this lethality. However, reducing the amount of Rho in this way at 18°C was shown to strongly suppress both the lethality and the *GMR>ΔBRCTpbl* rough eye phenotype (**Figure 4.13b**). When virgin females of the genotype *GMR>ΔBRCTpbl / CyO* were crossed to $RhoA^{720}$ / *CyO* males to test for suppression, equal numbers of the genotypes *GMR>ΔBRCTpbl / CyO*, *GMR>ΔBRCTpbl /* $RhoA^{720}$ and $RhoA^{720}$ / *CyO* were expected (*CyO/ CyO* is embryonic lethal). While *GMR>ΔBRCTpbl / CyO* flies made up only 11% of the total progeny at 18°C, 49% of the progeny were *GMR>ΔBRCTpbl /* $RhoA^{720}$, compared to 40% $RhoA^{720}$ / *CyO*. Therefore even though the protein lacks 286 of its 853 amino acids, it is still capable of interacting with Rho.

The *GMR>ΔBRCTpbl* rough eye phenotype was then tested for genetic interactions with mutant alleles or deficiencies covering other characterised members of the Rho family of small GTPases, including Rac 1 and 2, Mtl and Cdc42. In all cases, as with the *GMR>pbl* and *GMR>ΔNLSpbl* rough eye phenotypes, loss of one copy of the gene did not result in suppression of the *GMR>ΔBRCTpbl* rough eye phenotype. Thus the ΔBRCT form of PBL

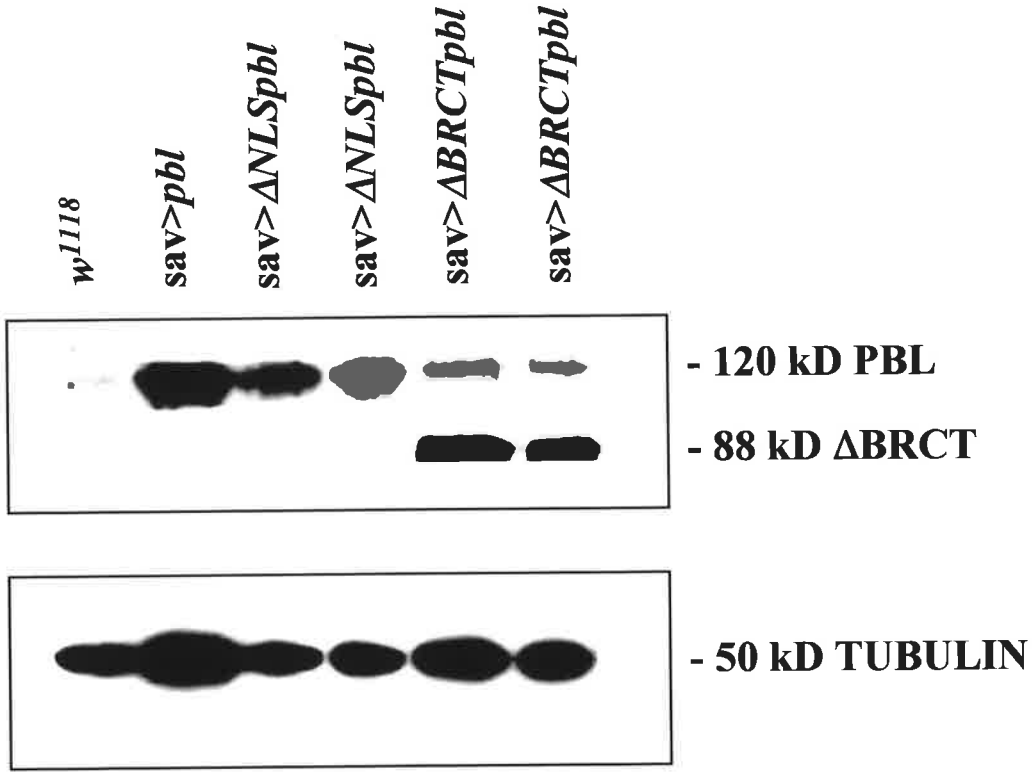

Figure 4.12 Western analysis of sav>*GAL4* expression levels in the salivary gland.

w^{1118}, sav *GAL4::UAS pbl*, sav *GAL4::UAS ΔNLSpbl* and sav *GAL4::UAS ΔBRCTpbl* salivary glands were dissected at 25°C, boiled and run on a 10% SDS polyacrylamide gel, which was then transferred to a nitrocellulose filter.
The filter was then probed with an anti-PBL antibody, which produced a band of approximately 120 kD in size in each lane. The ΔBRCT form of PBL removes 286 amino acids, and is approximately 88 kD in size.
The filter was then stripped and reprobed with an alpha-tubulin antibody, which served as a loading control. This produced a band of approximately 50 kD in size.
As can be seen from the filter, ΔBRCT PBL is expressed at a similar or lower level in the salivary gland than full length PBL.

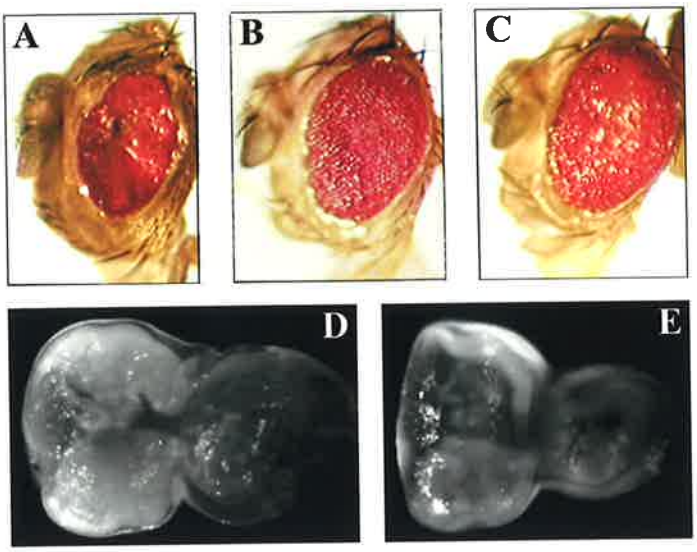

Figure 4.13 Suppression of the *GMR GAL4::UAS ΔBRCTpbl* rough eye phenotype by *RhoA*.

A. A *GMR GAL4::UAS ΔBRCTpbl* adult eye at 18 degrees C. Eye development is disrupted by the overexpression of ΔBRCT PBL posterior to the morphogenetic furrow of the developing larval eye disc.

B. Suppression of the *GMR GAL4::UAS ΔBRCTpbl* rough eye phenotype in $RhoA^{720}$ heterozygotes at 18 degrees C. The rough eye phenotype caused by the overexpression of ΔBRCT PBL posterior to the morphogenetic furrow is strongly suppressed when a *RhoA* mutant allele is introduced into the genetic background of these flies.

C. Suppression of the *GMR GAL4::UAS ΔBRCTpbl* rough eye phenotype by *GMR>p35*. The rough eye phenotype can be suppressed at 18 degrees C by the overexpression of the cell death inhibitor P35 (compare to A).

D. Acridine orange stain of a *GMR GAL4::UAS pbl* larval eye disc.

E. Acridine orange stain of a *GMR GAL4::UAS ΔBRCTpbl* larval eye disc. There is a slight increase in the number of staining cells.

maintained its specificity for RhoA (**Table 4.1**).

To ascertain whether the ΔBRCT mutant form of the protein was acting as a dominant negative, two *pbl* null mutant alleles were tested for their ability to dominantly enhance this phenotype. Again, as with the ΔNLS form of the protein, both were found to have no effect on the *GMR>ΔBRCTpbl* rough eye phenotype. Therefore ΔBRCT PBL is not interfering with normal PBL function to cause the severe phenotypes observed, but is functioning through its GEF domains to activate RhoA (**Table 4.1**).

The *GMR>ΔBRCTpbl* rough eye phenotype was then screened against mutant alleles of numerous other genes, including genes involved in cell death, cytokinesis and DNA damage checkpoints (**Table 4.1**). The only gene found to dominantly modify the phenotype, other than *RhoA,* was *p35*. As with the *GMR>ΔNLSpbl* rough eye phenotype, *GMR>p35* was found to suppress the *GMR>ΔBRCTpbl* phenotype at 18°C (**Figure 4.13c**). This was in direct contrast to the *GMR>pbl* phenotype which was enhanced by *GMR>p35* (O'Keefe, pers comm). As discussed in the previous chapter, the suppression by this gene may be secondary to a disruption of eye disc cells. Cells which may normally be removed by programmed cell death, contributing to the rough eye phenotype, may be kept alive by the expression of this apoptosis inhibitor. Acridine orange staining for cell death in larval eye discs indicated that the levels of cell death are slightly increased in *GMR>ΔBRCTpbl* eye discs compared to that of *GMR>pbl* (**Figure 4.13d-e**). It is therefore likely that cell death is occurring later in development to remove cells damaged by the expression of the ΔBRCT mutant form of PBL.

Table 4.1 Screening for enhancement or suppression of the *GMR GAL4::UASΔBRCTpbl* rough eye phenotype.

Flies of the genotype *GMR GAL4::UASΔBRCTpbl* were crossed to produce flies heterozygous for loss of function alleles or deficiencies covering the genes listed in the table. *RhoA, Rac1, Rac2, cdc42,* and *Mtl* are all Rho family members. $RhoA^{720}$ is a null allele (Strutt *et al.*, 1997). $cdc42^{3}$ is a lethal allele (Fehon *et al.*, 1997) and *ΔMtl* is a deletion which removes the entire *Mtl* open reading frame (Hakeda-Suzuki *et al.*, 2002). There were no specific mutations available in *Rac1* and *Rac2* and so deficiency stocks were used. The deficiency *Df(3L)Ar14-8* removes *Rac1*. *Df(3L)RM5-2* is a large deficiency which deletes the *pbl* gene as well as *Rac2*. This stock was tested alone, as well as with a cosmid (*cos34*), which carries the entire *pbl* gene, recombined onto the same chromosome. This cosmid is known to completely rescue PBL function (J. Wong and R. Saint, unpublished observations). pbl^{2} and pbl^{3} are both null alleles of *pbl* (Prokopenko *et al.*, 1999). Dia^{2} has a specific mutation in *Diaphanous*, a *Drosophila* formin protein required for actin re-organisation and cytokinesis (Castrillon and Wasserman, 1994). $chic^{221}$ has a mutation in *chickadee* which encodes profilin and acts downstream of *Diaphanous* during actin re-organisation (Verheyen and Cooley, 1994). acu^{E636} has a specific mutation in *act-up* which controls actin polymerisation and acts in the opposite direction to *chickadee* (Benlali *et al.*, 2000). *Diaphanous*, *chickadee* and *act-up* are all Rho effectors. *Df(3R)H99* is a deficiency which takes out the cell death genes *Hid*, *Grim*, and *Reaper*. *GMR>p35* overexpresses the apoptosis inhibitor *p35* (Hay *et al.*, 1994). grp^{1} is a maternal-effect lethal mutation in the checkpoint gene *grapes* (Fogarty *et al.*, 1994). RBF^{14} is a null allele of the *Drosophila* retinoblastoma family protein (Du *et al.*, 1996; Du and Dyson, 1999).

Gene screened	Effect on phenotype of *GMR GAL4::UASΔBRCTpbl*
RhoA^{720}	Strong suppression
Df(3L)Ar14-8 (*Rac1*)	No effect
Df(3L)RM5-2 (*Rac2* and *pbl*)	No effect
Df(3L)RM5-2,cos34 (*pbl*$^{+}$)	No effect
cdc 42^{3}	No effect
ΔMtl	No effect
pbl^{2}	No effect
pbl^{3}	No effect
Dia^{2}	No effect
chic^{221}	No effect
acu^{E636}	No effect
Df(3R)H99	No effect
GMR>p35	Medium suppression
grp^{1}	No effect
RBF^{14}	No effect

4:9 Genetic analysis of the salivary gland phenotype- ΔBRCT PBL does not interact with Rho

In the eye, PBL, ΔNLS PBL and ΔBRCT PBL were shown to act predominantly through RhoA. And as demonstrated in the previous chapter, while the *UAS pbl* phenotype was suppressible by RhoA in the salivary gland, *UAS ΔNLSpbl* was unable to genetically interact with RhoA in this tissue. To test whether the *UAS ΔBRCTpbl* phenotype was suppressible by Rho, the $RhoA^{720}$ null allele was recombined onto the *UAS ΔBRCTpbl* chromosome, which was then crossed to the sav *GAL4* driver. Reduction of Rho in this way was unable to suppress the *UAS ΔBRCTpbl* phenotype at 25°C (**Figure 4.14 a-b**). Given the severity of the phenotype at this temperature, the experiment was repeated at 18°C. At this lower temperature, sav *GAL4* is not as highly expressed, leading to a less severe effect on salivary gland structure. However, as was the case with the *ΔNLSpbl* phenotype, reducing the amount of RhoA still could not rescue the *ΔBRCTpbl* salivary gland phenotype (**Figure 4.14 c-d**). Therefore while ΔBRCT PBL was shown to act through RhoA in the eye, it does not appear to act through RhoA in the salivary gland. As discussed previously, this is most likely due to either a differing role of PBL in this tissue, or a differing mode of regulation.

Figure 4.14 Removal of one copy of *RhoA* does not suppress the ΔBRCT PBL salivary gland phenotype.

UAS ΔBRCTpbl and *UAS ΔBRCTpbl, RhoA*^{720} flies were crossed to the gut and salivary gland specific driver sav *GAL4.* Salivary glands from third instar larvae were then dissected, fixed and stained with phalloidin, which binds to filamentous actin (shown in red), and α–PBL (shown in green).

A. sav *GAL4::UASΔBRCTpbl* salivary gland at 25°C stained with phalloidin (10x mag). This same gland is shown in (A') stained with phalloidin (red) and PBL (green). ΔBRCT PBL localises to the nucleus. The cells are rounded, and actin structure is disrupted.

B. sav *GAL4::UAS ΔBRCTpbl, RhoA*^{720} salivary gland at 25°C stained with phalloidin (10x mag). Removal of one copy of *RhoA* does not suppress the disruption of actin structure or cell shape. This same gland is shown in (B') stained with phalloidin (red) and PBL (green).

C. sav *GAL4::UASΔBRCTpbl* salivary gland at 18°C stained with phalloidin (10x mag). At this lower temperature there is a less severe effect on actin structure, but cells are still rounded. This same gland is shown in (C') stained with phalloidin (red) and PBL (green).

D. sav *GAL4::UAS ΔBRCTpbl, RhoA*^{720} salivary gland at 18°C stained with phalloidin (10x mag). Removal of one copy of *RhoA* at this lower temperature does not suppress the disruption of actin structure or cell shape. This same gland is shown in (D') stained with phalloidin (red) and PBL (green).

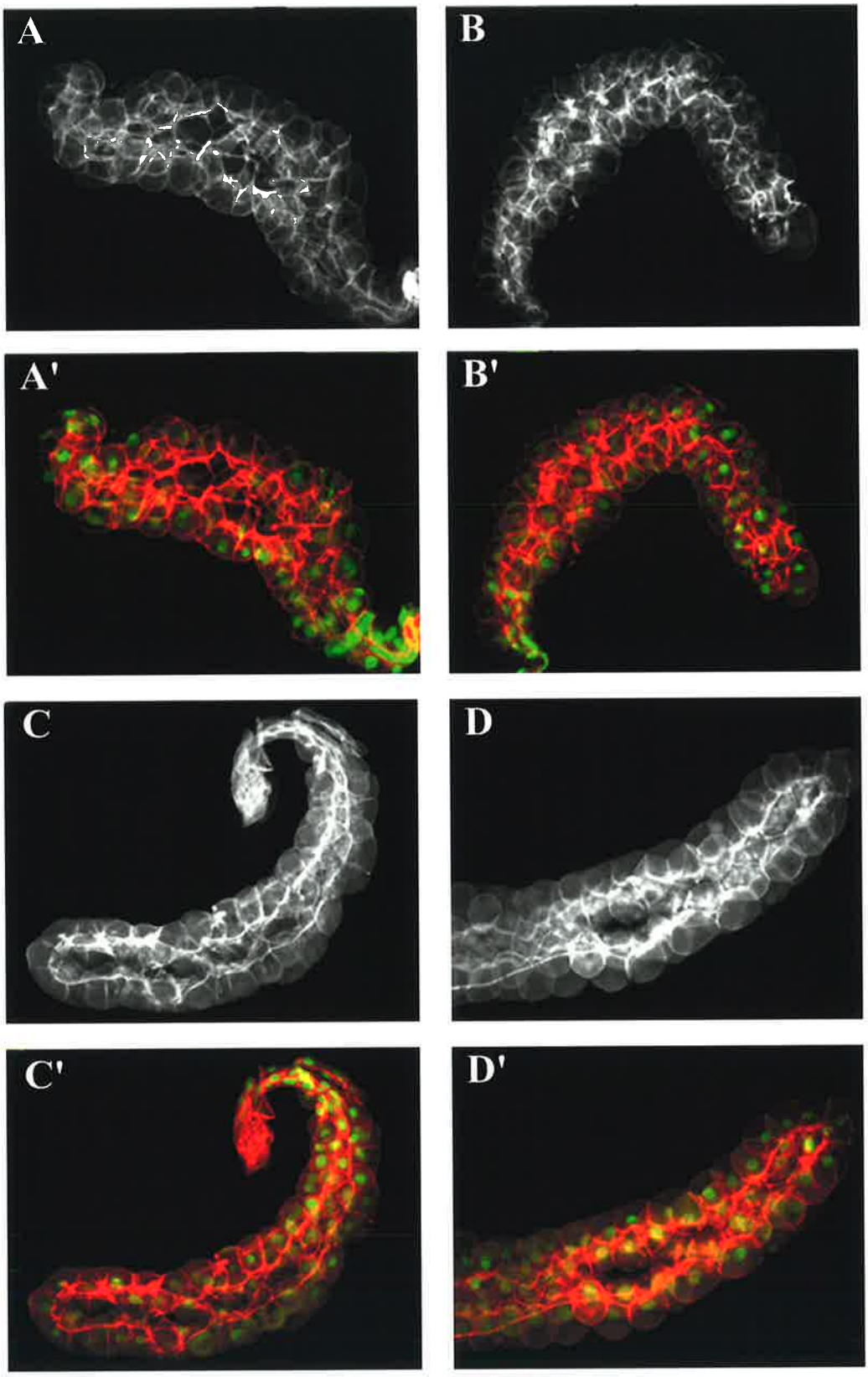
A
B
A'
B'
C
D
C'
D'

4:10 The RadECl region and BRCT domains are required for cytokinesis

As discussed in the previous sections, deletion of the RadECl region and BRCT domains causes extreme phenotypes in a variety of tissues. Despite maintaining the localisation of the full-length wild type protein, the phenotypes generated were far more severe, indicating the importance of these domains for the maintenance of normal cellular processes during development. However, are these domains required for the role of PBL in cytokinesis? To answer this question, ΔBRCT PBL was expressed in a *pbl* mutant embryonic background using the *prd GAL4* driver. As discussed in the previous chapter, expression of wild type PBL using this driver has been shown to completely rescue the cytokinetic defect of *pbl* mutants (**Figure 4.15a-c**). Expression of ΔBRCT PBL on the other hand was unable to rescue the cytokinetic defect of *pbl* mutants (**Figure 4.15d-f**). Thus the RadECl region and BRCT domains are required for cytokinesis.

4:11 Discussion

While evidence strongly suggests that PBL functions as a Rho GEF in the cytoplasm, playing an essential role in cytokinesis, the presence of nuclear BRCT domains also suggests a potentially separate nuclear role. When the nuclear localisation signal was mutated and the protein was completely cytoplasmic a range of severe phenotypes were observed. The severity of these phenotypes may simply reflect the importance of sequestering the protein in the nucleus to remove the Rho GEF activity from the cytoplasm at the appropriate time in the cell cycle. However, as shown previously, expression of full length, nuclear PBL in the salivary gland also disrupted the structure of the cytoskeleton, challenging the concept that nuclear localisation is simply a sequestering mechanism.

In an attempt to address whether there is a separate nuclear role for PBL, the conserved N-terminal sequences encoding the potential nuclear functional domains of the protein were removed by *in vitro* mutagenesis, and the effect of this deletion was examined in transgenic flies. While deletion of the RadECl region and two BRCT domains did not

appear to change the nuclear localisation of the protein when it was overexpressed in a variety of tissues, a range of severe phenotypes were observed. Compared to full-length wild type PBL, which caused a mild roughening of the eye when overexpressed in the developing larval eye disc, ΔBRCT PBL caused an extreme effect on eye development. The *GMR>ΔBRCTpbl* adult eye was characteristically small and glassy in appearance. Initial analysis of this phenotype indicated a disruption in the morphology of larval eye disc cells and nuclei. Although some nuclei appeared to be blocked in mid-mitosis, western analysis using a mitosis specific antibody showed this not to be the case, suggesting that nuclear morphology, rather than the process of mitosis itself, is affected. However, this phenotype in the eye may be due to unregulated activity of PBL, and if so, the effect of ectopic activity cannot be interpreted as indicating normal PBL function. In support of this, reducing the amount of PBL in the *GMR>ΔBRCTpbl* flies, through the introduction of a *pbl* null mutant allele, had no effect on the rough eye phenotype. This indicated that ΔBRCT PBL is not acting as a dominant negative form of the protein, and is not interfering with normal PBL function to produce the severe phenotype observed, consistent with an ectopic activity.

The patterning of the eye was also affected, with the neural clusters of ELAV expressing cells completely destroyed. However, unlike the *ΔNLSpbl* phenotype where a reduction in the number of ELAV expressing cells was observed, cells of the *GMR>ΔBRCTpbl* larval eye disc were still observed to express ELAV, despite their lack of organisation into clusters. This disruption of patterning early in development was also observed later in development, with a disruption to the patterning of the pupal eye disc. While expression of *ΔBRCTpbl* at 25°C caused a severely necrotic disc, the weaker expression at 18°C caused a disruption in the number of interommatidial and cone cells, with an occasional bristle defect. This phenotype was surprisingly similar to that of full length PBL and ΔNLS PBL, despite their very different final phenotypic appearances, indicating differences in the later effects of the mutant proteins on eye cell morphogenesis.

The *ΔBRCTpbl* construct was also shown to affect the proliferating cells of the wing disc, the differentiating cells of the eye disc when driven by the *elav GAL4* promoter and the non-cytokinetic cells of the salivary gland. Expression of the ΔBRCT form of PBL can therefore affect a variety of tissues, regardless of whether they are proliferating or have ceased proliferation and are differentiating.

The rough eye phenotype caused by the overexpression of the *ΔBRCTpbl* construct was strongly suppressed by reducing the amount of RhoA but not other Rho family G

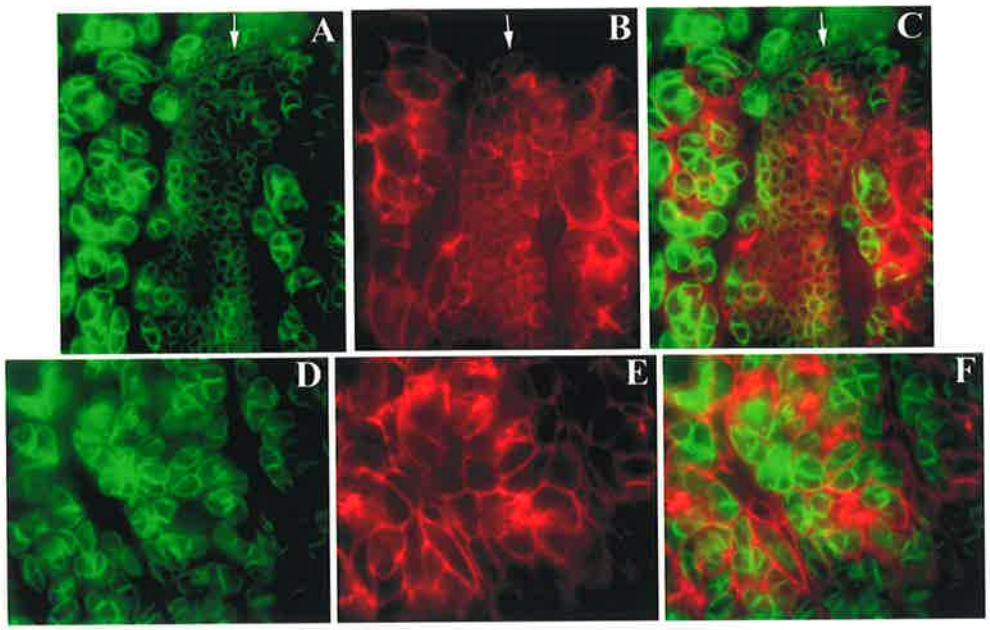

Figure 4.15 ΔBRCT PBL cannot rescue cytokinesis in a *pbl* mutant background.

A- C. A *prd GAL4, pbl^2/UAS pbl, pbl^3* embryo expressing wild type PBL in a *pbl* mutant background. The embryo was fixed and stained with anti-lamin which highlights the nuclear envelope, shown in green in (A), and anti-spectrin which stains the cell cortex, shown in red in (B). The merge of these two images is shown in (C). Expression of wild type PBL in alternate stripes along the embryo using *prd GAL4*, completely rescued the cytokinetic defect of the *pbl* mutant within those stripes. The rescue stripe is indicated by the white arrows.

D- F. A *prd GAL4, pbl^2/UAS ΔBRCTpbl, pbl^3* embryo expressing ΔBRCT PBL in a *pbl* mutant background. The embryo was fixed and stained with lamin (D) and spectrin (E). The merge of these two images is shown in (F). Expression of ΔBRCT PBL in alternate stripes along the embryo using *prd GAL4*, could not rescue the cytokinetic defect of the *pbl* mutant within those stripes. Three adjacent mutant stripes are shown.

proteins, indicating that despite lacking these nuclear domains, the protein continues to act through Rho. However, as discussed in the previous chapter, the redundancy between Rac1, Rac2 and Mtl (Hakeda-Suzuki *et al.*, 2002) poses a problem in that unless all three are removed at the same time, it cannot be concluded that ΔBRCT PBL does not act through Rac. Also, the fact that the only available Rac alleles were deficiencies that take out large regions of the chromosome, introduces the possibility that other genetic interactions may mask any potential interaction with Rac.

Overexpression of the cell death inhibitor P35, as with the *GMR>ΔNLSpbl* eye phenotype, was found to moderately suppress the *GMR>ΔBRCTpbl* rough eye phenotype. No dramatic differences in larval eye disc apoptosis were observed, indicating that the suppression by *GMR>p35* is likely to be due to blocking a secondary apoptotic effect induced by the extreme disruption to cell function caused by the expression of *ΔBRCTpbl*.

In the salivary gland, expression of the *ΔBRCTpbl* construct, like the expression of full length PBL, was found to cause a severe rounding of cells. However in the *ΔBRCTpbl* salivary glands, actin structure also appeared to be completely disrupted, with sheets of actin filaments forming in the cytoplasm. Interestingly, this phenotype resembles the actin stress fibre phenotype induced in tissue culture cells by the overexpression of activated Rho. Expression of activated Rho in the *Drosophila* salivary gland using the sav *GAL4* driver would therefore show whether this salivary gland phenotype is also due to inappropriate Rho activation. However, while the phenotype caused by the overexpression of full length PBL could be suppressed in this tissue by reducing the amount of RhoA, the reduction of Rho had no effect on the *ΔBRCTpbl* severe phenotype. Whether this phenotype is just too severe to be suppressed by reducing Rho activity, or whether the ΔBRCT form is acting through another pathway in this tissue remains to be seen. Another possibility is that expression driven by sav *GAL4* in the salivary gland is higher than that of *GMR GAL4* in the eye, allowing other G proteins to be activated in this tissue. Analysis of the ability of other Rho family members to suppress these phenotypes would therefore resolve this question.

The ability of both the wild type and ΔBRCT nuclear forms of the protein to have such a strong effect on the cytoskeleton was highly surprising, challenging the notion that nuclear localisation is a simply a sequestering mechanism. This effect could be explained by nuclear-cytoplasmic shuttling of the proteins, with the BRCT domains being required for anchoring the protein in the nucleus. However, this cannot be the sole explanation for this phenotype, as the completely cytoplasmic form of the protein containing the BRCT domains

was not observed to have such a severe effect on cytoplasmic actin. Lack of some unknown BRCT domain function in the cytoplasm would also be required to explain this disruption.

In accordance with a potentially cytoplasmic role, the RadECl region and BRCT domains were shown to be required for cytokinesis. This is a completely novel finding, and challenges the notion that such domains are only involved in DNA damage and cell cycle checkpoint type processes. However, the question that remains concerns whether these domains are required in the nucleus or cytoplasm for cytokinesis to occur.

In conclusion, the range of severe phenotypes observed when the RadECl and BRCT domains of PBL were deleted indicate that these nuclear domains are highly important for the maintenance of normal cellular processes during development. However, the ability of the nuclear protein lacking these domains to affect the cytoskeleton and cell morphology, even in non-dividing cells, suggests one of two possibilities. Either there is a novel Rho-dependent nuclear function for PBL, or the PBL protein is capable of shuttling between the nucleus and the cytoplasm, with the BRCT domains being required for some unknown cytoplasmic process. In support of a potential cytoplasmic role, the RadECl and BRCT domains were found to be required for cytokinesis. A cytoplasmic role for these domains is therefore examined in more detail in the next chapter, where *in vitro* mutagenesis was used to remove RadECl and BRCT domain function from the cytoplasm.

Chapter 5: Analysis of a cytoplasmic role for the RadECl region and BRCT domains

5:1 Introduction

As discussed in the previous chapters, PBL plays an essential role in cytokinesis. Through its DH and PH domains, PBL is thought to activate Rho, leading to the correct formation and function of the contractile ring which divides the cytoplasm in two (Prokopenko *et al.*, 1999). In addition to these cytoplasmic domains, PBL contains a consensus bipartite nuclear localisation signal, a potentially nuclear RadECl region, and two BRCT domains. In chapter 3, the importance of sequestering PBL to the nucleus was examined through the mutation of the nuclear localisation signal. While nuclear localisation of PBL was found not to be essential for its role in cytokinesis, the range of severe phenotypes caused by the cytoplasmic form of the protein indicated the importance of sequestering the protein to the nucleus for the maintenance of normal cellular processes. This finding suggested that nuclear localisation could simply be a sequestering mechanism. However, the ability of the apparently nuclear wild type form of the protein to modify the cytoskeleton when expressed in the salivary gland suggested that, at least in this tissue, nuclear sequestration is not sufficient to prevent PBL activity. Nuclear localisation is also not the only known method of regulating the cytoplasmic action of a protein. Post translational modifications such as phosphorylation or degradation could be used to regulate PBL function in the cytoplasm. Therefore it remained a possibility that nuclear localisation could be associated with a completely separate nuclear role.

In the previous chapter, we saw that deletion of the RadECl/BRCT domains did not disrupt the nuclear localisation of the wild type protein. However, this ΔBRCT form caused a range of severe phenotypes when expressed in a variety of tissues and failed to rescue cytokinesis. The question that remains concerns whether these domains are required in the nucleus or the cytoplasm for this role. To test this, *in vitro* mutagenesis was used to combine the ΔNLS and ΔBRCT mutations to remove RadECl and BRCT domain function from the cytoplasmic form of the protein.

5:2 Site directed mutation of the nuclear localisation signal within the ΔBRCT PBL construct

To combine both the ΔNLS and ΔBRCT mutations, site directed *in vitro* mutagenesis was again employed. Using the two complementary primers described in chapter 3, the nuclear localisation signal was specifically mutated on the ΔBRCT PBL construct by using the *ΔBRCTpbl* cDNA as a template (**Figure 5.1a**). Sequences of the resulting potential mutant clones were then determined to ensure that they carried both the specific NLS mutation and the ΔBRCT deletion, but no other mutations (**Figure 5.1b**).

A ΔNLSΔBRCT mutant *pbl* cDNA sequence was then cloned into the multiple cloning site of the pUAST vector, described previously, using the enzymes XhoI/XbaI. The pUAST–*ΔNLSΔBRCTpbl* cDNA construct was transformed into *Drosophila* by microinjection and after subsequent crosses, 15 separate transgenic lines were established. The chromosome into which the construct was inserted was then determined by genetic mapping. One line mapped to the X chromosome, eight lines mapped to the second chromosome, and six mapped to the third chromosome. All but three of these inserts were homozygous viable.

5:3 Expression of ΔNLSΔBRCT PBL in the *Drosophila* eye disc causes a severe rough eye

To analyse the effect of removing the RadECl region and BRCT domains from the cytoplasmic form of the protein, the eye specific enhancer *GMR* was used, as before, to drive the expression of the ΔNLSΔBRCT mutant protein in the developing eye disc. *GMR*-driven expression of ΔNLSΔBRCT PBL resulted in the most severe of the eye phenotypes generated in this study. All 15 transgenic lines were larval lethal at 25°C when crossed to *GMR GAL4*. As previously discussed, lethality is presumably due to leaky GAL4 expression in other tissues. At the lower temperature of 18°C, 12 out of 15 were larval or pupal lethal. The other 3 lines gave an extremely rough eye phenotype at 18°C. Eyes were almost completely

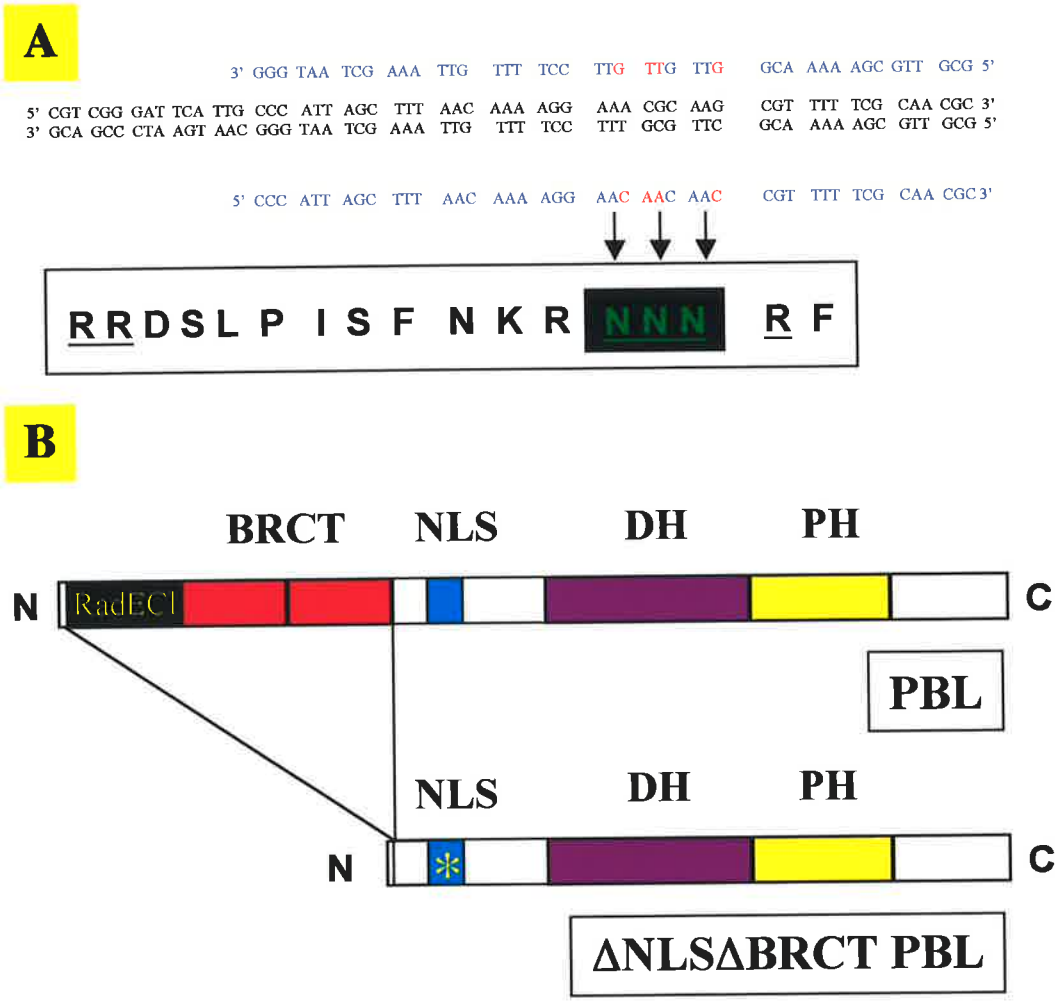

Figure 5.1 Site directed mutagenesis of the consensus bipartite nuclear localisation signal of ΔBRCT PBL.

A. The DNA sequence of the nuclear localisation signal of PBL is shown in black, with the primers designed to mutate 4 base pairs of this sequence shown in blue. The 4 mutant base pairs are shown in red. Beneath is the amino acid sequence of the mutated nuclear localisation signal. The critical basic residues of this signal are underlined, and the lysine/arginine/lysine (K/R/K) residues which were changed to asparagine residues (N) are shown in green, highlighted by a black box. The *ΔBRCTpbl* construct was used as the template in this *in vitro* mutagenesis reaction to combine the *ΔNLS* and *ΔBRCT* mutations in one construct.
B. A schematic diagram of the structure of the PBL protein, with the RadEC1 region boxed in black, the 2 consensus BRCT domains in red, the consensus bipartite nuclear localisation signal in blue, the Dbl homology domain (DH) in purple, and the Pleckstrin homology domain (PH) in yellow. Underneath is the ΔNLSΔBRCT construct which specifically removes both the BRCT domains and the RadEC1 region, has a mutated NLS (indicated by a yellow *), but contains the DH/PH domains.

ablated, with a blister remaining where the eye once was (**Figure 5.2c**). As such, they were phenotypically quite different to both *GMR>ΔNLSpbl* (**Figure 5.2a)** and *GMR>ΔBRCTpbl* (**Figure 5.2b**) eyes raised at the same temperature. Given the extreme nature of the phenotype, it was deemed pointless to attempt to section them.

In order to confirm the expected cytoplasmic localisation of the ΔNLSΔBRCT PBL protein, *GMR>ΔNLSΔBRCTpbl* larvae were grown at 18°C to enable their survival to the third instar, so that eye discs could be dissected and fixed. At this lower temperature, *GMR* is comparatively weakly expressed and, as a result, a very low level of expression was observed. However, the ΔNLSΔBRCT PBL protein was observed to be completely cytoplasmic as expected (**Figure 5.2d**).

To discount the possibility that the severity of the *ΔNLSΔBRCTpbl* phenotype is simply due to expression at a much higher level than that of the other constructs, western analysis was performed. Wild type, *GMR>pbl*, *GMR>ΔNLSpbl*, *GMR>ΔBRCTpbl*, and *GMR>ΔNLSΔBRCTpbl* eye discs were dissected at 18 and 25°C, boiled, and run on a 10% SDS polyacrylamide gel, which was then transferred to nitrocellulose and probed with an anti-PBL antibody. As can be seen from **Figure 5.3**, while *pbl* and *ΔNLSpbl* are expressed at a lower level at 18°C compared to 25°C, no band was observed for the *ΔBRCTpbl* sample at 18°C, presumably because expression was too low to detect on the western. For the *ΔNLSΔBRCTpbl* construct at 18°C, one sample had a very faint band, and the other had no band at all. However, the alpha-tubulin load control shows that a large amount of protein has been loaded for both of these samples. Thus it seems that the faint or absent band for the *ΔNLSΔBRCTpbl* samples is due to a very low level of the protein. Furthermore, the *ΔNLSΔBRCTpbl* construct appears to be expressed at a substantially lower level than *ΔNLSpbl*. Thus the increased severity of the *ΔNLSΔBRCTpbl* construct must be due to the absence of RadECl/BRCT domain function in the cytoplasm. In support of this is the fact that all 15 *ΔNLSΔBRCTpbl* lines were lethal with *GMR* at 25°C. It is highly improbable that all 15 lines would be expressed at a higher level than all of the *ΔNLSpbl* or *ΔBRCTpbl* lines.

5:4 Characterisation of the ΔNLSΔBRCT PBL phenotype in the eye

Expression of ΔNLSΔBRCT PBL caused a severe disruption to the development of the adult eye. This phenotype was far more severe than that of ΔNLS PBL, suggesting that the RadECl/BRCT domains play some unknown but important role in the cytoplasm. As a first step towards characterising this phenotype in the eye, larval eye disc cells were dissociated and examined. As discussed in the previous two chapters, the larval eye disc has a compact columnar epithelial structure, making dissociation necessary for the examination of individual cells. *GMR>ΔNLSΔBRCTpbl* flies were crossed to a *UAS-GFP* line so that those cells overexpressing ΔNLSΔBRCT PBL would also be expressing GFP, allowing identification and visualisation of these cells without fixation and antibody staining. The crosses were performed at 18°C, because of the lethality of this construct at 25°C.

Like the *GMR>ΔNLSpbl* phenotype at 25°C, *GMR>ΔNLSΔBRCTpbl* eye discs at 18°C were found to contain both multinucleate and anucleate cells (**Figure 5.4a-b**). However, quite surprisingly, considering the severe nature of the *GMR>ΔNLSΔBRCTpbl* adult eye phenotype at 18°C, most of the dissociated cells appeared normal (**Figure 5.4c**). There were also no examples of the fused sister chromatids which were characteristic of the *GMR>ΔBRCTpbl* phenotype (**refer to Figure 4.5b-d**). Given the relatively mild phenotype observed in the *ΔNLSΔBRCTpbl* eye disc cells at the larval stage, it seemed likely that later developmental defects must be responsible for the severe adult phenotype observed. To examine the further development of the eye, pupal eye discs were examined. *GMR>ΔNLSΔBRCTpbl* pupal discs raised at 18°C were dissected, fixed and stained for the epithelial cell contact marker Armadillo. Hoechst 33258 stain was used to visualise the DNA. Like both the *GMR>ΔNLSpbl* and *GMR>ΔBRCTpbl* phenotypes, *GMR>ΔNLSΔBRCTpbl* pupal discs had too many interommatidial and bristle cells (**Figure 5.5c-d**). However, in contrast to both the *ΔNLSpbl* and *ΔBRCTpbl* phenotypes, which had too few cone cells, *ΔNLSΔBRCTpbl* pupal eye discs occasionally had too many cone cells (**Figure 5.5c**). Given the fact that a difference in cone cell number alone is unlikely to explain the almost complete ablation of the *ΔNLSΔBRCTpbl* adult eyes, later developmental defects must be responsible.

To determine when the patterning process of the eye begins to fail, *GMR>ΔNLSΔBRCTpbl* larval eye discs were fixed and stained with anti-ELAV. As

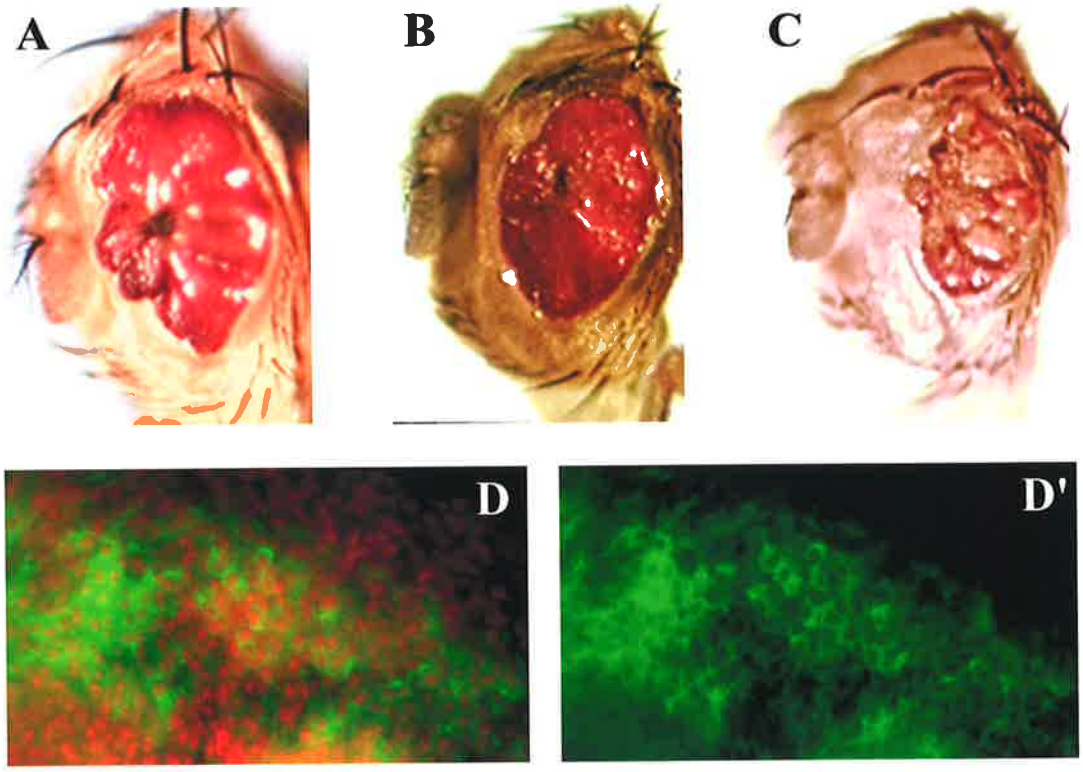

Figure 5.2 Expression of ΔNLSΔBRCT PBL in the eye disc causes an extremely rough eye.

A. A *GMR GAL4::UAS ΔNLSpbl* adult eye. A severe rough eye phenotype is caused by the overexpression of ΔNLS PBL posterior to the morphogenetic furrow in the developing eye disc at 18 degrees C.
B. A *GMR GAL4::UAS ΔBRCTpbl* adult eye. A severe, but phenotypically distinct, rough eye phenotype is caused by the overexpression of ΔBRCT PBL posterior to the morphogenetic furrow in the developing eye disc at 18 degrees C.
C. A *GMR GAL4::UAS ΔNLSΔBRCTpbl* adult eye. An extreme rough eye phenotype is caused by the overexpression of ΔNLSΔBRCT PBL posterior to the morphogenetic furrow in the developing eye disc at 18 degrees C. This phenotype is different to both *GMR>ΔNLSpbl* and *GMR>ΔBRCTpbl* eyes raised at the same temperature.
D. A *GMR GAL4::UAS ΔNLSΔBRCTpbl* third instar larval eye disc at 18 degrees fixed and stained with anti-PBL antibody (shown in green) and hoechst 33258 DNA stain (shown in red). ΔNLSΔBRCT PBL is observed to localise to the cytoplasm. The anti-PBL stain alone is shown in D'.

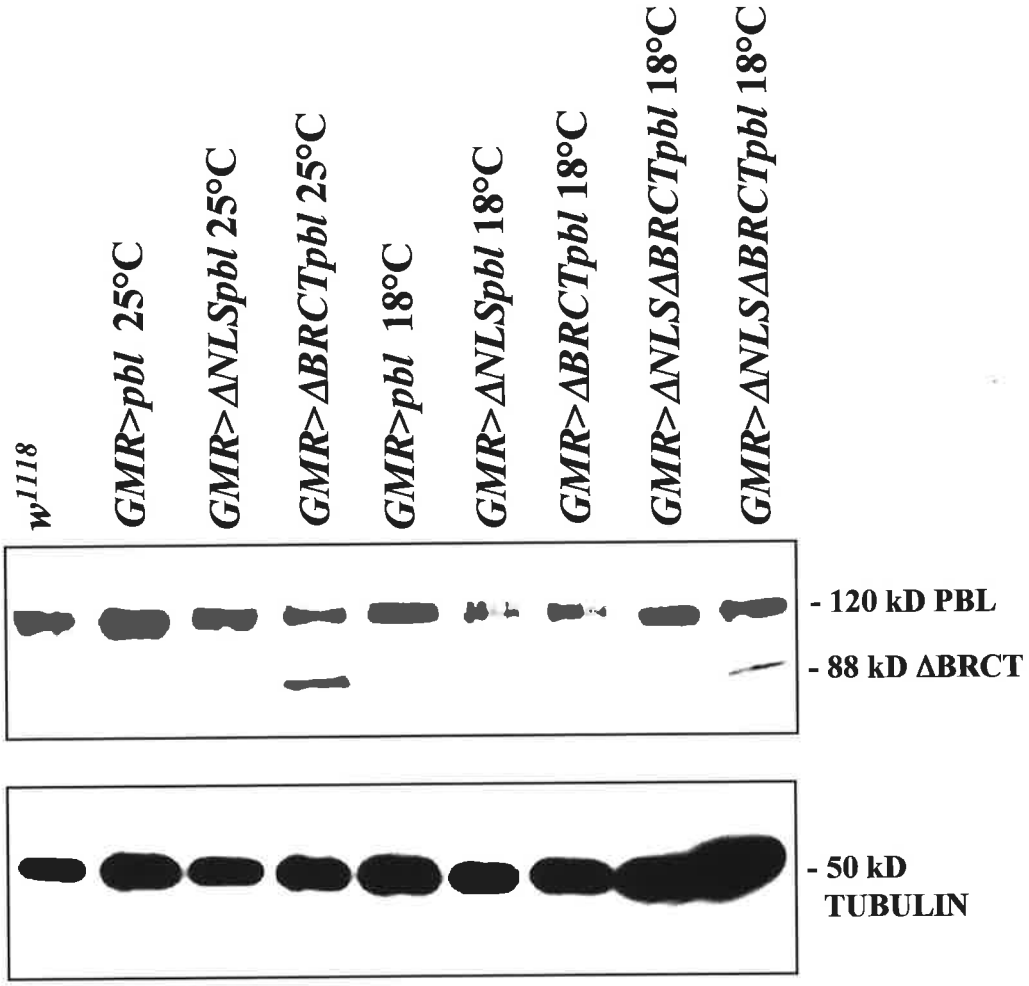

Figure 5.3 Western analysis of *GMR>GAL4* expression levels in the eye.

w^{1118}, *GMR GAL4::UAS pbl*, *GMR GAL4::UAS ΔNLSpbl*, *GMR GAL4::UAS ΔBRCTpbl* and *GMR GAL4::UAS ΔNLSΔBRCTpbl* eye discs were dissected at both 18 and 25°C, boiled and run on a 10% SDS polyacrylamide gel, which was then transferred to a nitrocellulose filter. The filter was then probed with an anti-PBL antibody, which produced a band of approximately 120 kD in size in each lane. The ΔBRCT form of PBL removes 286 amino acids, and is approximately 88 kD in size.
The filter was then stripped and reprobed with an alpha-tubulin antibody, which served as a loading control. This produced a band of approximately 50 kD in size.
As can be seen from the filter, ΔNLSΔBRCT PBL is expressed at a very low level compared to the other constructs. In one lane a very weak band was observed, and in another, no band was observed, presumably because not enough protein was present to be detected on the western.

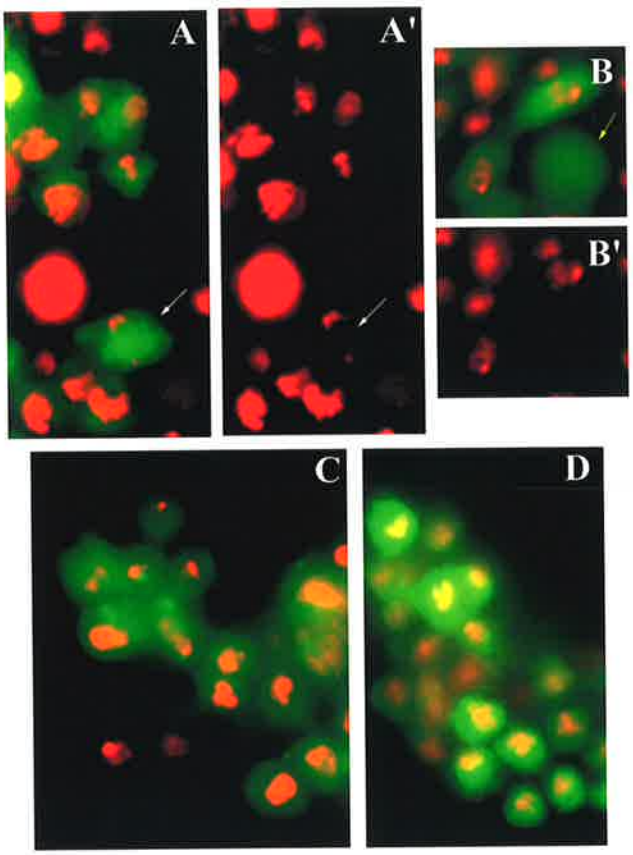

Figure 5.4 Dissociation of eye disc cells and visualisation by epifluorescence.

GMR GAL4::UAS ΔNLSΔBRCTpbl, and *GMR GAL4::UAS pbl* eye discs were dissociated and stained with hoechst to visualise the DNA (shown in red). *UAS GFP* was co-expressed to enable visualisation of the cells overexpressing the *pbl* constructs (shown in green). All images were taken at 100x magnification.

A. *GMR GAL4::UAS ΔNLSΔBRCTpbl* dissociated eye disc cells. Some cells are multinucleate, as indicated by the white arrow. The DNA stain alone is shown in A'.

B. *GMR GAL4::UAS ΔNLSΔBRCTpbl* dissociated eye disc cells. Some cells appear to be anucleate (yellow arrow). The DNA stain alone is shown in B'.

C. *GMR GAL4::UAS ΔNLSΔBRCTpbl* dissociated eye disc cells. Some cells appear to be quite normal, like the *GMR>pbl* eye disc cells shown in D.

D. *GMR GAL4::UAS pbl* dissociated eye disc cells. Cells are mononucleate.

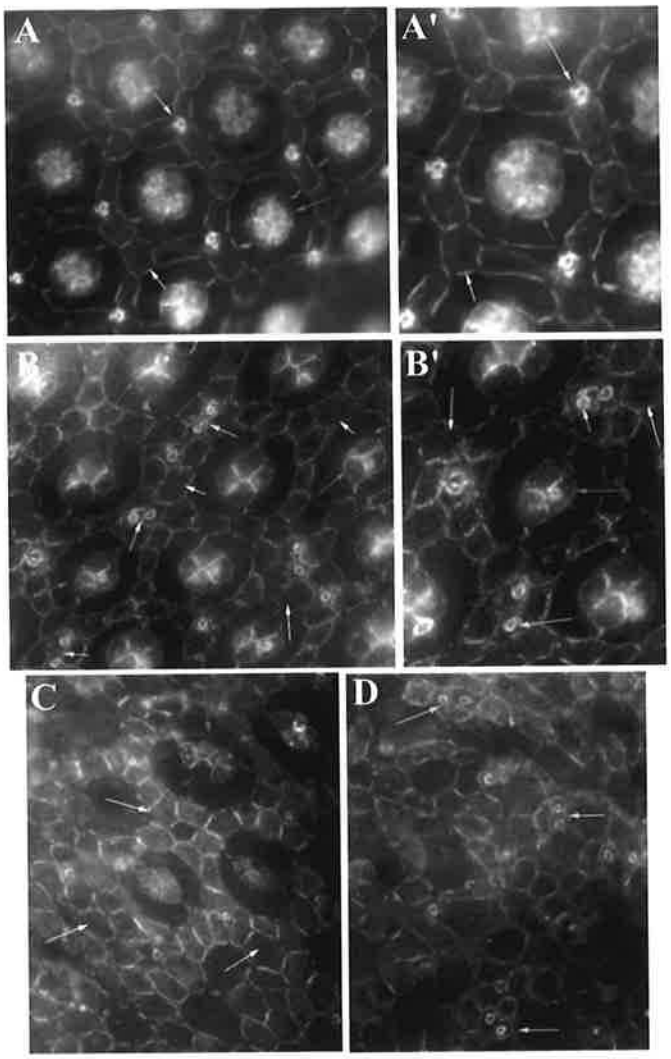

Figure 5.5 Disruption of pupal eye disc structure in *GMR GAL4::UAS ΔNLSΔBRCTpbl* eye discs.

All pupal discs were stained with antibodies against the cell contact marker Armadillo. Images were taken at 100x magnification.
A. Wild type pupal eye disc at 42 hr APF at 25 degrees C. The white arrow indicates an interommatidial cell, the yellow arrow a bristle cell, and the red arrow points to a group of cone cells. A'. Close up view of a wt pupal ommatidium.
B. *GMR GAL4::UAS ΔNLSpbl* eye disc at 84 hr APF at 18 degrees C. The pupal disc has more interommatidial cells than wild type (white arrows), more bristle cells (yellow arrows), and some ommatidia have too few cone cells (red arrows). B'. Close up view of a *GMR>ΔNLSpbl* ommatidium.
C. *GMR GAL4::UAS ΔNLSΔBRCTpbl* eye disc at 84 hr APF at 18 degrees C. The pupal disc has too many interommatidial cells (white arrows), and the occasional ommatidium has too many cone cells (red arrow).
D. *GMR GAL4::UAS ΔNLSΔBRCTpbl* eye disc at 84 hr APF at 18 degrees C. This pupal disc has a more severely disrupted structure with too many interommatidial cells and too many bristle cells (yellow arrows).

discussed previously, ELAV is expressed only in those cells of the eye disc that have adopted a neural fate (Campos *et al.*, 1987; Robinow and White, 1988). *GMR>ΔNLSΔBRCTpbl* eye discs were observed to have a reduction in the number of ELAV-expressing cell clusters (**Figure 5.6g-l**), a phenotype that was identical to that of *GMR>ΔNLSpbl* eye discs (**Figure 5.6d-f**). The morphogenetic furrow still progresses in these discs, but the adoption of neural cell fate seems to be delayed. Thus, early patterning events are disrupted in the *GMR>ΔNLSΔBRCTpbl* eye discs.

5:5 The effect of ΔNLSΔBRCT expression in the wing disc

As described above, expression of the cytoplasmic ΔNLSΔBRCT PBL in the proliferating and differentiating cells of the eye using the enhancer *GMR* was found to cause disruptions to both cytokinesis and the patterning of the eye disc. To examine whether expression of this construct can affect other proliferating tissues, ΔNLSΔBRCT PBL was expressed in the developing wing disc using the driver *71B*. While the expression of wild type PBL was previously shown to have no effect on the development of the adult wing (**Figure 5.7a**), expression of both *ΔNLSpbl* and *ΔBRCTpbl* was found to result in blistered and crumpled wings which frequently lacked the two cross veins. Expression of ΔNLSΔBRCT PBL produced a very similar phenotype. Wings were small, blistered, and fluid filled (**Figure 5.7b-c**), and also lacked the two cross veins (**Figure 5.7d**). Thus expression of the ΔNLSΔBRCT mutant form of PBL in the proliferating cells of both the eye and wing disc, causes severe disturbances to the development of both of these tissues.

5:6 The effect of ΔNLSΔBRCT expression in differentiating cells of the eye disc

To analyse the effect on differentiating tissues, ΔNLSΔBRCT PBL was expressed under the control of the *elav GAL4* driver, specific for the differentiating neural cells of the eye. As discussed in the previous chapters, when wild type PBL was expressed under the control of *elav GAL4*, no discernible disruption to eye development was observed (**Figure 4.10a**). When ΔNLS PBL and ΔBRCT PBL were expressed at 25°C, almost identical severe rough eye phenotypes were observed. Eyes for both of these constructs were small and glassy in appearance, with a characteristic ring of necrosis in the middle of the eye (**Figure 4.10b** and **c**), indicating that expression of these constructs can affect post mitotic cells. When ΔNLSΔBRCT PBL was expressed under the control of this driver at 25°C, the effect was embryonic lethal. The cross failed to take numerous times, and dead embryos with necrotic nervous systems were observed. This was presumably due to the fact that *elav GAL4* is expressed in a range of neural tissues throughout development. Reducing the temperature to 18°C or even 13°C did not prevent the embryonic lethality, indicating that ΔNLSΔBRCT PBL has a severely toxic effect on differentiating neural cells. The increased severity of this construct compared to both ΔNLS PBL and ΔBRCT PBL was consistent with that observed with the *GMR GAL4* driver. Thus like ΔNLS PBL and ΔBRCT PBL, the ΔNLSΔBRCT PBL construct can also affect cells that have ceased dividing.

5:7 The effect of ΔNLSΔBRCT PBL expression in salivary glands

The effect of ΔNLSΔBRCT PBL on the non-proliferating tissues of the larva was examined further using the salivary gland. As discussed in the previous chapters, the sav *GAL4* construct drives expression in a set of cells that have ceased cytokinesis. When full length PBL was expressed in these cells, it was observed to be nuclear and to have a significant effect on both cell size and cell shape, with a rounding of the cell cortex. The ΔNLS cytoplasmic form was found to have a similar, but more severe effect, with the glands

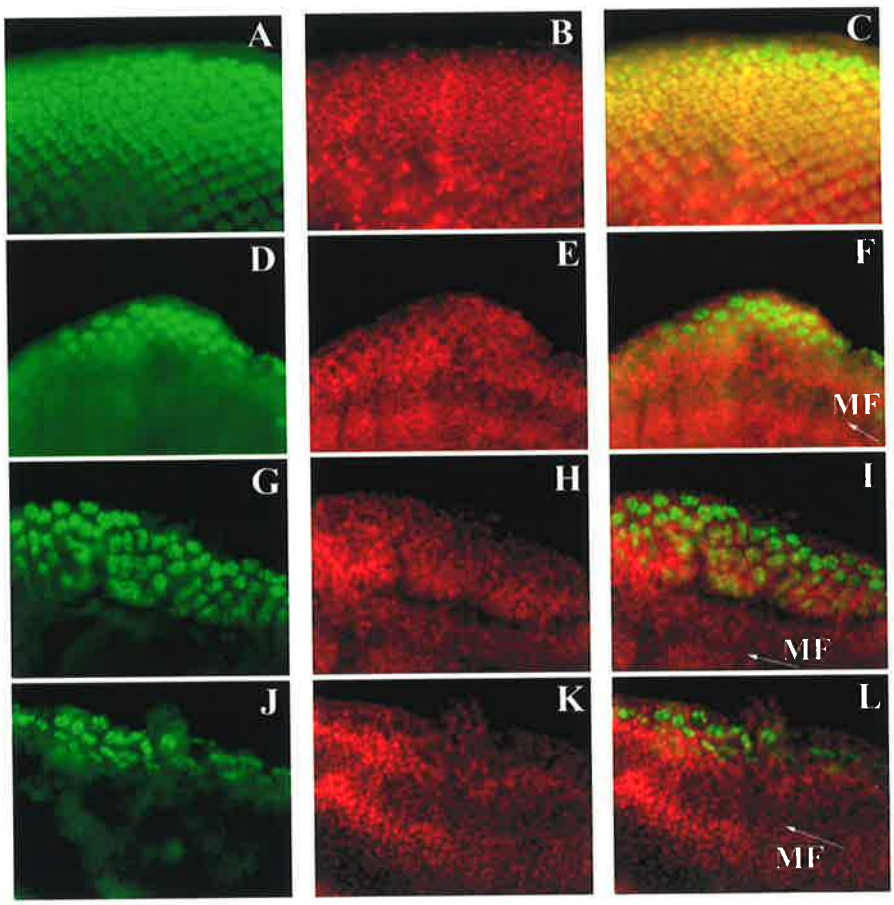

Figure 5.6 Adoption of neural cell fate is disrupted in *GMR GAL4::UAS ΔNLSΔBRCTpbl* eye discs.

Third larval instar eye discs were stained with the neural specific antibody ELAV, and hoechst 33258 stain for the DNA at 25 degrees C (unless otherwise indicated). ELAV is normally expressed in all cells posterior to the morphogenetic furrow which have adopted a neural fate.

A - C. Wild type eye disc stained with α–ELAV in green (A), and DNA stain in red (B). The merge of these two images is shown in C.

D - F. *GMR GAL4::UAS ΔNLSpbl* eye disc stained with α–ELAV in green (D), and DNA stain in red (E). A large reduction in the number of ELAV-staining cells is observed posterior to the morphogenetic furrow. However the clustered organisation of the ELAV-expressing cells remains. The merge of these two images is shown in F. The furrow still progresses (white arrow), but only those cells furthest from the furrow are expressing ELAV.

G - I. *GMR GAL4::UAS ΔNLSΔBRCTpbl* eye disc stained with α–ELAV in green (G), and DNA stain in red (H) at 18 degrees C. A similar phenotype to that of *GMR>ΔNLSpbl* eye discs at 25 degrees is observed. There is a reduction in the number of ELAV-expressing clusters posterior to the morphogenetic furrow (white arrow). The merge of these images is shown in I.

J-L. *GMR GAL4::UAS ΔNLSΔBRCTpbl* eye disc stained with α–ELAV in green (J), and DNA stain in red (K) at 18 degrees C. This disc has a more severe reduction in the number of ELAV-expressing clusters. The merge is shown in L.

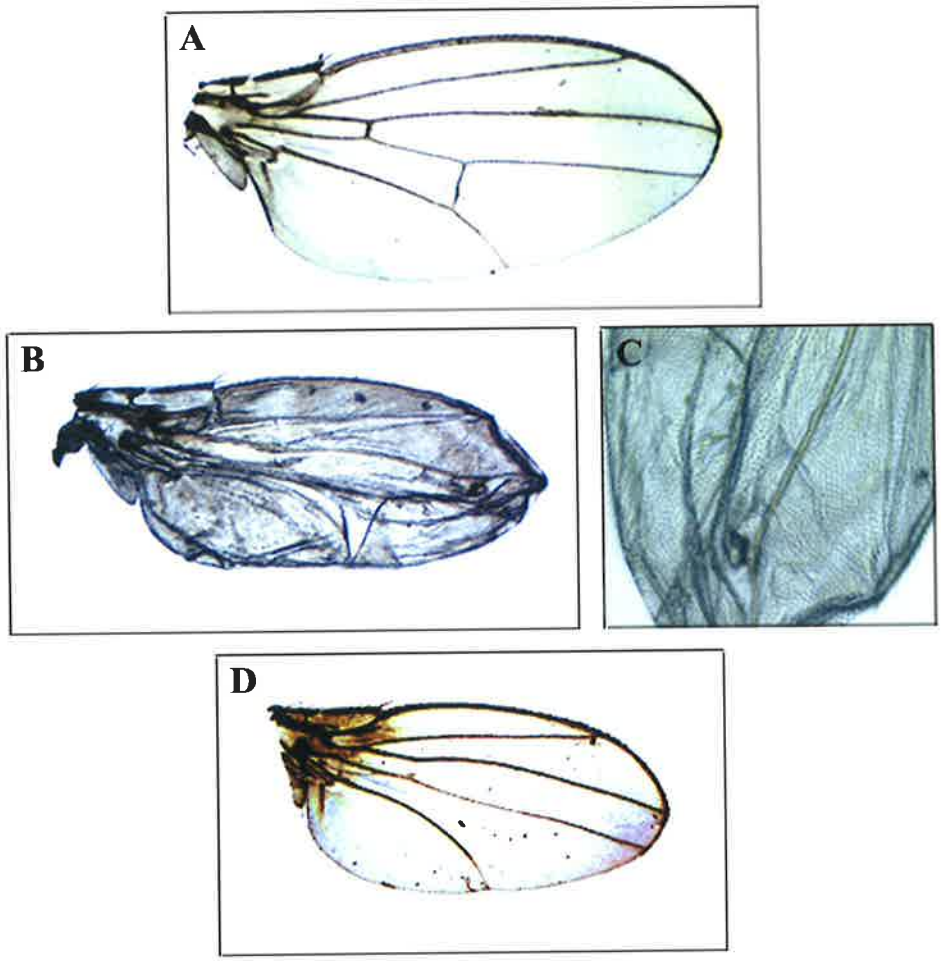

Figure 5.7 ΔNLSΔBRCT PBL disrupts wing development.

A. *71B GAL4::UAS pbl* adult wing (5x mag). Overexpressing PBL has no effect on wing development. Adult wings of normal size are produced, with normal venation.

B. *71B GAL4::UAS ΔNLSΔBRCTpbl* adult wing (5x mag). Overexpression of ΔNLSΔBRCT PBL disrupts wing development, producing blistered, fluid filled wings.

C. Close up view of the wing shown in B.

D. *71B GAL4::UAS ΔNLSΔBRCTpbl* adult wing (5x mag). This wing is not as disrupted, but clearly shows the lack of the two cross veins.

being significantly smaller, and their cells severely rounded. When ΔBRCT PBL was expressed, in addition to a reduction in gland size, and a significant rounding of the cells, a severe disruption of the actin cytoskeleton was observed. What was surprising was the ability of the apparently nuclear PBL and ΔBRCT PBL to have such a strong effect on the actin cytoskeleton. ΔNLSΔBRCT PBL was therefore expressed and its phenotype compared to that of the other constructs.

In line with that observed in other tissues, the *ΔNLSΔBRCTpbl* construct gave the most severe of the salivary gland phenotypes observed. Glands were dramatically reduced in size, and a severe disruption of the actin cytoskeleton was observed (**Figure 5.8c**), a phenotype which was very similar to that caused by expression of the ΔBRCT PBL construct (**Figure 5.8b**). Sheets of filamentous actin were observed in the cytoplasm and, as expected, anti-PBL stains showed ΔNLSΔBRCT PBL to localise to the cytoplasm (**Figure 5.8c'**).

In an attempt to examine the expression level of this construct, western analysis was performed. Wild type, sav>*pbl*, sav>*ΔNLSpbl*, sav>*ΔBRCTpbl* and sav>*ΔNLSΔBRCTpbl* salivary glands were dissected, boiled and run on a 10% SDS polyacrylamide gel, which was then transferred to nitrocellulose and probed with an anti-PBL antibody. As can be seen from **Figure 5.9**, ΔNLSΔBRCT PBL is present at a much lower level than the other constructs. Thus the severe phenotype of these salivary glands is due to the absence of RadECl/BRCT domain function in the cytoplasm.

One explanation for the similarity of the ΔNLSΔBRCT PBL salivary gland phenotype to that produced by expression of the ΔBRCT PBL construct, is that ΔBRCT PBL shuttles out into the cytoplasm, and it is the absence of some unknown RadECl or BRCT domain function in the cytoplasm which causes the severe disruption of the actin cytoskeleton observed. Assuming that shuttling of PBL occurs, the ΔBRCT form of PBL would only shuttle into the cytoplasm from the nucleus, while the ΔNLSΔBRCT form would be continuously in the cytoplasm, explaining the increased severity caused by expression of this construct. This nuclear-cytoplasmic shuttling theory would explain how the ΔBRCT PBL protein could have such an effect on the actin cytoskeleton, and is examined in the following section. Here the shuttling of both PBL and ΔBRCT PBL between the nucleus and the cytoplasm is specifically tested using a heterokaryon model system.

5:8 The heterokaryon model system to examine the nuclear-cytoplasmic shuttling of PBL

The heterokaryon system is a technique used to examine the shuttling of a protein between the nucleus and cytoplasm (Pinol-Roma and Dreyfuss, 1992; Michael *et al.*, 1995; Michael *et al.*, 1997; Fan and Steitz, 1998). First the nuclear localised, tagged protein is expressed using a constitutive chicken β-actin promoter in human cells. After a set amount of time, cycloheximide treatment is used to inhibit further protein expression, ensuring that the tagged protein is restricted to the human nuclei. The human cell population is then fused to a mouse cell line to form heterokaryon cells, consisting of both mouse and human nuclei. The cells are then fixed, and stained with an antibody against the tag (in this case anti-FLAG) and with hoechst 33258 to stain the nuclei. Human and mouse nuclei are phenotypically distinct, and hoechst staining allows the two to be differentiated via microscopy. If FLAG tagged protein is observed in the mouse nuclei of heterokaryons, then the protein must be capable of shuttling from the human nuclei to the cytoplasm and then it must enter the mouse nuclei via nuclear import. This technique was therefore used to examine whether the apparently nuclear localised PBL and ΔBRCT PBL are capable of shuttling between the nucleus and the cytoplasm.

Site directed mutagenesis was used to add a FLAG tag to the 5' end, immediately 3' of the initiating ATG, of both the *pbl* and *ΔBRCTpbl* cDNA constructs contained within the pBLUESCRIPT vector. This was accomplished by designing two complementary primers containing the FLAG tag sequence (5' GAC TAC AAG GAC GAC GAT GAC AAG 3'), flanked on either side by 14 and 12 bp of non-mutated sequence. *In vitro* site directed mutagenesis was performed on both the *pbl1A* and *ΔBRCTpbl* cDNA sequences using the Stratagene *in vitro* mutagenesis kit. As both *pbl 1A* and *ΔBRCTpbl* have the same sequence around their 5' ends, the same primer set was used on both constructs. Sequences of the resulting potential mutant clones were then determined to ensure they had the FLAG sequence inserted directly after the initiating ATG, but no other mutations.

A FLAG tagged *pbl* and *ΔBRCTpbl* cDNA sequence were then both cloned separately into the pACT vector using the enzymes NcoI/XbaI. This vector places the gene of interest under the direct control of a constitutively active chicken β-actin promoter, for expression in human cells. As a positive control, a FLAG tagged p160 construct was obtained. p160 is a

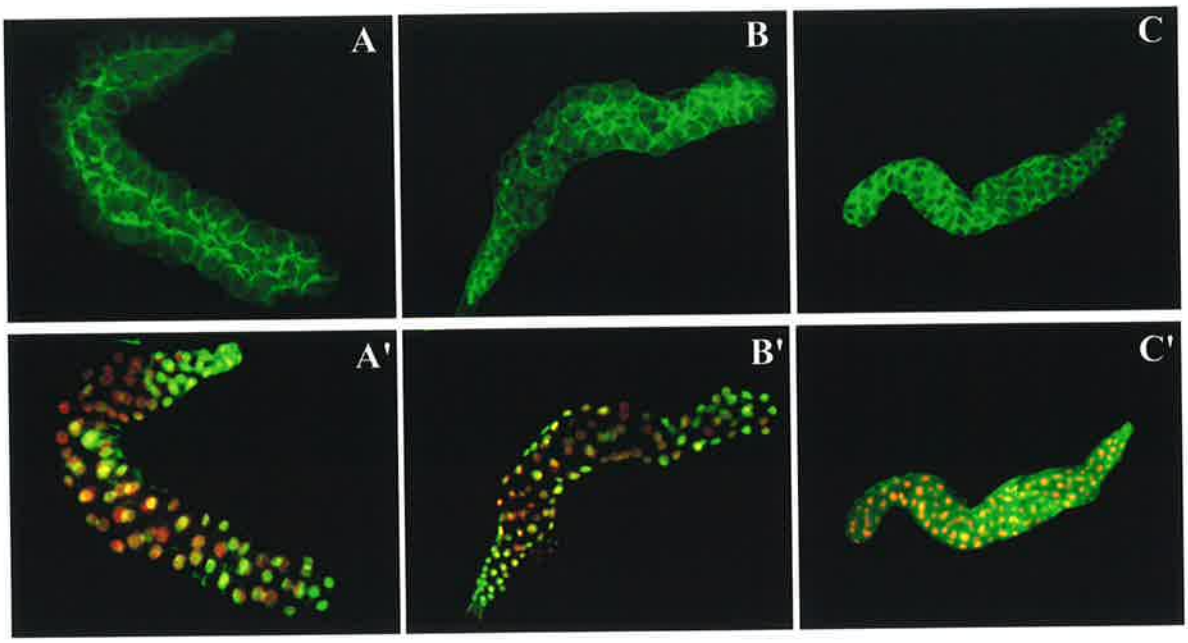

Figure 5.8 Expression of ΔNLSΔBRCT PBL in salivary glands disrupts actin structure.

UAS pbl, UAS ΔBRCTpbl and *UAS ΔNLSΔBRCTpbl* flies were crossed to the gut and salivary gland specific driver sav::*GAL4*. Salivary glands were then dissected from third instar larvae, fixed and stained with phalloidin which binds to filamentous actin (shown in green in A-C), α-PBL (shown in green in A'-C') and hoechst 33258 stain for the DNA (shown in red in A'-C'). All images were taken at 10x magnification.

A. sav *GAL4::UAS pbl* salivary gland stained with phalloidin showing the rounding of the cells that is observed when PBL is expressed. The same gland is shown in A' stained with α–PBL (green) and DNA (red). PBL localises to the nucleus.

B. sav *GAL4::UAS ΔBRCTpbl* salivary gland stained with phalloidin showing the disruption to both gland size and actin structure that is observed when ΔBRCT PBL is expressed. The same gland is shown in B' stained with α–PBL (green) and DNA (red). PBL maintains its nuclear localisation.

C. sav *GAL4::UAS ΔNLSΔBRCTpbl* salivary gland stained with phalloidin showing a more severe disruption to both gland size and actin structure. The same gland is shown in C' stained with α–PBL (green) and DNA (red). PBL localises to the cytoplasm as expected.

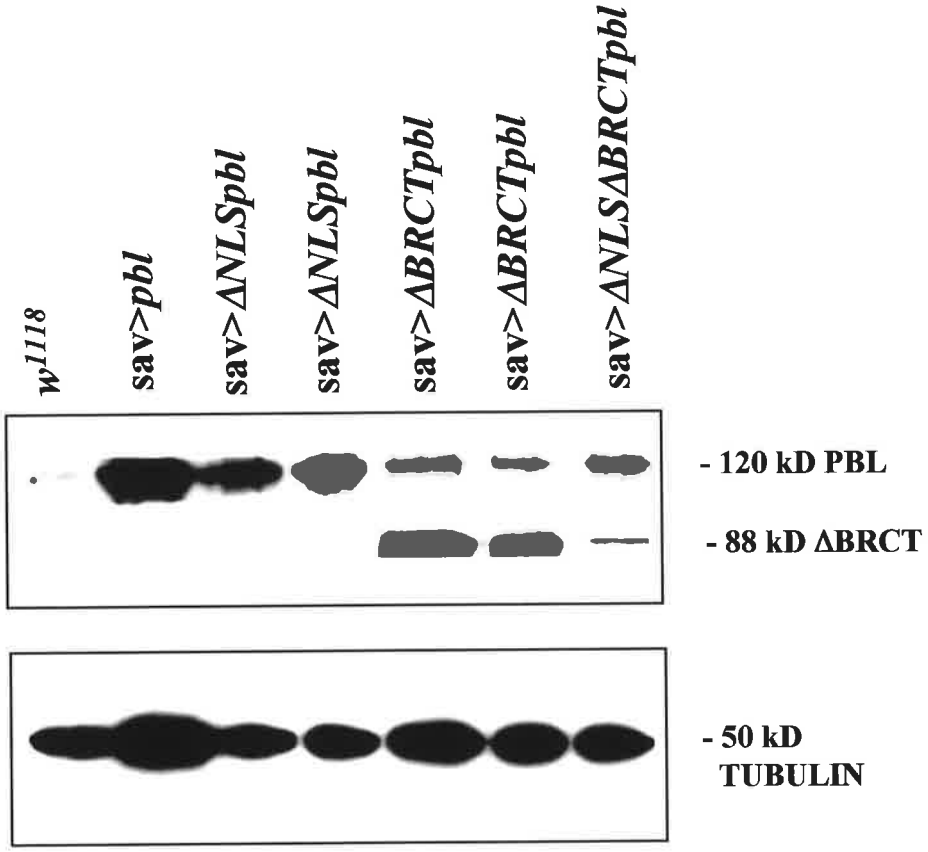

Figure 5.9 Western analysis of sav>*GAL4* expression levels in the salivary gland.

w^{1118}, sav *GAL4::UAS pbl*, sav *GAL4::UAS ΔNLSpbl*, sav *GAL4::UAS ΔBRCTpbl* and sav *GAL4::UAS ΔNLSΔBRCTpbl* salivary glands were dissected at 25°C, boiled and run on a 10% SDS polyacrylamide gel, which was then transferred to a nitrocellulose filter.
The filter was then probed with an anti-PBL antibody, which produced a band of approximately 120 kD in size in each lane. The ΔBRCT form of PBL removes 286 amino acids, and is approximately 88 kD in size.
The filter was then stripped and reprobed with an alpha-tubulin antibody, which served as a loading control. This produced a band of approximately 50 kD in size.
As can be seen from the filter, ΔNLSΔBRCT PBL is expressed at a very low level compared to all of the other constructs. Thus the extreme phenotype of these salivary glands is due to the absence of RadECl and BRCT domain function.

nucleolar localised protein which has been previously shown to be capable of shuttling using this method (L. McMillan, pers comm).

FLAG tagged p160, PBL and ΔBRCT PBL were expressed separately in human HEK 293T cells. The cells were cycloheximide treated to stop further protein expression, and then fused to the mouse cell line NIH-3T3. After a recovery period, the cells were fixed, and stained with hoechst and an anti-FLAG antibody. For each sample the following controls were included: HEK 293T human cells alone, mouse NIH-3T3 cells alone, and HEK 293T human cells transfected with the FLAG tagged construct pACT vector to ensure that the construct was being expressed.

Microscopic analysis of the resulting heterokaryon cells showed that both PBL and ΔBRCT PBL are capable of shuttling from the nucleus to the cytoplasm and back again. p160 was observed within the nucleoli of the mouse nuclei as expected (**Figure 5.10a**), while both PBL and ΔBRCT PBL were observed in the mouse nuclei of heterokaryon cells (**Figure 5.10b-c**). Therefore both PBL and ΔBRCT PBL are capable of shuttling from the nucleus to the cytoplasm.

Figure 5.10a The nucleolar protein p160 is capable of shuttling between the nucleus and the cytoplasm.

The nucleolar protein p160 was used as a positive control for shuttling between the nucleus and the cytoplasm. Human HEK 293T cells were transfected with the pACT expression vector driving constitutive expression of FLAG tagged p160 under the control of the chicken β–actin promoter. 24 hours post transfection cycloheximide treatment was used to prevent further protein expression and the cells were fused with mouse NIH-3T3 cells to create heterokaryon cells. These were then fixed and stained with anti-FLAG (false coloured in green) and hoechst 33258 to stain the DNA (false coloured red).

A-C. Mouse cells alone stained with hoechst (A) and anti-FLAG (B). The merge of these two images is shown in (C).

D-F. Human cells alone stained with hoechst (D) and anti-FLAG (E). The merge of these two images is shown in (F).

G-I. Human cells transfected with FLAG tagged p160, stained with hoechst (G) and anti-FLAG (H). The merge of these images is shown in (I). p160 is observed to localise to the nucleoli of expressing cells.

J-L. Human cells transfected with FLAG tagged p160 and fused with mouse cells. The cells were stained with hoechst (J) and anti-FLAG (K). The merge of these two images is shown in (L). p160 is observed to shuttle from the human nucleus, into the mouse nucleus, indicated by the white arrows.

M-O. Another example of a human/mouse heterokaryon, showing the shuttling of p160 from the human nucleus into the mouse nucleus. The cells were stained with hoechst (M) and anti-FLAG (N). The merge of these images is shown in (O) and the heterokaryon cell is indicated by the white arrows.

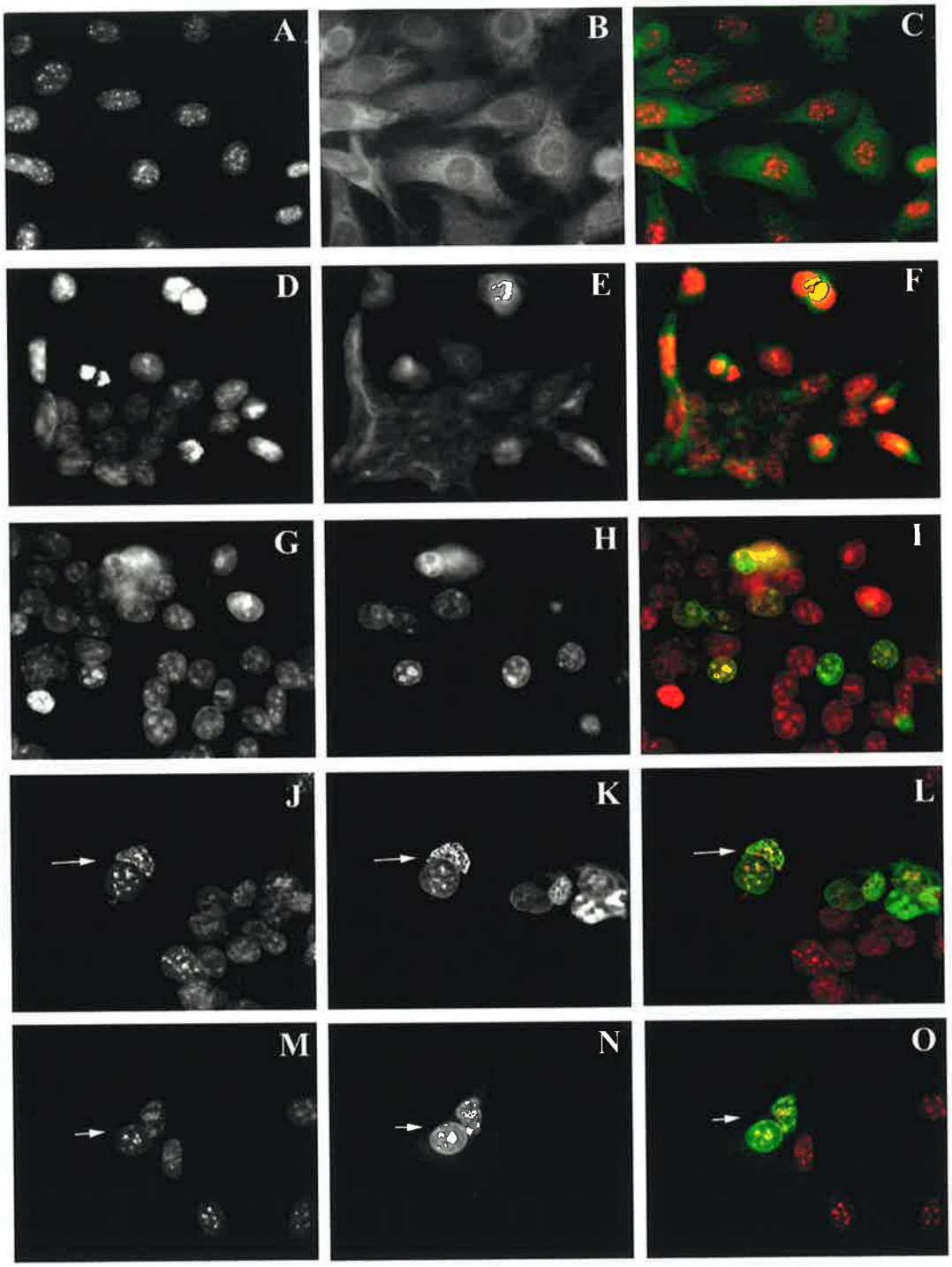
A
B
C
D
E
F
G
H
I
J
K
L
M
N
O

Figure 5.10b PBL is capable of shuttling between the nucleus and the cytoplasm.

Human HEK 293T cells were transfected with the pACT expression vector driving constitutive expression of FLAG tagged PBL under the control of the chicken β–actin promoter. 24 hours post transfection cycloheximide treatment was used to prevent further protein expression and the cells were fused with mouse NIH-3T3 cells to create heterokaryon cells. These were then fixed and stained with anti-FLAG (false coloured in green) and hoechst 33258 to stain the DNA (false coloured red).

A-C. Mouse cells alone stained with hoechst (A) and anti-FLAG (B). The merge of these two images is shown in (C).

D-F. Human cells alone stained with hoechst (D) and anti-FLAG (E). The merge of these two images is shown in (F).

G-I. Human cells transfected with FLAG tagged PBL, stained with hoechst (G) and anti-FLAG (H). The merge of these images is shown in (I). PBL is observed to localise to the nucleus of expressing cells.

J-L. Human cells transfected with FLAG tagged PBL and fused with mouse cells. The cells were stained with hoechst (J) and anti-FLAG (K). The merge of these two images is shown in (L). PBL is observed to shuttle from the human nucleus, into the mouse nucleus.

M-O. Another example of a human/mouse heterokaryon, showing the shuttling of PBL from the human nucleus into the mouse nucleus. The cells were stained with hoechst (M) and anti-FLAG (N). The merge of these images is shown in (O). PBL is absent from the mouse nuclei of separate cells.

P-R. A third example of a human/mouse heterokaryon, showing the shuttling of PBL from the human nucleus into the mouse nucleus. The cells were stained with hoechst (P) and anti-FLAG (Q). The merge of these two images is shown in (R). In this case there is also an example where PBL apparently fails to shuttle (yellow arrows). However in such cases it is difficult to ascertain whether failure to shuttle is simply because the two nuclei are in separate cells.

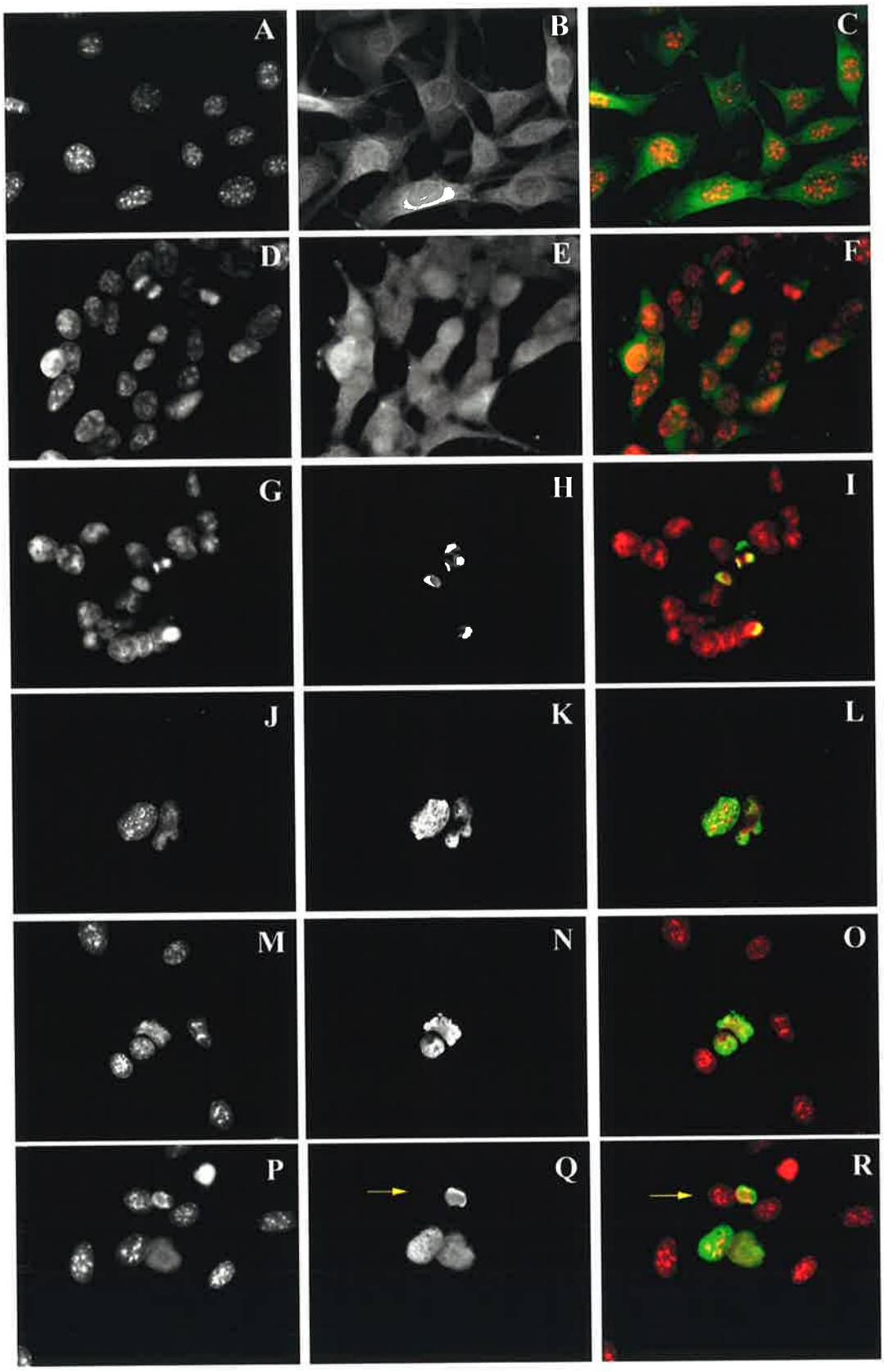
A
B
C
D
E
F
G
H
I
J
K
L
M
N
O
P
Q
R

Figure 5.10c ΔBRCT PBL is capable of shuttling between the nucleus and the cytoplasm.

Human HEK 293T cells were transfected with the pACT expression vector driving constitutive expression of FLAG tagged ΔBRCT PBL under the control of the chicken β–actin promoter. 24 hours post transfection cycloheximide treatment was used to prevent further protein expression and the cells were fused with mouse NIH-3T3 cells to create heterokaryon cells. These were then fixed and stained with anti-FLAG (false coloured in green) and hoechst 33258 to stain the DNA (false coloured red).

A-C. Mouse cells alone stained with hoechst (A) and anti-FLAG (B). The merge of these two images is shown in (C).

D-F. Human cells alone stained with hoechst (D) and anti-FLAG (E). The merge of these two images is shown in (F).

G-I. Human cells transfected with FLAG tagged ΔBRCT PBL, stained with hoechst (G) and anti-FLAG (H). The merge of these images is shown in (I). ΔBRCT PBL is observed to localise to the nucleus of expressing cells.

J-L. Human cells transfected with FLAG tagged ΔBRCT PBL and fused with mouse cells. The cells were stained with hoechst (J) and anti-FLAG (K). The merge of these two images is shown in (L). ΔBRCT PBL is observed to shuttle from the human nucleus, into the mouse nucleus. ΔBRCT PBL is absent from the mouse nuclei of separate cells

M-O. A human/mouse heterokaryon containing multiple nuclei. ΔBRCT PBL is present in several of the human nuclei, and has shuttled into the mouse nucleus indicated by the white arrow. The cells were stained with hoechst (M) and anti-FLAG (N). The merge of these images is shown in (O).

P-R. A third example of a human/mouse heterokaryon, showing the shuttling of ΔBRCT PBL from the human nucleus into the mouse nucleus. The cells were stained with hoechst (P) and anti-FLAG (Q). The merge of these two images is shown in (R). ΔBRCT PBL is absent from the nuclei of separate cells.

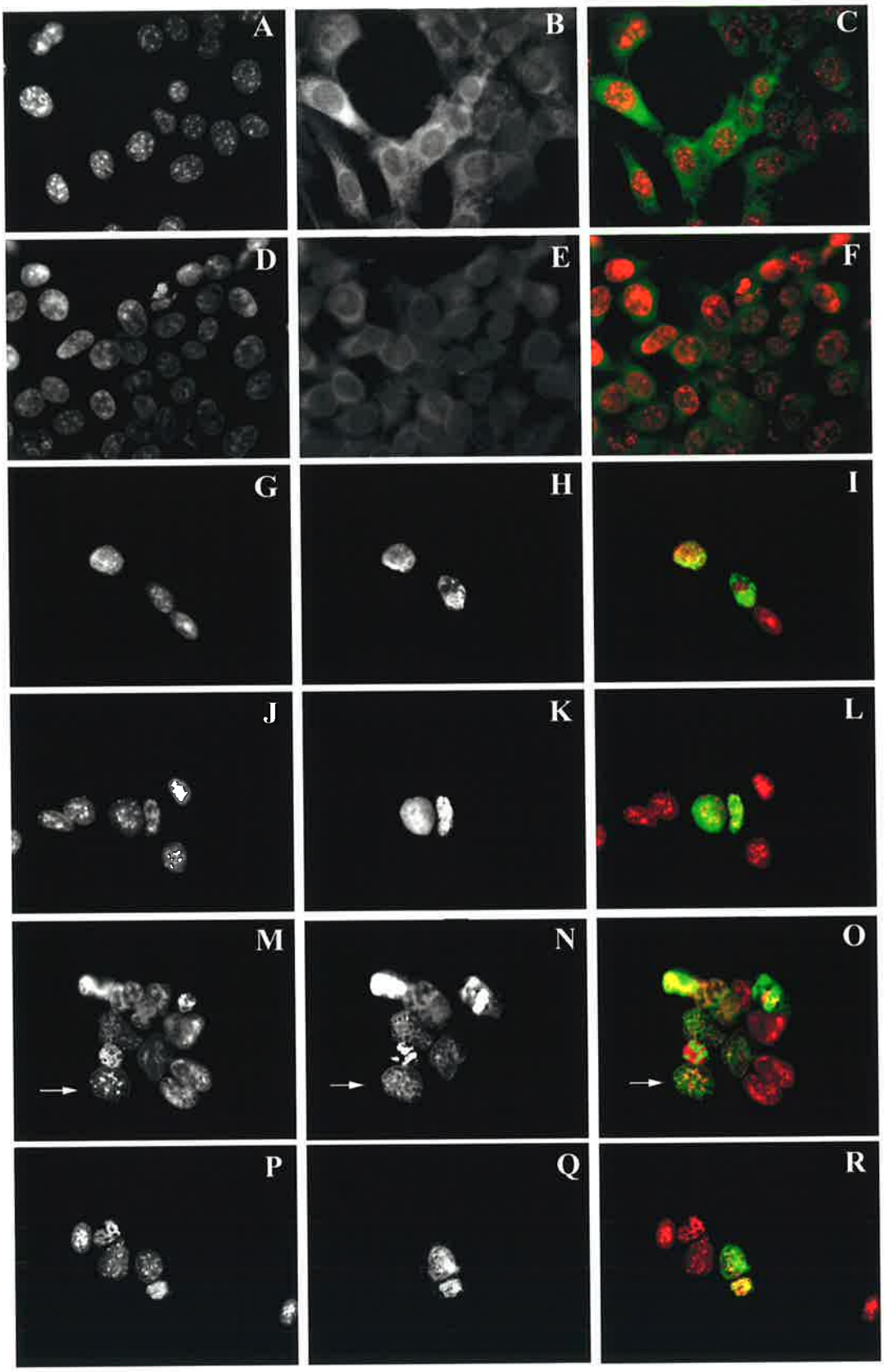
A
B
C
D
E
F
G
H
I
J
K
L
M
N
O
P
Q
R

5:9 Genetic analysis of the eye and salivary gland phenotypes- ΔNLSΔBRCT PBL interacts with Rho in the eye but not in the salivary gland

While ΔNLS and ΔBRCT PBL were both shown to maintain their specificity for RhoA in the eye, both mutant forms were unable to genetically interact with Rho in the salivary gland. In order to test the ΔNLSΔBRCT form for its ability to genetically interact with Rho in the eye, a $RhoA^{720}$ mutant allele was introduced into the *GMR>ΔNLSΔBRCTpbl* background. The *GMR>ΔNLSΔBRCTpbl* stock was lethal at 25°C. The reduction of Rho through the introduction of a $RhoA^{720}$ mutant allele was unable to suppress this lethality. However, reducing the amount of Rho at 18°C was found to mildly suppress the *GMR>ΔNLSΔBRCTpbl* rough eye phenotype (**Figure 5.11b**). When the temperature was further decreased to 13°C, reducing the amount of Rho was found to quite strongly suppress the *GMR>ΔNLSΔBRCTpbl* rough eye phenotype (**Figure 5.11d**). Therefore, when the protein lacks both a functional NLS, and its RadECl region and two BRCT domains, it is still capable of interacting with Rho. To test whether it had maintained its specificity for RhoA over the other Rho family members, the *GMR>ΔNLSΔBRCTpbl* stock was then tested for genetic interactions with mutant alleles or deficiencies covering other characterised members of the Rho family of small GTPases, including Rac1 and 2, Mtl and Cdc42. In all cases, as with the other constructs generated in this study, loss of one copy of any of these genes did not result in suppression of the *GMR>ΔNLSΔBRCTpbl* rough eye phenotype. Therefore it seems that the presence of DH and PH domains alone is enough to target the protein specifically to RhoA.

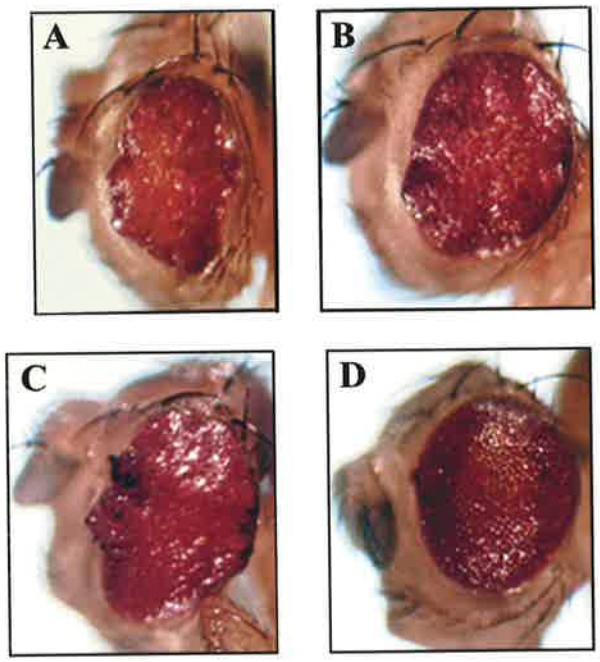

Figure 5.11 Suppression of the *GMR GAL4::UAS ΔNLSΔBRCTpbl* rough eye phenotype by *RhoA*.

A. A *GMR GAL4::UAS ΔNLSΔBRCTpbl* adult eye at 18 degrees C. Eye development is severely disrupted by the overexpression of ΔNLSΔBRCT PBL posterior to the morphogenetic furrow of the developing larval eye disc.

B. Suppression of the *GMR GAL4::UAS ΔNLSΔBRCTpbl* rough eye phenotype in $RhoA^{720}$ heterozygotes at 18 degrees. The rough eye phenotype caused by the overexpression of ΔNLSΔBRCT PBL posterior to the morphogenetic furrow is mildly suppressed when a *RhoA* mutant allele is introduced into the genetic background of these flies.

C. A *GMR GAL4::UAS ΔNLSΔBRCTpbl* adult eye at 13 degrees C. A significantly rough eye is produced by the overexpression of ΔNLSΔBRCT PBL posterior to the morphogenetic furrow at this temperature.

D. Suppression of the *GMR GAL4::UAS ΔNLSΔBRCTpbl* rough eye phenotype in $RhoA^{720}$ heterozygotes at 13 degrees. The rough eye phenotype caused by the overexpression of ΔNLSΔBRCT PBL posterior to the morphogenetic furrow is strongly suppressed when a *RhoA* mutant allele is introduced into the genetic background of these flies.

To test whether the ΔNLSΔBRCT phenotype in the salivary gland was suppressible by Rho, the *RhoA*^{720} null allele was recombined onto the *UAS ΔNLSΔBRCTpbl* chromosome, which was then crossed to the sav *GAL4* driver. Reduction of Rho in this way was unable to suppress the sav>*ΔNLSΔBRCTpbl* phenotype at 25°C (**Figure 5.12a-b**). Given the severity of the phenotype at this temperature, the experiment was then repeated at 18°C. At this lower temperature, sav *GAL4* is not as highly expressed, leading to a less severe effect on salivary gland structure. Reducing the amount of RhoA still could not suppress the *ΔNLSΔBRCTpbl* salivary gland phenotype (**Figure 5.12c-d**). Therefore, as was the case with both ΔNLS and ΔBRCT PBL, while ΔNLSΔBRCT PBL acts specifically through RhoA in the eye, it does not appear to act through Rho in the salivary gland. As discussed previously, this may reflect the fact that the phenotype is too severe to be suppressed by merely removing one copy of *RhoA*, or may be indicative of a different mode of regulation in this tissue.

Figure 5.12 Removal of one copy of *RhoA* does not suppress the ΔNLSΔBRCT PBL salivary gland phenotype.

UAS ΔNLSΔBRCTpbl and *UAS ΔNLSΔBRCTpbl, RhoA*^{720} flies were crossed to the gut and salivary gland specific driver sav *GAL4.* Salivary glands from third instar larvae were then dissected, fixed and stained with phalloidin, which binds to filamentous actin (shown in red), and α–PBL (shown in green). All images were taken at 10x magnification.

A. sav *GAL4::UAS ΔNLSΔBRCTpbl* salivary gland at 25°C stained with phalloidin. This same gland is shown in (A') stained with phalloidin (red) and PBL (green). ΔNLSΔBRCT PBL localises to the cytoplasm. The cells are rounded, and F-actin structure is severely disrupted.

B. sav *GAL4::UAS ΔNLSΔBRCTpbl, RhoA*^{720} salivary gland at 25°C stained with phalloidin. Removal of one copy of *RhoA* does not suppress the disruption of F-actin structure or cell shape. This same gland is shown in (B') stained with phalloidin (red) and PBL (green).

C. sav *GAL4::UAS ΔNLSΔBRCTpbl* salivary gland at 18°C stained with phalloidin. At this lower temperature there is a slightly less severe effect on F-actin structure and cell size, but cells are still rounded. This same gland is shown in (C') stained with phalloidin (red) and PBL (green). ΔNLSΔBRCT PBL still localises to the cytoplasm.

D. sav *GAL4::UAS ΔNLSΔBRCTpbl, RhoA*^{720} salivary gland at 18°C stained with phalloidin. Removal of one copy of *RhoA* at this lower temperature does not suppress the disruption of F-actin structure or cell shape. This same gland is shown in (D') stained with phalloidin (red) and PBL (green).

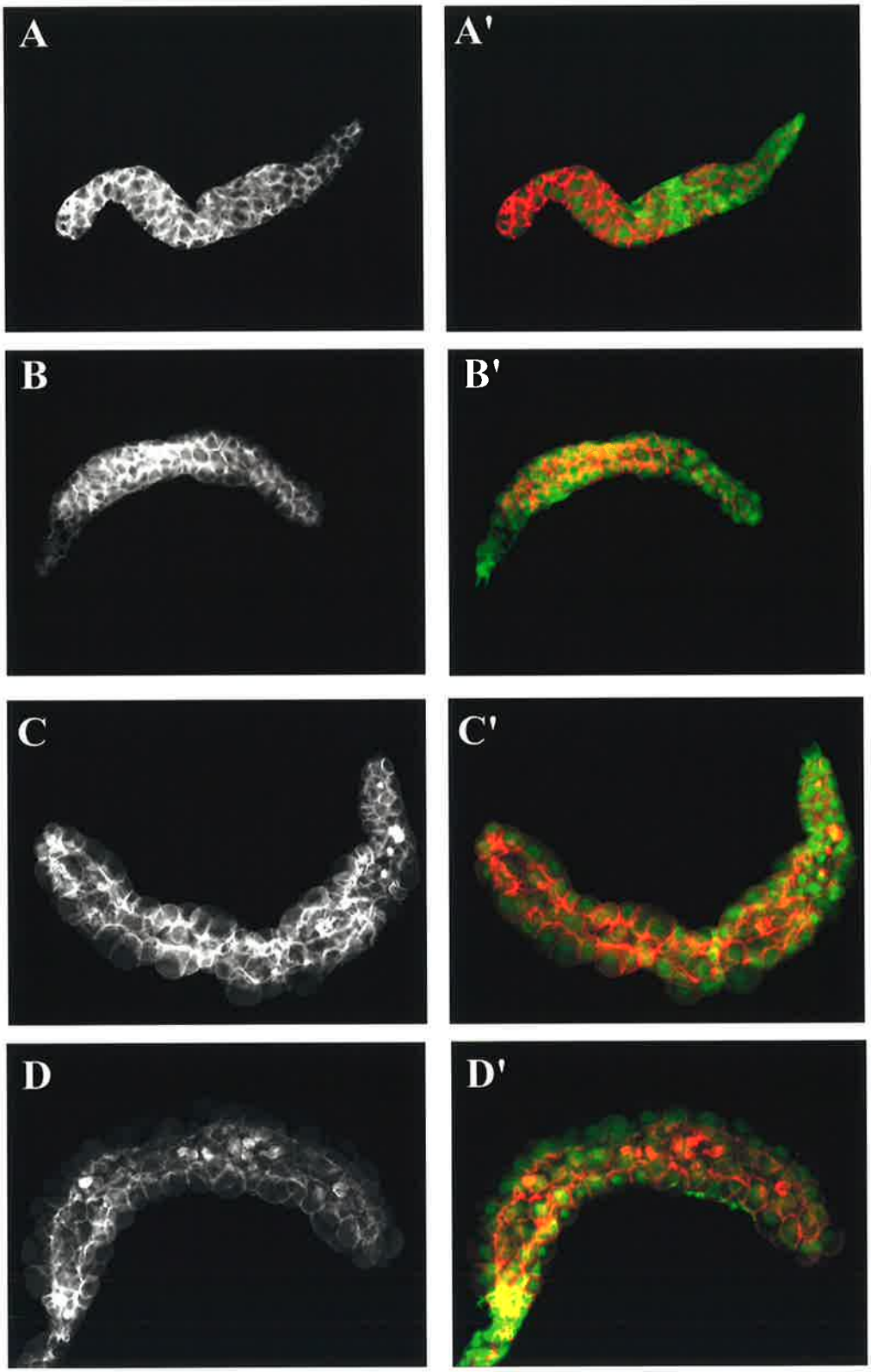
A
A'
B
B'
C
C'
D
D'

5:10 The RadECl region and BRCT domains are required in the cytoplasm for cytokinesis

As shown in the previous chapter, the potentially nuclear-functioning RadECl and BRCT domains are essential for PBL cytokinetic function. When these domains were removed from the PBL protein, the resultant ΔBRCT mutant form was unable to rescue the cytokinetic defect of the *pbl* mutant when it was expressed in stripes along the anterior-posterior axis of the mutant embryo using the driver *prd GAL4*. However, nuclear localisation of the protein was shown to be non-essential for cytokinesis. The ΔNLS cytoplasmic form was found to completely rescue the cytokinetic defect of the *pbl* mutant embryo when expressed in the same way. These two observations imply that the RadECl region and BRCT domains must be playing a cytoplasmic role in cytokinesis. To confirm this, the ΔNLSΔBRCT mutant form was expressed in the mutant embryo using the *prd GAL4* driver.

prd GAL4-driven embryonic expression of ΔNLSΔBRCT PBL was unable to rescue the cytokinetic defect of the *pbl* mutant (**Figure 5.13g-i**). Therefore while the cytoplasmic form of the protein containing the RadECl and BRCT domains can activate cytokinesis (**Figure 5.13 d-f**), the cytoplasmic form lacking these domains cannot. Thus the RadECl region and BRCT domains are required in the cytoplasm for cytokinesis.

Figure 5.13 ΔNLSΔBRCT PBL cannot rescue cytokinesis in a *pbl* mutant background.

A- C. A *prd GAL4, pbl*^{2}*/UAS pbl, pbl*^{3} embryo expressing wild type PBL in a *pbl* mutant background. The embryo was fixed and stained with anti-lamin which highlights the nuclear envelope, shown in green in (A), and anti-spectrin which stains the cell cortex, shown in red in (B). The merge of these two images is shown in (C). Expression of wild type PBL in alternate stripes along the embryo using *prd GAL4*, completely rescues the cytokinetic defect of the *pbl* mutant within those stripes. The rescue stripe is indicated by the white arrows.

D- F. A *prd GAL4, pbl*^{2}*/UAS ΔNLSpbl, pbl*^{3} embryo expressing ΔNLS PBL in a *pbl* mutant background. The embryo was fixed and stained with lamin (D) and spectrin (E). The merge of these two images is shown in (F). Expression of ΔNLS PBL in stripes along the embryo using *prd GAL4*, completely rescues the cytokinetic defect of the *pbl* mutant within those stripes (white arrows).

G- I. A *prd GAL4, pbl*^{2}*/UAS ΔNLSΔBRCTpbl, pbl*^{3} embryo expressing ΔNLSΔBRCT PBL in a *pbl* mutant background. The embryo was fixed and stained with lamin (G) and spectrin (H). The merge of these two images is shown in (I). Expression of ΔNLSΔBRCT PBL in stripes along the embryo using *prd GAL4*, cannot rescue the cytokinetic defect of the *pbl* mutant within those stripes. Two adjacent mutant stripes are shown.

J- K. A *prd GAL4, pbl*^{2}*/UAS ΔNLSΔBRCTpbl, pbl*^{3} embryo expressing myc-tagged ΔNLSΔBRCT PBL in a *pbl* mutant background. The embryo was fixed and stained with anti-myc, shown in green, and hoechst 33258 stain for the DNA, shown in red. A 10x magnification picture of the embryo in (J) shows the *prd GAL4* driven stripes of ΔNLSΔBRCT PBL expression. A 100x magnification view of one stripe is shown in (K). ΔNLSΔBRCT PBL is clearly cytoplasmic.

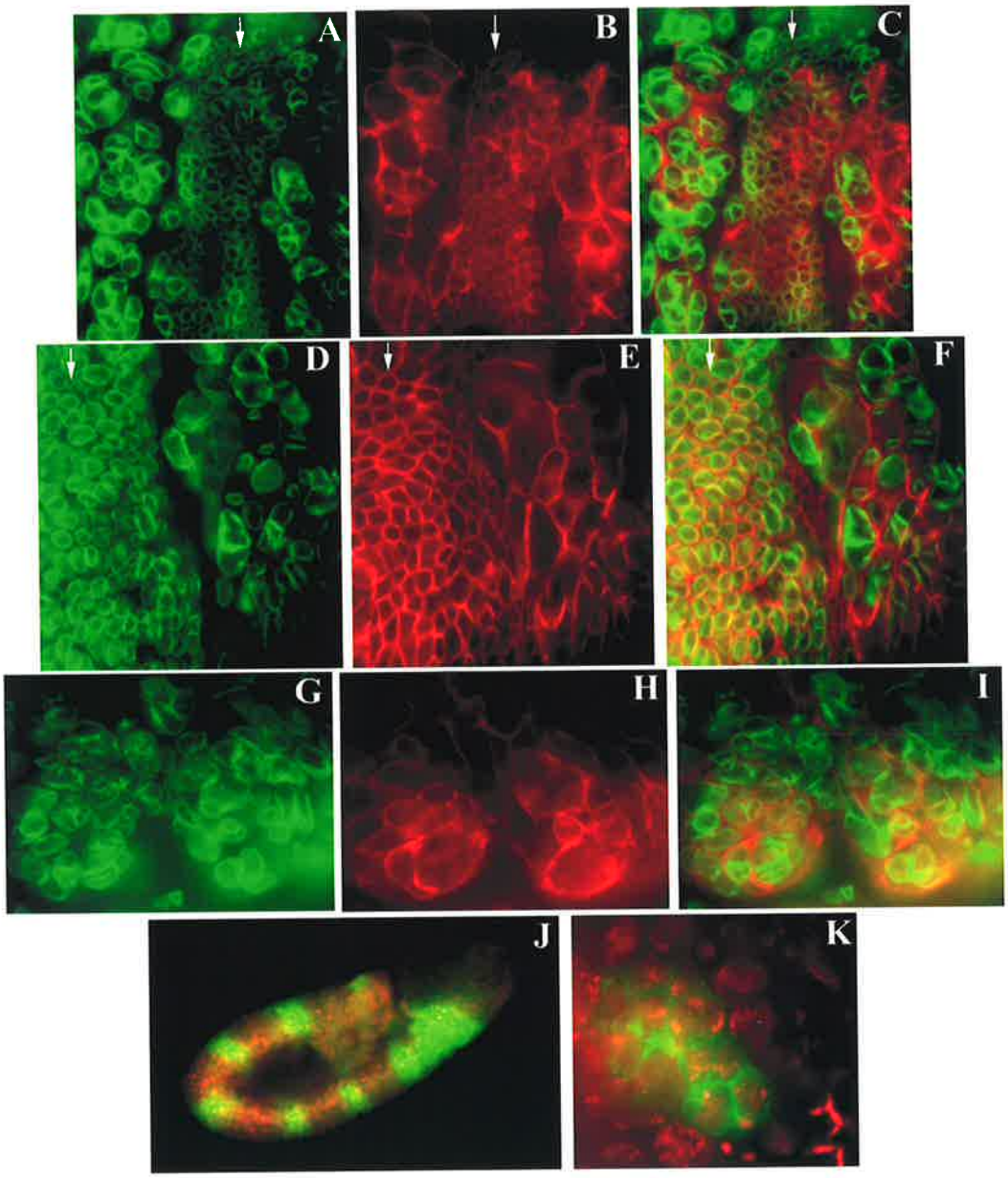
A
B
C
D
E
F
G
H
I
J
K

5:11 Discussion

As discussed in previous chapters, nuclear localisation is not essential for the cytokinetic function of PBL, however it is essential for the maintenance of normal cellular processes, given the extreme phenotypes caused by the expression of the ΔNLS cytoplasmic form. This finding suggested that the localisation of PBL to the nucleus during interphase could be a means of sequestering PBL function once it has activated Rho and stimulated cytokinesis. However, the observation that apparently nuclear localised PBL could affect the cytoskeleton of the salivary gland suggested that, at least in this tissue, nuclear localisation is not enough. It was therefore possible that nuclear localisation could be associated with a separate nuclear role and the presence of the potentially nuclear RadECl region and BRCT domains added further weight to this possibility. Deletion of these potential nuclear domains was found to cause a range of severe phenotypes when the mutant form was expressed in a variety of tissues, highlighting their important role in normal cellular processes. In addition to this, the severe disruption to cytoplasmic actin that was observed when the ΔBRCT construct was expressed in salivary glands, suggested the possibility that the PBL protein may shuttle between the nucleus and the cytoplasm, with the RadECl/BRCT domains playing some unknown cytoplasmic role. The RadECl/BRCT domains were then shown to be required for cytokinesis. This observation, combined with the fact that nuclear localisation itself is not required for cytokinesis, provided further support for a cytoplasmic role for these domains.

To investigate this further, the ΔNLS and ΔBRCT mutations were combined to examine the effect of removing RadECl/BRCT domain function from a purely cytoplasmic form of PBL. The ΔNLSΔBRCT construct was found to cause the most severe of the *GMR*-driven eye phenotypes generated in this study. Similar to the *GMR>ΔNLSpbl* phenotype, *GMR>ΔNLSΔBRCTpbl* larval eye discs were found to have both multinucleate and anucleate cells, suggesting a disruption in cytokinesis. Given the similarity to the *ΔNLSpbl* phenotype, this disruption is most likely due to the inappropriate action of the DH/PH domains. Unlike the *GMR>ΔBRCTpbl* phenotype, no examples of fused sister telophase nuclei were observed, suggesting that this phenotype is due to the absence of some RadECl/BRCT domain function in the nucleus. Given that this fused sister telophase phenotype has not been observed in *pbl* mutant embryos, it must be due to a dominant effect of overexpressing the ΔBRCT construct.

A similar disruption to tissue patterning in the pupal disc was observed with the ΔNLSΔBRCT construct to that observed with both the ΔNLS and ΔBRCT constructs. This suggested that later developmental defects must explain the massive increase in the disruption to the eye structure observed with the *GMR*-driven expression of ΔNLSΔBRCT PBL. The effect on the early patterning events of the eye disc was examined using the ELAV antibody, which is specific for those cells that have adopted a neural fate. The ΔNLSΔBRCT construct was found to cause an identical effect on the differentiating neural cells of the eye disc to that of the ΔNLS construct, reducing the number of ELAV expressing clusters. This suggested that this phenotype is most likely due to deregulated cytoplasmic DH/PH domain function rather than a lack of RadECI/BRCT domain function in the cytoplasm. The destruction of organisation of the ELAV expressing clusters observed with the ΔBRCT construct, on the other hand, is possibly due to absence of some unknown RadECI/BRCT domain function in the nucleus.

In contrast to the eye or salivary gland where differences in the resultant phenotypes were observed, the ΔNLS, ΔBRCT, and ΔNLSΔBRCT constructs all gave very similar phenotypes when expressed in developing wing tissue. Blistering and a disruption to the two cross veins were observed with all three constructs, suggesting either that PBL plays a different role in the wing compared to the eye or salivary gland, or that different modes of regulation are present in this tissue. It remains to be seen whether the wing phenotypes generated by all three of these constructs are suppressible by reducing the amount of Rho.

In line with the more severe phenotype observed in the eye, the ΔNLSΔBRCT construct was also found to cause a far more severe phenotype when expressed in neural tissues under the control of the *elav* GAL4 driver. While expression of ΔNLS and ΔBRCT PBL both caused a similar rough eye phenotype, expression of ΔNLSΔBRCT PBL was found to be embryonic lethal. An apparently necrotic nervous system was observed, suggesting that expression of ΔNLSΔBRCT PBL is far more toxic to the neural cells than either ΔNLS or ΔBRCT PBL alone.

In line with the general increase in phenotype severity observed with expression of the ΔNLSΔBRCT construct, the sav>*ΔNLSΔBRCTpbl* phenotype was found to be the most severe of the salivary phenotypes generated. The salivary glands were extremely small, with a severe disruption of filamentous actin, forming sheets of actin in the cytoplasm. This phenotype was like a severe version of the sav>*ΔBRCTpbl* phenotype. Given that ΔBRCT PBL is apparently nuclear and has a similar effect on the actin cytoskeleton as the

cytoplasmic ΔNLSΔBRCT form, this suggests that ΔBRCT PBL shuttles out into the cytoplasm, so that trapping the protein in the cytoplasm with the ΔNLS mutation enhances this effect.

A heterokaryon model system showed that both PBL and ΔBRCT PBL do indeed shuttle, with FLAG tagged versions of the protein migrating from human nuclei into mouse nuclei. It remains to be shown whether the murine homologue of PBL, ECT2, also shuttles in this system. The fact that both PBL and ΔBRCT PBL appear solely nuclear in fixed *Drosophila* tissues can be explained by the nuclear exit rate being substantially lower than the entrance rate. This finding also provided an explanation as to how these apparently nuclear proteins can affect the cytoskeleton. The increased severity caused by the ΔBRCT deletion is therefore most likely due to the absence of some unknown RadECl/BRCT domain function in the cytoplasm. In accordance with that observed for the ΔNLS and ΔBRCT salivary phenotypes, the sav>*ΔNLSΔBRCTpbl* phenotype was not suppressible by genetically reducing the amount of Rho. Again it remains to be seen whether the mutant forms of PBL target other Rho family members in this tissue, or whether the phenotypes generated by their expression are just too severe to be suppressed by removing one copy of *RhoA*.

One of the most significant findings of this study was the fact that the ΔNLSΔBRCT construct could not rescue the cytokinetic defect of the *pbl* mutant embryo when expressed under the control of the *prd GAL4* driver. This indicated that the RadECl/BRCT domains are required in the cytoplasm for the cytokinetic function of PBL. This is a novel finding for these normally nuclear domains, and extends the range of functions attributed to them beyond DNA damage sensing and repair processes to include cytokinesis. The ability of such domains to control cytokinesis could, in theory, provide a link between DNA damage sensing and the cell cycle, and should be investigated further.

In conclusion, the phenotypes caused by the expression of the ΔNLSΔBRCT construct, when compared to that caused by the expression of ΔNLS and ΔBRCT PBL, has enabled the identification of novel cytoplasmic roles for the RadECl and BRCT domains and raised the possibility that PBL also plays novel nuclear roles. A cytoplasmic role for these domains in cytokinesis has been identified, but the exact nature of the nuclear role, or roles, for these domains remains undefined. In an attempt to determine whether the BRCT domains of PBL play a role in DNA damage sensing and repair, as they do in other proteins, an x-ray sensitivity assay was performed. This involved comparing the sensitivity of *pbl* hypomorphic mutant larvae to that of wild type, and is described in the following chapter.

Chapter 6: Investigation of a potential role for PBL in DNA repair

6:1 Introduction

In the previous chapter, a cytoplasmic role for the RadECl/BRCT domains in cytokinesis was identified. This was a completely novel and surprising finding, given that these domains have only previously been implicated in nuclear processes. BRCT domains in particular, have previously been identified in many proteins that have roles in DNA damage response and repair pathways (Bork *et al.*, 1997; Callebaut and Mornon, 1997). A role for these domains in cytokinesis is therefore a very exciting finding, possibly providing a link between DNA damage and cell cycle control.

A cytoplasmic role for these domains was revealed by the severe effect on the cytoskeleton of a cytoplasmic form of the PBL protein that lacked these domains. Added to this was the discovery that wild type PBL protein shuttles between the nucleus and the cytoplasm, movement that would enable the RadECl/BRCT domains to have a direct cytoplasmic effect during interphase. It is therefore possible that the activity of PBL is regulated in part by its shuttling, as well as by its interaction, possibly through its RadECl/BRCT domains, with other proteins at specific points in the cell cycle. In support of this, the RadECl/BRCT domains have recently been shown to interact with the *Drosophila* RacGAP (DRacGAP) protein (Somers and Saint, manuscript in preparation). CYK-4 and MgcRacGAP, the nematode and murine homologues of DRacGAP, have both been shown to be required for cytokinesis (Jantsch-Plunger *et al.*, 2000; Hirose *et al.*, 2001). The interaction of the RadECl/BRCT domains with such a protein, therefore sheds some light on the possible mechanism behind their role in cytokinesis.

However, in addition to any cytoplasmic process that the PBL BRCT domains may be involved in, the question remains as to whether they play a role in a DNA damage response or repair pathway. To answer this, an x-ray sensitivity assay was performed. Mutants in DNA damage response pathways are known to be hypersensitive to DNA damaging agents. Larval hypersensitivity assays have therefore been used in *Drosophila* as a means of identifying multiple components of DNA damage response and repair pathways (Boyd *et al.*, 1987;

Henderson *et al.*, 1987; Dusenbery and Smith, 1996; Sekelsky *et al.*, 1998; Henderson, 1999). *pbl* mutant larvae were therefore irradiated and their survival to adulthood was compared to that of wild type larvae.

6:2 *pbl*^{p3} hypomorphic larvae are hypersensitive to x-irradiation

pbl^{p3} is a homozygous viable, hypomorphic mutant allele, based on its trans-heterozygous lethality when combined with a *pbl* null allele. It is an EMS-induced allele with a point mutation in the PH domain, however the exact effect of this mutation on *pbl* function is unknown. Given the viability of these flies as homozygotes, this stock was used in an x-ray sensitivity assay. *pbl*^{p3} mutant larvae were collected, bathed and irradiated at a variety of doses, and their survival to adulthood was compared to that of wild type. Non-irradiated controls were always included. This experiment was initially performed using 20 and 25 Gy of irradiation. As can be seen from **Figure 6.1**, although the *pbl*^{p3} non-irradiated control larvae survived to adulthood in similar numbers to wild type, *pbl*^{p3} larvae were hypersensitive to both 20 and 25 Gy of irradiation. The experiment was then repeated using 25 Gy and 30 Gy of irradiation. Almost identical survival percentages were obtained as before for the 25 Gy dose, while at 30 Gy, *pbl*^{p3} were again hypersensitive compared to wild type. These data sets were then combined and used to create the graph shown in **Figure 6.1**.

To discount the possibility that the hypersensitivity may be due to some other mutation in this stock, a cosmid carrying the *pbl* gene was introduced into the *pbl*^{p3} mutant background. This cosmid, known as *cos34*, has previously been shown to rescue viability of *pbl* null alleles (J. Wong and R. Saint, pers comm). It was therefore introduced into the *pbl*^{p3} mutant background to create a stock that was homozygous for *cos34* on the second chromosome, and homozygous for *pbl*^{p3} on the third. Larvae of this genotype were then irradiated, and their survival to adulthood compared to that of *pbl*^{p3} homozygotes and wild type individuals.

As can be seen from **Figure 6.1**, introduction of the cosmid completely rescued the hypersensitivity of the *pbl*^{p3} mutant stock. This hypersensitivity is therefore due to a lack of PBL function, and not some other mutation within the stock. Surprisingly, not only did the

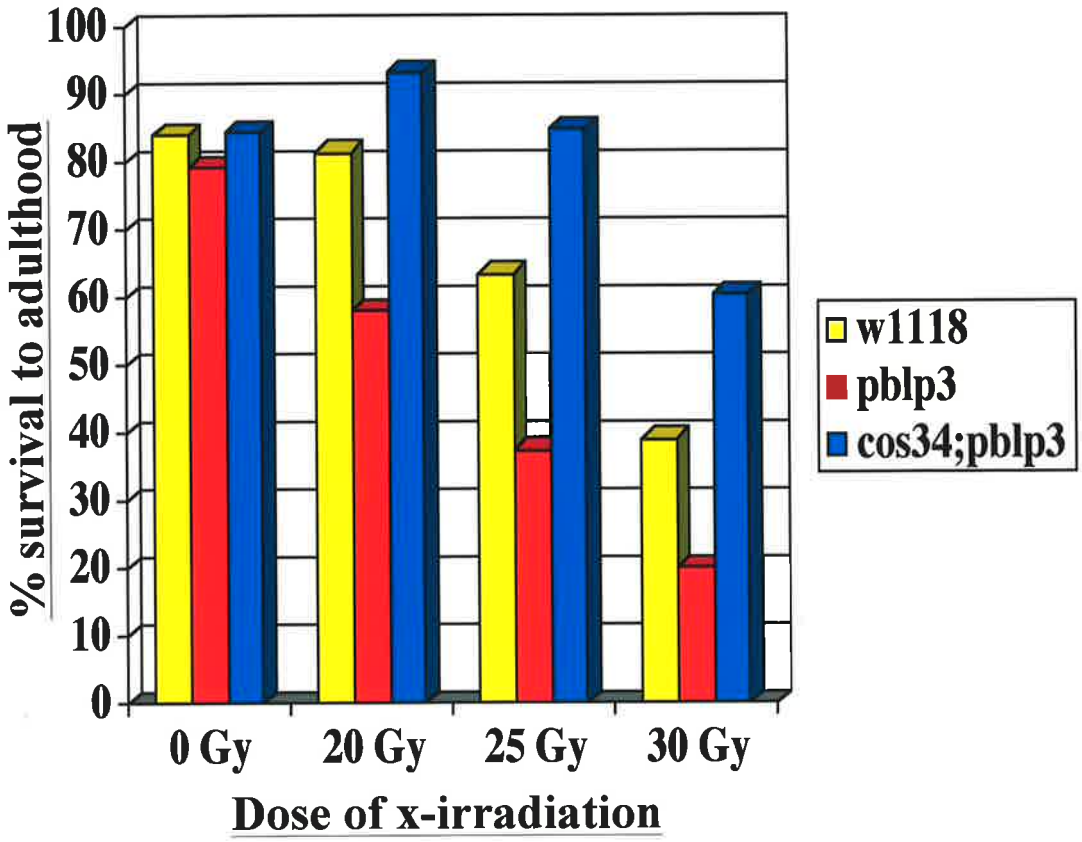

	0 Gy	20 Gy	25Gy	30 Gy
w^{1118}	390/464= **84.1%**	114/140= **81.4%**	173/273= **63.4%**	62/159= **39.0%**
pbl^{p3}	389/491= **79.2%**	203/350= **58.0%**	130/348= **37.4%**	32/159= **20.1%**
cos34;pbl^{p3}	355/420= **84.5%**	149/160= **93.1%**	253/298= **84.9%**	145/240= **60.4%**

Figure 6.1 Initial data indicated that pbl^{p3} mutant larvae are hypersensitive to x-irradiation.

w^{1118}, pbl^{p3} and *cos34;*pbl^{p3} third instar larvae were collected, bathed in water and irradiated in petri dishes at the doses indicated. The larvae were then transferred into vials containing food and the number of adults to hatch out of the vials were scored as a percentage of the number of larvae placed into the vials. The data are presented in both graphical and tabular form. As can be seen from the graph and the table, pbl^{p3} larvae appear to be hypersensitive to irradiation. Introduction of the cosmid known to rescue *pbl* function (*cos34*) resulted in complete rescue of this sensitivity. *cos34;*pbl^{p3} flies are not at all sensitive to 20 or 25 Gy of irradiation.

presence of the cosmid completely rescue the hypersensitivity of pbl^{p3}, but the *cos34;* pbl^{p3} flies survived better than wild type at every dose tested and were apparently immune to both 20 and 25 Gy of irradiation (**Figure 6.1**). This suggested that PBL might play a protective role against the damage associated with x-irradiation.

The irradiation experiments were then repeated several times with varying success. The doses 20 Gy and 30 Gy were used in an attempt to duplicate the previous data. In both of these instances, the non-irradiated controls performed more poorly than expected, and the survival data for larvae post irradiation was variable. Despite this, pbl^{p3} larvae were consistently more sensitive to irradiation than wild type, being hypersensitive to 20 Gy of irradiation and sensitive to 30 Gy. *cos34;* pbl^{p3} larvae consistently out-performed both wild type and pbl^{p3} at all doses given, and were still apparently immune to 20 Gy. This additional irradiation data were therefore pooled with previous data to produce the graph shown in **Figure 6.2**.

Using 25 and 30 Gy of irradiation, the survival experiments were again repeated on a series of successive days, and these data were combined to generate the graph shown in **Figure 6.3**. Although *cos34;* pbl^{p3} larvae consistently out-performed pbl^{p3} after irradiation, wild type larvae were quite variable in their survival and were observed to occasionally have a lower survival value than expected. The values for *cos34;* pbl^{p3} and pbl^{p3} larvae also varied. As a result of this variation, when these data were combined it had the effect of making wild type appear more sensitive to 30 Gy of irradiation than pbl^{p3} (**Figure 6.3**). However, *cos34;* pbl^{p3} larvae were still apparently immune to 25 Gy of irradiation. It was not possible to track down the source of variability in these assays in the time available for this work.

Despite variability in these experiments, pbl^{p3} larvae appear to be hypersensitive to both 20 and 25 Gy of irradiation. They are sensitive to 30 Gy, but not significantly more so than wild type. Introduction of the cosmid rescues the sensitivity observed at all doses tested, and *cos34;* pbl^{p3} flies are not at all sensitive to 20 or 25 Gy. Therefore, despite the significant variability observed in these experiments, the results suggest that *pbl* is involved in some sort of DNA damage response or repair type pathway, playing a protective role against the damage associated with ionizing radiation. In further support to this was the observation that the pbl^{p3} adult flies that did survive irradiation tended to die and not reproduce, while irradiated wild type and *cos34;* pbl^{p3} flies seemed to live longer and were observed to successfully reproduce. Taken together, these observations strongly suggest a role for PBL in DNA repair, and are justification for further investigation.

6:3 Is the hypersensitivity of *pbl*^{p3} enhanced by removing *Rho*?

To determine whether the hypersensitivity effect of *pbl* acts through Rho, the *RhoA*^{720} null allele was introduced in the *pbl*^{p3} mutant background with the purpose of examining the sensitivity of this stock to irradiation and comparing it to that of *pbl*^{p3}. *pbl*^{p3} however was found to be homozygous lethal when in a *RhoA* heterozygous mutant background. Although this finding is consistent with other work on the targets of PBL (Prokopenko *et al.*, 1999), it prevented this analysis from being performed. The only way to analyse the effect of Rho is therefore to repeat the experiments using *pbl*^{p3} heterozygotes instead of homozygotes and compare their sensitivity to that of *RhoA*^{720}; *pbl*^{p3} heterozygotes. However, flies heterozygous for *pbl*^{p3} are unlikely to show any hypersensitivity as their level of PBL function would probably approach that of wild type. Considering the difficulties in picking trans heterozygous larvae and the fact that these experiments were unlikely to provide clean cut results, it was deemed pointless to attempt them.

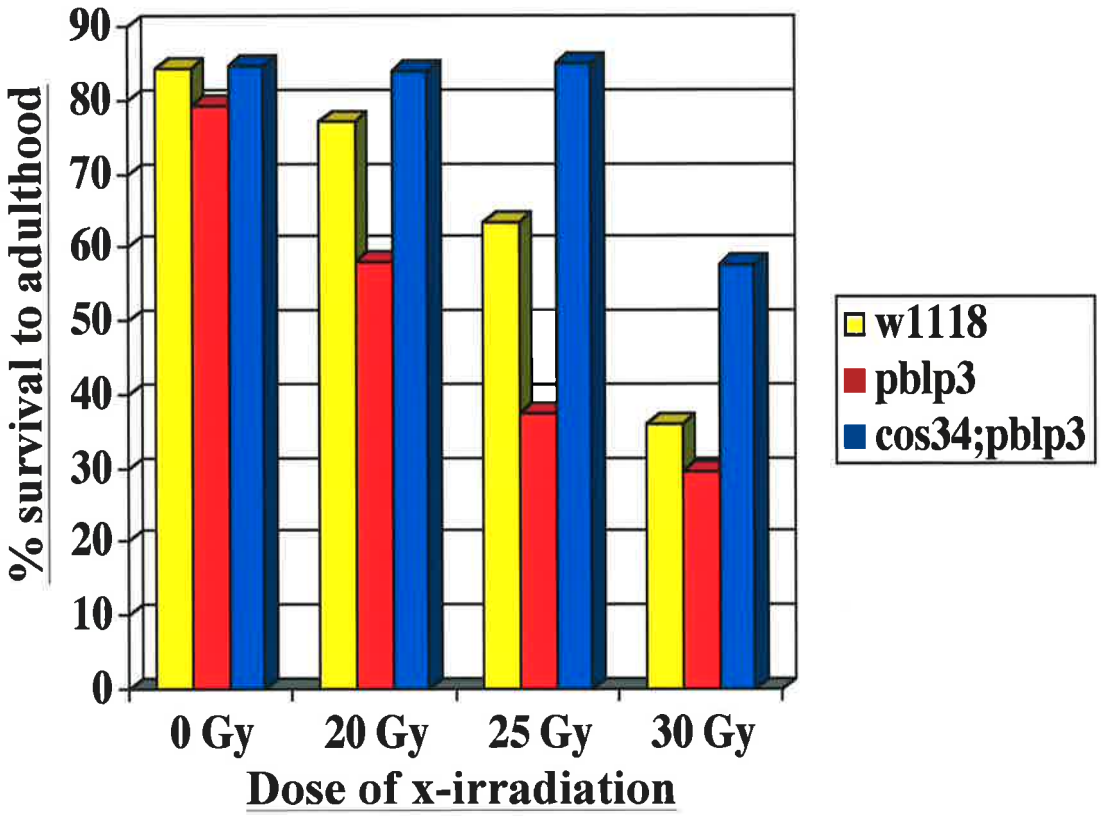

	0 Gy	20 Gy	25Gy	30 Gy
w^{1118}	390/464= **84.1%**	200/259= **77.2%**	173/273= **63.4%**	100/278= **36.0%**
pbl^{p3}	389/491= **79.2%**	353/609= **58.0%**	130/348= **37.4%**	129/439= **29.4%**
cos34;pbl^{p3}	355/420= **84.5%**	393/468= **84.0%**	253/298= **84.9%**	213/369= **57.7%**

Figure 6.2 Pooled data indicating that pbl^{p3} mutant larvae are hypersensitive to 20 and 25 Gy of x-irradiation.

w^{1118}, pbl^{p3} and *cos34;*pbl^{p3} third instar larvae were collected, bathed in water and irradiated in petri dishes at the doses indicated. The larvae were then transferred into vials containing food and the number of adults to hatch out of the vials were scored as a percentage of the number of larvae placed into the vials. The data are presented in both graphical and tabular form. As can be seen from the graph and the table, pbl^{p3} larvae appear to be hypersensitive to irradiation at both 20 and 25 Gy. They are sensitive to 30 Gy. Introduction of the cosmid known to rescue *pbl* function (*cos34*) resulted in complete rescue of the sensitivity observed at all doses. *cos34;*pbl^{p3} flies are not at all sensitive to 20 or 25 Gy of irradiation.

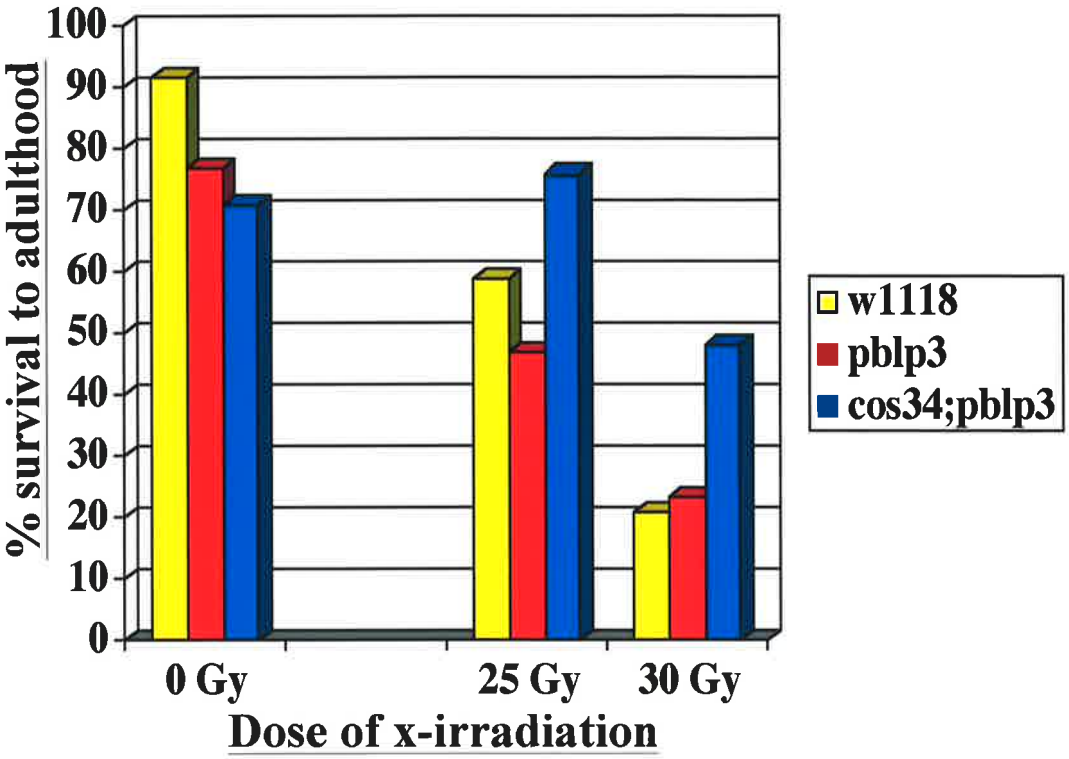

	0 Gy	25 Gy	30Gy
w^{1118}	412/450= **91.6%**	265/450= **58.9%**	62/300= **20.7%**
pbl^{p3}	345/450= **76.7%**	211/450= **46.9%**	70/300= **23.3%**
cos34;pbl^{p3}	319/450= **70.9%**	341/450= **75.8%**	144/300= **48.0%**

Figure 6.3 A third x-ray sensitivity test shows that both wild type and pbl^{p3} mutant larvae are sensitive to 25 and 30 Gy of x-irradiation.

w^{1118}, pbl^{p3} and *cos34;*pbl^{p3} third instar larvae were collected, bathed in water and irradiated in petri dishes at the doses indicated. The larvae were then transferred into vials containing food and the number of adults to hatch out of the vials were scored as a percentage of the number of larvae placed into the vials. The data are presented in both graphical and tabular form. As can be seen from the graph and the table, both wild type and pbl^{p3} larvae appear to be sensitive to irradiation at both 25 and 30 Gy. Introduction of the cosmid known to rescue *pbl* function (*cos34*) resulted in complete rescue of the sensitivity of pbl^{p3}. These *cos34;*pbl^{p3} flies are not at all sensitive to 25 Gy of irradiation.

6:4 Characterisation of the *pbl*^{p3} hypersensitivity phenotype: *pbl*^{p3} cells still arrest in response to DNA damage

In eukaryotic cells, DNA damage induces a block in the cell cycle. This cell cycle arrest enables the cell to repair any damage before the mutation is passed on to the next generation through DNA replication and cellular division (Weinert and Hartwell, 1988; Hartwell and Weinert, 1989; Weinert and Hartwell, 1989; Elledge, 1996; Walworth, 2000). In *Drosophila* cellularised embryos and larval tissues, it has been shown that DNA damage induces the cells to arrest in G2 (Brodsky *et al.*, 2000; Su *et al.*, 2000). Repair mechanisms are then activated and the damage is repaired before the cells continue into mitosis. The mitosis specific antibody anti-phosphorylated histone H3 (anti-PH3) can be used to examine this cell cycle arrest in irradiated tissues. The arrest of cells in G2 can be seen as a dramatic decrease in the number of cells in mitosis. Several *Drosophila* checkpoint genes including *mei-41* and *mus304* have been shown, using this antibody, to fail to undergo cell cycle arrest in response to DNA damage caused by x-irradiation. The larval wing and eye discs of mutants in these genes were observed to have just as many mitotic figures after irradiation as before, while wild type cells sense that damage has occurred and arrest the cell cycle (Brodsky *et al.*, 2000). Therefore, as a first step in understanding why *pbl*^{p3} mutants are hypersensitive, their ability to recognise DNA damage and arrest the cell cycle was examined. Wild type, *pbl*^{p3} and *cos34; pbl*^{p3} mutant larvae were irradiated at 40 Gy and, after 1 hour recovery at 25°C, eye and wing discs were dissected, fixed and stained with the anti-PH3 antibody. As can be seen from **Figure 6.4**, *pbl*^{p3} mutants, like wild type and *cos34; pbl*^{p3}, arrested the cell cycle.

Figure 6.4 *pbl*^{p3} mutant larvae detect DNA damage and arrest in G2.

Wild type, *pbl*^{p3} and *cos34;pbl*^{p3} third instar larvae were irradiated at 40 Gy and 1 hour post irradiation at 25°C, eye and wing discs were dissected, fixed and stained with the mitosis specific antibody anti-phosphorylated histone H3. Non-irradiated controls were included for each genotype. All images were taken at 10x magnification.

A. Wild type eye disc. Many cells are in mitosis.

B. Wild type eye disc 1hour post irradiation, showing a massive reduction in the number of cells in mitosis.

C. *pbl*^{p3} eye disc. There are just as many cells in mitosis as wild type.

D. *pbl*^{p3} eye disc 1 hour post irradiation. The same reduction in the number of mitotic cells was observed.

E. *cos34; pbl*^{p3} eye disc.

F. *cos34; pbl*^{p3} eye disc 1 hour post irradiation, showing the reduction in the number of mitotic cells.

G. Wild type wing disc. Many cells are in mitosis.

H. Wild type wing disc 1 hour post irradiation, showing few mitotic cells.

I. *pbl*^{p3} wing disc. There are just as many cells in mitosis as wild type.

J. *pbl*^{p3} wing disc 1 hour post irradiation also showing a dramatic reduction in the number of mitoses.

K. *cos34; pbl*^{p3} wing disc.

L. *cos34; pbl*^{p3} wing disc 1 hour post irradiation. Most cells are non-mitotic as expected.

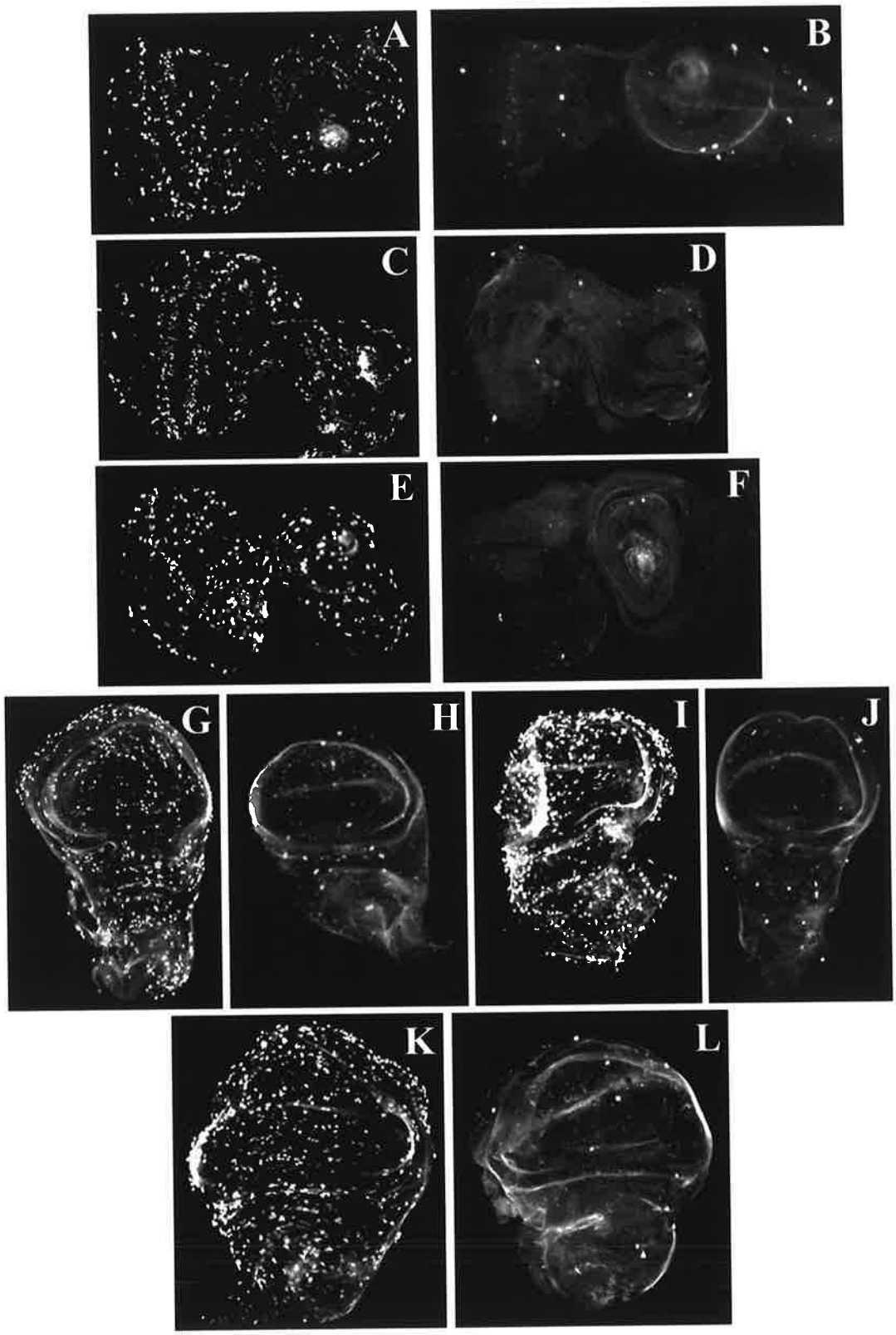
A
B
C
D
E
F
G
H
I
J
K
L

6:5 *pbl*^{p3} mutants appear to repair their DNA damage

The next question concerned whether *pbl*^{p3} mutants were capable of repairing DNA damage. If they were able to detect damage but unable to repair it, then this failure would explain their hypersensitivity to x-irradiation. To look at DNA damage directly, the anti-γ–H2AX antibody was used. Double stranded DNA breaks induced by ionizing radiation result in the phosphorylation of histone H2AX yielding a modified form known as γ–H2AX. Staining with a human antibody against this specific modified form has been shown to be a direct measure of the amount of DNA damage. Nuclear foci appear within one minute after irradiation, and the number of these foci has been shown to be directly comparable to the number of induced DNA double strand breaks. On westerns this human antibody has also been shown to cross react with *Drosophila* (Rogakou *et al.*, 1999). This antibody was therefore used in this study to quantify the amount of DNA damage induced, and to examine the repair process. If this antibody is in fact a direct measure of the amount of damage, then the level of staining should decrease with time after irradiation, as the repair process gradually resolves all of the DNA double strand breaks. A failure to repair would therefore be seen as a continuation of a high level of staining with this antibody.

As initial attempts to get this antibody to work on fixed *Drosophila* tissues failed, it was decided to utilise western analysis to show that this antibody could be used to follow the repair process in *Drosophila*. Wild type third instar larvae were irradiated at 40 Gy, and at 1 hour and 4 hours post irradiation, eye and wing discs were dissected for western analysis. The 1 hour time point was chosen as it was previously shown that tissues should have arrested the cell cycle by this stage. The 4 hour time point was chosen as previous studies on *Drosophila* larval tissues had shown that wild type cells given 40 Gy of irradiation should have re-entered the cell cycle by this time (Brodsky *et al.*, 2000). Non-irradiated controls were also included. As can be seen from **Figure 6.5**, 40 Gy induced a significant γ–H2AX band at 1 hour post irradiation in both eye and wing discs of wild type larvae. By 4 hours, this band decreased in intensity back to that of non-irradiated controls, indicating that the repair process can be followed in this way. The presence of a weak band in the non-irradiated control may be due to a low level of spontaneous DNA damage, but this possibility was not explored further. Thus staining with the human γ–H2AX antibody can be used to examine the process of irradiation-induced repair in *Drosophila* tissues.

pbl^{p3} mutant larvae were therefore irradiated at 40 Gy, and eye and wing discs were dissected at 1 hour and 4 hours post irradiation for western analysis using the γ–H2AX antibody. As is evident from **Figure 6.6**, *pbl*^{p3} mutants also appeared to repair their DNA damage. A significant band is induced 1 hour post irradiation, but this was observed to decrease in intensity by 4 hours to a level comparable to that of the non-irradiated control.

If *pbl*^{p3} mutants are capable of repair, then do they repair inefficiently? To answer this question, the time course of repair was examined and compared to that of *cos34; pbl*^{p3} larvae, which are not hypersensitive to irradiation. *pbl*^{p3} and *cos34; pbl*^{p3} larvae were irradiated at 40 Gy, and eye and wing discs were dissected at 1 hour, 2 hours, 3 hours and 4 hours post irradiation. Western analysis indicated that the repair time course was altered in *pbl*^{p3} compared to *cos34; pbl*^{p3} larvae. However, while *pbl*^{p3} wing disc cells appeared to be delayed in repairing their damage by 1 hour compared to *cos34; pbl*^{p3}, *pbl*^{p3} eye disc cells appeared to repair their damage 1 hour before that of *cos34; pbl*^{p3} larvae (**Figure 6.7**). Given these contradictory findings, the significance of the observations is uncertain.

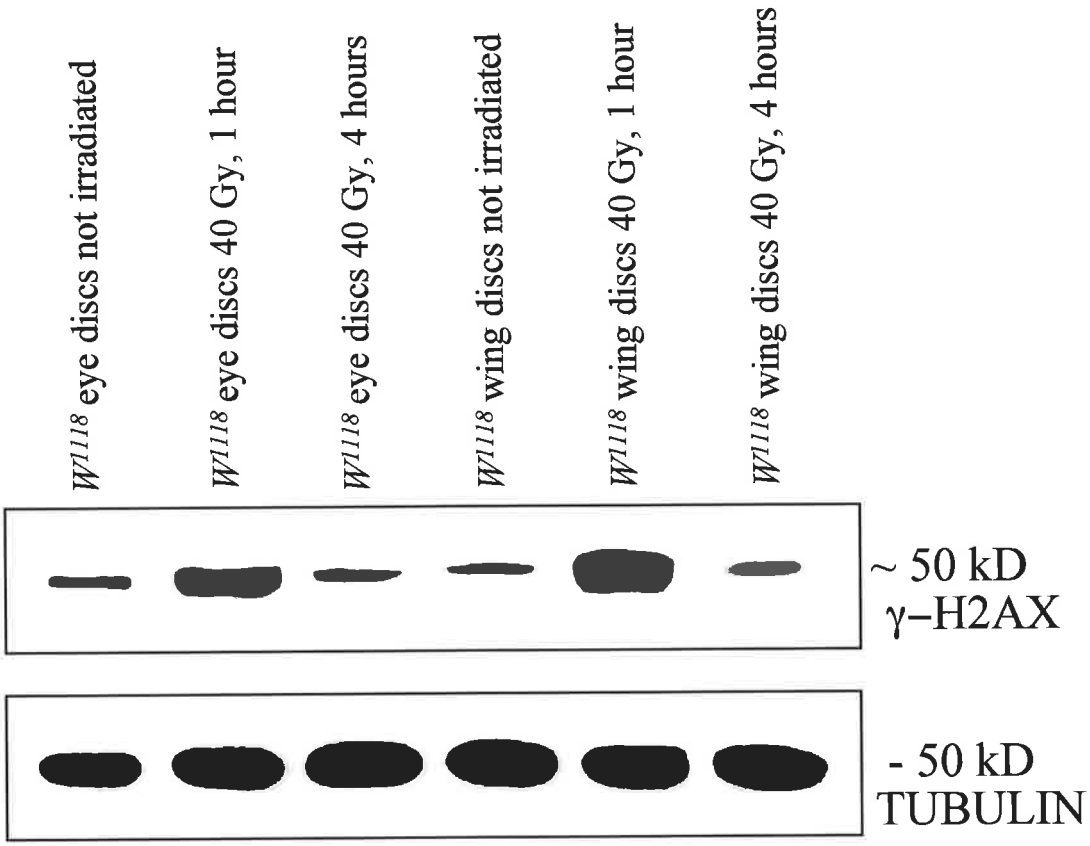

Figure 6.5 The γ–H2AX human antibody can be used to examine the DNA repair process in *Drosophila* larval tissues.

w^{1118} larvae were irradiated at 40 Gy. 1 hour and 4 hours post irradiation at 25°C, eye and wing discs were dissected, boiled and run on a 10% SDS polyacrylamide gel, which was then transferred to a nitrocellulose filter. Non-irradiated controls were also included.
The filter was then probed with an antibody specific for human γ–H2AX, which produced a band just above 50 kD in size in each lane.
The filter was then stripped and reprobed with an alpha-tubulin antibody, which served as a loading control. This also produced a band of approximately 50 kD in size.
As can be seen from the filter, irradiation of larval eye and wing discs produced a strong γ–H2AX signal 1 hour post irradiation. By 4 hours this signal decreased in intensity back to that of non-irradiated controls, indicating that the repair process can be followed in this way.

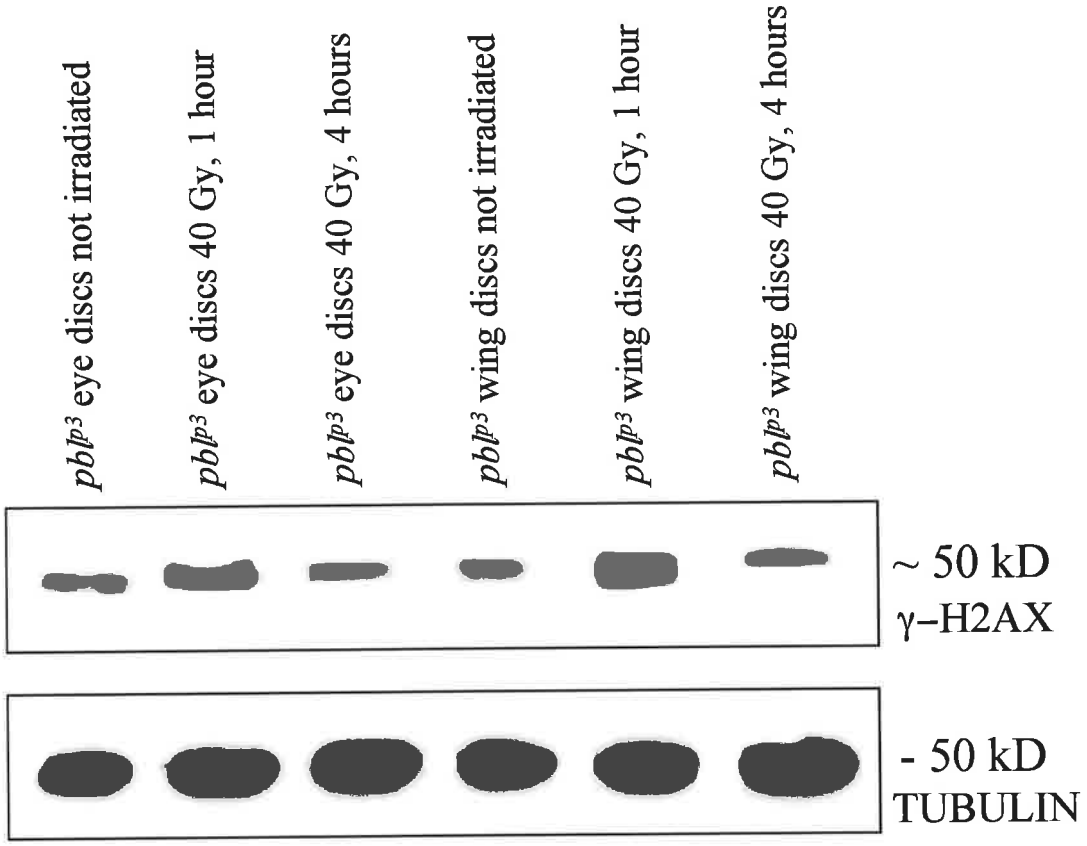

Figure 6.6 *pbl*^{p3} larval cells appear to repair their DNA damage.

pbl^{p3} larvae were irradiated at 40 Gy. 1 hour and 4 hours post irradiation at 25°C, eye and wing discs were dissected, boiled and run on a 10% SDS polyacrylamide gel, which was then transferred to a nitrocellulose filter. Non-irradiated controls were also included.
The filter was then probed with an antibody specific for γ–H2AX, which produced a band just above 50 kD in size in each lane.
The filter was then stripped and reprobed with an alpha-tubulin antibody, which served as a loading control. This also produced a band of approximately 50 kD in size.
As can be seen from the filter, irradiation of *pbl*^{p3} larval eye and wing discs produced a strong γ–H2AX signal 1 hour post irradiation. By 4 hours this signal decreased in intensity back to that of non-irradiated controls, indicating that *pbl*^{p3} larval cells are capable of repairing irradiation induced DNA damage.

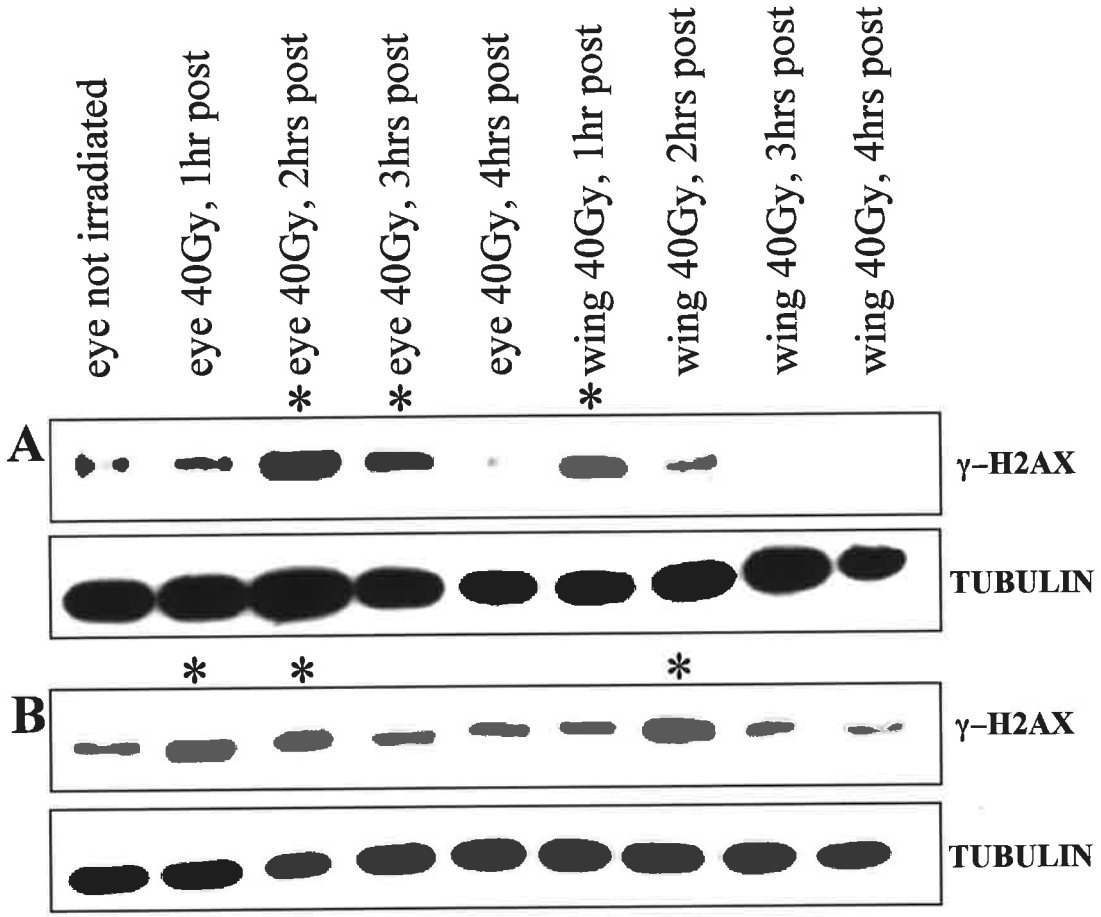

Figure 6.7 *pbl*^{p3} larval cells appear to repair their DNA damage, but with a slightly altered time course to that of *cos34; pbl*^{p3}.

cos34; pbl^{p3} and *pbl*^{p3} larvae were irradiated at 40 Gy. 1, 2, 3 and 4 hours post irradiation at 25°C, eye and wing discs were dissected, boiled and run on a 10% SDS polyacrylamide gel, which was then transferred to a nitrocellulose filter. Non-irradiated eye disc controls were also included.
The filter was then probed with an antibody specific for γ–H2AX, which produced a band of just above 50 kD in size in each lane. The filter was then stripped and reprobed with an alpha-tubulin antibody, which served as a loading control. This also produced a band of approximately 50 kD in size.
A. Irradiation of *cos34; pbl*^{p3} larval eye discs produced a strong γ–H2AX signal at 2 and 3 hours post irradiation (as indicated by the*). By 4 hours, this signal decreased in intensity back to that of the non-irradiated control. *cos34; pbl*^{p3} wing discs produced a strong γ–H2AX signal 1 hour post irradiation (*), which decreased in intensity by 2 hours.
B. Irradiation of *pbl*^{p3} larval eye discs produced a strong γ–H2AX signal at 1 hour and 2 hours post irradiation (*). This signal decreased in intensity in the 3 hours post irradiation tissues. *pbl*^{p3} eye discs therefore appeared to repair their damage 1 hour prior to *cos34; pbl*^{p3} eye discs. Irradiation of *pbl*^{p3} larval wing discs produced a strong γ–H2AX signal at 2 hours post irradiation (*). This signal decreased in intensity in the 3 hours post irradiation tissues. *pbl*^{p3} wing discs were therefore delayed in sensing and repairing their DNA damage by 1 hour compared to *cos34; pbl*^{p3}.

6:6 *pbl*^{p3} mutants are not delayed in re-entering the cell cycle after irradiation induced arrest

As discussed in the previous sections, although hypersensitive to x-irradiation, *pbl*^{p3} larvae sense that damage has occurred, arrest the cell cycle appropriately, and appear to repair their DNA. But do they then re-enter the cell cycle at the appropriate time? If, for example, they were capable of repair, but were deficient in a pathway that sensed that repair had occurred, then the cells would fail to re-enter the cell cycle. Such a failure could lead to a massive increase in apoptosis, which would explain the hypersensitivity. Wild type, *pbl*^{p3} and *cos34; pbl*^{p3} larvae were therefore irradiated at 40 Gy, and eye and wing discs were fixed and stained with the anti-PH3 antibody at various times post irradiation.

According to published data using these same *Drosophila* tissues, cells of wild type larvae are supposed to re-enter the cell cycle 4 hours after 40 Gy of x-irradiation at 25°C (Brodsky *et al.*, 2000). Indeed, as is evident in **Figures 6.5** and **6.6**, both wild type and *pbl*^{p3} eye and wing disc cells have repaired their irradiation induced damage by this time. However, the wild type cells used in this study did not re-enter the cell cycle until 6 hours post irradiation (**Figure 6.8c** and **l**). At this time, *pbl*^{p3} larval eye and wing discs had a few more cells in mitosis than wild type or *cos34; pbl*^{p3}, but this was variable and the difference was not dramatic (**Figure 6.8f** and **o**). However, when this 40 Gy dose of irradiation was used to examine the survival of larvae to adulthood, wild type larvae were found not to survive such a high level of irradiation (data not shown). It was therefore decided to repeat this analysis at a lower dose where *pbl*^{p3} larvae are clearly more sensitive to irradiation. At 25 Gy, most cells had re-entered the cell cycle by 1 hour post irradiation and wild type, *pbl*^{p3} and *cos34; pbl*^{p3} all appeared to have a similar level of cells in mitosis (**Figure 6.9**). Therefore, *pbl*^{p3} larval eye and wing disc cells do not appear to be delayed in re-entering the cell cycle after the irradiation-induced block.

Figure 6.8 *pbl*^{p3} eye and wing discs re-enter the cell cycle after irradiation-induced arrest at the same time as wild type.

Wild type, *pbl*^{p3} and *cos34;pbl*^{p3} third instar larvae were irradiated at 40 Gy. 1 hour and 6 hours post irradiation, eye and wing discs were dissected, fixed and stained with the mitosis specific antibody, anti-phosphorylated histone H3. Non-irradiated controls were included for each genotype. All images were taken at 10x magnification.

A. Wild type eye disc. Many cells are in mitosis.

B. Wild type eye disc 1hour post irradiation. Most cells have arrested, resulting in a massive decrease in the number of cells in mitosis.

C. Wild type eye disc 6 hours post irradiation. Cells have begun to re-enter mitosis after the irradiation-induced arrest.

D. *pbl*^{p3} eye disc. There are just as many cells in mitosis as wild type.

E. *pbl*^{p3} eye disc 1 hour post irradiation. Most cells have arrested like wild type.

F. *pbl*^{p3} eye disc 6 hours post irradiation. More cells have re-entered mitosis than wild type at the same time point. However, this is variable and not significant.

G. *cos34; pbl*^{p3} eye disc.

H. *cos34; pbl*^{p3} eye disc 1 hour post irradiation. Most cells have arrested.

I. *cos34; pbl*^{p3} eye disc 6 hours post irradiation. More cells have re-entered mitosis than wild type at this time point. However, the level of mitosis is similar to that of *pbl*^{p3}.

J. Wild type wing disc. Many cells are in mitosis.

K. Wild type wing disc 1 hour post irradiation. Most cells have arrested.

L. Wild type wing disc 6 hours post irradiation. Cells have begun to re-enter mitosis.

M. *pbl*^{p3} wing disc. There are just as many cells in mitosis as wild type.

N. *pbl*^{p3} wing disc 1 hour post irradiation. Most cells have arrested.

O. *pbl*^{p3} wing disc 6 hours post irradiation. Like wild type, cells have begun to re-enter mitosis.

P. *cos34; pbl*^{p3} wing disc.

Q. *cos34; pbl*^{p3} wing disc 1 hour post irradiation. Most cells have arrested.

R. *cos34; pbl*^{p3} wing disc 6 hours post irradiation. Many cells have re-entered mitosis by this stage.

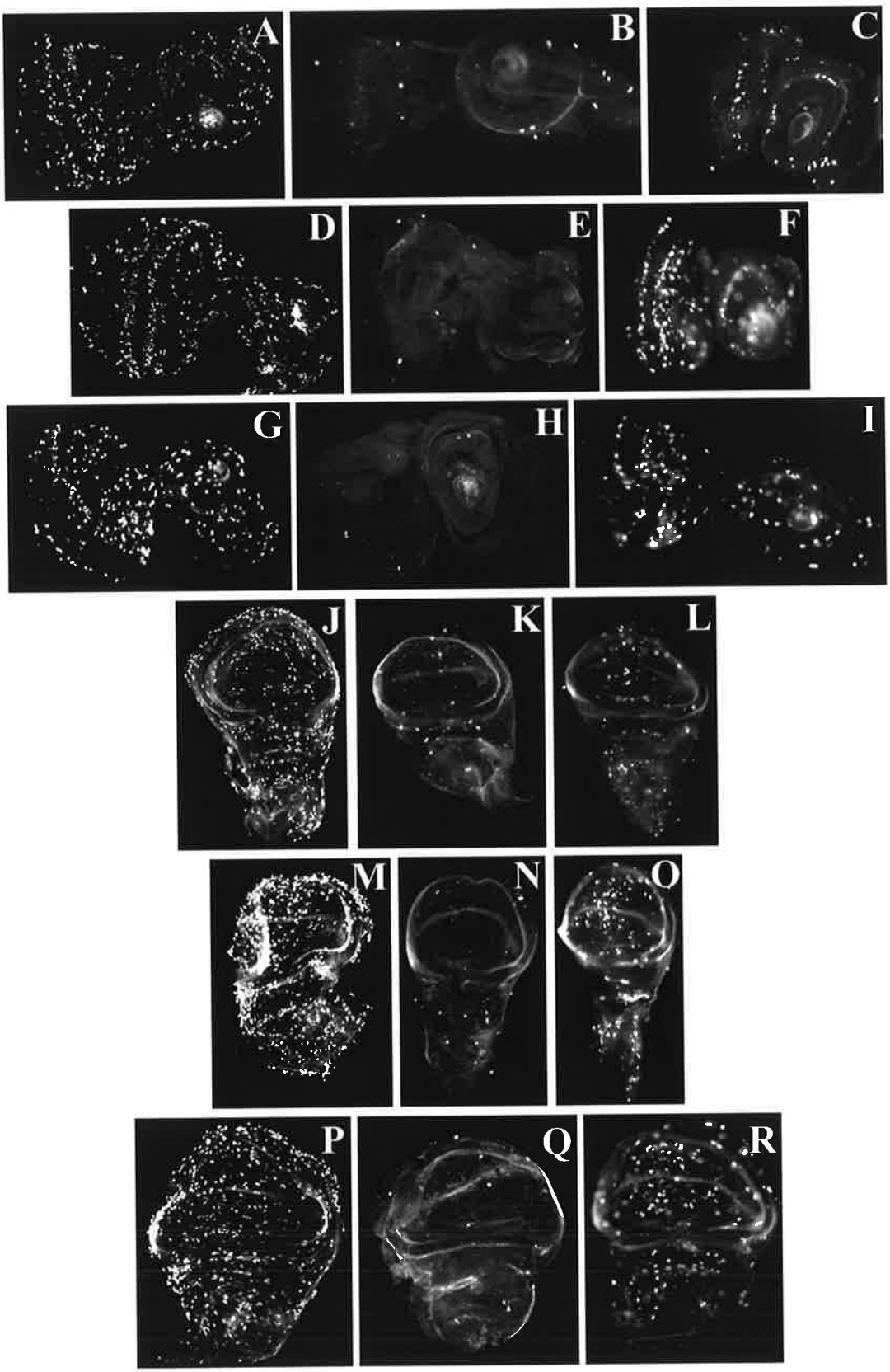
A
B
C
D
E
F
G
H
I
J
K
L
M
N
O
P
Q
R

Figure 6.9 After 25 Gy of irradiation, *pbl*^{p3} eye and wing discs re-enter the cell cycle at the same time as wild type.

Wild type and *pbl*^{p3} third instar larvae were irradiated at 25 Gy and 1 hour post irradiation eye and wing discs were dissected, fixed and stained with the mitosis specific antibody anti-phosphorylated histone H3. All images were taken at 10x magnification.

A. Wild type eye disc. Many cells are in mitosis.

B. Wild type eye disc 1hour post irradiation. Many cells have re-entered the cell cycle.

C. *pbl*^{p3} eye disc. There are just as many cells in mitosis as wild type.

D. *pbl*^{p3} eye disc 1 hour post irradiation. Just as many cells have re-entered mitosis as wild type.

E. Wild type wing disc. Many cells are in mitosis.

F. Wild type wing disc 1 hour post irradiation. Many cells have re-entered mitosis.

G. *pbl*^{p3} wing disc. There are just as many cells in mitosis as wild type.

H. *pbl*^{p3} wing disc 1 hour post irradiation. Just as many cells have re-entered mitosis as wild type wing discs at the same stage.

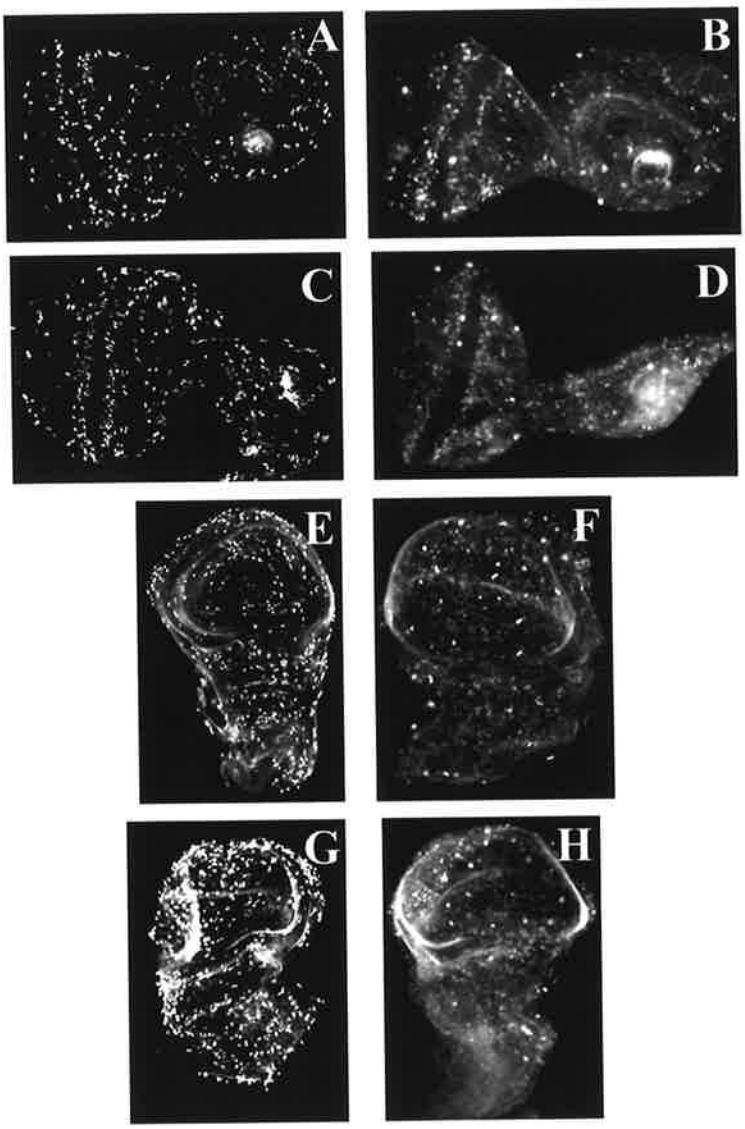
A
B
C
D
E
F
G
H

6:7 *pbl*^{p3} mutants do not have an excessive level of cell death after irradiation

To examine the level of cell death in response to irradiation, acridine orange staining was used. Acridine orange is a stain that can only penetrate cells whose membranes are breaking down. As a result, it can be used as a marker for both apoptosis and necrosis. If the repair within *pbl*^{p3} larval tissues is incomplete, or the tissues repair but fail to recognise that they have done so, then the tissues should have increased levels of acridine orange staining compared to wild type. Wild type, *pbl*^{p3} and *cos34; pbl*^{p3} larvae were therefore irradiated at 25 Gy, and eye and wing discs were dissected and stained at 7 hours post irradiation.

By 7 hours post 25 Gy of irradiation, a massive level of cell death was induced in wild type, *pbl*^{p3} and *cos34; pbl*^{p3} larval eye and wing discs (**Figure 6.10**). The level of cell death was similar in all three samples. *pbl*^{p3} and *cos34; pbl*^{p3} larval discs were then also examined at 8-9 hours and 9-10 hours post irradiation. By these later stages the level of cell death appeared to slightly increase, although the level of cells staining was similar between the two samples (**Figure 6.11** and **6.12**). Considering the high level of staining induced in both of the samples at this dose of irradiation, it was possible that any minor difference between them would go undetected. *pbl*^{p3} and *cos34; pbl*^{p3} larvae were therefore irradiated at 10 Gy and 2 Gy of irradiation, and the eye and wing discs were dissected and stained at 7-8 hours post irradiation (**Figure 6.13** and **6.14**). After 10 Gy of irradiation, a slightly lower level of cell death was induced compared to 25 Gy. However, the levels induced in *pbl*^{p3} and *cos34; pbl*^{p3} larval discs were not significantly different (**Figure 6.13**). After 2 Gy of irradiation a substantially lower level of cell death was induced. However, there was still no significant difference in the level of cell death between *pbl*^{p3} and *cos34; pbl*^{p3} samples (**Figure 6.14**).

Figure 6.10 *pbl*^{p3} eye and wing discs have a similar level of cell death as wild type at 7 hours post 25 Gy of irradiation.

Wild type, *pbl*^{p3} and *cos34;pbl*^{p3} third instar larvae were irradiated at 25 Gy and 7 hours post irradiation eye and wing discs were dissected and stained with the cell death specific marker acridine orange. Non-irradiated controls were included for each genotype. All images were taken at 10x magnification unless otherwise indicated.

A. Wild type eye disc. There are very few cells undergoing cell death.

B. Wild type eye disc 7 hours post irradiation. A massive increase in the level of cell death is observed. B' is a close up view of the same disc taken at 20x magnification.

C. *pbl*^{p3} eye disc. Very few cells are undergoing cell death like wild type.

D. *pbl*^{p3} eye disc 7 hours post irradiation. A massive increase in cell death is observed, but this is not significantly greater than the increase observed in wild type. D' is a close up of the same disc taken at 20x magnification.

E. *cos34; pbl*^{p3} eye disc. Very few cells are undergoing cell death.

F. *cos34; pbl*^{p3} eye disc 7 hours post irradiation. A massive increase in cell death is observed, similar to that of *pbl*^{p3} and wild type eye discs. F' is a close up of the same disc taken at 20x magnification.

G. Wild type wing disc. Very few cells are undergoing cell death.

H. Wild type wing disc 7 hours post irradiation. A massive increase in cell death is observed. H' is a close up of the same disc taken at 20x magnification.

I. *pbl*^{p3} wing disc. Very few cells are undergoing cell death like wild type.

J. *pbl*^{p3} wing disc 7 hours post irradiation. A massive increase in cell death is observed, to a level similar to that of wild type wing discs. J' is a close up of the same disc taken at 20x magnification.

K. *cos34; pbl*^{p3} wing disc. Very few cells are undergoing cell death.

L. *cos34; pbl*^{p3} wing disc 7 hours post irradiation. A massive increase in cell death is observed, similar to that of *pbl*^{p3} and wild type eye discs. L' is a close up view of the same disc taken at 20x magnification.

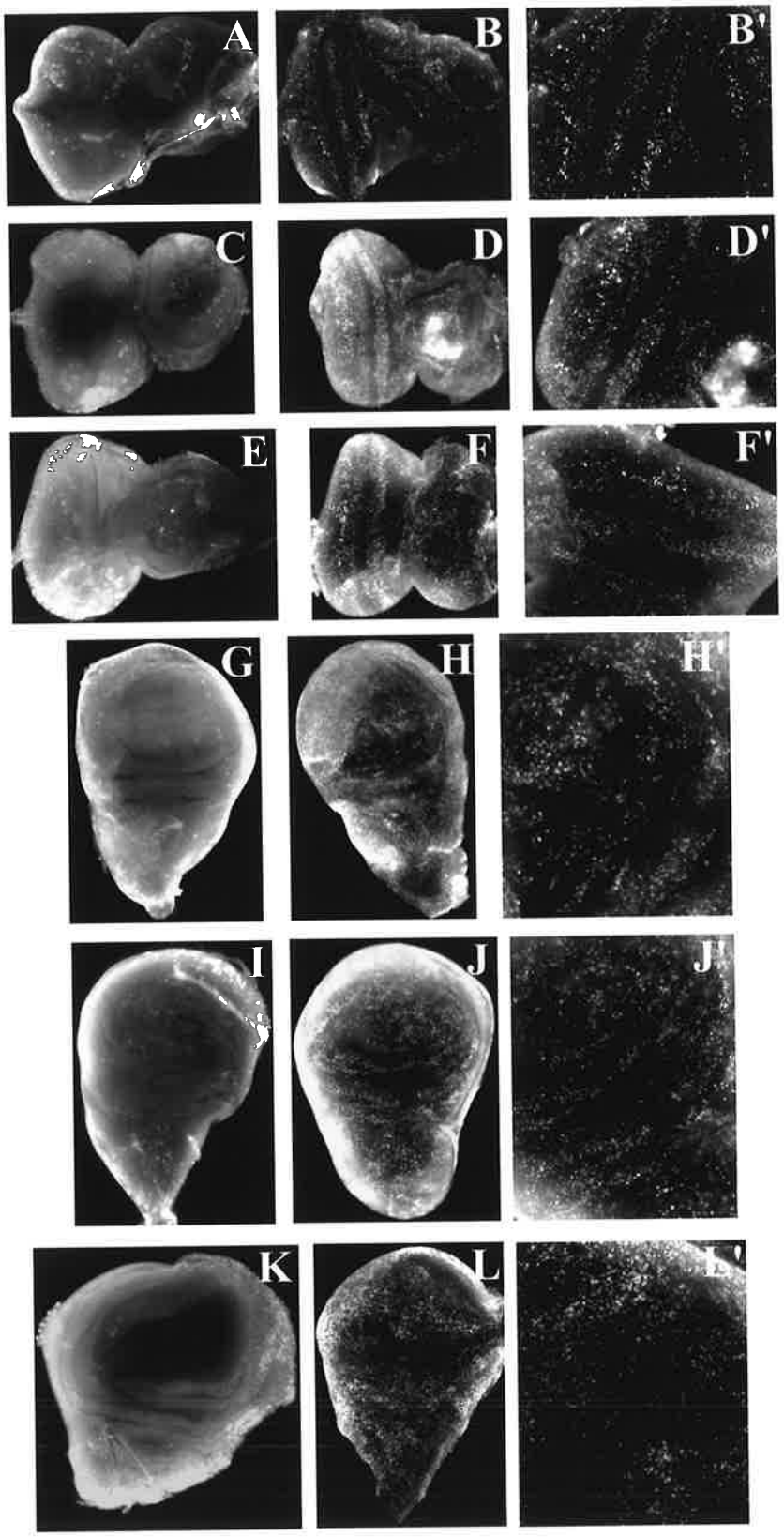
A
B
B'
C
D
D'
E
F
F'
G
H
H'
I
J
J'
K
L
L'

Figure 6.11 *pbl*^{p3} eye and wing discs have a similar level of cell death as *cos34; pbl*^{p3} discs at 8-9 hours post 25 Gy of irradiation.

pbl^{p3} and *cos34;pbl*^{p3} third instar larvae were irradiated at 25 Gy and 8-9 hours post irradiation eye and wing discs were dissected and stained with the cell death specific marker acridine orange. All images were taken at 10x magnification unless otherwise indicated.

A. *cos34; pbl*^{p3} eye disc. Very few cells are undergoing cell death.

B. *cos34; pbl*^{p3} eye disc 8-9 hours post irradiation. A massive increase in cell death is observed. B' is a close up of the same disc taken at 20x magnification.

C. *pbl*^{p3} eye disc. Very few cells are undergoing cell death.

D. *pbl*^{p3} eye disc 8-9 hours post irradiation. A massive increase in cell death is observed, but this is similar to the increase observed in *cos34; pbl*^{p3}. D' is a close up of the same disc taken at 20x magnification.

E. *cos34; pbl*^{p3} wing disc. Very few cells are undergoing cell death.

F. *cos34; pbl*^{p3} wing disc 8-9 hours post irradiation. A massive increase in cell death is observed. F' is a close up view of the same disc taken at 20x magnification.

G. *pbl*^{p3} wing disc. Very few cells are undergoing cell death.

H. *pbl*^{p3} wing disc 8-9 hours post irradiation. A massive increase in cell death is observed, to a level similar to that of *cos34; pbl*^{p3} wing discs. H' is a close up of the same disc taken at 20x magnification.

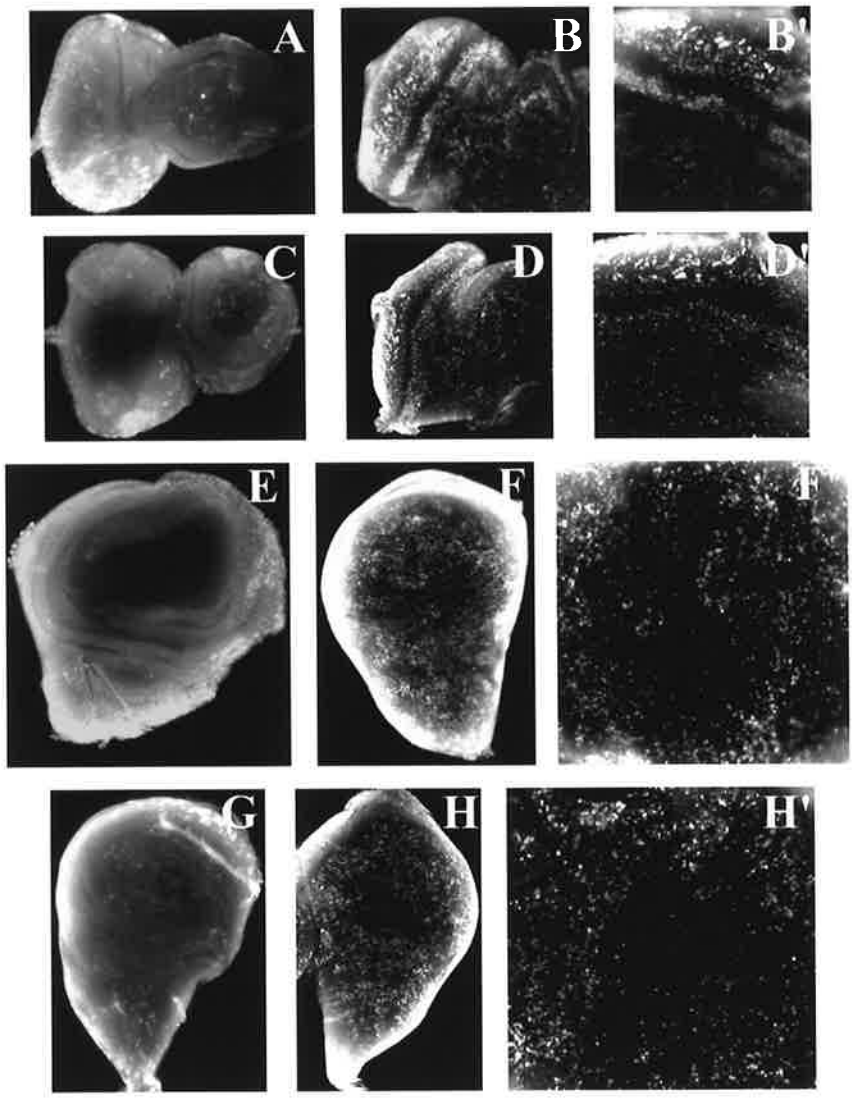
A
B
B'
C
D
D'
E
F
F'
G
H
H'

Figure 6.12 *pbl*^{p3} eye and wing discs have a similar level of cell death as *cos34; pbl*^{p3} discs at 9-10 hours post 25 Gy of irradiation.

pbl^{p3} and *cos34;pbl*^{p3} third instar larvae were irradiated at 25 Gy and 9-10 hours post irradiation eye and wing discs were dissected and stained with the cell death specific marker acridine orange. All images were taken at 10x magnification unless otherwise indicated.

A. *cos34; pbl*^{p3} eye disc. Very few cells are undergoing cell death.

B. *cos34; pbl*^{p3} eye disc 9-10 hours post irradiation. A massive increase in cell death is observed. B' is a close up of the same disc taken at 20x magnification.

C. *pbl*^{p3} eye disc. Very few cells are undergoing cell death.

D. *pbl*^{p3} eye disc 9-10 hours post irradiation. A massive increase in cell death is observed, but this is similar to the increase observed in *cos34; pbl*^{p3}. D' is a close up of the same disc taken at 20x magnification.

E. *cos34; pbl*^{p3} wing disc. Very few cells are undergoing cell death.

F. *cos34; pbl*^{p3} wing disc 9-10 hours post irradiation. A massive increase in cell death is observed. F' is a close up view of the same disc taken at 20x magnification.

G. *pbl*^{p3} wing disc. Very few cells are undergoing cell death.

H. *pbl*^{p3} wing disc 9-10 hours post irradiation. A massive increase in cell death is observed, to a level similar to that of *cos34; pbl*^{p3} wing discs. H' is a close up of the same disc taken at 20x magnification.

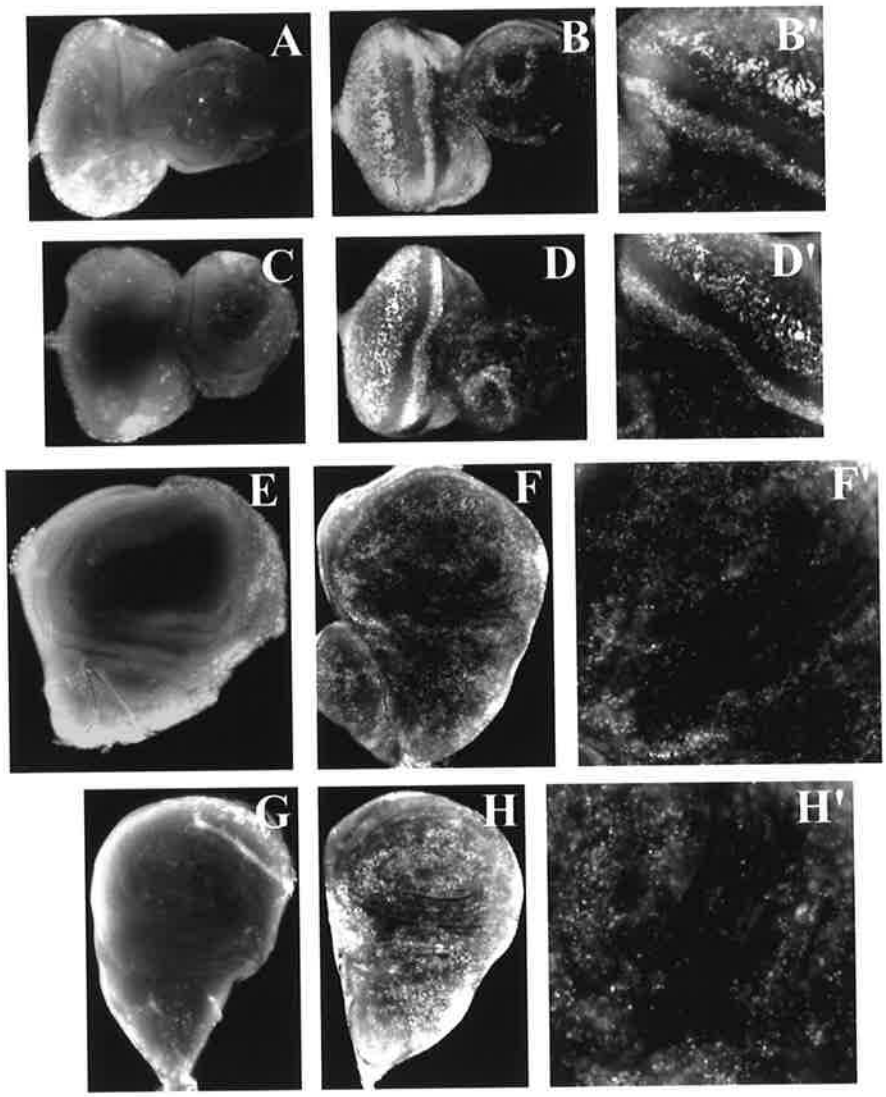
A
B
B'
C
D
D'
E
F
F'
G
H
H'

Figure 6.13 *pbl*^{p3} eye and wing discs have a similar level of cell death as *cos34; pbl*^{p3} discs at 7-8 hours post 10 Gy of irradiation.

pbl^{p3} and *cos34;pbl*^{p3} third instar larvae were irradiated at 10 Gy and 7-8 hours post irradiation eye and wing discs were dissected and stained with the cell death specific marker acridine orange. All images were taken at 10x magnification unless otherwise indicated.

A. *cos34; pbl*^{p3} eye disc. Very few cells are undergoing cell death.

B. *cos34; pbl*^{p3} eye disc 7-8 hours post irradiation. A large increase in cell death is observed. B' is a close up of the same disc taken at 20x magnification.

C. *pbl*^{p3} eye disc. Very few cells are undergoing cell death.

D. *pbl*^{p3} eye disc 7-8 hours post irradiation. A large increase in cell death is observed, but this is similar to the increase observed in *cos34; pbl*^{p3}. D' is a close up of the same disc taken at 20x magnification.

E. *cos34; pbl*^{p3} wing disc. Very few cells are undergoing cell death.

F. *cos34; pbl*^{p3} wing disc 7-8 hours post irradiation. A large increase in cell death is observed. F' is a close up view of the same disc taken at 20x magnification.

G. *pbl*^{p3} wing disc. Very few cells are undergoing cell death.

H. *pbl*^{p3} wing disc 7-8 hours post irradiation. A large increase in cell death is observed, to a level similar to that of *cos34; pbl*^{p3} wing discs. H' is a close up of the same disc taken at 20x magnification.

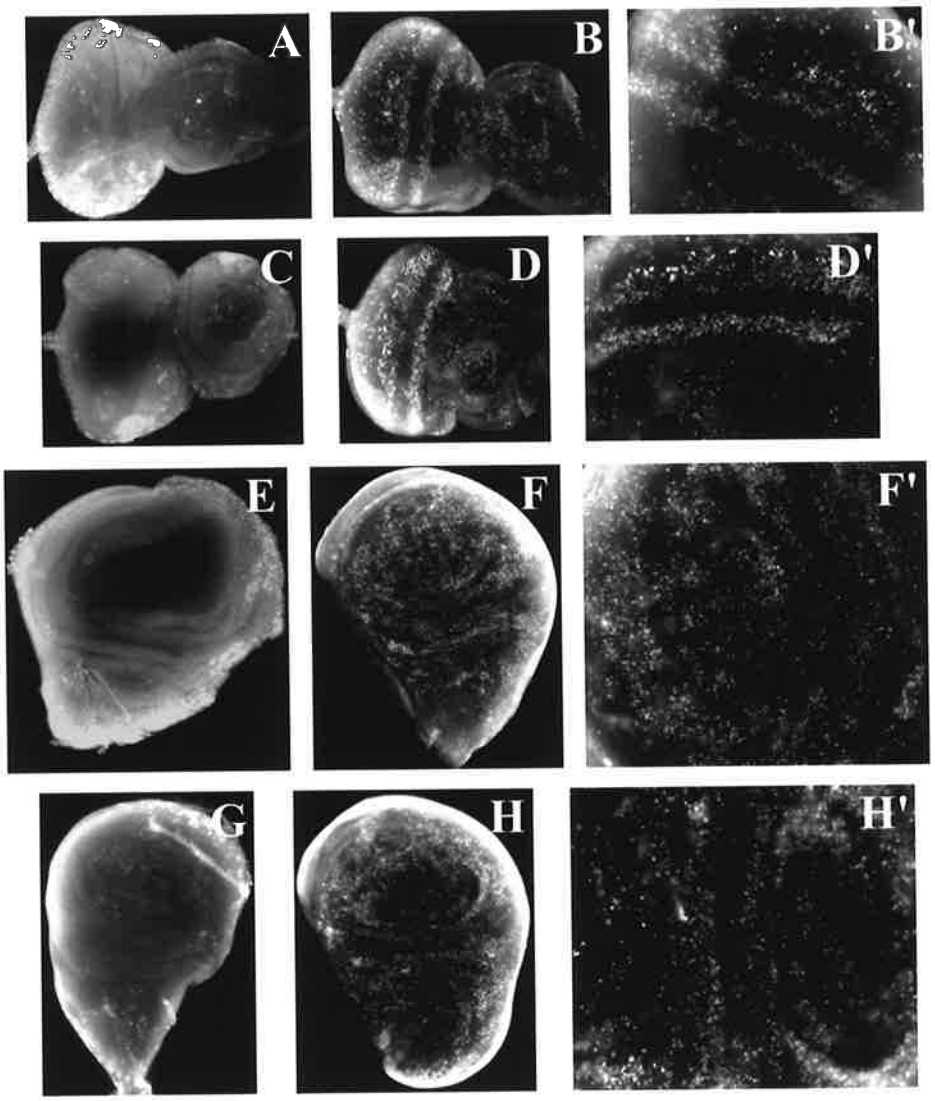
A
B
B'
C
D
D'
E
F
F'
G
H
H'

Figure 6.14 *pbl*^{p3} eye and wing discs have a similar level of cell death as *cos34; pbl*^{p3} discs at 7-8 hours post 2 Gy of irradiation.

pbl^{p3} and *cos34;pbl*^{p3} third instar larvae were irradiated at 2 Gy and 7-8 hours post irradiation eye and wing discs were dissected and stained with the cell death specific marker acridine orange. All images were taken at 10x magnification unless otherwise indicated.

A. *cos34; pbl*^{p3} eye disc. Very few cells are undergoing cell death.

B. *cos34; pbl*^{p3} eye disc 7-8 hours post irradiation. A small increase in cell death is observed compared to higher doses of irradiation. B' is a close up of the same disc taken at 20x magnification.

C. *pbl*^{p3} eye disc. Very few cells are undergoing cell death.

D. *pbl*^{p3} eye disc 7-8 hours post irradiation. A small increase in cell death is observed, but this is similar to the increase observed in *cos34; pbl*^{p3}. D' is a close up of the same disc taken at 20x magnification.

E. *cos34; pbl*^{p3} wing disc. Very few cells are undergoing cell death.

F. *cos34; pbl*^{p3} wing disc 7-8 hours post irradiation. A small increase in cell death is observed compared to higher doses of irradiation. F' is a close up view of the same disc taken at 20x magnification.

G. *pbl*^{p3} wing disc. Very few cells are undergoing cell death.

H. *pbl*^{p3} wing disc 7-8 hours post irradiation. A similar small increase in cell death is observed. H' is a close up of the same disc taken at 20x magnification.

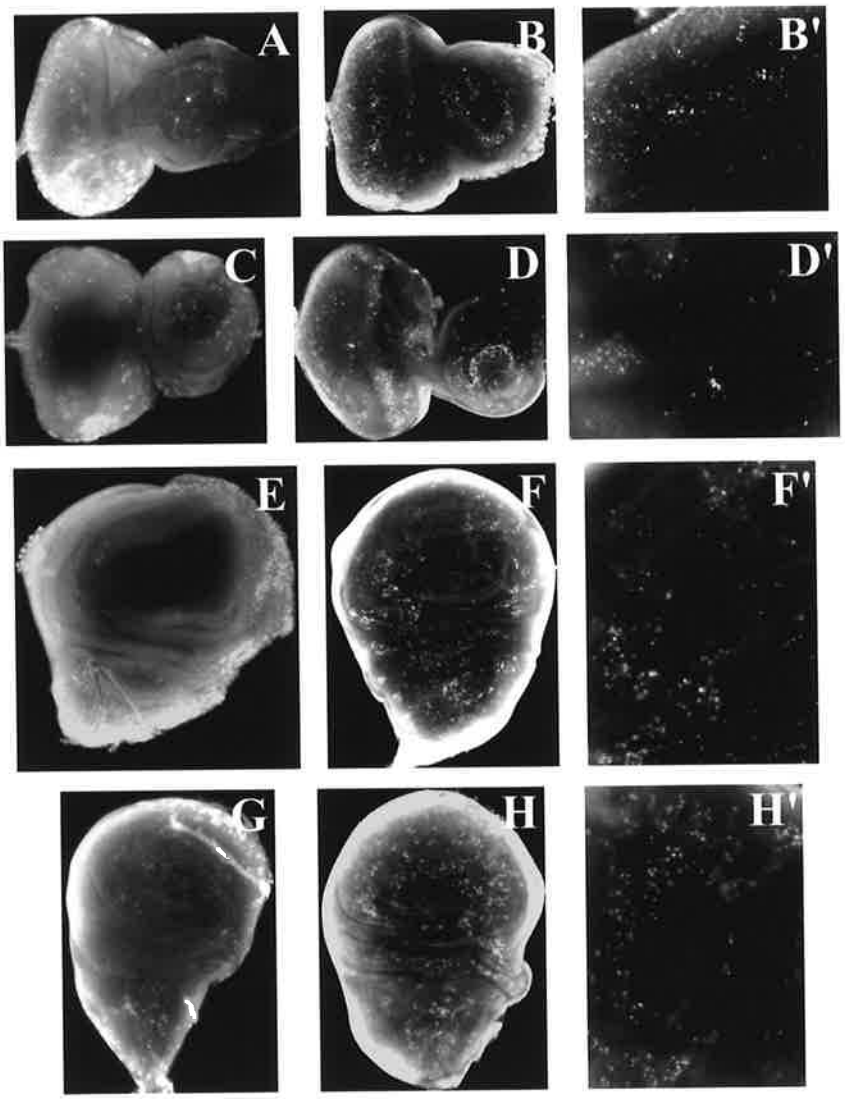
A
B
B'
C
D
D'
E
F
F'
G
H
H'

6:8 *pbl*^{p3} hypersensitivity is not due to a defect in cytokinesis

Although hypersensitive to x-irradiation, irradiated *pbl*^{p3} larval cells were found to arrest the cell cycle and apparently repair the damage, as they re-entered the cell cycle at the same time as wild type cells. They also showed no significant increase in the level of cell death. It remained a possibility that *pbl*^{p3} mutants were hypersensitive not because of a lack of a DNA repair process, but because of a failure in cytokinesis in the post-damage proliferative phase. After the massive level of cell death that is induced in response to the doses given in this study, a significant level of cell division would be needed to replenish those cells. If *pbl*^{p3} larvae were unable to replace those cells lost to apoptosis due to a mild cytokinetic defect, then this would explain their hypersensitivity to irradiation. *pbl*^{p3} and *cos34; pbl*^{p3} larvae were therefore irradiated at 25 Gy, and their subsequent development was analysed.

Although some larvae for both *pbl*^{p3} and *cos34; pbl*^{p3} samples were observed to not survive past the third larval instar after irradiation, numerous larvae were observed to continue to develop. Both *pbl*^{p3} and *cos34; pbl*^{p3} pupae formed, and many of these were observed to fully develop to stages just prior to eclosion (data not shown). *pbl*^{p3} pupae were found to contain apparently normal adult structures, but a high proportion were found to die within the pupal case without eclosing (data not shown). As development to this stage requires the proliferation of a multitude of different cell types, a defect in cytokinesis is an unlikely explanation for their hypersensitivity.

6:9 Discussion

Although widely reputed to play a role in DNA repair and other nuclear processes, the RadECl/BRCT domains were shown in the previous chapter to play an essential cytoplasmic role in cytokinesis. Despite its unique nature, this finding enabled the explanation of some of the phenotypes observed when the PBL constructs were expressed. In accordance with a cytoplasmic role for these domains, the PBL protein was also shown to shuttle between the nucleus and the cytoplasm. It was therefore proposed that the shuttling of the protein, combined with its interaction with other proteins via the RadECl/BRCT domains, could be a major factor in its regulation. In support of this, the RadECl/BRCT domains were recently shown to interact with a *Drosophila* RacGAP protein, a protein whose homologues in mice and nematodes have been shown to be essential for cytokinesis. These findings point to an important cytokinetic function for these domains in the cytoplasm. However, although known to be protein/protein interaction domains, the fact remains that BRCT domains have been identified in many proteins that have roles in DNA repair. Given the nuclear localisation of the PBL protein, and the presence of two of these highly conserved BRCT domains, it remained a possibility that PBL could also play a role in DNA repair. Not only would this point to a novel DNA repair mechanism, it could also provide a possible link between the response to DNA damage and control of the cell cycle.

In an attempt to investigate a potential role for PBL in the DNA damage response pathway, a larval X-ray sensitivity assay was performed. pbl^{p3} hypomorphic mutant larvae were x-irradiated, and their survival to adulthood was compared to that of wild type. pbl^{p3} larvae were found to be hypersensitive to both 20 and 25 Gy, suggesting that PBL does play a role in a DNA damage response or repair type pathway. The ability to completely rescue this hypersensitivity through the introduction of a cosmid carrying the *pbl* gene, proved that the sensitivity of the pbl^{p3} stock was in fact due to a lack of PBL function. In addition to rescuing the hypersensitivity, the presence of the cosmid enabled the flies to perform better than wild type in the sensitivity assay. Not only did a higher percentage of *cos34;* pbl^{p3} larvae survive to adulthood, but they were apparently immune to 20 and 25 Gy of irradiation. This provided further evidence that PBL may play a protective role against the damage induced by x-irradiation. However, it must be said that these experiments were highly variable. The significant degree of variation that was observed was most likely due to difficulties in controlling the experiments. An example of this was the occasional bacterial infection of the

fly food into which the larvae were placed. Such infections were generally observed in vials from which a lower than expected number of adult flies emerged. In addition to this, it was difficult to decide whether a fly had actually survived to adulthood. Many of the survivors, particularly in the pbl^{p3} samples, appeared to be severely unwell and died within a day of eclosing. For this reason it is likely that the survival values for pbl^{p3} samples presented here are overestimates, and that the hypersensitivity of pbl^{p3} is substantially more significant. It is therefore suggested that future studies examining larval sensitivity look not only at the number of adults which eclose, but also score the length of time that adult flies survive, and the percentage of developmental abnormalities. A detailed analysis of the reproductive ability of surviving flies is also suggested, as most pbl^{p3} surviving flies appeared to be sterile. Therefore, although the results presented in this thesis represent a preliminary investigation into the possible role of *pbl* in DNA damage sensing and repair, the consistent poor survival of pbl^{p3} and the apparent immunity of *cos34;* pbl^{p3} flies to two doses of irradiation, strongly implicate *pbl* in a DNA damage response pathway.

In an attempt to determine the cellular basis behind the apparent hypersensitivity of pbl^{p3}, a variety of molecular techniques were employed. pbl^{p3} mutant larvae were found to detect the DNA damage and arrest the cell cycle like wild type, presumably in G2 phase. They were found to repair their DNA as judged by measuring the levels of γ–H2AX. They were also found to re-enter the cell cycle after repair at the appropriate time. They were not found to have a significantly higher level of cell death than wild type after irradiation, and were deemed to be capable of replenishing cells lost to apoptosis on the basis of their completion of development to late pupal stages. So exactly why are they hypersensitive to x-irradiation? There are two possibilities; either they have a defect that is too small to detect using the current methods available, or the sensitivity is due to a specific tissue not tested in this study. It is indeed feasible that even a small difference in repair ability could lead to the hypersensitivity observed, the detection of which, in the context of the whole organism, would be impossible. Especially if, for some reason, this difference was limited to a particular tissue type. To overcome these problems, it may be better to utilise the relatively simpler cell culture system. It has recently been shown that, through the use of dsRNA targeted to the *pbl* transcript, PBL function can be specifically destroyed, resulting in the formation of multinucleate cells (C. McCleod, pers comm). Therefore, not only is cell culture a simpler system, but PBL function can be completely abolished through the use of double stranded RNA. This is an impossibility in the context of a whole organism, as the animal would not survive past embryogenesis without *pbl* function. Cells treated with *pbl* dsRNA

could therefore be irradiated, and their ability to repair DNA damage examined using the anti-γ–H2AX antibody.

Another possible future direction in the attempt to understand the molecular basis behind the hypersensitivity of pbl^{p3} larvae, is the use of genetic analysis. The pbl^{p3} mutation could be combined with other mutations in known DNA damage response and repair pathways, and the sensitivity of these double mutants analysed. The use of genetic analysis in this way could point to the exact molecular pathway that PBL could be part of in the response to DNA damage.

In conclusion, although pbl^{p3} larvae were found consistently to be hypersensitive to irradiation, the exact cellular mechanism behind this sensitivity remains unresolved. It appears as though *pbl* may play a protective role against the damage caused by x-irradiation. However, the difference between pbl^{p3} larvae and wild type is either too small to be detected with the current methods available, or for some unknown reason the sensitivity is due to a specific tissue not tested in this study. Considering that the processes of DNA damage response and repair are general cellular mechanisms, it seems unlikely that *pbl* would only play a role in one particular cell type. It is therefore more likely that the difference between pbl^{p3} larvae and wild type is small and has remained undetected in this study. It is indeed entirely feasible that even a small difference in the ability to repair damage could explain the increase in sensitivity observed. Considering the general large scale of the responses studied here, it is likely that any small difference would go unnoticed. The relatively simpler cell culture system should therefore be pursued in future experiments as a means to define the molecular role that PBL plays in the DNA damage response and repair pathway.

Chapter 7: Final Discussion

7:1 PBL is a Rho GEF that also contains BRCT domains

The PBL protein is required for cytokinesis in *Drosophila*. Through its DH and PH domains, PBL is known to activate Rho, leading to both the formation and correct function of the contractile ring (Prokopenko *et al.*, 1999). However, in addition to these cytoplasmic Rho GEF domains, PBL also contains two highly conserved nuclear BRCT domains, and a third conserved region, named the RadECl region, found otherwise in nuclear proteins. The presence of such domains within a Rho GEF protein is both unique and intriguing in that it could enable PBL to play a dual role in both cytokinesis and DNA repair, perhaps providing a novel mechanism by which the sensing of DNA damage and cell cycle control are linked. For this reason, a potential nuclear role for PBL was examined in this thesis.

7:2 The importance of sequestering PBL to the nucleus

In an attempt to determine the importance of nuclear localisation, the consensus bipartite nuclear localisation signal of PBL was specifically mutated with the aim of rendering it functionless. This ΔNLS mutant form of the protein was then expressed in a variety of tissues to examine the consequences of trapping PBL in the cytoplasm, and to determine whether nuclear localisation is important for its role in cytokinesis. The results detailed in this study indicate that nuclear localisation itself is not required for cytokinesis. However, the severe phenotypes that resulted from cytoplasmic expression indicate that sequestering the protein to the nucleus at the appropriate time is highly important for the maintenance of normal cellular processes. These observations supported the idea that nuclear localisation is simply a sequestering mechanism, removing PBL Rho GEF function from the cytoplasm at the appropriate time.

7:3 Is there a separate nuclear role for PBL?

Although the phenotypes caused by the cytoplasmic ΔNLS mutant form of PBL could be caused by deregulated Rho GEF activity in the cytoplasm, nuclear localisation is not the only known way of removing PBL function from the cytoplasm at the appropriate time. Post translational modifications such as degradation or phosphorylation could be used to regulate PBL function in the cytoplasm, while nuclear localisation could be associated with a completely separate nuclear role. Indeed, although wild type PBL expressed in the salivary gland was localised to the nucleus, it was still capable of affecting the cytoplasm, suggesting that in this non-cytokinetic tissue, nuclear localisation is not enough to suppress its activity. The presence of two BRCT domains also lent support to a separate nuclear role. Why would a protein whose only function is in the cytoplasm contain two conserved nuclear domains?

7:4 The role of the RadECI/BRCT domains

In an attempt to determine the importance of the RadECI/BRCT domains in the function of PBL, *in vitro* mutagenesis was used to specifically delete these domains from the PBL protein. While removal of these domains did not change the nuclear localisation of the protein, deletion of these domains caused significantly more severe phenotypes than the expression of wild type PBL, highlighting their importance to normal PBL function. In the salivary gland, although apparently nuclear, ΔBRCT PBL was found to severely disrupt the cytoskeleton, with sheets of filamentous actin forming in the cytoplasm. This observation suggested that either ΔBRCT PBL shuttles into the cytoplasm to have this cytoplasmic effect, or it is capable of affecting the cytoskeleton from the nucleus.

Through the use of the heterokaryon model system, both PBL and ΔBRCT PBL were then shown to be capable of shuttling from the nucleus to the cytoplasm. Although this observation enables an explanation as to how nuclear PBL can have a cytoplasmic effect, it does not resolve whether the nuclear localisation of PBL is used as a sequestering mechanism. Could a protein that shuttles between the nucleus and the cytoplasm use nuclear localisation as a sequestering mechanism? This would indeed be a possibility if the shuttling of wild type PBL were specifically regulated. Rather than just cycling back and forth from

the nucleus to the cytoplasm, the movement of PBL would need to be regulated at specific points in the cell cycle, presumably through its interaction with other proteins.

7:5 A cytoplasmic role for the RadECl/BRCT domains in cytokinesis

The phenotypes observed when the ΔBRCT form of PBL was overexpressed, strongly suggested that these domains play a cytoplasmic role. To examine this possibility, their function was specifically removed from the cytoplasm by combining the ΔNLS mutation with the ΔBRCT deletion. In line with a potential cytoplasmic role for these domains, trapping this deleted form of PBL in the cytoplasm was found to cause the most severe of all of the phenotypes generated in this study. While the cytoplasmic ΔNLS form of PBL was shown to be able to completely rescue cytokinesis in a *pbl* mutant background, the ΔNLSΔBRCT form lacking RadECl/BRCT domain function in the cytoplasm was unable to activate cytokinesis. This experiment proved that these domains are required in the cytoplasm for cytokinesis, extending the range of functions attributed to these domains. An important experiment that remains to be performed, however, is to remove the RadECl region and two BRCT domains individually to determine if any one domain in particular, or all three, are required for cytokinesis.

While the ΔNLS cytoplasmic form of the protein was only observed to round the cells of the non-cytokinetic salivary gland, the cytoplasmic form lacking the RadECl/BRCT domains was observed to severely disrupt cytoplasmic actin, stimulating the formation of sheets of filamentous actin, a phenotype that was similar to the well documented actin stress fibre phenotype in tissue culture cells. The differences between the ΔNLS and ΔNLSΔBRCT phenotypes and between the wild type PBL and ΔBRCT phenotypes, together with the demonstration that nuclear PBL shuttles through the cytoplasm, suggests that the RadECl/BRCT domains could play an unknown cytoplasmic role in interphase. Given the severe disruption to the actin structure that was observed, it is possible that this role involves maintaining the cytoskeletal structure itself. A direct role in cytoskeletal organisation for a nuclear Rho GEF that shuttles through the cytoplasm is a distinct possibility. It should be noted that a role for PBL in the nucleus, such as in transcriptional regulation, which has

secondary consequences on cytoplasmic cytoskeletal structures, cannot be ruled out. However, the weight of evidence favours a cytoplasmic interphase function via nuclear-cytoplasmic shuttling.

7:6 PBL may also play a role in a DNA damage response pathway

Irrespective of the demonstration that the RadECl/BRCT domains are required for cytokinesis, the possibility remained that PBL could also play a role in DNA repair. The apparent hypersensitivity of pbl^{p3} larvae to x-irradiation supports this possibility. Not only were pbl^{p3} larvae hypersensitive to 20 and 25 Gy of irradiation, but the introduction of the cosmid carrying the entire *pbl* gene completely rescued this sensitivity. Surprisingly, these rescued flies performed even better than wild type, and were apparently immune to both 20 and 25 Gy of irradiation. Although these experiments cannot be considered conclusive, owing to the variability in the survival assay itself, they strongly implicate PBL in a DNA damage response or repair pathway. However, initial attempts to characterise the cellular basis of this sensitivity were not successful. Perhaps the sensitivity is due to a small difference in some aspect of the damage response pathway, or perhaps the sensitivity is limited to a specific tissue that was not examined in this study. Rather than test every single tissue type in the *Drosophila* larva, it is suggested that the relatively simpler cell culture system be used in future experiments to track down the molecular role. Through the use of dsRNA targeted to the *pbl* transcript, PBL function can be completely abolished in this system. The sensitivity of pbl^{p3} mutant larvae to other mutagens should also be analysed. Not only may pbl^{p3} mutants show an even greater sensitivity to these, but enhanced sensitivity to one particular mutagen type might help define which repair pathway, if any, PBL is involved in. It is also suggested that new *pbl* mutant alleles be generated for these analyses. Rather than using the pbl^{p3} hypomorphic mutant stock with a mutation within the PH domain of unknown effect, specific regions within the BRCT domains could be targeted through the use of homologous recombination mediated mutation of the genomic *pbl* locus (Rong and Golic, 2000). Such mutations may also enhance the sensitivity of *pbl* to irradiation and enable the specific regions of the protein responsible for this sensitivity to be further characterised.

The ability of PBL to play a role in both cytokinesis and the response to DNA damage suggests the possibility that PBL could provide a link between the DNA damage response pathway and the cell cycle. In response to DNA damage, the BRCT domains may associate with DNA repair type proteins, preventing their association with proteins such as the RacGAP, thus preventing cytokinesis until the DNA damage is resolved. PBL could therefore provide an extra control mechanism, preventing cell division before DNA repair is complete. This possibility should therefore be examined further.

7:7 Future directions

The results of this thesis have indicated many new roles for the RadECl/BRCT domains. Not only do they have an as yet undefined role in the cytoplasm and/or nucleus during interphase, they are also essential for cytokinesis. So far, however, we have no clear picture of the molecular nature of these roles. It has been shown that the RadECl/BRCT domains are required for cytokinesis, but it is not known exactly what they do. The generation of more specific deletions within these domains will enable the precise determination of which regions are important for cytokinesis. However, in order to understand the molecular role that they play, a range of different genetic and biochemical techniques should be employed.

The yeast 2-hybrid system using the RadECl/BRCT domains as bait has already identified a *Drosophila* RacGAP as an interactor with these domains, shedding some light on their possible molecular role in cytokinesis (Somers and Saint, in preparation). The murine and nematode homologues of *Drosophila* RacGAP have been shown to be required for cytokinesis (Jantsch-Plunger *et al.*, 2000; Hirose *et al.*, 2001). Despite the fact that the Rac proteins of *Drosophila* have not been shown to be required for cytokinesis (Harden *et al.*, 1995; Hakeda-Suzuki *et al.*, 2002; Ng *et al.*, 2002), this does not rule out the possibility that Rac needs to be downregulated for cytokinesis to proceed normally. Thus it is entirely feasible that the interaction of PBL with this RacGAP enables precise control of the down regulation of Rac with the simultaneous up regulation of Rho, leading to correct formation and function of the contractile ring which divides the cell in two. This possibility is currently being examined.

Considering the potentially highly significant nature of the yeast 2-hybrid interactor already analysed, this technique should be employed to chase down other proteins that interact with PBL as a means of understanding its complicated roles. Co-immunoprecipitation experiments could also be used in conjunction with a yeast 2-hybrid assay to test the specific regions of the PBL protein responsible for any interaction, in addition to testing known cytokinetic proteins for their interaction. Both yeast 2-hybrid and co-immunoprecipitation assays could also prove useful in tracking down the molecular role that PBL may play in DNA repair, through the isolation of known DNA damage response or repair proteins as interactors. It is also entirely possible that PBL may only interact with components of DNA damage repair pathways in response to DNA damage itself. It is therefore also suggested that co-immunoprecipitation experiments be performed using extracts from irradiated tissues as well as those prepared from non-irradiated samples.

In addition to *in vitro* and *in vivo* biochemical techniques, further genetic analysis could prove highly useful. The rough eye phenotypes generated by the expression of the mutant constructs generated in this study could be used as the basis for further, saturating genetic screens as a means of identifying more interactors. Indeed, with the release of the complete *Drosophila* genome sequence, such an analysis should prove highly productive, enhancing our understanding of PBL function. In addition to dominant modifier screens, genetic analysis could be used in the x-ray sensitivity assay. Known mutants in the various pathways used in the detection and repair of DNA damage could be introduced into the pbl^{p3} or another *pbl* mutant allele background. By manipulating the genetic background of the *pbl* mutants in this way, and analysing their sensitivity to irradiation, PBL may be shown to be involved in one particular DNA damage response or repair pathway.

7:8 Final conclusions

The results of this thesis have indicated that PBL is a Rho GEF protein that shuttles between the nucleus and the cytoplasm, explaining how nuclear PBL can influence cytoplasmic structure. While the nuclear localisation of PBL was shown to be non-essential for cytokinesis, sequestering the protein to the nucleus at the appropriate time was found to be highly important for the maintenance of normal cellular processes. The PBL RadECl/BRCT domains were also found to be required in the cytoplasm for cytokinesis. This was a novel and exciting finding, extending the range of functions attributed to these domains beyond DNA damage response to include cytokinesis.

In addition to its role in cytokinesis, the phenotypes observed when PBL and its mutant forms were expressed in non-cytokinetic tissues suggested a novel cytoplasmic and/or nuclear role for PBL in interphase. In line with the documented role for BRCT domains, preliminary evidence also suggested that PBL may play a role in the DNA damage response pathway. Thus, rather than being a simple Rho GEF that activates Rho in the cytoplasm through its DH/PH domains, PBL appears to be a multifunctional protein that utilises different conserved domains for its diverse cellular roles.

References

Abbott, D. W., Thompson, M. E., Robinson-Benion, C., Tomlinson, G., Jensen, R. A. and Holt, J. T. (1999). *BRCA1* expression restores radiation resistance in *BRCA1*-defective cancer cells through enhancement of transcription-coupled DNA repair. *Journal of Biological Chemistry* **274**: 18808-12.

Abe, H., Obinata, T., Minamide, L. S. and Bamburg, J. R. (1996). *Xenopus laevis* actin-depolymerizing factor/cofilin: a phosphorylation-regulated protein essential for development. *Journal of Cell Biology* **132**: 871-885.

Adam, J. C., Pringle, J. R. and Peifer, M. (2000). Evidence for functional differentiation among Drosophila septins in cytokinesis and cellularization. *Molecular Biology of the Cell* **11**: 3123-35.

Adams, R. R., Tavares, A. A., Salzberg, A., Bellen, H. J. and Glover, D. M. (1998). *pavarotti* encodes a kinesin-like protein required to organize the central spindle and contractile ring for cytokinesis. *Genes and Development* **12**: 1483-94.

Afshar, K., Stuart, B. and Wasserman, S. A. (2000). Functional analysis of the Drosophila diaphanous FH protein in early embryonic development. *Development* **127**: 1887-97.

Althaus, F. R. and Richter, C. (1987). ADP-ribosylation of proteins. Enzymology and biological significance. *Mol. Biol. Biochem. Biophys.* **37**: 1-237.

Amano, M., Ito, M., Kimura, K., Fukata, Y., Chihara, K., Nakano, T., Matsuura, Y. and Kaibuchi, K. (1996). Phosphorylation and activation of myosin by Rho-associated kinase (Rho-kinase). *Journal of Biological Chemistry* **271**: 20246-9.

Anderson, L., Henderson, C. and Adachi, Y. (2001). Phosphorylation and rapid relocalization of 53BP1 to nuclear foci upon DNA damage. *Molecular and Cellular Biology* **21**: 1719-29.

Anderson, S. F., Schlegel, B. P., Nakajima, T., Wolpin, E. S. and Parvin, J. D. (1998). BRCA1 protein is linked to the RNA polymerase II holoenzyme complex via RNA helicase A. *Nature Genetics* **19**: 254-6.

Araki, H., Leem, S. H., Phongdara, A. and Sugino, A. (1995). Dpb11, which interacts with DNA polymerase II(ε) in *Saccharomyces cerevisiae*, has a dual role in S-phase progression and at a cell cycle checkpoint. *Proceedings of the National Academy of Sciences of the United States of America* **92**: 11791-11795.

Ausubel, S. F., Brent, R. E., Kingston, R. E., Moore, D., Seidman, J. G., Smith, J. A. and Struhl, K. (1994). Current Protocols in Molecular Biology. New York: WILEY.

Bamburg, J. R. (1999). Proteins of the ADF/cofilin family: essential regulators of actin dynamics. *Annual Review of Cell and Developmental Biology* **15**: 185-230.

Barrett, K., Leptin, M. and Settleman, J. (1997). The Rho GTPase and a putative RhoGEF mediate a signaling pathway for the cell shape changes in Drosophila gastrulation. *Cell* **91**: 905-15.

Bashaw, G. J., Hu, H., Nobes, C. D. and Goodman, C. S. (2001). A novel Dbl family RhoGEF promotes Rho-dependent axon attraction to the central nervous system midline in *Drosophila* and overcomes Robo repulsion. *The Journal of Cell Biology* **155**: 1117-1122.

Benlali, A., Draskovic, I., Hazelett, D. J. and Treisman, J. E. (2000). *act up* controls actin polymerization to alter cell shape and restrict Hedgehog signaling in the Drosophila eye disc. *Cell* **101**: 271-81.

Bennett, M. K., Garcia, A. J., Elferink, L. A., Peterson, K., Fleming, A. M., Hazuka, C. D. and Scheller, R. H. (1993). The syntaxin family of vesicular transport receptors. *Cell* **74**: 863-873.

Bergeret, E., Pignot-Paintrand, I., Guichard, A., Raymond, K., Fauvarque, M. O., Cazemajor, M. and Griffin-Shea, R. (2001). RotundRacGAP functions with Ras during spermatogenesis and retinal differentiation in Drosophila melanogaster. *Molecular and Cellular Biology* **21**: 6280-91.

Billuart, P., Winter, C. G., Maresh, A., Zhao, X. and Luo, L. (2001). Regulating axon branch stability. The role of p190 RhoGAP in repressing a retraction signaling pathway. *Cell* **107**: 195-207.

Bishop, A. L. and Hall, A. (2000). Rho GTPases and their effector proteins. *Biochemical Journal* **348 (2)**: 241-55.

Bluemink, J. G. and deLaat, S. W. (1973). New membrane formation during cytokinesis in normal and cytochalasin B-treated eggs of *Xenopus laevis*. I. Electron microscope observations. *Journal of Cell Biology* **59**: 89-108.

Bonaccorsi, S., Giansanti, M. G. and Gatti, M. (1998). Spindle self-organization and cytokinesis during male meiosis in asterless mutants of Drosophila melanogaster. *Journal of Cell Biology* **142**: 751-61.

Bork, P., Hofmann, K., Bucher, P., Neuwald, A. F., Altschul, S. F. and Koonin, E. V. (1997). A superfamily of conserved domains in DNA damage-responsive cell cycle checkpoint proteins. *FASEB Journal* **11**: 68-76.

Bowerman, B. and Severson, A. F. (1999). Cell division: plant-like properties of animal cell cytokinesis. *Current Biology* **9**: R658-60.

Boyd, J. B., Golino, M. D., Nguyen, T. D. and Green, M. M. (1976). Isolation and characterization of X-linked mutants of *Drosophila melanogaster* which are sensitive to mutagens. *Genetics* **84**: 485-506.

Boyd, J. B., Mason, J. M., Yakamoto, A. H., Brodberg, R. K., Banga, S. S. and Sakaguchi, K. (1987). A genetic and molecular analysis of DNA repair in Drosophila. *Journal of Cell Science* **6**: 39-60.

Boyd, J. B. and Setlow, R. B. (1976). Characterization of postreplication repair in mutagen-sensitive strains of *Drosophila melanogaster*. *Genetics* **84**: 507-526.

Brand, A. H. and Perrimon, N. (1993). Targeted gene expression as a means of altering cell fates and generating dominant phenotypes. *Development* **118**: 401-415.

Brodsky, M. H., Sekelsky, J. J., Tsang, G., Hawley, R. S. and Rubin, G. M. (2000). *mus304* encodes a novel DNA damage checkpoint protein required during *Drosophila* development. *Genes and Development.* **14**: 666-678.

Brown, T. C. and Boyd, J. B. (1981). Postreplication repair-defective mutants of *Drosophila melanogaster* fall into two classes. *Mol. Gen. Genet.* **183**: 356-362.

Burgess, R. W., Deitcher, D. L. and Schwarz, T. L. (1997). The synaptic protein syntaxin1 is required for cellularization of Drosophila embryos. *Journal of Cell Biology* **138**: 861-75.

Caldecott, K. W., Aoufouchi, S., Johnson, P. and Shall, S. (1996). XRCC1 polypeptide interacts with DNA polymerase β and possibly poly(ADP-ribose) polymerase, and DNA ligase III is a novel molecular "nick sensor" *in vitro*. *Nucleic Acids Research* **24**: 4387-4394.

Caldecott, K. W., McKeown, C. K., Tucker, J. D., Ljungquist, S. and Thompson, L. H. (1994). An interaction between the mammalian DNA repair protein XRCC1 and DNA ligase III. *Molecular and Cellular Biology* **14**: 68-76.

Caldecott, K. W., Tucker, J. D., Stanker, L. H. and Thompson, L. H. (1995). Characterisation of the XRCC1-DNA ligase III complex *in vitro* and its absence from mutant hamster cells. *Nucleic Acids Research* **23**: 4836-4843.

Callebaut, I. and Mornon, J. P. (1997). From BRCA1 to RAP1: A widespread BRCT module closely associated with DNA repair. *FEBS Lett.* **400**: 25-30.

Calvi, B. R. and Spradling, A. C. (1999). Chorion gene amplification in *Drosophila*: a model for metazoan origins of DNA replication and S-phase control. *Methods* **18**: 407-417.

Campos, A. R., Rosen, D. R., Robinow, S. N. and White, K. (1987). Molecular analysis of the locus elav in Drosophila melanogaster: a gene whose embryonic expression is neural specific. *EMBO Journal* **6**: 425-431.

Campos-Ortega, J. A. and Hartenstein, V. (1985). The embryonic development of *Drosophila melanogaster*. Berlin: Springer-Verlag.

Cantor, S. B., Bell, D. W., Ganesan, S., Kass, E. M., Drapkin, R., Grossman, S., Wahrer, D. C., Sgroi, D. C., Lane, W. S., Haber, D. A. *et al.,*. (2001). BACH1, a novel helicase-like protein, interacts directly with BRCA1 and contributes to its DNA repair function. *Cell* **105**: 149-60.

Cao, L. G. and Wang, Y. L. (1990). Mechanism of the formation of contractile ring in dividing cultured animal cells. II. Cortical movement of microinjected actin filaments. *Journal of Cell Biology* **111**: 1905-11.

Cao, L. G. and Wang, Y. L. (1996). Signals from the spindle midzone are required for the stimulation of cytokinesis in cultured epithelial cells. *Molecular Biology of the Cell* **7**: 225-32.

Cappelli, E., Taylor, R., Cevasco, M., Abbondandolo, A., Caldecott, K. and Frosina, G. (1997). Involvement of XRCC1 and DNA ligase III gene products in DNA base excision repair. *Journal of Biological Chemistry* **272**: 23970-23975.

Carmena, M., Riparbelli, M. G., Minestrini, G., Tavares, A. M., Adams, R., Callaini, G. and Glover, D. M. (1998). Drosophila polo kinase is required for cytokinesis. *Journal of Cell Biology* **143**: 659-71.

Castrillon, D. H. and Wasserman, S. A. (1994). Diaphanous is required for cytokinesis in Drosophila and shares domains of similarity with the products of the limb deformity gene. *Development* **120**: 3367-77.

Chang, F., Drubin, D. and Nurse, P. (1997). cdc12p, a protein required for cytokinesis in fission yeast, is a component of the cell division ring and interacts with profilin. *Journal of Cell Biology* **137**: 169-82.

Chapman, M. S. and Verma, I. M. (1996). Transcriptional activation by BRCA1. *Nature* **382**: 678-679.

Cherfils, J. and Chardin, P. (1999). GEFs: structural basis for their activation of small GTP-binding proteins. *Trends in Biochemical Sciences* **24**: 306-311.

Cortez, D., Wang, Y., Qin, J. and Elledge, S. J. (1999). Requirement of ATM-dependent phosphorylation of BRCA1 in the DNA damage response to double-strand breaks. *Science* **286**: 1162-1166.

Couch, F. J. and Weber, B. L. (1996). Mutations and polymorphisms in the familial early-onset breast cancer (BRCA1) gene. Breast Cancer Information Core. *Human Mutation* **8**: 8-18.

Crawford, J. M., Harden, N., Leung, T., Lim, L. and Kiehart, D. P. (1998). Cellularization in Drosophila melanogaster is disrupted by the inhibition of rho activity and the activation of Cdc42 function. *Developmental Biology* **204**: 151-64.

Critchlow, S. E., Bowater, R. P. and Jackson, S. P. (1997). Mammalian DNA double-strand break repair protein XRCC4 interacts with DNA ligase IV. *Current Biology* **7**: 588-598.

De Murcia, G. and Menissier-De Murcia, J. (1994). Poly(ADP-ribose) polymerase: a molecular nick-sensor. *Trends in Biochemical Sciences* **19**: 172-176.

Devore, J. J., Conrad, G. W. and Rappaport, R. (1989). A model for astral stimulation of cytokinesis in animal cells. *Journal of Cell Biology* **109**: 2225-32.

Di Cunto, F., Imarisio, S., Hirsch, E., Broccoli, V., Bulfone, A., Migheli, A., Atzori, C., Turco, E., Triolo, R., Dotto, G. P. *et al.,*. (2000). Defective neurogenesis in citron kinase knockout mice by altered cytokinesis and massive apoptosis. *Neuron* **28**: 115-27.

Dickson, B. J. (2001). Rho GTPases in growth cone guidance. *Current Opinion in Neurobiology* **11**: 103-110.

Drechsel, D. N., Hyman, A. A., Hall, A. and Glotzer, M. (1997). A requirement for Rho and Cdc42 during cytokinesis in Xenopus embryos. *Current Biology* **7**: 12-23.

Du, W. and Dyson, N. (1999). The role of RBF in the introduction of G1 regulation during *Drosophila* embryogenesis. *EMBO Journal* **18**: 916-925.

Du, W., Vidal, M., Xie, J. E. and Dyson, N. (1996). RBF, a novel RB-related gene that regulates E2F activity and interacts with cyclin E in Drosophila. *Genes and Development* **10**: 1206-1218.

Dulic, A., Bates, P. A., Zhang, X., Martin, S. R., Freemont, P. S., Lindahl, T. and Barnes, D. E. (2001). BRCT domain interactions in the heterodimeric DNA repair protein XRCC1-DNA ligase III. *Biochemistry* **40**: 5906-13.

Dumontier, M., Hocht, P., Mintert, U. and Faix, J. (2000). Rac1 GTPases control filopodia formation, cell motility, endocytosis, cytokinesis and development in Dictyostelium. *Journal of Cell Science* **113 (12)**: 2253-65.

Dusenbery, R. L. and Smith, P. D. (1996). Cellular responses to DNA damage in *Drosophila melanogaster*. *Mutation Research* **364**: 133-145.

Dutartre, H., Davoust, J., Gorvel, J. P. and Chavrier, P. (1996). Cytokinesis arrest and redistribution of actin-cytoskeleton regulatory components in cells expressing the Rho GTPase CDC42Hs. *Journal of Cell Science* **109 (2)**: 367-77.

Earnshaw, W. C. and Cooke, C. A. (1991). Analysis of the distribution of the INCENPs throughout mitosis reveals the existence of a pathway of structural changes in the chromosomes during metaphase and early events in cleavage furrow formation. *Journal of Cell Science* **98 (4)**: 443-61.

Eckley, D. M., Ainsztein, A. M., Mackay, A. M., Goldberg, I. G. and Earnshaw, W. C. (1997). Chromosomal proteins and cytokinesis: patterns of cleavage furrow formation and inner centromere protein positioning in mitotic heterokaryons and mid-anaphase cells. *Journal of Cell Biology* **136**: 1169-83.

Eda, M., Yonemura, S., Kato, T., Watanabe, N., Ishizaki, T., Madaule, P. and Narumiya, S. (2001). Rho-dependent transfer of Citron-kinase to the cleavage furrow of dividing cells. *Journal of Cell Science* **114**: 3273-84.

Edgar, B. A. (1995). Diversification of cell cycle controls in developing embryos. *Current Opinion in Cell Biology.* **7**: 815-824.

Edgar, B. A. and O'Farrell, P. H. (1990). The three postblastoderm cell cycles of Drosophila embryogenesis are regulated in G2 by *string*. *Cell* **62**: 469-80.

Elledge, S. J. (1996). Cell cycle checkpoints: preventing an identity crisis. *Science* **274**: 1664-1672.

Ellis, M. C., O'Neill, E. M. and Rubin, G. M. (1993). Expression of *Drosophila* glass protein and evidence for negative regulation of its activity in non-neuronal cells by another DNA binding protein. *Development* **119**: 855-865.

Evangelista, M., Blundell, K., Longtine, M. S., Chow, C. J., Adames, N., Pringle, J. R., Peter, M. and Boone, C. (1997). Bni1p, a yeast formin linking cdc42p and the actin cytoskeleton during polarized morphogenesis. *Science* **276**: 118-22.

Fan, X. C. and Steitz, J. A. (1998). Overexpression of HuR, a nuclear-cytoplasmic shuttling protein, increases the *in vivo* stability of ARE-containing mRNAs. *EMBO Journal* **17**: 3448-3460.

Fehon, R. G., Oren, T., LaJeunesse, D. R., Melby, T. E. and McCartney, B. M. (1997). Isolation of mutations in the Drosophila homologues of the human Neurofibromatosis 2 and yeast CDC42 genes using a simple and efficient reverse-genetic method. *Genetics* **146**: 245-52.

Field, C. M., al-Awar, O., Rosenblatt, J., Wong, M. L., Alberts, B. and Mitchison, T. J. (1996). A purified Drosophila septin complex forms filaments and exhibits GTPase activity. *Journal of Cell Biology* **133**: 605-16.

Field, C. M. and Alberts, B. M. (1995). Anillin, a contractile ring protein that cycles from the nucleus to the cell cortex. *Journal of Cell Biology* **131**: 165-78.

Fishkind, D. J. and Wang, Y. L. (1993). Orientation and three-dimensional organization of actin filaments in dividing cultured cells. *Journal of Cell Biology* **123**: 837-48.

Foe, V. E. (1989). Mitotic domains reveal early commitment of cells in Drosophila embryos. *Development* **107**: 1-22.

Fogarty, P., Kalpin, R. F. and Sullivan, W. (1994). The *Drosophila* maternal-effect mutation *grapes* causes a metaphase arrest at nuclear cycle 13. *Development* **120**: 2131-2142.

Friedman, L. S., Ostermeyer, E. A., Szabo, C. I., Dowd, P., Lynch, E. D., Rowell, S. E. and King, M.-C. (1994). Confirmation of *BRCA1* by analysis of germline mutations linked to breast and ovarian cancer in ten families. *Nature Genetics* **8**: 399-404.

Gatti, M., Smith, D. A. and Baker, B. S. (1983). A gene controlling condensation of heterochromatin in *Drosophila melanogaster*. *Science* **221**: 83-85.

Genova, J. L., Jong, S., Camp, J. T. and Fehon, R. G. (2000). Functional analysis of Cdc42 in actin filament assembly, epithelial morphogenesis, and cell signaling during Drosophila development. *Developmental Biology* **221**: 181-94.

Giansanti, M. G., Bonaccorsi, S., Williams, B., Williams, E. V., Santolamazza, C., Goldberg, M. L. and Gatti, M. (1998). Cooperative interactions between the central spindle and the contractile ring during Drosophila cytokinesis. *Genes and Development* **12**: 396-410.

Giansanti, M. G., Gatti, M. and Bonaccorsi, S. (2001). The role of centrosomes and astral microtubules during asymmetric division of Drosophila neuroblasts. *Development* **128**: 1137-45.

Giet, R. and Glover, D. M. (2001). Drosophila aurora B kinase is required for histone H3 phosphorylation and condensin recruitment during chromosome condensation and to organize the central spindle during cytokinesis. *Journal of Cell Biology* **152**: 669-82.

Glotzer, M. (1997a). Cytokinesis. *Current Biology* **7**: R274-R276.

Glotzer, M. (1997b). The mechanism and control of cytokinesis. *Current Opinion in Cell Biology.* **9**: 815-823.

Glotzer, M. (2001). Animal Cell Cytokinesis. *Annual Review of Cell and Developmental Biology* **17**: 351-386.

Glover, D. M., Leibowitz, M. H., McLean, D. A. and Parry, H. (1995). Mutations in aurora prevent centrosome separation leading to the formation of monopolar spindles. *Cell* **81**: 95-105.

Goto, H., Kosako, H. and Inagaki, M. (2000). Regulation of intermediate filament organization during cytokinesis: possible roles of Rho-associated kinase. *Microscopy Research and Technique* **49**: 173-82.

Goto, H., Kosako, H., Tanabe, K., Yanagida, M., Sakurai, M., Amano, M., Kaibuchi, K. and Inagaki, M. (1998). Phosphorylation of vimentin by Rho-associated kinase at a unique amino-terminal site that is specifically phosphorylated during cytokinesis. *Journal of Biological Chemistry* **273**: 11728-36.

Gowen, L. C., Avrutskaya, A. V., Latour, A. M., Koller, B. H. and Leadon, S. A. (1998). BRCA1 required for transcription-coupled repair of oxidative DNA damage. *Science* **281**: 1009-1012.

Gu, X. and Verma, D. P. (1996). Phragmoplastin, a dynamin-like protein associated with cell plate formation in plants. *EMBO Journal* **15**: 695-704.

Gunsalus, K. C., Bonaccorsi, S., Williams, E. V., Verni, F., Gatti, M. and Goldberg, M. L. (1995). Mutations in *twinstar*, a *Drosophila* gene encoding a cofilin/ADF homologue, result in defects in centrosome migration and cytokinesis. *Journal of Cell Biology* **131**: 1243-59.

Hacker, U. and Perrimon, N. (1998). DRhoGEF2 encodes a member of the Dbl family of oncogenes and controls cell shape changes during gastrulation in Drosophila. *Genes and Development* **12**: 274-84.

Hakeda-Suzuki, S., Ng, J., Tzu, J., Dietzl, G., Sun, Y., Harms, M., Nardine, T., Luo, L. and Dickson, B. J. (2002). Rac function and regulation during *Drosophila* development. *Nature* **416**: 438-442.

Harden, N., Loh, H. Y., Chia, W. and Lim, L. (1995). A dominant inhibitory version of the small GTP-binding protein Rac disrupts cytoskeletal structures and inhibits developmental cell shape changes in *Drosophila*. *Development* **121**: 903-914.

Harden, N., Ricos, M., Ong, Y. M., Chia, W. and Lim, L. (1999). Participation of small GTPases in dorsal closure of the *Drosophila* embryo: distinct roles for Rho subfamily proteins in epithelial morphogenesis. *Journal of Cell Science* **112**: 273-284.

Harris, S. D., Hamer, L., Sharpless, K. E. and Hamer, J. E. (1997). The *Aspergillus nidulans* sepA gene encodes an FH1/2 protein involved in cytokinesis and the maintenance of cellular polarity. *EMBO Journal* **16**: 3474-3483.

Hart, M. J., Eva, A., Zangrilli, D., Aaronson, S. A., Evans, T., Cerione, R. A. and Zheng, Y. (1994). Cellular transformation and guanine nucleotide exchange activity are catalyzed by a common domain on the dbl oncogene product. *Journal of Biological Chemistry* **269**: 62-65.

Hartwell, L. H. and Weinert, T. A. (1989). Checkpoints: controls that ensure the order of cell cycle events. *Science* **246**: 629-634.

Hay, B. A., Wolff, T. and Rubin, G. M. (1994). Expression of baculovirus P35 prevents cell death in Drosophila. *Development* **120**: 2121-2129.

Henderson, D. S. (1999). DNA repair defects and other *mu*stakes in *Drosophila melanogaster*. *Methods* **18**: 377-400.

Henderson, D. S., Bailey, D. A., Sinclair, D. A. R. and Grigliatti, T. A. (1987). Isolation and characterization of second chromosome mutagen-sensitive mutations in *Drosophila melanogaster*. *Mutation Research* **177**: 83-93.

Hendzel, M. J., Wei, Y., Mancini, M. A., Van Hooser, A., Ranalli, T., Brinkley, B. R., Bazett-Jones, D. P. and Allis, C. D. (1997). Mitosis-specific phosphorylation of histone H3 initiates primarily within pericentromeric heterochromatin during G2 and spreads in an ordered fashion coincident with mitotic chromosome condensation. *Chromosoma* **106**: 348-360.

Hicks, M. S., O'Leary, V., Wilkin, M., Bee, S. E., Humphries, M. J. and Baron, M. (2001). DrhoGEF3 encodes a new Drosophila DH domain protein that exhibits a highly dynamic embryonic expression pattern. *Development Genes and Evolution* **211**: 263-267.

Hime, G. and Saint, R. (1992). Zygotic expression of the *pebble* locus is required for cytokinesis during the postblastoderm mitoses of *Drosophila*. *Development* **114**: 165-171.

Hinshaw, J. E. and Schmid, S. L. (1995). Dynamin self-assembles into rings suggesting a mechanism for coated vesicle budding. *Nature* **374**: 190-192.

Hirose, K., Kawashima, T., Iwamoto, I., Nosaka, T. and Kitamura, T. (2001). MgcRacGAP is involved in cytokinesis through associating with mitotic spindle and midbody. *Journal of Biological Chemistry* **276**: 5821-5828.

Holt, J. T., Thompson, M. E., Szabo, C., Robinson-Benion, C., Arteaga, C. L., King, M.-C. and Jensen, R. A. (1996). Growth retardation and tumour inhibition by *BRCA1*. *Nature Genetics* **12**: 298-302.

Honda, Y., Tojo, M., Matsuzaki, K., Anan, T., Matsumoto, M., Ando, M., Saya, H. and Nakao, M. (2002). Cooperation of HECT-domain ubiquitin ligase hHYD and DNA topoisomerase II-binding protein for DNA damage response. *Journal of Biological Chemistry* **277**: 3599-3605.

Hu, Y. F., Hao, Z. L. and Li, R. (1999). Chromatin remodeling and activation of chromosomal DNA replication by an acidic transcriptional activation domain from BRCA1. *Genes and Development* **13**: 637-642.

Imamura, H., Tanaka, K., Hihara, T., Umikawa, M., Kamei, T., Takahashi, K., Sasaki, T. and Takai, Y. (1997). Bni1p and Bnr1p: downstream targets of the Rho family small G-proteins which interact with profilin and regulate actin cytoskeleton in Saccharomyces cerevisiae. *EMBO Journal* **16**: 2745-55.

Iwabuchi, K., Bartel, P. L., Li, B., Marraccino, R. and Fields, S. (1994). Two cellular proteins that bind to wild-type but not mutant p53. *Proceedings of the National Academy of Sciences of the United States of America* **91**: 6098-6102.

Iwabuchi, K., Li, B., Massa, H. F., Trask, B. J., Date, T. and Fields, S. (1998). Stimulation of p53-mediated transcriptional activation by the p53-binding proteins, 53BP1 and 53BP2. *Journal of Biological Chemistry* **273**: 26061-26068.

Jantsch-Plunger, V. and Glotzer, M. (1999). Depletion of syntaxins in the early Caenorhabditis elegans embryo reveals a role for membrane fusion events in cytokinesis. *Current Biology* **9**: 738-45.

Jantsch-Plunger, V., Gonczy, P., Romano, A., Schnabel, H., Hamill, D., Schnabel, R., Hyman, A. A. and Glotzer, M. (2000). CYK-4: A Rho family gtpase activating protein (GAP) required for central spindle formation and cytokinesis. *Journal of Cell Biology* **149**: 1391-1404.

Jordan, P. and Karess, R. (1997). Myosin Light Chain-activating phosphorylation sites are required for oogenesis in Drosophila. *Journal of Cell Biology* **139**: 1805-1819.

Jurgens, G., Wieschaus, E., Nusslein-Volhard, C. and Kluding, H. (1984). Mutations affecting the pattern of the larval cuticle in *Drosophila melanogaster*. *Roux's Archives of Developmental Biology* **193**: 283-295.

Kaitna, S., Mendoza, M., Jantsch-Plunger, V. and Glotzer, M. (2000). Incenp and an aurora-like kinase form a complex essential for chromosome segregation and efficient completion of cytokinesis. *Current Biology* **10**: 1172-81.

Kerr, P. and Ashworth, A. (2001). New complexities for BRCA1 and BRCA2. *Current Biology* **11**: R668-R676.

Khodjakov, A. and Rieder, C. L. (2001). Centrosomes enhance the fidelity of cytokinesis in vertebrates and are required for cell cycle progression. *Journal of Cell Biology* **153**: 237-242.

Kimura, K., Ito, M., Amano, M., Chihara, K., Fukata, Y., Nakafuku, M., Yamamori, B., Feng, J., Nakano, T., Okawa, K. *et al.*,. (1996). Regulation of myosin phosphatase by Rho and Rho-associated kinase (Rho-kinase). *Science* **273**: 245-8.

Kimura, K., Tsuji, T., Takada, Y., Miki, T. and Narumiya, S. (2000). Accumulation of GTP-bound RhoA during cytokinesis and a critical role of ECT2 in this accumulation. *The Journal of Biological Chemistry* **275**: 17233-17236.

Kinoshita, M., Kumar, S., Mizoguchi, A., Ide, C., Kinoshita, A., Haraguchi, T., Hiraoka, Y. and Noda, M. (1997). Nedd5, a mammalian septin, is a novel cytoskeletal component interacting with actin-based structures. *Genes and Development* **11**: 1535-1547.

Kishi, K., Sasaki, T., Kuroda, S., Itoh, T. and Takai, Y. (1993). Regulation of cytoplasmic division of Xenopus embryo by rho p21 and its inhibitory GDP/GTP exchange protein (rho GDI). *Journal of Cell Biology* **120**: 1187-95.

Knoblich, J. A. and Lehner, C. F. (1993). Synergistic action of Drosophila cyclins A and B during the G2-M transition. *EMBO Journal* **12**: 65-74.

Komatsu, S., Yano, T., Shibata, M., Tuft, R. A. and Ikebe, M. (2000). Effects of the regulatory light chain phosphorylation of myosin II on mitosis and cytokinesis of mammalian cells. *Journal of Biological Chemistry* **275**: 34512-20.

Koonin, E. V., Altschul, S. F. and Bork, P. (1996). BRCA1 protein products: functional motifs. *Nature Genetics* **13**: 266-268.

Kosako, H., Amano, M., Yanagida, M., Tanabe, K., Nishi, Y., Kaibuchi, K. and Inagaki, M. (1997). Phosphorylation of glial fibrillary acidic protein at the same sites by cleavage furrow kinase and Rho-associated kinase. *Journal of Biological Chemistry* **272**: 10333-6.

Kosako, H., Goto, H., Yanagida, M., Matsuzawa, K., Fujita, M., Tomono, Y., Okigaki, T., Odai, H., Kaibuchi, K. and Inagaki, M. (1999). Specific accumulation of Rho-associated kinase at the cleavage furrow during cytokinesis: cleavage furrow-specific phosphorylation of intermediate filaments. *Oncogene* **18**: 2783-8.

Kosako, H., Yoshida, T., Matsumura, F., Ishizaki, T., Narumiya, S. and Inagaki, M. (2000). Rho-kinase/ROCK is involved in cytokinesis through the phosphorylation of myosin light chain and not ezrin/radixin/moesin proteins at the cleavage furrow. *Oncogene* **19**: 6059-6064.

Kubota, Y., Nash, R. A., Klungland, A., Schar, P., Barnes, D. E. and Lindahl, T. (1996). Reconstitution of DNA base excision repair with purified human proteins: interaction between DNA polymerase beta and the XRCC1 protein. *EMBO Journal* **15**: 6662-6670.

Lamarche, N. and Hall, A. (1994). GAPs for rho-related GTPases. *Trends in Genetics* **10**: 436-440.

Larochelle, D. A., Gerald, N. and De Lozanne, A. (2000). Molecular analysis of racE function in Dictyostelium. *Microscopy Research and Technique* **49**: 145-51.

Larochelle, D. A., Vithalani, K. K. and De-Lozanne, A. (1996). A novel member of the rho family of small GTP-binding proteins is specifically required for cytokinesis. *Journal of Cell Biology* **133**: 1321-9.

Lee, J.-S., Collins, K. M., Brown, A. L., Lee, C.-H. and Chung, J. H. (2000a). hCds1-mediated phosphorylation of BRCA1 regulates the DNA damage response. *Nature* **404**: 201-204.

Lee, T., Winter, C., Marticke, S. S., Lee, A. and Luo, L. (2000b). Essential roles of Drosophila RhoA in the regulation of neuroblast proliferation and dendritic but not axonal morphogenesis. *Neuron* **25**: 307-16.

Lehner, C. F. (1992). The *pebble* gene is required for cytokinesis in *Drosophila*. *Journal of Cell Science* **103**: 1021-1030.

Li, S., Chen, P., Subramanian, T., Chinnadurai, G., Tomlinson, G., Osborne, C. K., Sharp, Z. D. and Lee, W. (1999). Binding of CtIP to the BRCT repeats of BRCA1 involved in the transcription regulation of p21 is disrupted upon DNA damage. *Journal of Biological Chemistry* **274**: 11334-11338.

Liu, X., Wang, H., Eberstadt, M., Schnuchel, A., Olejniczak, E. T., Meadows, R. P., Schkeryantz, J. M., Janowick, D. A., Harlan, J. E., Harris, E. A. *et al.*,. (1998). NMR structure and mutagenesis of the N-terminal Dbl homology domain of the nucleotide exchange factor Trio. *Cell* **95**: 269-277.

Longtine, M. S., DeMarini, D. J., Valencik, M. L., Al-Awar, O. S., Fares, H., De Virgilio, C. and Pringle, J. R. (1996). The septins: roles in cytokinesis and other processes. *Current Opinion in Cell Biology* **8**: 106-19.

Longtine, M. S., Fares, H. and Pringle, J. R. (1998). Role of the yeast Gin4p protein kinase in septin assembly and the relationship between septin assembly and septin function. *Journal of Cell Biology* **143**: 719-36.

Ludwig, T., Fisher, P., Ganesan, S. and Efstratiadis, A. (2001). Tumorigenesis in mice carrying a truncating *Brca1* mutation. *Genes and Development* **15**: 1188-93.

Lukowitz, W., Mayer, U. and Jurgens, G. (1996). Cytokinesis in the *Arabidopsis* embryo involves the syntaxin-related KNOLLE gene product. *Cell* **84**: 61-71.

Luo, L., Liao, Y. J., Jan, L. Y. and Jan, Y. N. (1994). Distinct morphogenetic functions of similar small GTPases: Drosophila Drac1 is involved in axonal outgrowth and myoblast fusion. *Genes and Development* **8**: 1787-802.

Mabuchi, I., Hamaguchi, Y., Fujimoto, H., Morii, N., Mishima, M. and Narumiya, S. (1993). A rho-like protein is involved in the organisation of the contractile ring in dividing sand dollar eggs. *Zygote* **1**: 325-31.

Mack, G. and Rattner, J. B. (1993). Centrosome repositioning immediately following karyokinesis and prior to cytokinesis. *Cell Motility and the Cytoskeleton* **26**: 239-247.

Madaule, P., Eda, M., Watanabe, N., Fujisawa, K., Matsuoka, T., Bito, H., Ishizaki, T. and Narumiya, S. (1998). Role of citron kinase as a target of the small GTPase Rho in cytokinesis. *Nature* **394**: 491-4.

Maekawa, M., Ishizaki, T., Boku, S., Watanabe, N., Fujita, A., Iwamatsu, A., Obinata, T., Ohashi, K., Mizuno, K. and Narumiya, S. (1999). Signaling from Rho to the actin cytoskeleton through protein kinases ROCK and LIM-kinase. *Science* **285**: 895-898.

Magie, C. R., Meyer, M. R., Gorsuch, M. S. and Parkhurst, S. M. (1999). Mutations in the Rho1 small GTPase disrupt morphogenesis and segmentation during early Drosophila development. *Development* **126**: 5353-64.

Makiniemi, M., Hillukkala, T., Tuusa, J., Reini, K., Vaara, M., Huang, D., Pospiech, H., Majuri, I., Westerling, T., Makela, T. P. *et al.*,. (2001). BRCT Domain-containing Protein TopBP1 Functions in DNA Replication and Damage Response. *The Journal of Biological Chemistry* **276**: 30399-30406.

Marintchev, A., Robertson, A., Dimitriadis, E. K., Prasad, R., Wilson, S. H. and Mullen, G. P. (2000). Domain specific interaction in the XRCC1-DNA polymerase beta complex. *Nucleic Acids Research* **28**: 2049-59.

Masson, M., Niedergang, C., Schreiber, V., Muller, S., Menissier-De Murcia, J. and De Murcia, G. (1998). XRCC1 Is Specifically Associated with Poly(ADP-Ribose) Polymerase and Negatively Regulates Its Activity following DNA damage. *Molecular and Cellular Biology* **18**: 3563-3571.

McFarlane, R. J., Carr, A. M. and Price, C. (1997). Characterisation of the *Schizosaccharomyces pombe rad4/cut5* mutant phenotypes: dissection of DNA replication and G2 checkpoint control function. *Molecular and General Genetics* **255**: 332-40.

Megraw, T. L., Kao, L. and Kaufman, T. C. (2001). Zygotic development without functional mitotic centrosomes. *Current Biology* **11**: 116-120.

Michael, W. M., Choi, M. and Dreyfuss, G. (1995). A nuclear export signal in hnRNP A1: a signal-mediated, temperature-dependent nuclear protein export pathway. *Cell* **83**: 415-422.

Michael, W. M., Eder, P. S. and Dreyfuss, G. (1997). The K nuclear shuttling domain: a novel signal for nuclear import and nuclear export in the hnRNP K protein. *EMBO Journal* **16**: 3587-3598.

Miki, T., Smith, C. L., Long, J. E., Eva, A. and Fleming, T. P. (1993). Oncogene *ect2* is related to regulators of small GTP-binding proteins. *Nature* **362**: 462-465.

Miyake, T., Hu, Y. F., Yu, D. S. and Li, R. (2000). A functional comparison of BRCA1 C-terminal domains in transcription activation and chromatin remodeling. *Journal of Biological Chemistry* **275**: 40169-73.

Monteiro, A. N., August, A. and Hanafusa, H. (1996). Evidence for a transcriptional activation function of BRCA1 C-terminal region. *Proceedings of the National Academy of Sciences of the United States of America* **93**: 13595-13599.

Moore, J. D. and Endow, S. A. (1996). Kinesin proteins: a phylum of motors for microtubule-based motility. *Bioessays* **18**: 207-19.

Moriyama, K., Iida, K. and Yahara, I. (1996). Phosphorylation of Ser-3 of cofilin regulates its essential function on actin. *Genes Cells* **1**: 73-86.

Moynahan, M. E., Chiu, J. W., Koller, B. H. and Jasin, M. (1999). Brca1 controls homology-directed DNA repair. *Molecular Cell* **4**: 511-518.

Murphy, A. M. and Montell, D. J. (1996). Cell type-specific roles for Cdc42, Rac, and RhoL in Drosophila oogenesis. *Journal of Cell Biology* **133**: 617-30.

Murray, A. W., Solomon, M. J. and Kirschner, M. W. (1989). The role of cyclin synthesis and degradation in the control of maturation promoting factor activity. *Nature* **339**: 280-6.

Nagase, T., Seki, N., Ishikawa, K., Ohira, M., Kawarabayasi, Y., Ohara, O., Tanaka, A., Kotani, H., Miyajima, N. and Nomura, N. (1996). Prediction of the coding sequences of unidentified human genes. VI. The coding sequences of 80 new genes (KIAA0201-KIAA0280) deduced by analysis of cDNA clones from cell line KG-1 and brain. *DNA research* **3**: 321-329.

Nash, R. A., Caldecott, K. W., Barnes, D. E. and Lindahl, T. (1997). XRCC1 protein interacts with one of two distinct forms of DNA ligase III. *Biochemistry* **36**: 5207-5211.

Neish, A. S., Anderson, S. F., Schlegel, B. P., Wei, W. and Parvin, J. D. (1998). Factors associated with the mammalian RNA polymerase II holoenzyme. *Nucleic Acids Research* **26**: 847-853.

Nern, A. and Arkowitz, R. A. (2000). Nucleocytoplasmic shuttling of the Cdc42p exchange factor Cdc24p. *Journal of Cell Biology* **148**: 1115-1122.

Neufeld, T. P. and Rubin, G. M. (1994). The *Drosophila peanut* gene is required for cytokinesis and encodes a protein similar to yeast putative bud neck filament proteins. *Cell* **77**: 371-9.

Newsome, T. P., Schmidt, S., Dietzl, G., Keleman, K., Asling, B., Debant, A. and Dickson, B. J. (2000). Trio combines with dock to regulate Pak activity during photoreceptor axon pathfinding in Drosophila. *Cell* **101**: 283-94.

Ng, J., Nardine, T., Harms, M., Tzu, J., Goldstein, A., Sun, Y., Dietzl, G., Dickson, B. J. and Luo, L. (2002). Rac GTPases control axon growth, guidance and branching. *Nature* **416**: 442-447.

Nicholas, K. B., Nicholas, H. B. and Deerfield, D. W. (1997). GeneDoc: Analysis and Visualization of Genetic Variation. *EMBNEW.NEWS* **4**: 14.

Nobes, C. D. and Hall, A. (1995). Rho, rac, and cdc42 GTPases regulate the assembly of multimolecular focal complexes associated with actin stress fibers, lamellipodia, and filopodia. *Cell* **81**: 53-62.

O'Connell, C. B., Wheatley, S. P., Ahmed, S. and Wang, Y. L. (1999). The small GTP-binding protein rho regulates cortical activities in cultured cells during division. *Journal of Cell Biology* **144**: 305-13.

O'Farrell, P. H. (1992). Cell cycle control: many ways to skin a cat. *Trends in Cell Biology.* **2**: 159-162.

O'Shea, E. K. and Herskowitz, I. (2000). The ins and outs of cell-polarity decisions. *Nature Cell Biology* **2**: E39-E41.

Oei, S. L., Griesenbeck, J. and Schweiger, M. (1997). The role of poly ADP-ribosylation. *Rev. Physiol. Biochem. Pharmacol.* **131**: 4135-4137.

Olofsson, B. (1999). Rho guanine dissociation inhibitors: pivotal molecules in cellular signalling. *Cell Signalling* **11**: 545-554.

Opas, J. and SoÇtyÑska, M. S. (1978). Reorganization of the cortical layer during cytokinesis in mouse blastomeres. *Experimental Cell Research* **113**: 208-11.

Ouchi, T., Lee, S. W., Ouchi, M., Aaronson, S. A. and Horvath, C. M. (2000). Collaboration of signal transducer and activator of transcription 1 (STAT1) and BRCA1 in differential regulation of IFN-gamma target genes. *Proceedings of the National Academy of Sciences of the United States of America* **97**: 5208-5213.

Ouchi, T., Monteiro, A. N., August, A., Aaronson, S. A. and Hanafusa, H. (1998). BRCA1 regulates p53-dependent gene expression. *Proceedings of the National Academy of Sciences of the United States of America* **95**: 2302-6.

Palmieri, S. J., Nebl, T., Pope, R. K., Seastone, D. J., Lee, E., Hinchcliffe, E. H., Sluder, G., Knecht, D., Cardelli, J. and Luna, E. J. (2000). Mutant Rac1B expression in Dictyostelium: effects on morphology, growth, endocytosis, development, and the actin cytoskeleton. *Cell Motility and the Cytoskeleton* **46**: 285-304.

Parnas, D., Haghighi, A. P., Fetter, R. D., Kim, S. W. and Goodman, C. S. (2001). Regulation of postsynaptic structure and protein localization by the Rho-type guanine nucleotide exchange factor dPix. *Neuron* **32**: 415-24.

Parry, D. H. and O'Farrell, P. H. (2001). The schedule of destruction of three mitotic cyclins can dictate the timing of events during exit from mitosis. *Current Biology* **11**: 671-83.

Piel, M., Nordberg, J., Euteneuer, U. and Bornens, M. (2001). Centrosome-dependent exit of cytokinesis in animal cells. *Science* **291**: 1550-3.

Pinol-Roma, S. and Dreyfuss, G. (1992). Shuttling of pre-mRNA binding proteins between nucleus and cytoplasm. *Nature* **355**: 730-732.

Prokopenko, S. N., Brumby, A., O'Keefe, L., Prior, L., He, Y., Saint, R. and Bellen, H. J. (1999). A putative exchange factor for Rho1 GTPase is required for initiation of cytokinesis in *Drosophila. Genes and Development.* **13**: 2301-2314.

Rameh, L. E., Arvidsson, A., Carraway, K. L. R., Couvillon, A. D., Rathbun, G., Crompton, A., VanRenterghem, B., Czech, M. P., Ravichandran, K. S., Burakoff, S. J. *et al.,*. (1997). A comparative analysis of the phosphoinositide binding specificity of pleckstrin homology domains. *Journal of Biological Chemistry* **272**: 22059-22066.

Rao, V. N., Shao, N., Ahmad, M. and Reddy, E. S. (1996). Antisense RNA to the putative tumor suppressor gene BRCA1 transforms mouse fibroblasts. *Oncogene* **12**: 523-528.

Rappaport, R. (1961). Experiments concerning the cleavage stimulus in sand dollar eggs. *Journal of Experimental Zoology* **148**: 81-89.

Rappold, I., Iwabuchi, K., Date, T. and Chen, J. (2001). Tumor Suppressor p53 Binding Protein1 (53BP1) is involved in DNA damage-signaling pathways. *Journal of Cell Biology* **153**: 613-620.

Rechsteiner, M. and Rogers, S. W. (1996). PEST sequences and regulation by proteolysis. *Trends in Biochemical Sciences* **21**: 267-71.

Ridley, A. J. and Hall, A. (1992). The small GTP-binding protein rho regulates the assembly of focal adhesions and actin stress fibers in response to growth factors. *Cell* **70**: 389-399.

Ridley, A. J., Paterson, H. F., Johnston, C. L., Diekmann, D. and Hall, A. (1992). The small GTP-binding protein rac regulates growth factor-induced membrane ruffling. *Cell* **70**: 401-410.

Robbins, J., Dilworth, S. M., Laskey, R. A. and Dingwall, C. (1991). Two interdependent basic domains in nucleoplasmin nuclear targeting sequence: identification of a class of bipartite nuclear targeting sequence. *Cell* **64**: 615- 623.

Robinow, S. N. and White, K. (1988). The locus *elav* of *Drosophila melanogaster* is expressed in neurons at all developmental stages. *Developmental Biology* **126**: 294-303.

Rogakou, E. P., Boon, C., Redon, C. and Bonner, W. M. (1999). Megabase chromatin domains involved in DNA double-strand breaks *in vivo*. *The Journal of Cell Biology* **146**: 905-915.

Rong, Y. S. and Golic, K. G. (2000). Gene targeting by homologous recombination in *Drosophila*. *Science* **288**: 2013-2018.

Rubin, G. M. and Spradling, A. C. (1982). Genetic transformation of *Drosophila* with transposable element vectors. *Science* **218**: 348-353.

Saint, R. B. and Wigley, P. L. (1992). Developmental regulation of the cell cycle. *Current Opinion in Genetics and Development.* **2**: 614-620.

Saka, Y., Esashi, F., Matsusaka, T., Mochida, S. and Yanagida, M. (1997). Damage and replication checkpoint control in fission yeast is ensured by interactions of Crb2, a protein with BRCT motif, with Cut5 and Chk1. *Genes and Development* **11**: 3387-400.

Saka, Y., Fantes, P., Sutani, T., McInerny, C., Creanor, J. and Yanagida, M. (1994). Fission yeast cut5 links nuclear chromatin and M phase regulator in the replication checkpoint control. *EMBO Journal* **13**: 5319-5329.

Saka, Y. and Yanagida, M. (1993). Fission yeast *cut5*$^{+}$, required for S phase onset and M phase restraint, is identical to the radiation-damage repair gene *rad4*$^{+}$. *Cell* **74**: 383-393.

Salzberg, A., Prokopenko, S. N., He, Y., Tsai, P., Pal, M., Maroy, P., Glover, D. M., Deak, P. and Bellen, H. J. (1997). P-element insertion alleles of essential genes on the third chromosome of Drosophila melanogaster: mutations affecting embryonic PNS development. *Genetics* **147**: 1723-41.

Sambrook, J., Fritsch, E. F. and Maniatis, T. (1989). Molecular Cloning: A laboratory manual. Cold Spring Harbor, NY: Cold Spring Harbor Laboratory Press.

Schmidt, A. and Hall, A. (2002). The Rho exchange factor Net1 is regulated by nuclear sequestration. *Journal of Biological Chemistry* **277**: 14581-14588.

Schultz, L. B., Chehab, N. H., Malikzay, A. and Halazonetis, T. D. (2000). p53 binding protein 1 (53BP1) is an early participant in the cellular response to DNA double-strand breaks. *Journal of Cell Biology* **151**: 1381-90.

Schumacher, J. M., Golden, A. and Donovan, P. J. (1998). AIR-2: An Aurora/Ipl1-related protein kinase associated with chromosomes and midbody microtubules is required for polar body extrusion and cytokinesis in Caenorhabditis elegans embryos. *Journal of Cell Biology* **143**: 1635-46.

Scully, R., Anderson, S. F., Chao, D. M., Wei, W., Ye, L., Young, R. A., Livingston, D. M. and Parvin, J. D. (1997a). BRCA1 is a component of the RNA polymerase II holoenzyme. *Proceedings of the National Academy of Sciences of the United States of America* **94**: 5605-5610.

Scully, R., Chen, J., Ochs, R. L., Keegan, K., Hoekstra, M., Feunteun, J. and Livingston, D. M. (1997b). Dynamic changes of BRCA1 subnuclear location and phosphorylation state are initiated by DNA damage. *Cell* **90**: 425-35.

Scully, R., Chen, J., Plug, A., Xiao, Y., Weaver, D., Feunteun, J., Ashley, T. and Livingston, D. M. (1997c). Association of BRCA1 with Rad51 in mitotic and meiotic cells. *Cell* **88**: 265-275.

Scully, R., Ganesan, S., Vlasakova, K., Chen, J. J., Sokolovsky, M. and Livingston, D. M. (1999). Genetic analysis of BRCA1 function in a defined tumor cell line. *Molecular Cell* **4**: 1093-1099.

Scully, R. and Livingston, D. M. (2000). In search of the tumor-suppressor functions of BRCA1 and BRCA2. *Nature* **408**: 429-432.

Sekelsky, J. J., Burtis, K. C. and Hawley, R. S. (1998). Damage control: the pleiotropy of DNA repair genes in *Drosophila melanogaster*. *Genetics* **148**: 1587-1598.

Severson, A. F., Hamill, D. R., Carter, J. C., Schumacher, J. and Bowerman, B. (2000). The aurora-related kinase AIR-2 recruits ZEN-4/CeMKLP1 to the mitotic spindle at metaphase and is required for cytokinesis. *Current Biology* **10**: 1162-71.

Shao, N., Chai, Y. L., Shyam, E., Reddy, P. and Rao, V. N. (1996). Induction of apoptosis by the tumor suppressor protein BRCA1. *Oncogene* **13**: 1-7.

Shimada, Y., Gulli, M. P. and Peter, M. (2000). Nuclear sequestration of the exchange factor Cdc24 by Far1 regulates cell polarity during yeast mating. *Nature Cell Biology* **2**: 117-124.

Sigrist, S., Jacobs, H., Stratmann, R. and Lehner, C. F. (1995). Exit from mitosis is regulated by Drosophila fizzy and the sequential destruction of cyclins A, B and B3. *EMBO Journal* **14**: 4827-38.

Sisson, J. C., Field, C., Ventura, R., Royou, A. and Sullivan, W. (2000). Lava lamp, a novel peripheral golgi protein, is required for *Drosophila melanogaster* cellularization. *Journal of Cell Biology* **151**: 905-18.

Smith, D. A., Baker, B. S. and Gatti, M. (1985). Mutations in genes encoding essential mitotic functions in *Drosophila melanogaster*. *Genetics* **110**: 647-670.

Somasundaram, K., Zhang, H., Zeng, Y. X., Houvras, Y., Peng, Y., Wu, G. S., Licht, J. D., Weber, B. L. and El-Deiry, W. S. (1997). Arrest of the cell cycle by the tumour-suppressor BRCA1 requires the CDK-inhibitor p21WAF1/CiP1. *Nature* **389**: 187-190.

Sone, M., Hoshino, M., Suzuki, E., Kuroda, S., Kaibuchi, K., Nakagoshi, H., Saigo, K., Nabeshima, Y. and Hama, C. (1997). Still life, a protein in synaptic terminals of *Drosophila* homologous to GDP-GTP exchangers. *Science* **275**: 543-7.

Sotillos, S. and Campuzano, S. (2000). DRacGAP, a novel Drosophila gene, inhibits EGFR/Ras signalling in the developing imaginal wing disc. *Development* **127**: 5427-38.

Soulier, J. and Lowndes, N. F. (1999). The BRCT domain of the *S. cerevisiae* checkpoint protein Rad9 mediates a Rad9-Rad9 interaction after DNA damage. *Current Biology* **9**: 551-4.

Spradling, A. C. and Rubin, G. M. (1982). Transposition of cloned P elements into *Drosophila* germline chromosomes. *Science* **218**: 341-347.

Strutt, D. I., Weber, U. and Mlodzik, M. (1997). The role of RhoA in tissue polarity and Frizzled signalling. *Nature* **387**: 292-5.

Su, T., Walker, J. and Stumpff, J. (2000). Activating the DNA damage checkpoint in a developmental context. *Current Biology* **10**: 119-126.

Sumi, T., Matsumoto, K., Takai, Y. and Nakamura, T. (1999). Cofilin phosphorylation and actin cytoskeletal dynamics regulated by rho- and Cdc42-activated LIM-kinase 2. *Journal of Cell Biology* **147**: 1519-1532.

Swan, K. A., Severson, A. F., Carter, J. C., Martin, P. R., Schnabel, H., Schnabel, R. and Bowerman, B. (1998). *cyk-1*: a *C. elegans* FH gene required for a late step in embryonic cytokinesis. *Journal of Cell Science* **111**: 2017-2027.

Tatsumoto, T., Xie, X., Blumenthal, R., Okamoto, I. and Miki, T. (1999). Human ECT2 is an Exchange Factor for Rho GTPases, Phosphorylated in G2/M Phases, and Involved in Cytokinesis. *The Journal of Cell Biology* **147**: 921-927.

Taylor, R. M., Wickstead, B., Cronin, S. and Caldecott, K. W. (1998). Role of a BRCT domain in the interaction of DNA ligase III-α with the DNA repair protein XRCC1. *Current Biology* **8**: 877-880.

Theurkauf, W. E. and Hawley, R. S. (1992). Meiotic spindle assembly in *Drosophila* females: behaviour of nonexchange chromosomes and the effects of mutations in the nod kinesin-like protein. *Journal of Cell Biology* **116**: 1167-1180.

Thompson, J. D., Higgins, D. G. and Gibson, T. J. (1994). CLUSTAL W: improving the sensitivity of progressive multiple sequence alignment through sequence weighting, position-specific gap penalties and weight matrix choice. *Nucleic Acids Res* **22**: 4673-4680.

Thompson, L. H., Brookman, K. W., Jones, N. J., Allen, S. A. and Carrano, A. V. (1990). Molecular cloning of the human *XRCC1* gene, which corrects defective DNA strand break repair and sister chromatid exchange. *Molecular and Cellular Biology* **10**: 6160-6171.

Tibbetts, R. S., Cortez, D., Brumbaugh, K. M., Scully, R., Livingston, D., Elledge, S. J. and Abraham, R. T. (2000). Functional interactions between BRCA1 and the checkpoint kinase ATR during genotoxic stress. *Genes and Development* **14**: 2989-3002.

Toenjes, K. A., M.M., S. and Johnson, D. I. (1999). The guanine-nucleotide-exchange factor Cdc24p is targeted to the nucleus and polarized growth sites. *Current Biology* **9**: 1183-6.

Tsubouchi, H. and Ogawa, H. (1998). A novel mre11 mutation impairs processing of double-strand breaks of DNA during both mitosis and meiosis. *Molecular and Cellular Biology* **18**: 260-268.

Verheyen, E. M. and Cooley, L. (1994). Profilin mutations disrupt multiple actin-dependent processes during Drosophila development. *Development* **120**: 717-28.

Verkade, H. M. and O'Connell, M. J. (1998). Cut5 is a component of the UV-responsive DNA damage checkpoint in fission yeast. *Molecular and General Genetics* **260**: 426-33.

Walworth, N. C. (2000). Cell-cycle checkpoint kinases: checking in on the cell cycle. *Current Opinion in Cell Biology* **12**: 697-704.

Wang, Y., Cortez, D., Yazdi, P., Neff, N., Elledge, S. J. and Qin, J. (2000). BASC, a super complex of BRCA1-associated proteins involved in the recognition and repair of aberrant DNA structures. *Genes and Development* **14**: 927-939.

Watanabe, N., Madaule, P., Reid, T., Ishizaki, T., Watanabe, G., Kakizuka, A., Saito, Y., Nakao, K., Jockusch, B. M. and Narumiya, S. (1997). p140mDia, a mammalian homolog of Drosophila diaphanous, is a target protein for Rho small GTPase and is a ligand for profilin. *EMBO Journal* **16**: 3044-56.

Weinert, T. and Hartwell, L. (1989). Control of G2 delay by the *rad9* gene of *Saccharomyces cerevisiae*. *Journal of Cell Science Suppl* **12**: 145-148.

Weinert, T. A. and Hartwell, L. H. (1988). The RAD9 gene controls the cell cycle response to DNA damage in *Saccharomyces cerevisiae*. *Science* **241**: 317-322.

Werner, L. A. and Manseau, L. J. (1997). A *Drosophila* gene with predicted rhoGEF, pleckstrin homology and SH3 domains is highly expressed in morphogenic tissues. *Gene* **187**: 107-14.

Wheatley, S. P., Hinchcliffe, E. H., Glotzer, M., Hyman, A. A., Sluder, G. and Wang, Y. l. (1997). CDK1 inactivation regulates anaphase spindle dynamics and cytokinesis in vivo. *Journal of Cell Biology* **138**: 385-93.

Wheatley, S. P., O'Connell, C. B. and Wang, Y. I. (1998). Inhibition of chromosomal separation provides insights into cleavage furrow stimulation in cultured epithelial cells. *Molecular Biology of the Cell* **9**: 2173-84.

Wheatley, S. P. and Wang, Y. (1996). Midzone microtubule bundles are continuously required for cytokinesis in cultured epithelial cells. *Journal of Cell Biology* **135**: 981-9.

Williams, B. C., Riedy, M. F., Williams, E. V., Gatti, M. and Goldberg, M. L. (1995). The *Drosophila* kinesin-like protein KLP3A is a midbody component required for central spindle assembly and initiation of cytokinesis. *Journal of Cell Biology* **129**: 709-23.

Winter, C. G., Wang, B., Ballew, A., Royou, A., Karess, R., Axelrod, J. D. and Luo, L. (2001). *Drosophila* Rho-associated kinase (Drok) links Frizzled-mediated planar polarity signaling to the actin cytoskeleton. *Cell* **105**: 81-91.

Wissmann, A., Ingles, J., McGhee, J. D. and Mains, P. E. (1997). *Caenorhabditis elegans* LET-502 is related to Rho-binding kinases and human myotonic dystrophy kinase and interacts genetically with a homolog of the regulatory subunit of smooth muscle myosin phosphatase to affect cell shape. *Genes and Development* **11**: 409-22.

Wolff, T. and Ready, D. F. (1993). Pattern formation in the *Drosophila* retina. In *The Development of Drosophila melanogaster*, (ed. Bate, M. and Martinez Arias, A.), pp. 1277-1326. Cold Spring Harbour, NY: Cold Spring Harbor Laboratory Press.

Xia, Z., Morales, J. C., Dunphy, W. G. and Carpenter, P. B. (2001). Negative cell cycle regulation and DNA damage-inducible phosphorylation of the BRCT protein 53BP1. *Journal of Biological Chemistry* **276**: 2708-2718.

Xu, B., Kim St, S. and Kastan, M. B. (2001). Involvement of Brca1 in S-phase and G(2)-phase checkpoints after ionizing irradiation. *Molecular and Cellular Biology* **21**: 3445-50.

Xu, X., Weaver, Z., Linke, S. P., Li, C., Gotay, J., Wang, X. W., Harris, C. C., Ried, T. and Deng, C. X. (1999). Centrosome amplification and a defective G2-M cell cycle checkpoint induce genetic instability in BRCA1 exon 11 isoform-deficient cells. *Molecular Cell* **3**: 389-395.

Yamamoto, R. R., Axton, J. M., Yamamoto, Y., Saunders, R. D., Glover, D. M. and Henderson, D. S. (2000). The *Drosophila mus101* gene, which links DNA repair, replication and condensation of heterochromatin in mitosis, encodes a protein with seven BRCA1 C-terminus domains. *Genetics* **156**: 711-21.

Yamane, K., Kawabata, M. and Tsuruo, T. (1997). A DNA-topoisomerase-II-binding protein with eight repeating regions similar to DNA-repair enzymes and to cell-cycle regulator. *European Journal of Biochemistry* **250**: 794-799.

Yamane, K. and Tsuruo, T. (1999). Conserved BRCT regions of TopBP1 and of the tumor suppressor BRCA1 bind strand breaks and termini of DNA. *Oncogene* **18**: 5194-5203.

Yamano, H., Gannon, J. and Hunt, T. (1996). The role of proteolysis in cell cycle progression in *Schizosaccharomyces pombe*. *EMBO Journal* **15**: 5268-79.

Yarden, R. I., Pardo-Reoyo, S., Sgagias, M., Cowan, K. H. and Brody, L. C. (2002). BRCA1 regulates the G2/M checkpoint by activating Chk1 kinase upon DNA damage. *Nature Genetics* **30**: 285-289.

Yasui, Y., Amano, M., Nagata, K., Inagaki, N., Nakamura, H., Saya, H., Kaibuchi, K. and Inagaki, M. (1998). Roles of Rho-associated kinase in cytokinesis; mutations in Rho-associated kinase phosphorylation sites impair cytokinetic segregation of glial filaments. *Journal of Cell Biology* **143**: 1249-58.

Ye, Q., Hu, Y., Zhong, H., Nye, A. C., Belmont, A. S. and Li, R. (2001). BRCA1-induced large-scale chromatin unfolding and allele-specific effects of cancer-predisposing mutations. *Journal of Cell Biology* **155**: 911-921.

Yoffe, K. B., Manoukian, A. S., Wilder, E. L., Brand, A. H. and Perrimon, N. (1995). Evidence for engrailed-independent wingless autoregulation in Drosophila. *Developmental Biology* **170**: 636-50.

Zachariae, W. (1999). Progression into and out of mitosis. *Current Opinion in Cell Biology* **11**: 708-16.

Zhang, D. and Nicklas, R. B. (1996). 'Anaphase' and cytokinesis in the absence of chromosomes. *Nature* **382**: 466-8.

Zhang, H., Somasundaram, K., Peng, Y., Tian, H., Zhang, H., Bi, D., Weber, B. L. and El-Deiry, W. S. (1998a). BRCA1 physically associated with p53 and stimulates its transcriptional activity. *Oncogene* **16**: 1713-1721.

Zhang, H., Tombline, G. and Weber, B. L. (1998b). BRCA1, BRCA2, and DNA damage response: collision or collusion? *Cell* **92**: 433-436.

Zhang, X., Morera, S., Bates, P. A., Whitehead, P. C., Coffer, A. I., Hainbucher, K., Nash, R. A., Sternberg, M. J., Lindahl, T. and Freemont, P. S. (1998c). Structure of an XRCC1 BRCT domain: a new protein-protein interaction module. *EMBO Journal* **17**: 6404-11.

Zheng, Y., Zangrilli, D., Cerione, R. A. and Eva, A. (1996). The pleckstrin homology domain mediates transformation by oncogenic dbl through specific intracellular targeting. *Journal of Biological Chemistry* **271**: 19017-19020.

Zhong, Q., Chen, C. F., Li, S., Chen, Y., Wang, C. C., Xiao, J., Chen, P. L., Sharp, Z. D. and Lee, W. H. (1999). Association of BRCA1 with the hRad50-hMre11-p95 complex and the DNA damage response. *Science* **285**: 747-750.